

IAEA-TECDOC-726

# ***Isotopic and geochemical precursors of earthquakes and volcanic eruptions***

*Proceedings of an Advisory Group Meeting  
held in Vienna, 9–12 September 1991*



INTERNATIONAL ATOMIC ENERGY AGENCY

IAEA

November 1993

The IAEA does not normally maintain stocks of reports in this series.  
However, microfiche copies of these reports can be obtained from

INIS Clearinghouse  
International Atomic Energy Agency  
Wagramerstrasse 5  
P.O. Box 100  
A-1400 Vienna, Austria

Orders should be accompanied by prepayment of Austrian Schillings 100,—  
in the form of a cheque or in the form of IAEA microfiche service coupons  
which may be ordered separately from the INIS Clearinghouse.

The originating Section of this document in the IAEA was:

Section of Isotope Hydrology  
International Atomic Energy Agency  
Wagramerstrasse 5  
P.O. Box 100  
A-1400 Vienna, Austria

ISOTOPIC AND GEOCHEMICAL PRECURSORS  
OF EARTHQUAKES AND VOLCANIC ERUPTIONS  
IAEA, VIENNA, 1993  
IAEA-TECDOC-726  
ISSN 1011-4289

Printed by the IAEA in Austria  
November 1993

## **FOREWORD**

Every year natural catastrophes, such as earthquakes and volcanic eruptions, cause heavy death tolls, human suffering and disastrous damage, despite continuous progress in the understanding of natural hazards and the mitigation of their effects. But the prediction of such events within a reasonable time is still a problem.

In recent years, investigations have shown that, under certain circumstances, some geochemical tools, including environmental isotopes, can provide useful indications for predicting earthquakes and volcanic eruptions. However, the natural processes and the geological causes which govern the geochemical behaviour of these precursors are still far from being fully understood. The International Atomic Energy Agency therefore convened an Advisory Group Meeting on the Isotopic and Geochemical Precursors of Earthquakes and Volcanic Eruptions to review the state of the art in this field, which has such important practical implications.

The Advisory Group meeting was held in Vienna from 9 to 12 September 1991 and was attended by twenty-three invited experts and observers from eleven countries and two international organizations.



## *EDITORIAL NOTE*

*In preparing this document for press, staff of the IAEA have made up the pages from the original manuscripts as submitted by the authors. The views expressed do not necessarily reflect those of the governments of the nominating Member States or of the nominating organizations.*

*The use of particular designations of countries or territories does not imply any judgement by the publisher, the IAEA, as to the legal status of such countries or territories, of their authorities and institutions or of the delimitation of their boundaries.*

*The mention of names of specific companies or products (whether or not indicated as registered) does not imply any intention to infringe proprietary rights, nor should it be construed as an endorsement or recommendation on the part of the IAEA.*

*The authors are responsible for having obtained the necessary permission for the IAEA to reproduce, translate or use material from sources already protected by copyrights.*

## CONTENTS

Summary of the Advisory Group Meeting . . . . .	7
Radon as a precursor of earthquakes . . . . .	9
<i>V.T. Dubinchuk</i>	
Gas-geochemical approaches to earthquake prediction . . . . .	22
<i>Chi-Yu King</i>	
Radon measurements in Austria and some basic problems in earthquake prediction research . . . . .	37
<i>H. Friedmann</i>	
Geochemical precursors of earthquakes — Experience in Italy . . . . .	44
<i>M. Valenza, P.M. Nuccio</i>	
Fluidodynamical and chemical features of radon 222 related to total gases: Implications for earthquake predictions . . . . .	48
<i>G. Martinelli</i>	
Some isotopic and geochemical anomalies observed in Mexico prior to large scale earthquakes and volcanic eruptions . . . . .	63
<i>S. de la Cruz-Reyna, M. A. Armienta-Hernandez, N. Segovia</i>	
Conclusions on the possible variations of chemical and isotopic composition of groundwater systems in response to changed hydrodynamic conditions (based on investigations of deep groundwater systems and thermal-mineral waters and brines in tectonic active areas) . . . . .	87
<i>W. Balderer</i>	
Principles and methods of volcanic surveillance: The case of Vulcano, Italy . . . . .	108
<i>P.M. Nuccio, M. Valenza</i>	
Buildup of CO <sub>2</sub> in Lake Nyos and evaluation of recurrence of future gas outbursts . .	116
<i>M. Kusakabe</i>	
The Lake Nyos gas disaster: Conclusions and predictions . . . . .	124
<i>S.J. Freeth</i>	
The need of real-time devices for measuring volcanic and seismic signals . . . . .	130
<i>M. Balcázar, N. Segovia, M. Monnin, A. Chávez, J.H. Flores</i>	
Geochemical surveillance of active volcanic areas in Italy: Campi Flegrei Caldera and Vulcano Island . . . . .	135
<i>D. Tedesco</i>	
List of Participants . . . . .	155

## SUMMARY OF THE ADVISORY GROUP MEETING

The fluids trapped and segregated in pores, fissures and fractures of deep geological formations may suddenly become mobile and migrate into shallow horizons or to the surface under conditions of tectonic stress and strain which precede and eventually cause earthquakes. In fact, the strain to which rocks are subjected determines the opening of cavities and the fluid release. In general, these fluids have a chemical and isotopic composition different from those of other fluids, like shallow groundwater, with which they mix. This produces the appearance of chemical and isotopic anomalies, which may announce the occurrence of an earthquake in the near future.

If this is the general mechanism producing variations of certain elements and isotopes, the details of their geochemical behaviour, and therefore their reliability as earthquake precursors, are still poorly understood. Radon 222 seems to be one of the most promising precursors and is the tracer for which more data are available: according to statistics elaborated in China, 70% of earthquakes are preceded by radon anomalies detectable in soil, air and/or in groundwater. However, 40% of the radon anomalies detected are not followed by earthquakes.

Other isotopes, the variations of which may potentially be suitable for earthquake prediction, are the stable and radioactive isotopes of light elements such as hydrogen, helium, oxygen and carbon. For these isotopes, however, the existing data are still very scarce, and much more research and observations are necessary to assess their reliability on a statistical basis.

In spite of all these shortcomings, the problem of earthquake prediction is of such importance that some national networks for geochemical and isotopic monitoring of earthquakes are already in place, and others will be established in the near future.

Volcanic eruptions are also frequently preceded by chemical and isotopic variations of fluids delivered by fumaroles, hot springs, etc. These variations are usually more pronounced and easier to detect than those announcing earthquakes. The reason lies in the fact that the magmatic fluids, which produce the geochemical and isotopic changes, are located at a lesser depth in the Earth's crust than those released before and during earthquakes. For instance, an increase of hydrogen generated by the interaction of magmatic fluid with rocks, in fumarole gases, is considered a good precursor of volcanic eruptions. Also other changes of the fluid chemical composition and variations of  $^3\text{He}/^4\text{He}$ ,  $^2\text{H}/^1\text{H}$ ,  $^{13}\text{C}/^{12}\text{C}$ ,  $^{18}\text{O}/^{16}\text{O}$  isotopic ratios have been detected.

Compared with that of earthquakes, the prediction of volcanic eruptions appears relatively easier, because the scientific understanding of volcanic processes is more advanced. In addition, in the case of volcanoes, the areas and the sites for continuous monitoring are well identified, and the data already available provide a good orientation for samples to collect and parameters to measure.

In conclusion, sufficient evidence has been accumulated that certain geochemical and isotopic tools can be used as precursors of earthquakes and volcanic eruptions. Variations of about 40 geochemical and isotopic indicators have been recorded before large and

moderate earthquakes at different sites and under different hydrogeological, tectonic and volcanic conditions, with a time advance ranging from hours to one year. Among these indicators one can mention variations in concentration and/or isotopic ratios of hydrogen, helium, carbon, oxygen, neon, radon, radium and uranium.

Nevertheless, there are still many scientific questions and methodological problems which need to be solved, in order to extract from the geochemical and isotopic signals a prediction with a high level of reliability. To this end, long term (preferably on-line) monitoring of geochemical, isotopic, hydrological and geophysical parameters should be organized, and an interdisciplinary approach should be used for elaborating the field data, which should lead to the formulation of complex geochemical and geophysical models.

In order to help in tackling these problems and to foster research, the participants recommended that further work be done on isotopic and geochemical precursors of earthquakes and volcanic eruptions. This work should concentrate on:

- (i) searching, selecting and using the most informative isotopic and geochemical precursors, to be monitored along with other hydrological and geophysical parameters;
- (ii) analysing precursor behaviour, and formulating theories and models for this;
- (iii) elaborating algorithms for data processing and event prediction;
- (iv) improving and developing monitoring networks.

# RADON AS A PRECURSOR OF EARTHQUAKES

V.T. DUBINCHUK\*

International Atomic Energy Agency,  
Vienna

## Abstract

*This is a short historical review on the use and study of radon concentration variations in groundwater and soil air as a possible precursor of earthquakes and other events affected by accumulation and variation of strains in rock massifs. An analysis of the main features of radon signals in hydrogeochemical systems is presented and possible mechanisms of radon earthquake forerunners are discussed. It is assumed that the initial stage of any radon transfer from a rock matrix mineral in a strained state into pore fluid has a thermo-molecular activation character obeying general kinetic laws. On this basis a new model for radon anomalies has been developed where so-called conversion coefficients, kinetic complexes, kinetics of radioactive decay, first order transfer processes (sorption, for example) and hydraulic transport (turnover) are involved. All of these kinetic parameters are related to some characteristic residence time for a given precursor in a given system. Both groups of parameters are governing amplitude and forms of radon precursor output curves. The main characteristics of precursors in hydrogeochemical systems are the residence time distribution functions for water (RTDFw) and precursor components (RTDFc). These functions can be evaluated by means of well known isotope hydrology tracer techniques. Some methodological consequences and recommendations how to use isotope hydrology data are given for the analysis and interpretation of the radon (and of other hydrochemical) precursor signals of earthquakes.*

## 1. INTRODUCTION

Earthquakes are a major threat to humanity and it is a great challenge for scientists and engineers to make efforts to prevent their disastrous consequences [9, 42, 57, 58, 65, 73, 79]. Almost all kinds of human activities are most sensible to and depend on seismo-tectonic and geo-dynamic conditions and events [58]. One should remember that modern city agglomerations, roads and pipelines, hydro-, nuclear-, coal- and gas-power stations, chemical and gas-oil industries, etc. are vulnerable to geodynamic processes connected with or activated by various strains in soil and rocks. The problem of earthquakes and other geodynamic processes requires an adequate and complex system approach to be analysed [30, 58, 72, 73, 75, 79].

The major problem to be solved is the earthquake forecast, i.e. determination of strength, place and time of possible future earthquakes [8, 28, 30, 43, 57, 58, 75]. It should be emphasized that regional ability to provide earthquake safety influences human activities in a different way, depending on the state of the art of environmental monitoring and, what is most important, of understanding seismotectonic precursor signals in order to make correct decision [7, 12, 28, 30, 60]. It is true that the great majority of catastrophic seismic events has not been forecast, nevertheless the hope of being more successful in future in predicting the site and strength of earthquakes has increased.

\* Present address: All-Russian Research Institute for Hydrology and Engineering Geology, Center for Geoenvironment, 142452 Zeleny Village, Noginsk District, Moscow Region, Russian Federation.

Earthquake prediction is one of the most important, yet infant disciplines within earth sciences and engineering. The history of development of earthquake prediction studies could be subdivided into the following stages:

- intuitive semi-scientific attempts were made till the end of the 19th century [37, 58];
- scientific formulation of the problem and possible ways to solve it were elaborated by Orlov A.P., Mushketov I.V., Golitsyn B.B., in the early 20th century;
- the first complex studies were made after the Ashkhabad earthquakes by Gamburtsev. His study was predominantly seismological, although there were some indications of possible hydrogeochemical and hydrogeological precursors [44];
- a "renaissance" of this problem came after the Tashkent earthquake of 1966 [4, 5, 70, 73, 78]. At that time the hydrogeological parameters (groundwater level, temperature, mineralization, turbidity, flow) and hydrogeochemical tracers (Rn, some other chemical soluted gas components,  $^{234}\text{U}/^{238}\text{U}$ , Ra, He) were tried out to forecast earthquakes. At the same time, analogous research started in the USA [38, 39, 42, 46, 54, 60, 63, 64, 71], in China [35, 74, 75, 83], in Japan [50, 82] and in other countries [23, 25, see also reviews 28, 54, 57, 71, 72];
- further prognostic studies were greatly intensified after the Armenian (1987) and the Californian (1989) earthquakes.

During the last two decades a number of hydrochemical precursor in different seismo-tectonical regions were observed. A review of such observations can be found in a series of publications [5, 12, 15, 28, 34, 43, 45, 57, 72, 75]. In the early 1970s researchers were very optimistic that the prediction problem would soon be solved. But the number of precursors, which has constantly increased, was hard to be monitored and nearly impossible to be interpreted.

There is a lot of evidence that such ground water constituents as Rn, He,  $\text{CO}_2$ ,  $\text{CH}_4$ , Ar,  $\text{H}_2$ ,  $\text{O}_2$ ,  $\text{N}_2$ , Na, Cl, Hg, Rb, Cs,  $\text{SiO}_2$  are changing their concentration before, during and after an earthquake [12, 15, 29-34, 44, 45, 49, 67, 75].

It was noted that not only chemical components, but also some isotopes such as D/H,  $^{18}\text{O}/^{16}\text{O}$ ,  $^{222}\text{Rn}/^{226}\text{Ra}$ ,  $^{234}\text{U}/^{238}\text{U}$ ,  $^{13}\text{C}/^{12}\text{C}$ ,  $^4\text{He}/^{40}\text{Ar}$  are varying their content or ratios at a detectable level [10, 12, 29-34, 39, 53]. Moreover, it has been recorded that in experiments by compression of rock materials [29, 30, 34, 36, 47], in landslide massifs [26, 27, 56], in mines and quarries before rock explosions, before and at the end of volcano eruptions [20, 22], and by artificial explosions [31], some volatile components (Rn, He, Ar,  $\text{H}_2$ , Hg, CO,  $\text{CH}_4$ ) are escaping.

Changes in the radon emission of groundwater were first observed as a precursory phenomenon of an earthquake. In several publications in the former Soviet Union [4, 67, 73] an abnormal increase of radon concentration in groundwater prior to the Tashkent earthquake of April 26, 1966 was reported. The radon concentration of groundwater obtained from several deep wells (1200-2400 m) in Tashkent and its surroundings had gradually increased for several years and reached a maximum concentration level (2-3 times higher than normal) just prior to the earthquake. Immediately after the main earthquake event, with a magnitude of 5.5, the radon concentration returned to the normal level of approximately  $5 \times 10^{-10}$  Ci/l. After more studies and continuous monitoring, an apparent correlation between the changes of radon concentration in groundwater and successive after-shocks was confirmed.

Since the Tashkent earthquake, hydrogeochemical precursor studies have been predominantly implemented in groundwater with increasing intensity in different regions of the Russian Federation: in Uzbekistan [2, 5, 32, 33, 67, 70, 73], in Kirgizia [1, 11-14, 29, 41], in Dagestan [53], in Ukraine [15, 45, 62], in Turkmenia [44] and in Armenia [6], etc.

In 1975 the US Geological Survey began to monitor radon contents in subsurface soil-gas along some active faults in central California in order to test whether this parameter might show any useful earthquake related changes [28, 38, 39, 42, 46, 63, 64]. American scientists thought that there were several reasons for choosing to monitor radon in soil-gas instead of in groundwater. The first result of it was that the very effective and inexpensive Track Etch Technique has been developed.

It was observed that soil-gas and gas exhalations in general are commonly enriched in Rn in fault zones and that the near surface-air shows significant increases in its radon content in the time of an earthquake occurrence [38, 39]. However, it is known that other environmental factors such as barometric pressure, temperature, rainfall, and wind speed can strongly effect the radon content of the air above and near the ground-surface.

It seems therefore that the observation of radon content in groundwaters is preferable because groundwater radon is a conservative indicator with regard to exogenic factors. Already in 1979 Shapiro et al. [63, 64] observed a radon anomaly which coincided with several other geophysical and geochemical anomalies and appeared to have been associated with an earthquake which occurred at a distance of 290 km from the site of the radon anomalies. In China and the Russian Federation, groundwater radon anomalies were observed 50–400 km from the earthquake epicenters.

Reports of supposed precursory radon anomalies at great distances (of several tens or hundreds of kilometers) from the subsequent earthquakes, were first received with considerable scepticism, particularly in the USA. It was said that the half-life of a radon atom is too short (3.8 days) to allow it to move more than tens of meters from the site of production, even if active subsurface transport mechanisms are involved [71, 72].

Even for soil-air radon content, King [38, 39] showed that there were some anomalies which appeared to be systematically related to earthquake events above a threshold magnitude of about 4.0. This was considered to be possibly caused by radon escaping in fault zones in response to source strain changes.

In China, hydrogeochemical observations related to earthquake prediction research, such as the study of radon variation in groundwater, have been made since 1968. It is worthwhile to note that radon data played an important role in the successful prediction of the Liaotung Peninsula earthquake on February 4, 1975 with a magnitude of 7.3 [75]. A review of radon and other hydrochemical precursor studies in China can be found in [75].

Japanese scientists started the same sort of study in 1973 [50, 82] by using the liquid scintillation techniques developed by Noguchi in 1964.

Nowadays, physicists, hydrogeologists and seismologists are using networks of stations to record several possible precursors in groundwater and soil-gas in an attempt to predict earthquakes of a magnitude greater than 4 on the Richter scale. Nevertheless the current situation can be described with the words of Guy Rerrier (cited by P. Lanoy, 1989): "The number of earthquakes is so great" "that there is every chance" "that any kind of monitoring" "will lead to something".

## 2. MEASUREMENT TECHNIQUES USED

Judging by published literature the most widely used techniques to measure radon content in groundwater and soil-air may be subdivided into the following groups:

- Emanometry by means of ionization chambers and counters [12, 15, 23, 24–27, 29–34, 40]
- Liquid scintillation counting [27, 50]
- Zn(S) scintillation counting [12, 27, 29–32]
- Track Etch Method [22, 50, 38, 39]
- Trap (charcoal, glass) technology [42]

It seems clear that dynamical on-line emanometry measurements on the base of ionization and scintillation chambers, plus some variations of trap techniques [42], are preferable. The liquid scintillation counting can be realized in a discrete sampling regime as all kinds of trap techniques based on continuing counting. The Track Etch Method using cellulose films is very cheap and simple but can be rather applied in air soil measurements and in a discrete regime only. Evidently, the measurement technique choice depends on goals and objectives as well as field conditions.

The requirements for earthquake forecast based on radon measurement are [12, 15, 27, 29–32, 50]:

- Low-level radiation measurement techniques are required because radon concentrations in groundwater are of the order of  $10^{-10}$  Ci/l and variations of Rn activity in seismo-tectonic regions range in about plus/minus one order of magnitude of this value.
- There is a need for outgassing systems to extract the gas-fraction from natural waters. The outgassing device has to be as simple and robust as possible, and it should not be easily affected by corrosion and precipitation of calcium carbonates, organic and suspended particles.
- Therefore care must be taken in processing groundwater to measure radon in an on-line regime.
- Stability of the measuring system has to be provided, and the variations of meteorological conditions (temperature, pressure, air humidity and so on) should be monitored, to correct the observation data.
- The instruments should not require much maintenance and should be easy to operate because observation sites (wells, springs, captages) are usually located in isolated areas.
- The relaxation characteristics of the system must not effect the natural variation of components which are being measured.
- The monitoring system should be located in the more sensitive sites which can be selected from the existing information.
- The system has to provide a continuous or discrete-continuous regime of measurements with the required accuracy.

## 3. MAIN FEATURES OF THE OBSERVED RADON SIGNALS

The analysis of the published materials allows to formulate some general and specific features of radon and other hydrochemical precursors [1, 2, 5, 7, 12–15, 28, 33, 45, 50, 51, 57, 63, 64, 67–75, 82–84] (see also Fig. 1–12, 16).

- 1 The observed anomalies have a wide space distribution with respect to the epicentral zones, precursors can be observed in a distance of several tens to hundreds kilometers from the

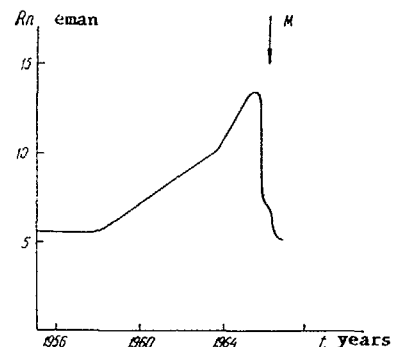


Fig. 1 Radon variations in Tashkent's groundwater  
(By Ulomov V.I. Mavashev B.Z., 1967 [78])

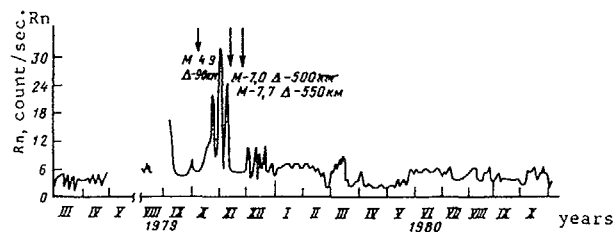


Fig. 2 Radon variations observed in thermomineral waters  
at the Ashkhabad station prior to the Kopet-Dag  
earthquakes of 1979-11-14 and 1979-11-27, Turkmenia  
(By Ataev S. et al., [30])

epicenter and at different depths from surface up to about 2 km. The anomalies have been observed before, during and after the main events. Nevertheless there might be no detectable anomalies prior to relatively strong earthquakes.

2. The anomalies occur in shallow and deep groundwaters, in springs and in soil air. Due to geological, structural and hydrochemical characteristics they may occur in cold groundwaters, in mineral and/or thermal waters, they may be found associated to faults, fissured and fractured zones, or be located in sedimentary aquifers.
3. A definite positive correlation exists between the earthquake strength (magnitude) and the
  - distance of the site where precursors appear
  - time of precursor appearance
  - amplitude of precursor signal
  - shape of precursor record

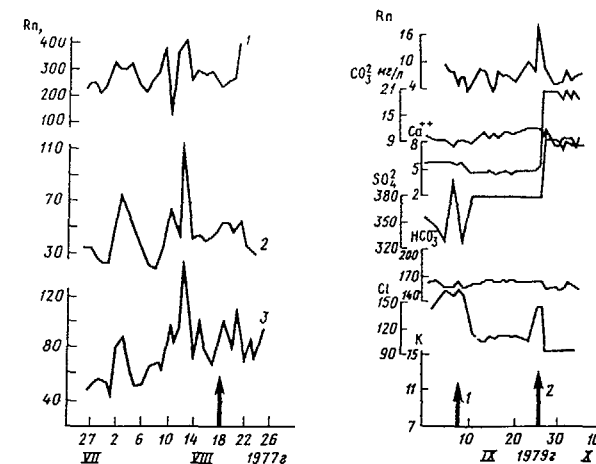


Fig. 3 Radon anomalies prior to the:  
(a) Tjup earthquake of 1977-08-18 ( $K=9.8$ ,  $L=73$  km) observed in the Djety-Oguz thermal waters, Kirgizia (wells)  
(b) Central Tan-Shan earthquake of 1979-09-07 ( $K=11.6$ ,  $L=200$  km)  
(c) Bakanass earthquake of 1979-09-25 ( $K=19.2$ ,  $L=220$  km) observed in the well Kurskaja at the shore of the Isyk-Kul lake  
(By Kalmurzajev K.L. et al. [30])

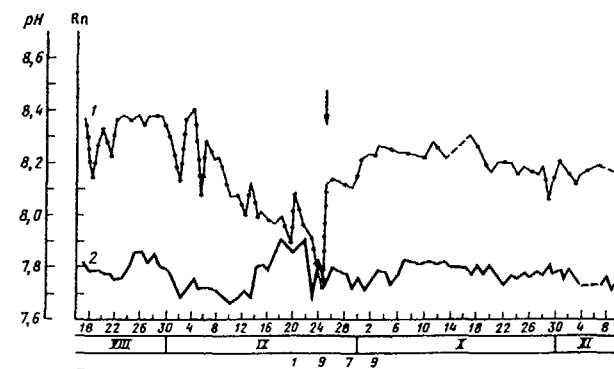


Fig. 4 Radon (2) and pH (1) variations prior to the Bakanass earthquake ( $M=6.1$ ), Kazakhstan  
(By Erzhanov Zh.S. et al. [30])

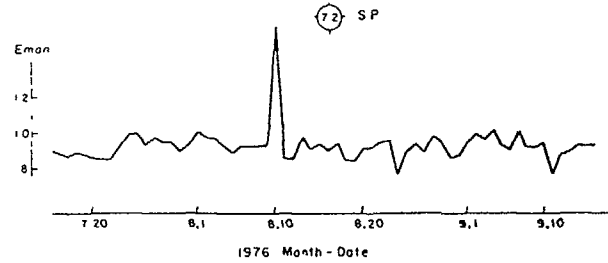


Fig 5 Spikelike groundwater radon anomaly observed at the Kutzan station 6 days before the  $M = 7.2$  Sungpan-Pingnu earthquake of 1976 (Fig. 5-11 are cited by Teng [74])

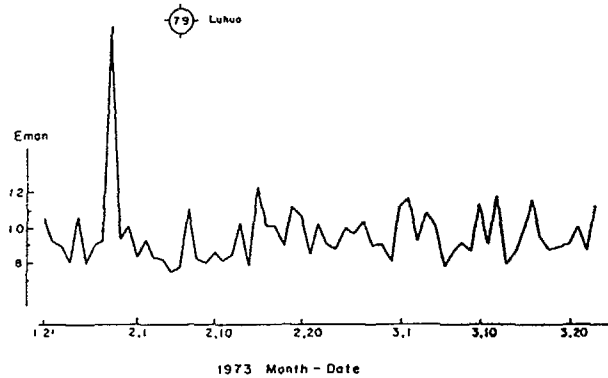


Fig. 6 Spikelike groundwater radon anomaly observed at the Kutzan station 8 days before the  $M = 7.9$  Luhuo earthquake of 1973.

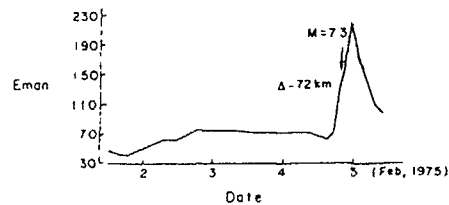


Fig 7 Spikelike groundwater anomaly before the 1973 Haicheng earthquake of  $M = 7.3$ , as observed at the Hotang hot spring site of Liaoyang, Liaoning province After *The Group of Hydro-Chemistry* [1977]

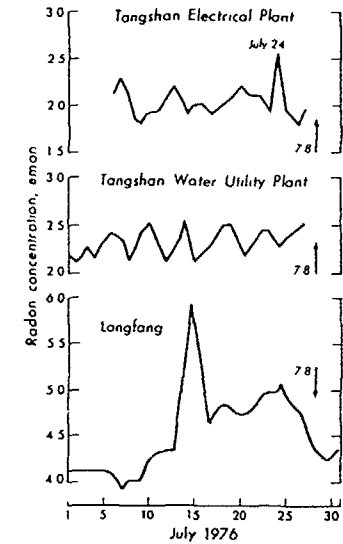


Fig 8 Groundwater radon anomalies observed at three stations before the 1976 Tangshan earthquake ( $M = 7.8$ ) Top two traces give data from sites in the epicentral region, bottom trace gives data from Langfang station, which is 130 km from the epicenter After Wang [1978]

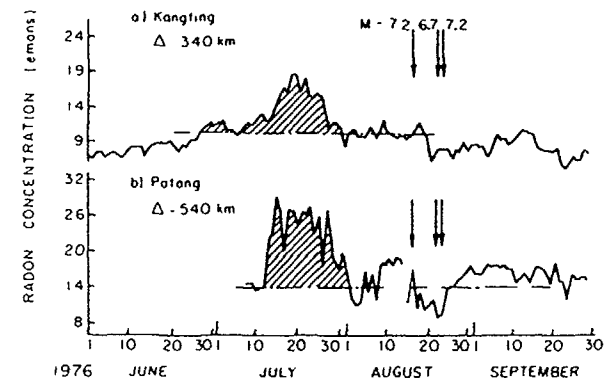


Fig 9 Groundwater radon anomalies observed before the Sunpan-Pingwu earthquake showing a much longer anomalous duration. After Wakua [1978] Cross-hatching indicates above average readings



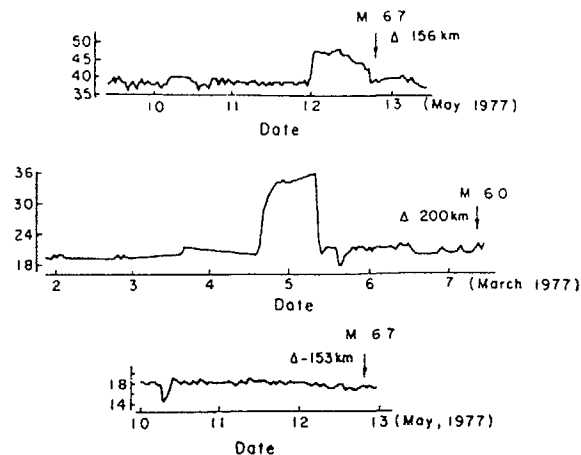


Fig 10 Groundwater radon anomalies observed at two locations in Peking by automatic groundwater radon monitoring systems (Top) Peking Shichiao well data before the Lutai event. (Middle) Peking Research well data before the Chien-an event (Bottom) Peking Research well data before the Lutai event. After *The Group of Hydro-Chemistry* [1977]

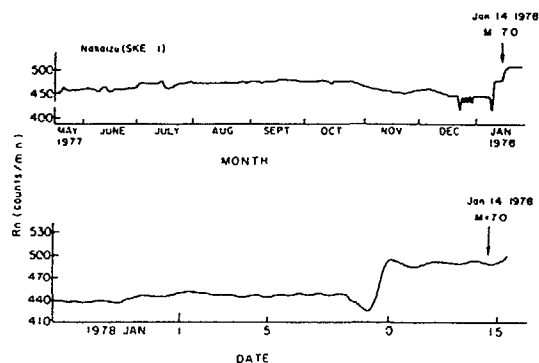


Fig 11 Groundwater radon anomaly observed before the 1978 Izu Peninsula earthquake ( $M = 7.0$ ) Bottom trace is an enlarged portion of part of the top trace (H Wakita, written communication, 1978)

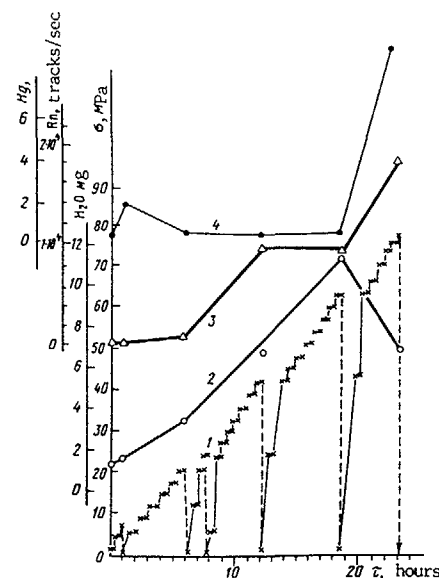


Fig. 12 An experimental discharge of water (2), radon (3) and Hg (4) as a function of strain value  $\sigma(t)$  MPa by compression of a basalt block (By Varshal G. M. et al., [30])

Generally, on the basis of observational data, one can state that the greater the magnitude of a seismic event,

- the greater is the distance where precursors can be recorded
- the earlier the precursor signals appear
- the larger is the signal amplitude

It is commonly thought that increasing radon concentrations indicate forthcoming seismo-tectonic events, but until now it has not been determined if there are any specific characteristics of radon output curves which could serve as an unequivocal indicator for the time of earthquake shocks

- 4 A wide variety of forms, durations and amplitudes of radon output curves have been recorded within the same regions and during similar events There might be (see also Fig 1-12, 16)
  - a single or several spike maximums
  - a monotonous increase in radon concentration with or without any steady state plateau before the main shock
  - a "wave"-type or faster chaotic fluctuations in radon contents without apparent regularities

The duration of precursor variations can be short (several hours) and long-term (several days, months and even years) The time before the shock can be of the same order as the background variation duration

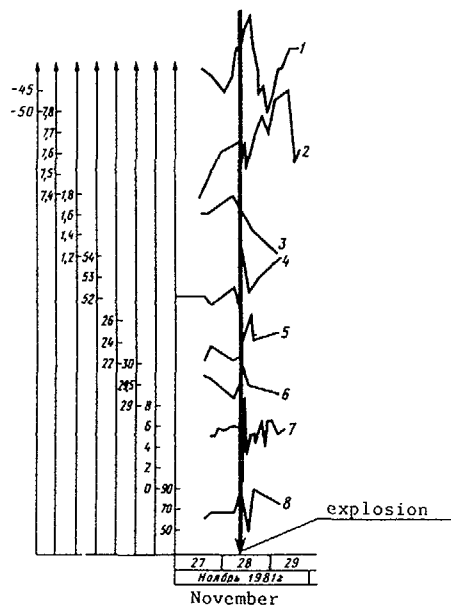


Fig. 13 Variations of hydrochemical parameters by the explosion:  
 1-Eh; 2-pH; 3- $\text{HCO}_3^-$ ; 4- $\text{SO}_4^{2-}$ ; 5- $\text{H}_2\text{SiO}_4$ ; 6- $\text{Cl}^-$ ; all in mg. eqv./l  
 7-He, ml/l  $\cdot 10^{-3}$ ; 8-Rn - eman.

5. Exhalations of radon in the soil-air and in groundwater only define the region where the strain is likely to exist and where changes may occur. This conclusion is supported by the fact that variations of radon concentrations have additionally been observed in strained rocky massifs and particularly in:
  - fault zones [12, 37, 39, 50, 59]
  - landslide massifs [26, 27, 56]
  - mines and quarries
  - experiments on compression and destruction of rock materials [30, 31, 34, 36, 47, 56]
  - rock massifs subjected to artificial explosions [30, 31]
  - volcanic areas [20].
6. Nevertheless, radon data collected in worldwide different tectonic regions show similar and consistent properties [28, 43, 57, 75].
7. Most of the observed radon anomalies occurred far away from the earthquake epicenter and model calculations indicate that strain fields of at most  $10^6$  to  $10^8$  strain were causing the anomalies. If these strains are divided by the appropriate precursor time, minimum strain rates from  $10^{-7}$  to  $10^{-10} \text{ day}^{-1}$  are obtained [28].

8. The observed radon anomalies are thought to be caused by small changes in the local stress intensity. Due to structural inhomogeneity of the geological bodies, there are several centers of stress concentration, where the internal free energy of particles (such as molecules of Rn, He, etc.) (see Fig. 14) can reach the potential barrier to be transferred from solid matrix into pore fluids [17-19, 76]. Generally speaking, such a strained state of the rocky massifs could be the main initial cause of geochemical precursors of earthquakes [26, 27, 29-33, 36, 47, 76].

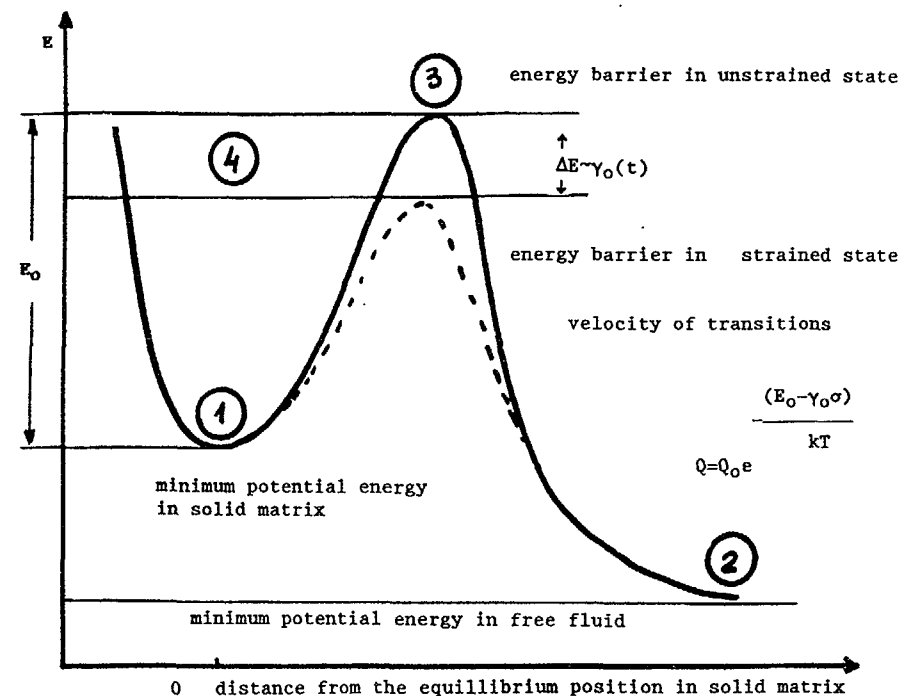


Fig. 14 Energy of particles in two-phase porous systems. Arbitrary particle can:  
 1 - be built into the mineral matrix structure and have a minimum potential energy occurring in a "potential pit";  
 2 - be a free one and located in the porous solution with new minimum energy less than for a solid matrix;  
 3 - appear to be at the top of the energy barrier where it may spontaneously return itself into the "potential pit" or transfer itself in the free state into the porous fluid;  
 4 - reach the energy to be equal or to prevail the potential barrier to transfer itself into a free porous fluid in strained condition; in unstrained condition such a particle is not able to overcome the energy barrier.

- 9 It has been noted that there is a wide spectrum of seismic background fluctuations of precursor content in the pore fluid which may deteriorate the record of useful signals. Investigations have shown that the background depends on local geological, hydrogeological and geochemical conditions and on local seismic background. But this appears to be suspicious, in the sense that the background has to be ruled by the same laws that are valid for the 'useful' precursor signals.
- 10 Once more this shows the importance of a good knowledge of the aseismic seismic hydrogeochemistry characteristics of hydrogeological systems selected for monitoring. The best are those which provide the maximum sensitivity to transform strain variations in geochemical signals. This means that any observation system must be tuned to the given site and precursor indicators. But so far there are no precise guidelines for this choice.
- 11 From the point of view of isotope hydrology, its scientific background and techniques [12, 21, 27, 29-34, and many others] provide a wide spectrum of possibilities to determine water and component turnover times in hydrogeochemical systems, which could play an important, perhaps even decisive, role. As is shown in [17-18 and many others], Mean Residence Times (MRT) of water and dissolved component may be the key parameters for a correct monitoring of hydrogeochemical precursor signals.
- 12 In fact significant anomalies have sometimes been observed not in the vicinity of some strong earthquake epicenters, but, on the contrary, where some weak seismic events were recorded. The author of this paper believes that there is no unique reason for this behaviour, but it seems that relaxation time characteristics of the hydrogeochemical systems are very important. However, till now the whole mechanism of the radon variation in groundwater, soil-air and gas exhalations, has not been fully understood nor satisfactorily described for processing and interpreting the observed anomalies in terms of space-time-strength prediction characteristics.

#### 4. ASSUMED MECHANISMS

A number of studies have been published in which an attempt has been made to explain radon and other hydrochemical precursor anomalies with theoretical models, which should enable to interpret and use the monitoring records for predicting earthquakes. Without pretending to give a complete overview, it is worthwhile to note the following hypotheses:

- rock dilatation and water diffusion [8, 16, 28, 43, 48],
- avalanche fissure forming [8, 16, 43],
- direct strain influence on emission of precursor component from solid into pore fluids [1, 5, 10, 12-15, 29-33, 62-64, 67-70, etc.],
- activation of convection-diffusion transport [10, 11-14, 45, 68-70, 73],
- ultra-sonic and/or a wider spectrum of wave extraction (shaking) [12, 26, 29-33, 37, 70, 73, 77],
- admixture of fluids from other (deeper) layers [2, 5, 10, 12, 33, 73, 77],
- changing of fissures and porosity [28, 30-33, 39, 43, 56, 59, etc.],
- mechanical deformations [30, 43, 77]

For a long time, studies on earthquake prediction were oriented towards the increase of observation networks and the establishment of new detectors, indicators, etc. The Californian earthquake (1989) showed that it is not sufficient to just make predictions. This earthquake occurred in an area where thousands of detectors were connected to a fully computerized tele-

metric system. Even so, this was not sufficient. This means that new and better concepts are needed more than additional new detectors [65].

Some specialists (Barsukov V.L., et al. [30, 31, 60]) now think that the idea of a modern nonlinear dynamics with its concepts of chaos and collective behavior of inhomogeneous structured media is the panacea long waited for. If this is so, one should revise all the interpretations recently made.

This approach may be connected with sinergetics [61] as well as with the theory of catastrophes which have been recently developed. In any case, new information is needed to fully understand the processes which are ruling hydrogeochemical (and other) precursors. Moreover, new ideas are required for the interpretation of recorded data.

#### 5. RADON PRECURSOR BEHAVIOR IN HYDROGEOCHEMICAL SYSTEMS (PERFECT MIXING MODEL)

Taking into account the relatively short life-time of radon (half life 3.8 days) and its origin as a radium decay product, one can conclude that radon anomalies observed in strain area are produced in the vicinity of observation sites. But, if radon is produced in the earthquake seats and then transported to surface and to far observation sites, it would require transport velocity and flow rate of fluids so high, that they would be impossible in groundwater [17]. This supports the occurrence of some unique initial mechanisms originated, as mentioned above, by the strain in the earthquake seats as well as at the distance from them.

Additional tectonic strain effects decrease the activation energy  $E_a$  of processes (see Fig 14) controlling the escape of chemical and isotopic components from the rock matrix into the pore solution. Those processes could be called dissolution, leaching, emanation, diffusion, formation and transport of defects in the mineral matrix lattice, etc. It is well known that dissolution rate is governed by the Arrhenius law, diffusion velocity by the Frenkel-Langmuir-Dashman-law, intensity of defect formation in solid bodies by the Schottky-law, as well as any other physico-chemical reactions by the Glasstone-Ehring law, are obeying an invariant function

$$Q(t) = Q_{oi}(t) e^{-E_0/kT} \quad (1)$$

$Q(t)$  is the variation of the component input into a solute phase from a mineral matrix,  $T$  is an absolute temperature in K,  $k$  is the Boltzmann constant,  $kT$  represents the average kinetic energy of a given particle (Rn molecule in our case) at the absolute temperature  $T$ ,  $Q_{oi}$  is a constant for the given particle in a given system,

If there is a strain  $\sigma(t)$ , then the activation energy (potential barrier) will change into [17, 55]

$$E_a = E_0 - \gamma_0 \sigma(t) \quad (2)$$

$E_0$  represents the mean activation energy needed to transfer a particle from the matrix into the pore solution in the unstrained state, and  $\gamma_0$  is a coefficient.

This fact is thoroughly proved in the thermo-kinetic theory of bodies [55]. Thus, the input flow rate in the stressed state may be recognized as a function of the internal mechanical strain developed in the body

$$Q_s = Q_{oi} e^{-(E_0 - \gamma_0 \sigma(t))/kT} = Q_{oi} e^{\gamma_0 \sigma(t)/kT} \quad (3)$$

where

$$Q_o(t) = Q_{oi}(t)e^{-E_d/kT} \quad (4)$$

The physico-geochemical meaning of eqs. (1)-(4) is very simple. The transition velocity of a particle from a solid matrix into a pore solution (more generally, a fluid) depends exponentially on the ratio of the activation energy of the given transition process to the mean kinetic energy  $kT$  of the given particle at temperature  $T$  K. The parameters  $Q_{oi}$  or  $Q_o$  and  $E_o$  characterize the process in unstrained condition ( $\sigma(t) = 0$ ).  $\gamma_o$  is an energetico-structural parameter of the solid matrix, having the dimension of a volume  $[L^3]$ .

The molecular-kinetic theory has shown that  $\gamma_o$  is proportional to a characteristic volume (in average occupied by the particle of given structural positions) and to a local overstrain of interparticle connections [55]. The parameter  $\gamma_o$  strongly depends on the structural scale effects, whereas  $Q_o$  and  $E_o$  do not depend on structural effects.  $E_o$  characterizes an activation energy of destruction of interparticle connections in the solid matrix. This means that the activation energy for any component built in a mineral lattice must have the same order of magnitude of sublimation energy, dissolution or self-diffusion processes [55].

This means that activation energy  $E_o$  must be of an order of:

- 50-200 kcal/mole for the escaping of particles from crystal lattices due to melting, solution, sublimation and diffusion;
- 20-200 kcal/mole for formation and migration of defects in crystal lattice as well as for migration of any particles with defects through the solid body;
- 2-5 kcal/mole for destruction of Van-der-Waals bonds between molecules;
- 2-10 kcal/mole for sorption-desorption at the contact surface between matrix and pore fluid.

In [27] we have already tried to evaluate activation energies of radon emanation in minerals using published data on temperature dependency of emanation velocity. They appear in the order of 8-13 kcal/mole (for uranium ores), that is two to three times higher than the binding energy in liquids and adsorbed layers, but 5-10 times less than the particle contact energy in solid lattices. This data is completely relevant to the energy of defect formation and defect migration in solid bodies. These facts also support activation energies of diffusion of He, Ne, Ar, Kr, Xe in the solid mineral phase (see references in [27]).

Despite all apparent discrepancies between such a variety of processes as emanation, diffusion, sorption-desorption, solution-precipitation, defect formation-migration, their kinetics is similar and depend on some parameters like  $Q_o$ ,  $\gamma_o$ ,  $E_o$  and  $E_a$ .

In order to obtain a more concrete result we can use the solution of our earlier publication [27] to describe the radon behavior in a stationary hydrological system with perfect mixing regime of water and its constituents. Additionally it is assumed that:

- the initial concentration of radon in pore fluid is zero, e.g.,  $C_o = C(t=0)$ ;
- the input of radon caused by strain variations is described by eq (3);
- the exponent in eq. (3) may be substituted by its Taylor's series development in the first approximation as

$$Q(t) = Q_{oi}(t) \left( 1 + \frac{\gamma_o(t)}{kT} + \dots \right) = Q_{oi}(t) + \gamma_o(t) + \dots \quad (5)$$

where

$$\gamma = Q_o \gamma_o / kT \quad (6)$$

This  $\gamma$ -value may be considered, in the framework of the model, as a generalized conversion coefficient of radon transfer from the solid matrix into the pore fluid.

Using such an approximation of the previously obtained solution for stationary hydrological perfect mixing models [17-19], the following expression for time variations of the hydrochemical precursor can be established:

$$C(t) = C_o e^{-\lambda t} + \int_0^t \lambda_w e^{-\lambda \Theta} C_i(t - \Theta) d\Theta + \frac{Q_o}{\Lambda} (1 - e^{-\lambda t}) + \int_0^t \lambda_w e^{-\lambda \Theta} \gamma_o(t - \Theta) d\Theta \quad (7)$$

It appears that  $t$  relates to the observation time moment, but  $\Theta$  is an integrating time variable in the interval  $(0, t)$ . The difference  $(t - \Theta)$  gives a time  $\Theta$  in days (months, years, etc.) before the observation time  $t$ .

It should be noticed that  $\lambda_w = q/V$  is a hydraulic kinetic parameter of the given hydrogeological system:  $q$  is a recharge-discharge volumetric flow rate and  $V$  the storage volume of water in the system; the inverse value of  $\lambda_w$  is  $\tau_w = \lambda_w^{-1} = V/q$  is the mean residence (turnover) time of water carrying radon or other components. If a precursor component is conservative and stable, then and only then is its residence time equal to that of water. A characterizes all possible processes obeying the first order kinetics by which components are lost because they are non-conservative and/or unstable. For example, for radon one should take into account:

- radioactive decay with the constant  $\lambda_a$ ;
- irreversible losses by any physico-chemical processes like sorption, precipitation, etc., with the constant  $\lambda_p$  and by the hydraulic discharge with constant  $\lambda_w$ .

Thus,

$$\Lambda = \lambda_w + \lambda_a + \lambda_p \dots \quad (8)$$

By introducing the residence time characteristic of each process, eq. (8) becomes:

$$\tau = (\tau_w^{-1} + \tau_a^{-1} + \tau_p^{-1} \dots)^{-1} \quad (9)$$

Now it is possible to transform eq. (7) from the " $\lambda$ -form" into the " $\tau$ -form":

$$C(t) = C_o e^{-t/\tau} + \int_0^t \tau_w^{-1} e^{-\Theta/\tau} C_i(t - \Theta) d\Theta + Q_o \tau (1 - e^{-t/\tau}) + \int_0^t \tau_w^{-1} e^{-\Theta/\tau} \gamma_o(t - \Theta) d\Theta \quad (10)$$

Let us return now to the physico-hydrogeochemical meaning of the solution expressed by eqs. (7) and (10).

The first exponential term on the right side of eqs (7), (10) describes the influence of the initial content. The second integral term characterizes the action of a hydraulic recharge with the input component concentration  $C_i(t)$ . The third term gives the injection of the precursor component caused by the normal strain state, i.e. by  $\sigma(t) = 0$ ,  $C_i(t) = 0$  and  $C_o = 0$ . The last integral term determines the required seismo-hydrogeochemical signal as a reaction of the system to the strain variation  $\sigma(t)$  in the bulk rock.

## 6. SOME USEFUL CONSEQUENCES

In spite of the relative simplicity of the model we reach some very important conclusions, especially from the isotope hydrological and geo-seismological points of view

1 A hydrogeochemical reaction of any system on strain stresses can be presented as a convolution operation or sum of time strain variations. These are converted into a component input from the matrix into porous fluid by means of a weighting function such as the Green's function for the given system and components

$$G(t) = \lambda_w e^{-\Lambda t} = \tau_w e^{-t/\tau} \quad (11)$$

It is well known in system analysis that this function is closely connected with the Residence Time Distribution Function (RTDFw) of water [17]

$$\Phi_w(t) = \lambda_w e^{-\lambda_w t} = \tau_w^{-1} e^{-t/\tau_w} \quad (12)$$

and with the RTDFc of a given precursor component (Rn, for example)

$$\Phi_c(t) = \Lambda e^{-\Lambda t} = \tau^{-1} e^{-t/\tau} \quad (13)$$

These functions are interconnected with each other by the following one-to-one relationship

$$G(t) = \lambda_w e^{-\Lambda t} = (\lambda_w/\Lambda) \Lambda e^{-\Lambda t} = (\lambda_w/\Lambda) \Phi_c(t) = \Phi_w(t) e^{-(\Lambda - \lambda_w)t} \quad (14)$$

The functions  $G$ ,  $\Phi_c$ , and  $\Phi_w$  express all the main properties (including relaxation) of water as a carrier and precursor components

It is clear that the kinetic parameters  $\Lambda$ ,  $\lambda_w$ ,  $\lambda_a$ ,  $\lambda_p$  and the time constants  $\tau$ ,  $\tau_w$ ,  $\tau_a$ ,  $\tau_p$  represent the mass turnover and relaxation characteristics of precursors and system

2 It is not difficult to prove that  $\Phi_w(t)$  and  $\Phi_c(t)$  are normalized to unit and have all properties needed for a statistical distribution. The first t-moments of  $\Phi_w$  and  $\Phi_c$  are  $\tau_w$  and  $\tau$ , respectively, which support  $\tau_w$  and  $\tau$  as the mean residence time of water and components in the system

3 With a long period observation ( $t \gg \tau = \Lambda^{-1}$ ) any system "forgets" the initial conditions and, in addition, any "background" term is relaxed to the level of  $Q_0/\Lambda$ , which reflects a steady "background" state. The  $Q_0/\Lambda$  value can be used to determine  $\Lambda$  or  $Q_0$  (or  $Q_{oi}$  and  $\lambda_0$ ) using the background observation data

4 "Pure" current hydrochemical signals caused only by additional strain  $\sigma(t)$  can be presented as

$$\begin{aligned} \Delta C(t) &= C(t) - Q_0/\Lambda = \int_0^t \lambda_w e^{-\lambda_w(t-\Theta)} \gamma_0(t-\Theta) d\Theta = \int_0^t (\lambda_w/\Lambda) \Lambda e^{-\lambda_w(t-\Theta)} \gamma_0(t-\Theta) d\Theta = \\ &= \int_0^t (\lambda_w/\Lambda) \Phi_c(\Theta) \gamma_0(t-\Theta) d\Theta = \int_0^t \Phi_w(\Theta) e^{-\lambda_a + \lambda_p + \lambda_w} \gamma_0(t-\Theta) d\Theta \end{aligned} \quad (15)$$

5 The maximum signal depends on maximal values of the conversion coefficient  $\gamma$  and the ratio  $\lambda_w/\Lambda = \tau/\tau_w$

It is clear that with any other constant conditions a maximal value of the parameter  $\lambda_w/\Lambda$  is 1, which can be reached when  $\Lambda \rightarrow \lambda_w$ , or  $\lambda_a$  and  $\lambda_p \rightarrow 0$ , e.g. when the precursor component is stable ( $\lambda_a = 0$ ) and conservative ( $\lambda_p = 0$ ) like He, for instance. For radon as a noble gas, the condition  $\lambda_p = 0$  can be adopted, but  $\lambda_a \neq 0$ . This means that the maximum value of a radon signal is proportional to

$$\frac{\lambda_w}{\Lambda} = \frac{\lambda_w}{\lambda_w + \lambda_a} = \frac{\tau_a}{\tau_w + \tau_a} \quad (16)$$

6 If the mean residence time of water  $\tau_w \gg \tau_a$  ( $\tau_w \gg 40$  days, practically), then  $\lambda_w/\Lambda \sim \tau_a/\tau_w \ll 1$  and the expected signals will be rather small. On the contrary, if  $\tau_w \ll \tau_a$  and  $\lambda_w/\Lambda \sim 1$ , then the signal will be maximal. It is therefore preferable to select the system which has  $\tau_w \ll \tau_a$  as monitoring site

7 There is yet another cause which decreases the possible useful hydrochemical signals. This means that there is an interrelation between the duration of the strain impact  $\sigma(t)$  and the mean residence time  $\tau$  of the precursor component. Supposing that a strain variation is an impulse one obtains

$$\sigma(t) = 0, \quad t \leq 0 \quad (17-1)$$

$$\sigma(t) = \sigma_0, \quad 0 < t < t_s \quad (17-2)$$

$$\sigma(t) = 0, \quad t \geq t_s \quad (17-3)$$

Substituting the above equations in eq (15), one obtains the following output concentrations of the precursor

$$\Delta C(t) = 0, \quad t \leq 0 \quad (18-1)$$

$$\Delta C(t) = \Delta C_{\max} (1 - e^{-\Lambda t}), \quad 0 < t < t_s \quad (18-2)$$

$$\Delta C(t) = \Delta C_{\max} \left( 1 - e^{-\Lambda t_s} \right) e^{-\Lambda(t-t_s)}, \quad t \geq t_s \quad (18-3)$$

$$\Delta C_{\max} = \lambda_w \gamma \sigma_0 / \Lambda = \tau \gamma \sigma_0 / \tau_w \quad (19)$$

is the *maximum maximorum* value of the signal. One can see that due to the proper relaxation characteristic  $\Lambda$  (or  $\tau$ ), the maximum value of  $\Delta C(t)$  by the given duration of the strain impacts  $t_s$  is

$$\Delta C(t) = (\lambda_w \gamma \sigma_0 / \Lambda) (1 - e^{-\Lambda t_s}) = (\tau \gamma \sigma_0 / \tau_w) (1 - e^{-t_s/\tau}) \quad (20)$$

The smaller the ratio  $t_s/\tau$ , the lesser is the signal achieved, and when  $t_s \gg 3\tau$  a maximum signal is reached. If one wants to record a precursor signal as early as possible and at its maximum level, the following condition has to be satisfied  $t_s \sim 3\tau$ . In order to get a good hydrogeochemical precursor signal a system with the relevant time characteristics must be monitored, as already emphasized above. This is the reason for tuning the observed system in order to get a good signal/background ratio

8 The form of the hydrogeochemical signals must strongly depend on the relevant RTDFw and RTDFc (see Fig. 15) and on the parameters which can be determined using isotope tracer techniques developed in isotope hydrology. For instance, the RTDFw of water ( $\phi_w$ ) is determined by isotopes such as tritium,  $^{18}\text{O}$  and deuterium. To estimate  $\phi_w$  and its parameter  $\tau_w$  (or  $\lambda_w$ ), some artificial tracers could also be used.

9 Such parameters as  $Q_o$  and  $\gamma$  (or  $Q_o$  and  $\gamma_0$ ) can be evaluated by using the hydrogeochemical data obtained during aseismic periods or by interpreting hydrochemical reactions of the system on sinusoidal tidal variations of strains.

10 The experimental work should concentrate on finding out the activation energy  $E_a$  of the transfer of possible precursor components (Rn, He, Ar, Kr, Xe,  $\text{CH}_4$ , etc.) from solid matrix into pore fluids. That is why it is so important to arrange the experiments in such a way that a temperature dependency of the transfer rate would be obtained.

11 Finally, the results given here for perfect mixing models can be generalized for any linear system. A reaction of a hydrochemical system under strain impact is approximately proportional to the convolution integral of the given strain space-time variation and to the residence time distribution functions of precursor components in the system.

## 7. CONCLUSION

There is a great need for

- elaborating adequate descriptive and predictive models of formation and transformation of hydrogeochemical precursor signals,
- working out algorithms to extract useful information from field data,
- evaluating proper conversion and relaxation characteristics of the monitored systems in order to predict earthquakes,
- widening isotope hydrology techniques to measure residence time parameters of the precursor components,
- generalizing and analysing typical precursor data in order to understand the mechanism of their formation,
- studying and measuring all the parameters needed (transport and dispersion characteristics, retardation factors due to sorption-desorption, emanation and/or leaching velocity and so on),
- selecting the criteria for the best sensitivity of hydrochemical (and other) precursors to the earthquakes and optimizing observation networks.

Once more, it should be emphasized that a solution of the problem of hydrogeochemical earthquake precursors demands consolidated and combined efforts and developments of a wide range of specialists in isotope hydrology, seismology, hydrogeology, geochemistry, physicochemistry, mechanics, mathematics, system analysis and so on. All these specialists should be gathered together within the framework of an international programme.

## 8. AN EPILOGUE

The present paper was almost ready for publication when two events occurred. In California another strong earthquake occurred and in the Soviet Union a new issue of the magazine 'Nauka i Zhizn' (Science and Life) [65-80] published a wide analysis of all aspects of the catastrophic

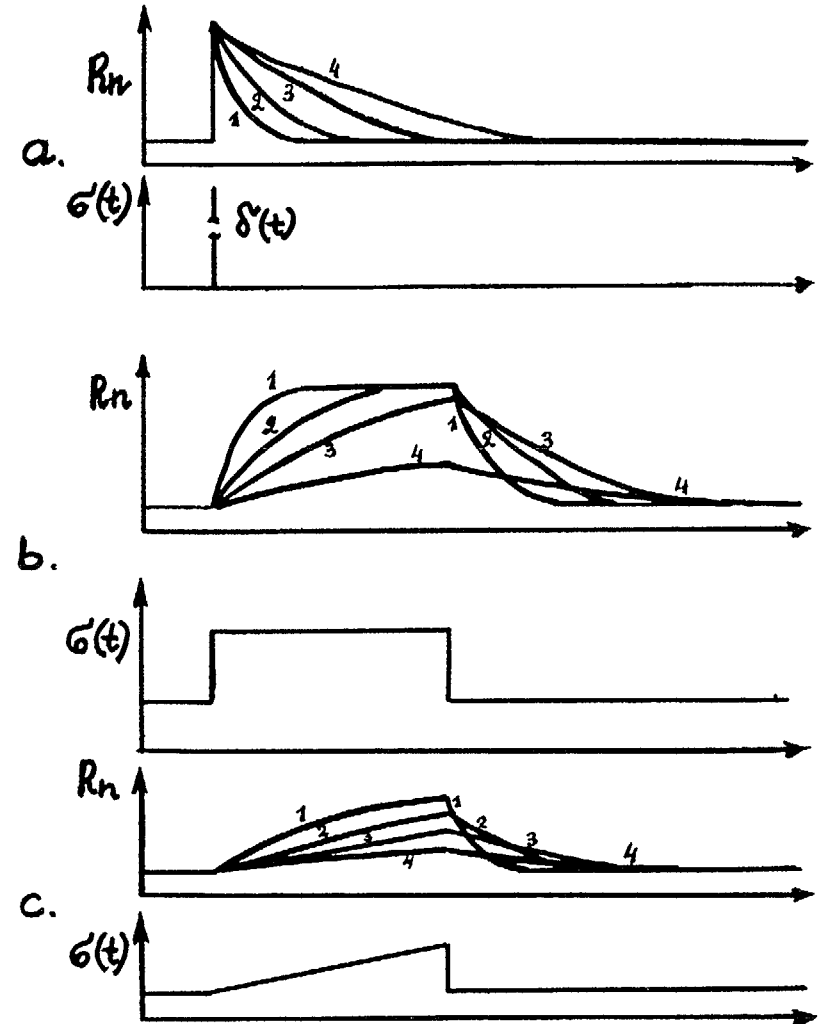


Fig. 15 Typical variation of radon and other hydrochemical precursor's concentrations in hydrogeological systems with a perfect mixing regime. Reactions on:  
a -  $\delta$ -stress  
b - constant impulse stress  
c - linear increasing strain stress  
The curves are related to different mean residence times  $\tau$  of the component in porous fluid:  
 $\tau_1 \leq \tau_2 \leq \tau_3 \leq \tau_4$

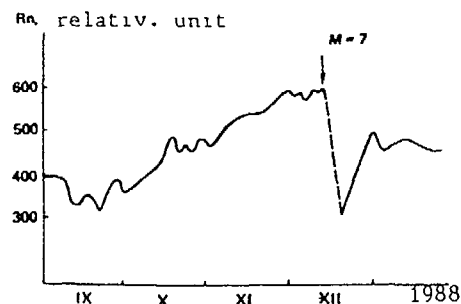


Fig 16 Rn concentration variation in subsoil atmosphere prior to and after the Spitak earthquake, Armenia, 1988

Spitak earthquake in Armenia on December 7, 1988 This enables us to add some data to those already shown

In Fig 16, a variation of the radon concentration in the subsoil atmosphere is given which was recorded before and after the main shock in Leninakan (Armenia), but analysed only after the earthquake It seems very likely that the earthquake could have been forecast on grounds of the radon anomalies which were easily detectable and which were similar to other strong earthquake forerunners like the Tashkent one There was a remarkable increase of subsoil radon which started to increase 3 months before the earthquake

The last measurement before the main shock was taken on the early morning of December 7, 1988 and after that, measurements were taken again on December 15, 1988 In the middle of November the radon concentration stabilized to a level of 30% above the background this was an almost definitive signal of warning of a forthcoming earthquake The radon signals were accompanied by groundwater level variations According to the data of G Vartanian from VSEGINGEO, Moscow, detectable variations of regional groundwater level distributions were observed which reflected the strain state of the region before the shock Unfortunately, these data were not known and interpreted in time, but only *a posteriori*

The Californian information from [66] clearly demonstrates that it is not sufficient to have hundreds of different monitors which are connected with computerized systems for the on-line processing of observed data it is also necessary to have good conceptual models and algorithms for interpreting precursor records, and drawing correct conclusions with respect to time, place and strength of an earthquake

From this point of view the author believes that without using the latest developments in isotope hydrology in order to evaluate proper relaxation parameters of the system it will not be possible to make a decisive step towards a reliable application of hydrogeological and hydro geochemical earthquake precursors

## REFERENCES

1. Abdullajev A.U., Medjitozova Z.A., Kriger L.P., Nurgazijeva V.V , Consequences of the appearing of precursors before the strong earthquake in northern Tian-Shan (in Russian), Fizika Zemli, 1988, N7, p.23-32
2. Abduvalijev A.K., Voitov G.I., Rudakov V.P., Radon precursor before some strong earthquakes in Central Asia (in Russian), Doklady Akademii Nauk SSSR, 1986, 291, N4, p.924-927
3. Andrews J.N., Radiogenic and inert gases in groundwaters, paper presented at 2nd International Symposium on Water-Rock Interaction, Strasbourg, France, Univ. Louis Pasteur, Centre Nat. Recherche Sci., Inst. Geol., Aug. 17-25, 1977
4. Antsilevich M.G., An attempt to forecast the moment of origin of recent tremors of the Tashkent earthquake through observations of the variation of radon (in Russian), Akad. Nauk. Uzb. SSR, 1971, p.188-200
5. Asimov M.S., Yerzhanov Z.S., Kalmurzaev K.Y., Kurbanov M.K., Mavlyanov G.A., Negmatullaev S.K., Nersesov I.L., Ulomov V.I., The state of earthquake prediction research in the Soviet Republics of Central Asia (in Russian), International Symposium on Earthquake Prediction, Rep. III-12, UNESCO, Paris, 1979, p.20
6. Basentsian M.M., Kuchmin O.A., Rudakov V.P., Some features of dynamics of subsoil radon fields in the condition of an Armenian prognostic poligone. Izvestija Akademii Nauk Arm. SSR, Nauki o Zemle XLI, N1, 1988, p.65-67
7. Birchard G.F., Libby W.F., Soil radon concentration changes preceding and following four magnitude 4.2-4.7 earthquakes on the San Jacinto fault in southern California, J. Geophys. Res., 85, 1980, p.3100
8. Brace V.F., Miachkin V.I., Dietrich G.H., Sobolev G.A., Two models to explain earthquake precursors. Collection of Soviet-American works on earthquake prediction, Dushanbe-Moscow, 1976, p.9-21
9. Brandes K., Earthquake prediction - interdisciplinary co-operation at Berlin on earthquake protection. Amts.-Mitteilungsbl. Bundesanst. Materialpruef. 1988, v.18(4), p.623-628
10. Bulashevich Y.P., Chalov P.I., Tuzova T.B., et al., Helium contents and relations between the uranium seria isotopes in waters on fault zones in northern Kirgizia (in Russian). Fizika Zemli, 1976, N1, p.78-84
11. Chalov P.I., Komissarov V.V., Vasiljev I.A., Radon migration during determination in the aquifer-well-system by accumulation of its decay products (in Russian). Geokhimiya, 1986, N7, p.1049-1052
12. Chalov P I., Tuzova T.V., Al'okhina V.M., Isotope parameters in groundwaters of the earth crust faults. 1980, Ilim, Frunze, p.104
13. Chalov P.I., Tuzova T.V., Al'ochina V.M., Short-time variations of radio isotope parameters of fault water in the earth crust (in Russian). Fizika Zemli, 1977, N8, p.62-71

14. Chalov P.I., Tuzova T.V., Al'ochina V.M., About earthquake forecasting by variation of radioactive parameters of fault waters in the earth crust (in Russian). *Fizika Zemli*, 1977, N8, p.56-58
15. Development of seismoprognostic studies at the Ukraine (in Russian). Kiev, "Naukova dumka", 1984
16. Dobrovolskij I.P., Zubkov S.I., Miachkin V.I., About the evaluation of the size of precursor appearance zones of earthquakes (in Russian). In: *Earthquake precursor modelling*, 1980, Moscow, "Nauka", p.7-44
17. Dubinchuk V.T., Analysis of using possibilities for Hydrochemical precursors of earthquakes (in Russian). *Water Resource*, 1983, No.5, p.130-136
18. Dubinchuk V.T., Kinetics and evolving some components from the rock matrix into the underground water by the action of mechanical forces (in Russian). In: *Hydrogeochemical precursors of earthquakes*. Moscow, "Nauka", 1984, p.31-34
19. Dubinchuk V.T., Theoretical basis of hydrochemical precursors by strained state of rocks. In: *Methods and organization of observation for earthquakes prognosis* (in Russian). Moscow, VSEGINGEO, 1983, p.57-60
20. Earthquakes and volcanos give chemical signals. "Chem. and Eng. News", 1979, 57, N16, p.20-22
21. Ferronsky V.I., Polyakov V.A., Environmental isotopes in the hydrosphere. Transl. from Russian, John Wiley and Son Ltd., Chichester, 1982, p.466
22. Flerov G.N., et al., Use of radon as a detector of volcanic processes (in Russian). 1985, Joint Institute for Nuclear Research, Dubna, USSR, p.7
23. Friedmann H., Hernegger F., A method for continuous measurement of radon in springwater for the earthquake prediction. *Geophys. Res. Lett.*, 1978, N7, p.565-568
24. Fukui M., Continious monitoring of  $^{222}\text{Rn}$  concentration in unconfined groundwater. *Journ. Hydr.*, 1985, 82, p.371-380
25. Ghosh P.G., et al., A method of radon monitoring in bore well waters for earthquake prediction. A case study at Pyntheromukzah. Shillong, India. *Indian J. Earth Sci.*, 1987, v.14(1), p.53-63
26. Gorbushina L.V., Riaboshtan M.S., Emanation techniques of geodynamic processes, indication by engineering geology surveying (in Russian). *Sovetskaya geologia*, 1975, N4, p.106-112
27. Gudzenko V.V., Dubinchuk V.T., Radium isotopes and radon in natural waters (in Russian). Moscow, "Nauka", 1987, p.160, Monography
28. Hauksson E., Goddard J., Radon earthquake precursor studies in Iceland, *J. Geophys. Res.*, 86, 1981, p.7037-7054
29. Hydrogeochemical and hydrodynamical studies at the prognostic poligones of Kirgizia (in Russian). Frunze, "Ilim", 1988
30. Hydrogeochemical precursors of earthquakes (in Russian). 1985, Moscow, "Nauka", p.286
31. Hydrogeochemistry studies at prognostic poligones. Alma-Ata, "Nauka", 1983, p.112
32. Hydrogeoseismological studies in eastern Fergana, 1978, Tashkent, "Fan", p.189
33. Isotopes in hydrology (in Russian). 1977, Tashkent, Fan, p.292
34. Isotope in hydrosphere (in Russian). Abstracts of the 3rd All-Union Symposium (29 May - 1 June, 1989, Kaunas), p.336
35. Jiang F., Li G., The application of geochemical methods in earthquake prediction in China, report, W.K. Kellogg Radiat. Lab., Calif. Inst. of Technol., Pasadena, 1980
36. Kabo V.A., Musin Y.A., Idrisova S., Some features of radon escape into water at long term uniaxial compression of rocks (in Russian). *Izvestia Akad. Nauk SSR, Fiz Zemli*, 1989, 7, p.103-106
37. Keilhak K., Groundwaters (in Russian). Transl. from German, Leningrad - Moscow, ONTI NKTP USSR, 1935, p.494
38. King C.Y., Episodoic radon changes in subsurface soil gas along active faults and possible relation to earthquakes, *J. Geophys. Res.*, 85, 1980, p.3065
39. King. C.Y., Geochemical measurements pertinent to earthquake prediction. *Journ. Geoph. Res.*, 1980, 85, NB6, p.3051
40. Komissarov V.V., Chalov P.I., On utilization of the water-gas system to seismoprediction goals (in Russian). *Geokhimiya*, 1987, 6, p.904-997
41. Materials of the IX Republic Scientific Conference of young scientists (in Russian). Frunze, "Ilim", 1988
42. Melvin J.D., Shapiro M.H., Copping N.A., An automated radon-thoron monitor for earthquake prediction research, *Nucl. Instrum. Methods*, 1978, p.153, 239
43. Miachkin V.I., Preparing processes of earthquakes (in Russian). M., Nauka, 1978, p.232
44. Milkis M.P., Hydrogeological and hydrometeorological precursors of the catastrophical earthquake in Ashkhabad. *Doklady Akademii Nauk SSSR*, 1983, 273, 5, p.1091-1094
45. Modern geodynamics and earthquake forcast (in Russian). 1987, Kiev



46. Mogro-Campero A., Fleischer R.L., Likes R.S., Changes in subsurface radon concentrations associated with earthquakes, *J. Geophys. Res.*, 85, 1980, p.3053
47. Musin J.A., Kabo V.A., Idrisova G., Analysis of a model of radon enrichment in groundwaters (in Russian). *Izvestia Akademii Nauk, Kirg. SSR*, 1986, 2, p.14-16
48. Nikolajevskij V.H., Dilatation and earthquake seat theory (in Russian). *Uspekhi mechaniki*, 1980, 3, N1, p.71-100
49. Nivin V.A., On possible gas-geochemical and gas-dynamical criteria for estimation of the tectonophysical state of local sections in igneous rocks. *Doklady Akademii Nauk SSSR*, 1989, 308, N6, p.1453-1458
50. Noguchi M., Wakita H., A method for continuous measurement of radon in groundwater for earthquake prediction. *Journ. Geop. Res.*, 1977, v.82, No.8, p.1353-1357
51. Observation techniques and organizations of groundwater regime on earthquakes forecast (in Russian). *VSEGINGEO*, Moscow, 1983, p.75
52. Ogilvi A.N., On captage of radioactive waters and variations of their radioactivity in dependence of debit (in Russian). *Trudy Gosbalneologicheskogo Instituta, Piatigorsk*, 1928, 6, p.85-93
53. Ossyka D.G., et al., Hydrochemical anomalies, fore-run tectonics earthquakes as a reflexion of earthquake seats (in Russian). *Doklady Akademii Nauk*, 1977, 233, N1, p.74-77
54. Radon detection and measurement. January 1970 - September 1988 (citation from compendix data base). National Technical Information Service, Springfield, 1988, p.135
55. Regel V.R., Slutsker A.I., Tomashevsky E.E, Kinetical nature of wreck of solid bodies (in Russian). Moscow, "Nauka", 1974, p.560
56. Riaboshan Y.S., Sultankhodjaev A.N., et al., On the behavior of radon in zones with dynamic strain (in Russian). *Doklady Akademii Nauk, Yzb. SSR*, 1978, N6, p.51-53
57. Rikitake T., Classification of earthquake precursors. "Tectonophysics" 1979, 54, N3-4, p.293-309
58. Rikitake T., Earthquake prediction. N.Y. Elsevier, 1976, XVI, p.375
59. Rudakov V.P., On subsoil radon concentration variation in seismoactive fault depositions (in Russian). *Geologia i razvedka, M.*, 1979, 18 Dep. in VINITI
60. Scholz C.H., Sykes L.R., Aggarwal Y.P., Earthquake prediction: A physical basis, *Science*, 181, 1973, p.803-810
61. Seidov D.G., Sincergetics of geophysical processes (in Russian). "Priroda", 1989, N9, p.25-34
62. Seismoprostnistical studies on the territory of the Ukrain SSR, 1988, Kiev, "Naukova Dumka"
63. Shapiro M.H., Melvin J.D., Tombrello T.A., Mendenhall M.H., Larson P.B., Whitcomb J.H., Relationship of the 1979 southern California radon anomaly to a possible regional strain event, *J. Geophys. Res.*, 86, 1981, p.1725-1730
64. Shapiro M.H., Melvin J.D., Tombrello T.A., Whitcomb J.H., Automated radon mintoring at a hard-rock site in the southern California transverse ranges, *J. Geophys. Res.*, 85, 1980, p.3058-3064
65. Shebalin N.V., About the Spitak earthquake of 7 December 1988 (in Russian). *Nauka i Zhizn* 1989, N4, p.16-20
66. Smirnov K., For applausing it is still too early. Soviet-American studies provide the predicting of San Francisco's earthquake (in Russian). *Pravda*, 1989, 2 November, N, p.307
67. Sultankhodjaev A.N., Chernov I.G., Zakirov T., Hydrogeoseismic precursors to the Gazli earthquake (in Russian). *Izv. Akad. Nauk. Uzb. SSR*, 7, 1976, p.51-53
68. Sultankhodjaev A.N., Hydrogeoseismological precursors of earthquakes. 27th International Geological Congress, Moscow, 4-14 August 1984, v.5, sect.10-1, M., 1984, p.409-411
69. Sultankhodjaev A.N., Khusamiddinov. Short term precursors of the catastrophical Gasli earthquakes (in Russian). *Doklady Akademii Nauk SSSR*, 1988, 301, 5, p.1087-1090
70. Sultankhodjaev A.N., Tyminskij B.T., Spiridonov A.I., Radioactive emanation to study geological processes (in Russian). Tashkent, Fan, 1979, p.119
71. Tanner A.B., Radon migration in the ground: A supplemental review, *Geol. Surv. Open File Rep. U.S.*, 1978, p.78-1050
72. Tanner A.B., Radon migration in the ground: A supplementary review, *Nat. Radiat. Environ.*, 1, 1980, p.5-57
73. Tashkent earthquake of 26 April 1966 (in Russian). Tashkent, Fan, 1971, p.672
74. Teng Ta-Liang, Some recent studies on groundwater radon content as an earthquake precursor., *Journ. Geoph. Res.*, 1980, 85, B6, p.3089-3099
75. Tsaj-Tsuhuan, Shi Huasin, Hydrochemical precursors of earthquakes (in Chinese). *Dichji Chubanshe* 1980, p.206

76. Tsarev V.P., Kuznetsov O.L., Kuznetsov Y.I., et al., An influence of mechanic energy, outloaded in strain discharge zones of the earth-crust on geochemical processes (in Russian). In: Studies of rock massif state by acoustics methods, 1980, M., NPO Neft'erazvedka, p.78
77. Tyminskij V.G., About the role of hydrochemical indicators in tectonic activity studies. *Geokhimiya*, 1971, N1, p.107-109
78. Ulomov V.I., Mavashev B.Z., About the precursor of the strong tectonic earthquake. *Doklady Akademii Nauk*, 1967, 176, N2, p.319-329
79. Vogel A., Brandes K., Earthquake prognostics: Hazard assessment, risk evolution and damage prevention. Friedrich Vieweg, Wiesbaden, 1988, p.544
80. Vojtov G.I., Popov E.A., Geochemical prognose of earthquakes. *Nauka i Zhizn'*, 1989, N12, p.60-64
81. Vorobjov A.A., Dmitrijevskij V.S., Sokolovskij O.N., Thermofluctuation theory of rock wrecking and earthquakes. In: "Physico-technical problems of deposit processing", 1980, N5, p.19-23
82. Wakita H., Iyarashi G., et al., Coseismic radon changes in groundwater, *Geoph. Res. Letters*, 1989, 16, No.5, p.417-420
83. Wallace R.E., Ta-Liang Teng, Prediction of the Sunpan-Pingwu earthquake. August 1976, "Bull-Seismol. Soc. Amer.", 1980, 70, N4, p.1199-1223
84. Zhai Xingyao, et al.,  $\alpha$ -method of current and automatic measurement of groundwater radon content. *Northwest Seismol J.*, 1984, 6, NY, p.83-88

## GAS-GEOCHEMICAL APPROACHES TO EARTHQUAKE PREDICTION

Chi-Yu KING  
US Geological Survey,  
Menlo Park, California,  
United States of America

### Abstract

Concentrations of a wide range of terrestrial gases in ground water and soil air have commonly been found to be anomalously high along active faults, suggesting that the faults may be paths of least resistance for the outgassing process of the "solid" earth. Anomalous temporal gas-concentration changes with durations of a few hours to many months have been recorded before many large and some smaller earthquakes at stations mostly located along active faults at epicentral distances of as much as several earthquake-source dimensions where the associated coseismic strain changes are estimated to be as small as  $10^{-8}$ . This result suggests that the earthquakes and the associated anomalies are both incidental results of some small but broad-scale episodic strain changes in the crust. Such strain changes may be amplified at the earthquake and anomaly sites and, together with sufficient pre-existing stresses, may reach some critical levels (above half fracture strengths) for generation of the earthquakes and anomalies. Significant gas-concentration changes have also been observed at times of other known crustal disturbances, such as underground explosions, ground-water pumping, and earth tide, and from stressed rock samples in laboratory experiments. These results suggest several possible mechanisms for the deformation-related gas-emission changes that involve movement of crustal fluids of non-uniform chemical composition or enhanced water/rock reaction at newly created rock surfaces. However, gas-concentration changes may also be caused by various non-tectonic environmental changes, which must be recognized in the search of true earthquake precursors.

### INTRODUCTION

Scientific measurements for earthquake prediction have been made extensively since the mid-1960's in many seismically active countries such as USSR, China, Japan, and USA. The geophysical and geochemical data often show temporal changes interpreted to be premonitory to some large or moderate earthquakes.

Some of the reported anomalies are considered by other investigators to be marginal in their tectonic significance, because similar changes may be caused by other concurrent environmental variations such as rainfall or groundwater pumping. In a previous paper (King, 1986)<sup>13</sup> I gave an overview of gas-geochemical studies carried out in various seismic regions of the world and discussed possible effects of various environmental changes. In the present supplementary paper, I show a collection of representative gas-geochemical data sets published in the literature and suggest a physical basis for some of the observed features in the data, which may still need to be substantiated by further studies.

### SPATIAL ANOMALIES AND ACTIVE FAULTS

Active faults are commonly characterized by anomalously high concentrations of a wide variety of terrestrially generated gases (e.g., radon, helium, hydrogen, mercury, and carbon dioxide) in ground water and soil air. This observation suggests that the faults may be paths of least resistance for gases in the "solid" earth to escape to the atmosphere. Figure 1 shows, for example, the result of Israel and Björnsson (1967)<sup>8</sup> who measured radon and thoron concentration in soil air at 1-m depth along transects perpendicular to the strikes of several faults near Aachen. They attributed the radon anomalies that were accompanied by thoron anomalies to enrichment of parent nuclides, and the other radon anomalies to upward migration of radon. Irwin and Barnes (1980)<sup>6</sup> showed that the worldwide distributions of springs in which the groundwater  $\text{HCO}_3^{-1}$  content exceeded 1,000 ppm generally coincided with major seismic belts (Figure 2). Figure 3 shows helium anomalies along active faults, especially at intersections of faults, observed by Yanitskiy et al. (1975)<sup>28</sup>, who measured helium concentration in ground water at depths of 30–50 m in north Kazakhstan. Similar anomalies were also observed for several other gases (e.g.,  $\text{H}_2$ ,  $\text{CO}_2$ , Rn, and Hg).

### TEMPORAL VARIATIONS ASSOCIATED WITH KNOWN CRUSTAL DEFORMATION

A number of field experiments have been conducted in which the gas concentrations in ground water or soil air were found to change in response to known crustal strain changes caused by such events as underground explosions, ground-water pumping, and earth tide. Figure 4 shows soil-air radon anomalies observed by Wollenberg et al. (1977)<sup>26</sup> at five monitoring sites near the nuclear explosion Esrom in the Nevada Test Site. The anomaly amplitudes decreased with increasing distance from ground zero, and were apparently not related to barometric pressure variations recorded nearby.

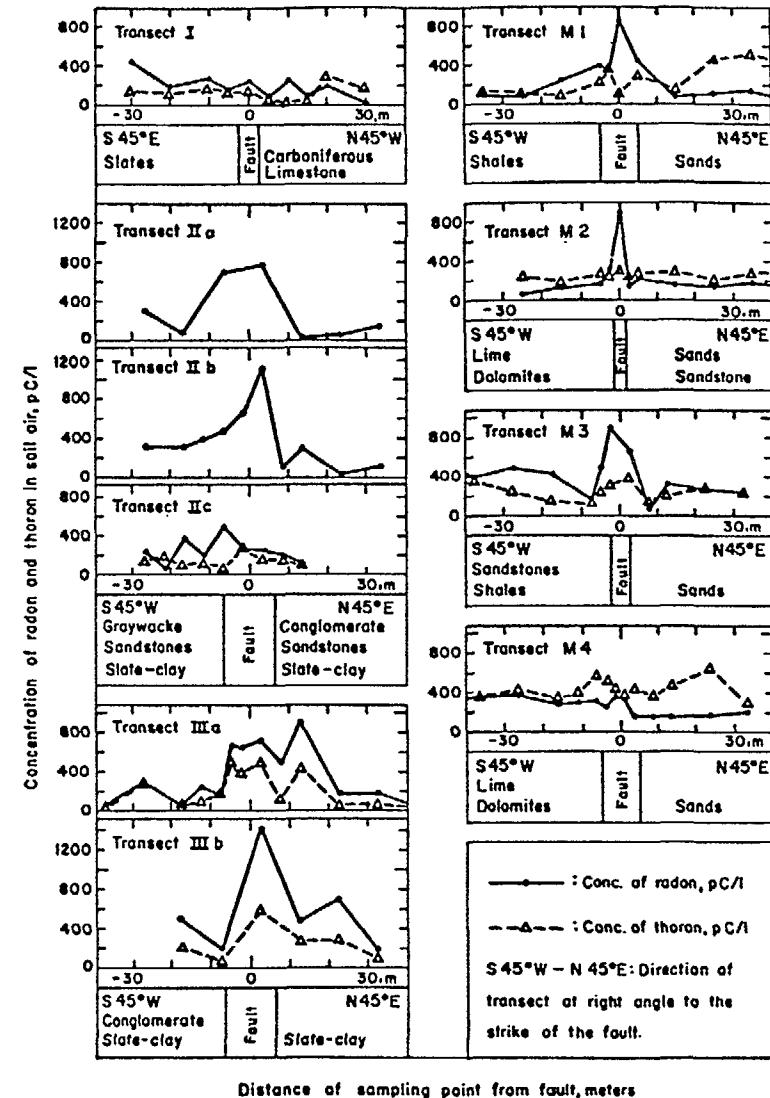


Figure 1. Concentration of radon and thoron at 1-m depth in soil air over faults near Aachen. The concentration was measured in transects at right angle to the strike of the faults, which had previously been located by geological methods. A section of the bedrock under each transect is schematically indicated. (After ISRAEL and BJÖRNSSON, 1967.)<sup>8</sup>

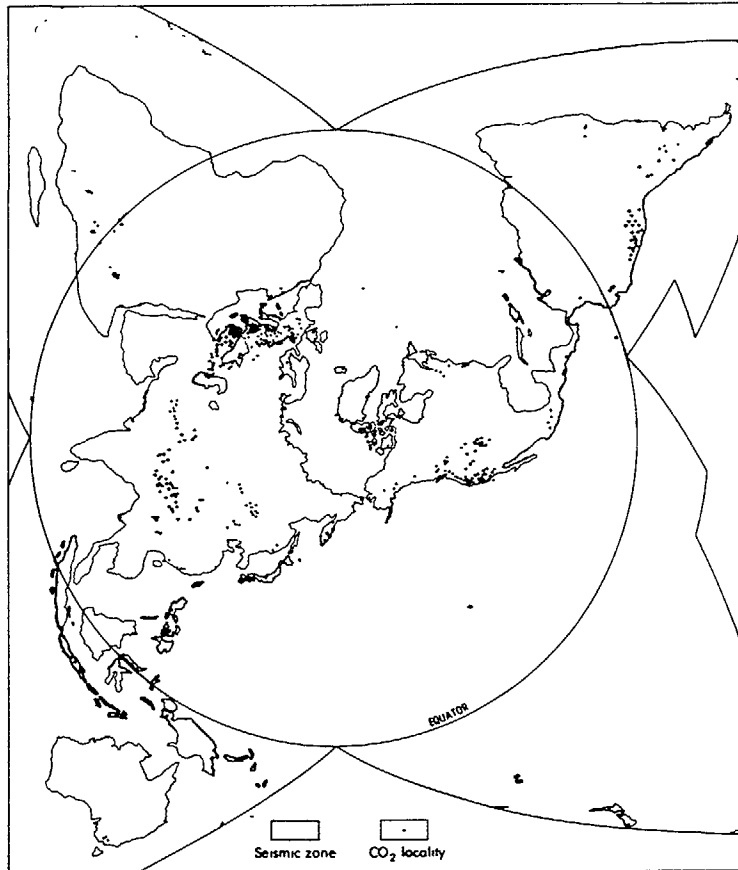


Figure 2. Worldwide distribution of seismic zones (shaded) and localities of springs with high  $\text{CO}_2$  discharges ( $\text{HCO}_3^-$  content  $\geq 1000$  ppm). (After IRWIN and BARNES, 1980)<sup>6)</sup>.

Figure 5 shows the result of Sugisaki (1981)<sup>23)</sup>, who observed a correlation between tidal strain and the He/Ar concentration ratio in gas bubbles from a mineral spring in Japan. Similar results were also observed for other gases at several other "sensitive" sites, suggesting that terrestrial gas emissions at such sites may be responsive to crustal strain changes as low as  $10^{-8}$ .

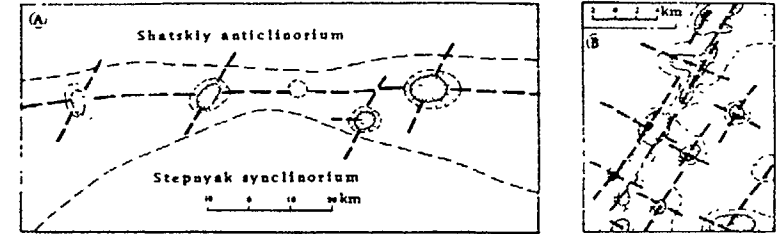


Figure 3. Anomalous high helium concentration in groundwater at depths of 30–50 m along consolidated and slightly permeable fault zones (dashed lines) (A), and along active fault zones (B), especially at intersections of faults in north Kazakhstan. The helium content in  $10^{-4}$  ml/l is  $<1$  in white areas, 1–12.5 in sparsely dotted areas, and 12.5–125 in the densely dotted areas. (After YANITSKIY et al., 1975.)<sup>28)</sup>

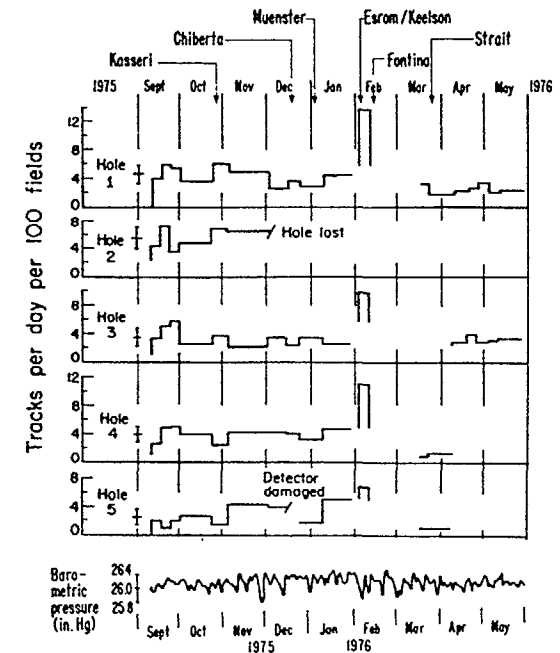


Figure 4. Temporal variations of soil-gas radon concentrations monitored at five shallow holes (0.7 m deep) near underground nuclear explosion Esrom in the Nevada Test Site. Holes 1–5 are, respectively, 0.2, 1.3, 2.7, 3.8, and 4.6 km from ground zero. Mean values and standard deviations from the pre-Esrom values at each site are indicated by error bars. Barometric pressure data at the NTS are shown at the bottom for comparison. (Modified from WOLLENBERG et al., 1977.)<sup>26)</sup>

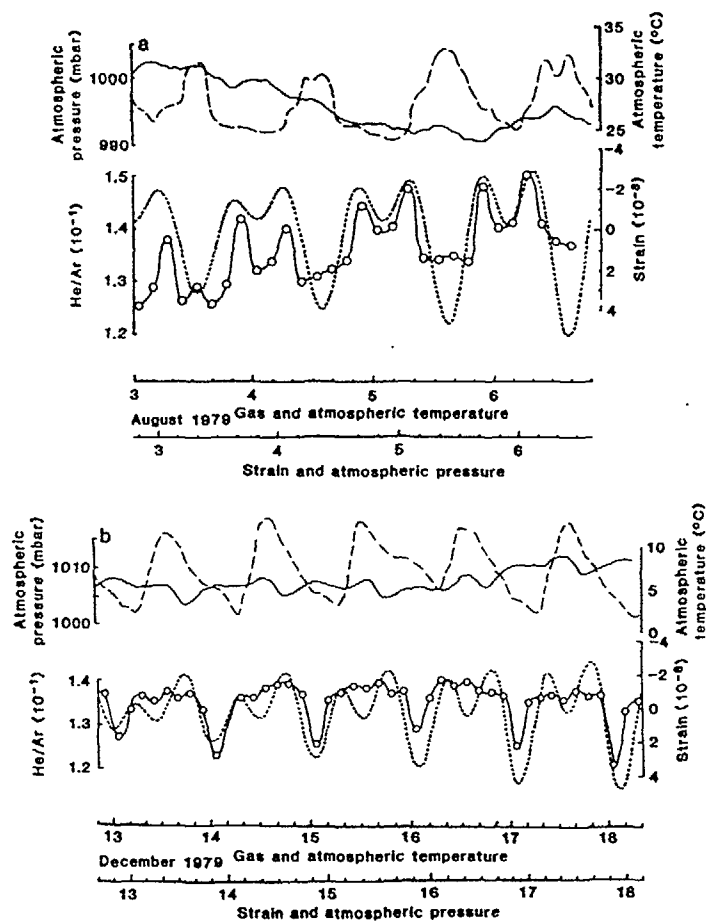


Figure 5. Comparison of temporal variations of He/Ar concentration ratio in gas bubbles in a mineral spring at Byakko Spa, Japan (circles) with theoretical tidal strain (areal dilation; dotted curve), atmospheric pressure (solid curve), and temperature (dashed curve) for two time periods. (After SUGISAKI, 1981.)<sup>23)</sup>

### EARTHQUAKE-RELATED GAS CHANGES

Gas-concentration changes have been reportedly observed before many large and some smaller earthquakes in various parts of the world. Some of these changes might be coincidental, caused by non-tectonic environmental changes, such as rainfall and ground-water pumping, or by instrumental or human error. Others

are probably truly related to earthquakes, and they appear to show some general features in common: (1) They tend to occur mostly along active faults, especially at the intersections and bends of faults, at epicentral distances up to several times the corresponding earthquake-source dimensions. (2) The durations range from a few hours to many months. The occurrence, or the increasing occurrences, of the short-term (spike-like) anomalies appears to be useful to predict the time of earthquakes (perhaps within a few days to a few weeks). (3) The spatial extent and the duration of the intermediate-term anomalies generally appear to increase with, and thus may be useful for predicting, earthquake magnitude. (4) The amplitude of the anomalies does not appear to show consistent correlation with either earthquake magnitude or epicentral distance (in contrast to the case of explosion shown in Figure 4). Following are some representative examples of earthquake-related gas changes, which are deemed relatively reliable, because they were recorded in multiple components, by independent methods or observers, or at multiple sites, or because they can be compared with a reasonably long set of background data.

### Radon Anomalies Before the Tangshan Earthquake

Radon content of ground water has been monitored at many wells in northern China shortly after the magnitude 7.2 Xingtai earthquake in 1966 (see King (1985)<sup>12)</sup>, for a review of radon studies in China). Figure 6 shows the location of the magnitude 7.8 Tangshan earthquake in 1976 and monitoring stations. Most of the stations that recorded the supposedly intermediate-term and/or short-term anomalies (increases, which are sometimes difficult to recognize, in Figures 7 and 9) were located along major or secondary fault zones up to an epicentral distance of about 500 km (Figures 8 and 10). The intermediate-term anomalies (gradual increases beginning in late 1973 and lasting up to several years) may be related to both the Haicheng (1975, magnitude 7.3) and Tangshan earthquakes on account of their proximity in time (1.5 years) and space (350 km). One station (Guanzhuang) was in operation long enough to cover the magnitude 7.4 Bohai earthquake in 1969 also; the associated anomaly, which peaked after the earthquake, is shorter in duration but comparable in amplitude. The anomaly amplitudes are small, ranging from 10 to 100% and do not depend significantly on epicentral distance (Figures 8 and 10). Short-term anomalies (spike-like increases mostly, Figure 9) were recorded in increasing numbers at the wells a few days to weeks before the Tangshan main shock and several strong aftershocks (Figure 11). However, very few of them were recorded in the immediate epicentral areas.

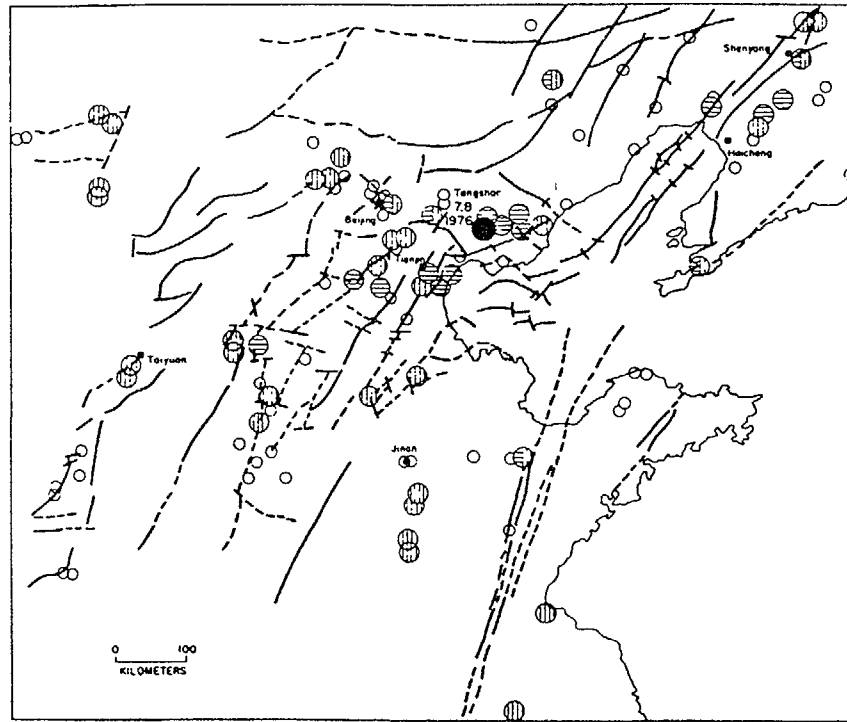


Figure 6. Locations of monitoring stations that showed intermediate-term ground-water radon-concentration changes (circles with horizontal stripes), short-term changes (circles with vertical stripes), and no significant change (small circles) before the 1976 Tangshan earthquake (solid circle) in northern China. Thick solid and dashed lines indicate observed and inferred major faults, respectively. (After YING et al., 1978.)<sup>29)</sup>

The above-mentioned radon anomalies typify those observed elsewhere in the world. Figure 12 shows a plot of anomaly amplitudes vs. epicentral distance for a worldwide data set compiled by Hauksson (1981)<sup>4)</sup>. The areal extents of anomaly occurrences are unexpectedly large, and increase with magnitudes of the associated earthquakes. However, the anomaly amplitudes do not depend significantly on epicentral distance or earthquake magnitude. The threshold of the related strain changes was estimated to be  $\sim 10^{-8}$ , comparable with tidal strain changes.

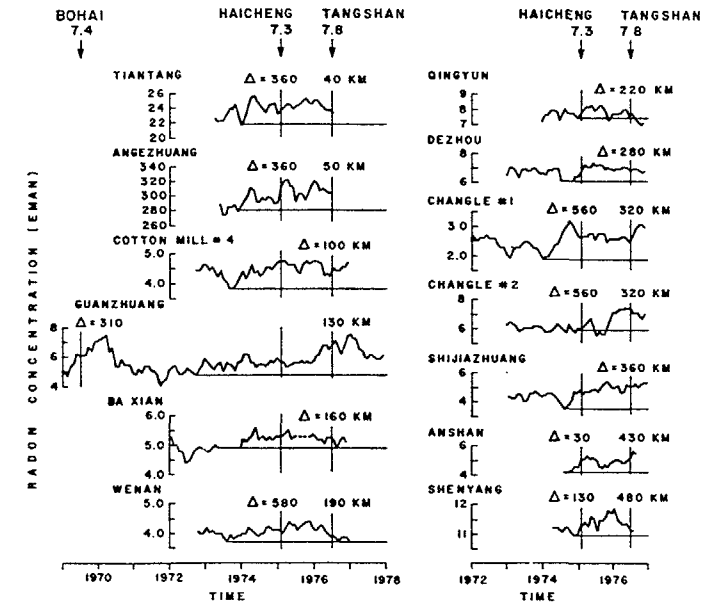


Figure 7. Time series of ground-water radon concentration (monthly average values) recorded at sensitive stations in northern China. Arrows indicate the times of 1975 Haicheng and 1976 Tangshan earthquakes. (After YING et al., 1978.)<sup>29)</sup>

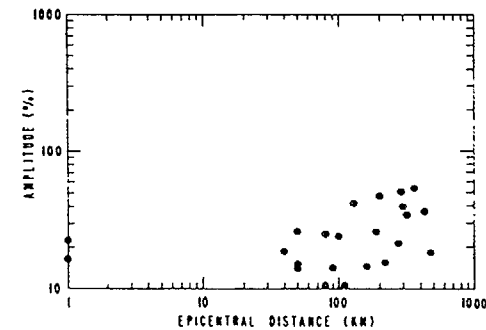


Figure 8. Amplitude of intermediate-term ground-water radon anomalies (relative to background level in monthly average values) as a function of epicentral distance from the 1976 Tangshan earthquake. (Based on data in YING et al., 1981.)<sup>30)</sup>

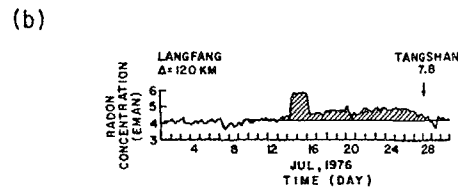
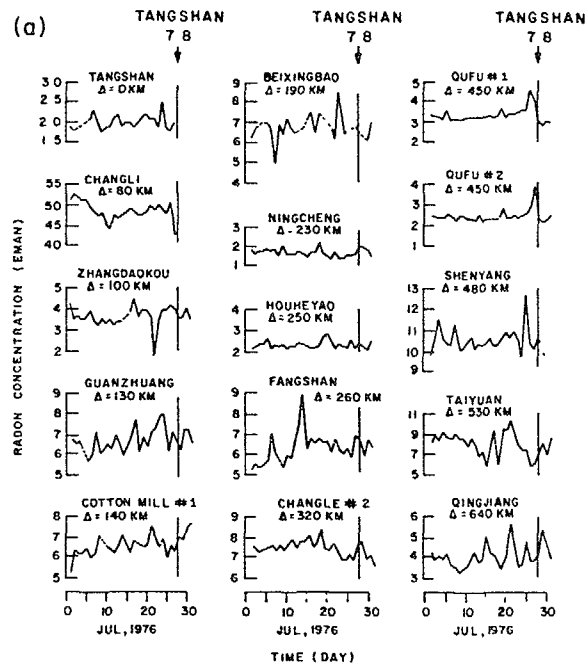


Figure 9. Time series of ground-water radon concentration, showing short-term changes before the 1976 Tangshan earthquake. (After YING et al., 1981.)<sup>30)</sup> (a) Daily readings. (b) Continuous data at Langfang station.

#### Gas-geochemical anomalies in southern California during 1979

Gas-geochemical measurements were made extensively in southern California by several research groups. Figure 13 shows helium and radon concentrations recorded by Chung (1985)<sup>1)</sup> and colleagues at Arrowhead hot spring on the San Andreas fault. These concentrations varied synchronously and were anomalous at the time of several significant local earthquakes including the magnitude 4.8 Big Bear earthquake in 1979, but not the magnitude 4.1 earthquake in 1983.

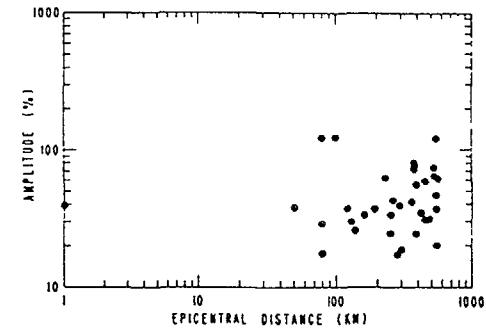


Figure 10. Amplitude of short-term ground-water radon anomalies (relative to background level in daily readings) as a function of epicentral distance before the 1976 Tangshan earthquake. (Based on data in YING et al., 1981.)<sup>30)</sup>

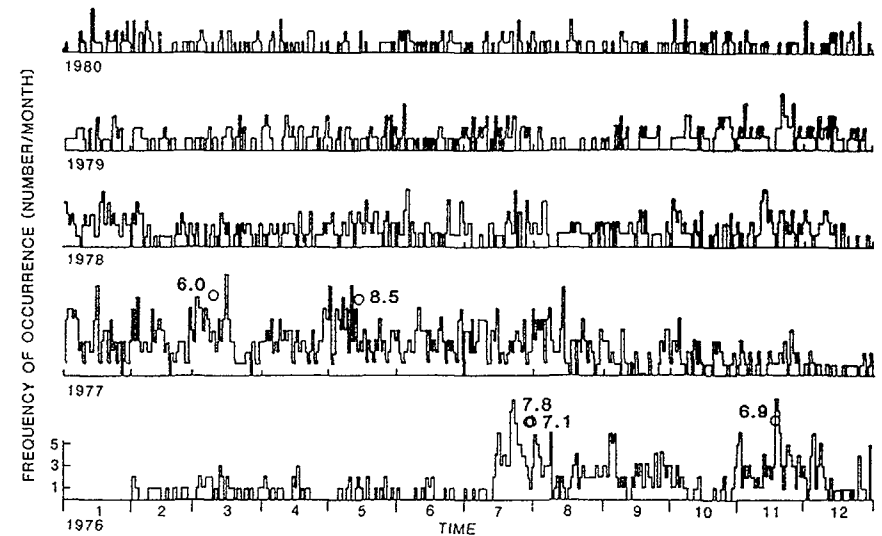


Figure 11. Frequency of occurrence of short-term radon anomalies recorded at water wells in northern China. Indicated are occurrences of Tangshan earthquake and larger aftershocks (magnitude  $\geq 6.0$ , circles) (After YANG et al., 1982)<sup>27)</sup>

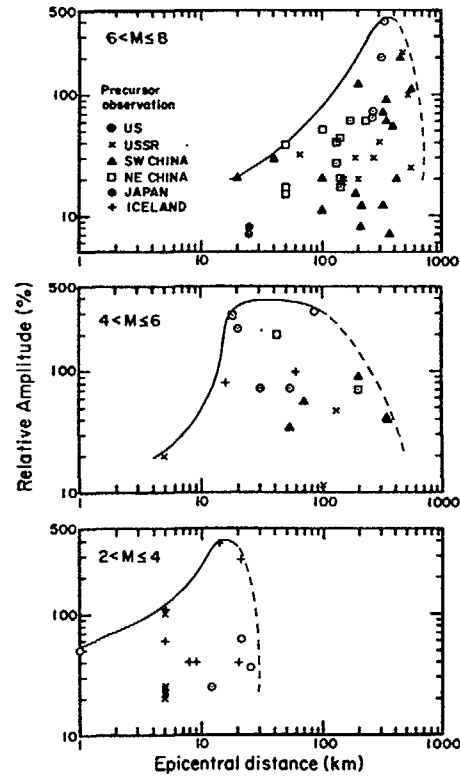


Figure 12. Amplitude of ground-water radon anomalies relative to background level as a function of epicentral distance for a worldwide data set. (After HAUSSON, 1981.)<sup>4)</sup>

Similar anomalies were recorded for methane, nitrogen, electric conductivity, and temperature, and they were all attributed to admixing of gas-rich water from a deep source with the regular shallow water within the spring. No such anomaly was recorded, however, at this group's other 15 monitoring sites. Teng and colleagues (see Teng and Sun, 1986)<sup>25)</sup> also recorded significant anomalies in 1979 at three of their 14 ground-water radon monitoring stations, located within 20 km of the Big Bear earthquake (Figure 14). So did Shapiro *et al.* (1985)<sup>22)</sup> at one of their monitoring sites along a frontal fault of the Transverse Ranges (Figure 15). Shapiro *et al.* considered the anomaly recorded at Kresge between June 1979 and early 1982 to be tectonic in origin, possibly as the result of a regional strain episode,

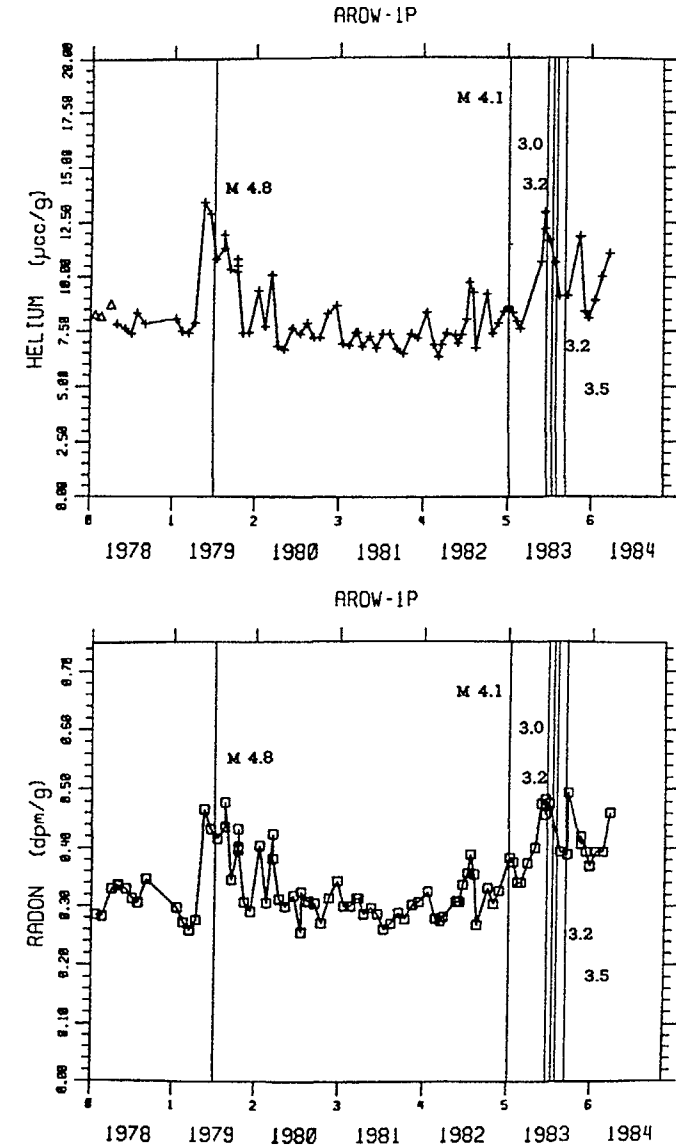


Figure 13. Time series of helium and radon concentrations in water samples taken monthly from the Arrowhead hot spring on the San Andreas fault in southern California. Vertical lines indicate the times of several local earthquakes with labeled magnitudes. (After CHUNG, 1985.)<sup>1)</sup>



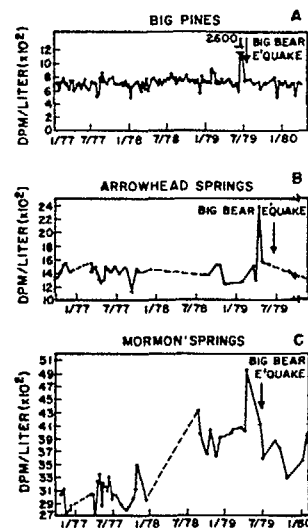


Figure 14. Time series of radon concentrations in water samples taken from three USC stations along the San Andreas fault within 20 km of the magnitude 4.8 Big Bear earthquake (indicated by arrows) in southern California. (After TENG and SUN, 1986.)<sup>25)</sup>

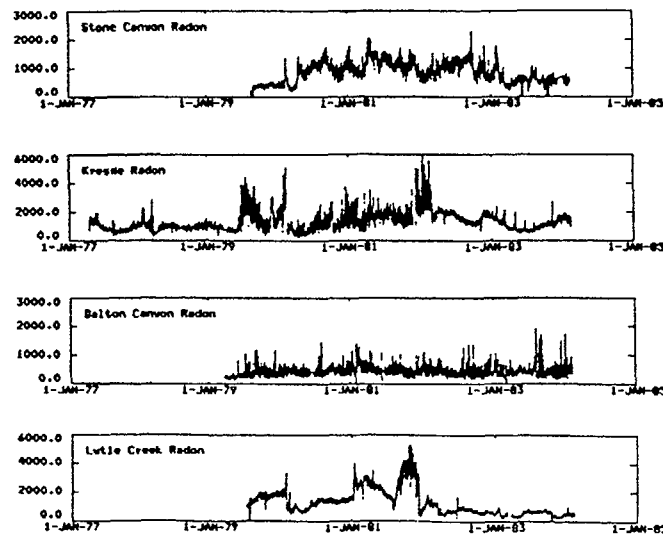


Figure 15. Time series of ground-water radon concentrations recorded at four Caltech stations in southern California. (After SHAPIRO et al., 1985.)<sup>22)</sup>

which may be responsible also for the increased number of moderate earthquakes in southern California, including the magnitude 6.6 Imperial Valley earthquake on October 15, 1979 about 290 km away from their sensitive stations.

#### Geochemical anomalies during 1980 in central California

King et al. (1981)<sup>16)</sup> and O'Neil and King (1981)<sup>19)</sup> recorded some gas and related chemical changes in ground water at two wells along the San Andreas fault near San Juan Bautista, California (Figure 16) at the beginning of a sequence of earthquakes in 1980; the largest of the earthquakes has a magnitude of 4.8 and epicentral distances of several kilometers. Figure 17 shows the result of *in situ* measurements of water level, temperature, salinity, electric conductivity, and pH at a 30-m deep artesian well (Mission Farm Campground). The water level had generally been rising since two years before the earthquake; it reached the ground surface (the well became self-flowing) at about the same time as a magnitude 4.0 earthquake that occurred 25 km away, or about two months before the magnitude 4.8 earthquake at an epicentral distance of 6 km. Simultaneously, the water temperature became more steady, and the salinity/conductivity increased by many standard deviations from the background level. Similar results were obtained from chemical analyses of water samples (taken from the well at the same time as the *in situ* measurement) in the laboratory, especially for contents of  $\text{Ca}^{++}$ ,  $\text{Mg}^{++}$ ,  $\text{F}^-$ ,  $\text{Cl}^-$ ,  $\text{NO}_3^-$ ,  $\text{SO}_4^-$ , and  $\text{HCO}_3^-$  (Figure 18) and stable isotopes  $\delta\text{D}$  and  $\delta^{18}\text{O}$  (Figure 19a). The isotopic contrast is shown more clearly on a plot of  $\delta\text{D}$  versus

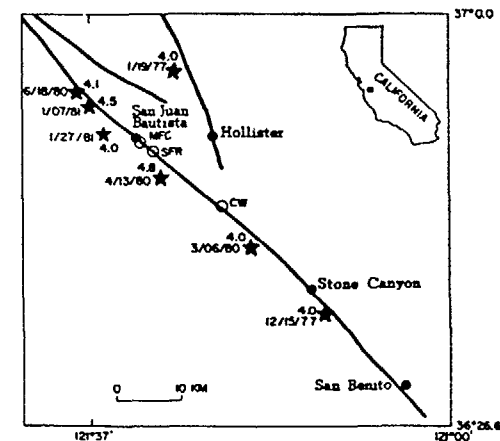


Figure 16. Location of water wells (circles) and earthquakes (stars) of magnitude 4.0 or larger that occurred during the study period of KING et al (1981).<sup>16)</sup>

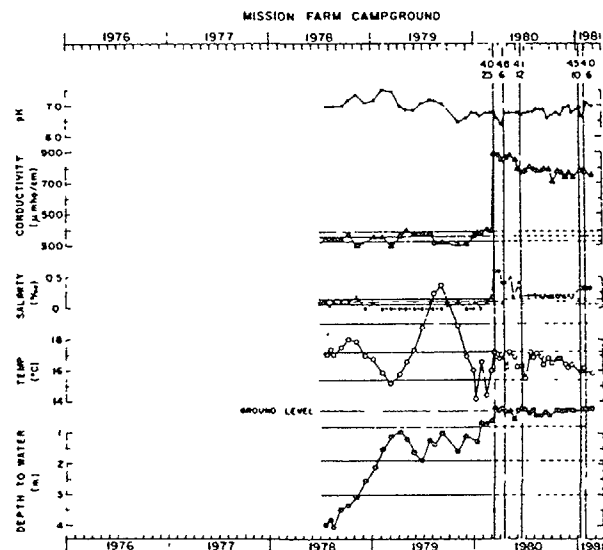


Figure 17. Time series of water level, temperature, salinity, electric conductivity, and pH at the MFC well. Horizontal lines indicate pre-anomaly mean value  $\pm$  one standard deviation. Vertical lines indicate occurrence of earthquakes of magnitude  $\geq 4.0$ ; labeled are magnitude and epicentral distance in km. (After KING et al., 1981.)<sup>16)</sup>

$\delta^{18}\text{O}$  (Figure 19b). Such changes were attributed to admixing of water from another aquifer that was normally not tapped by the well, possibly through cracks created in an intervenient aquiclude during a tectonic strain episode. Similar but generally opposite changes were observed at another well located on different side of the fault (San Francis Retreat, SFR in Figure 16) about 80 m deep and about 3 km southeast of the first (Figures 20–22). However, no significant changes were recorded at a third well (Cienega Winery, CW in Figure 16) somewhat farther away from the epicenter area. Measurements at the former two wells were interrupted shortly after the anomalies because the wells were then used for continuous radon monitoring that requires pumping.

#### Gas-geochemical anomalies before the 1984 W. Nagano earthquake

Gas-geochemical anomalies were recorded by three groups of researchers (Sano et al., 1986; Sugisaka and Sugiura, 1986; Katoh et al., 1986)<sup>20),24),10)</sup> at several stations near the magnitude 6.8 earthquake on September 14, 1984 in

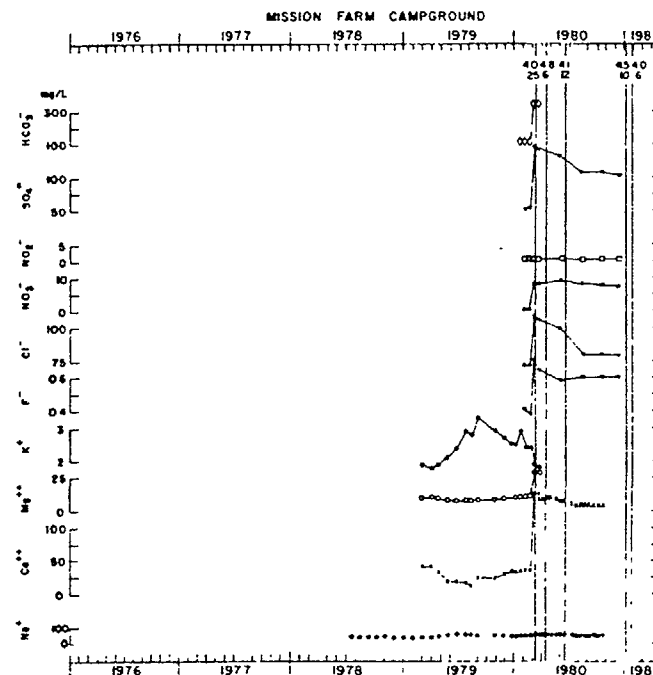
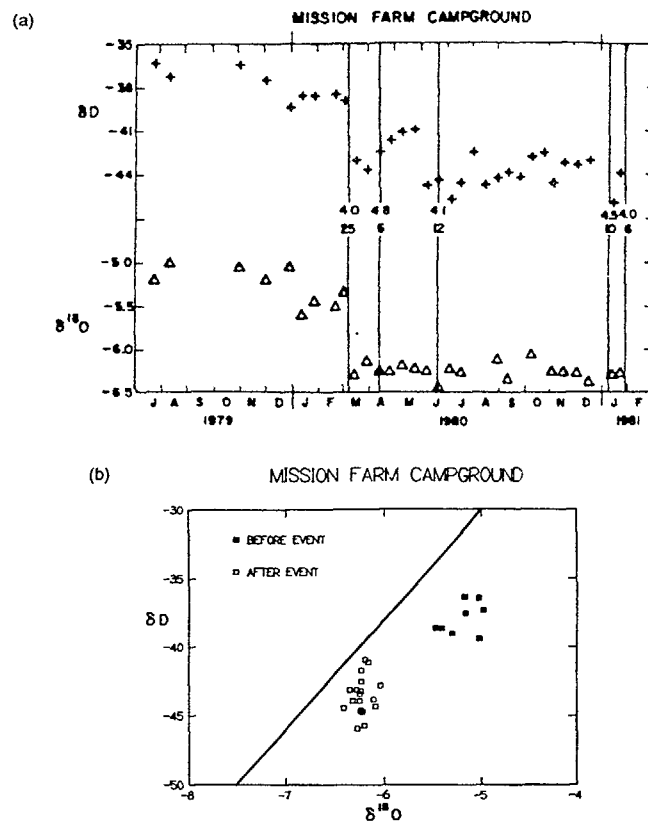
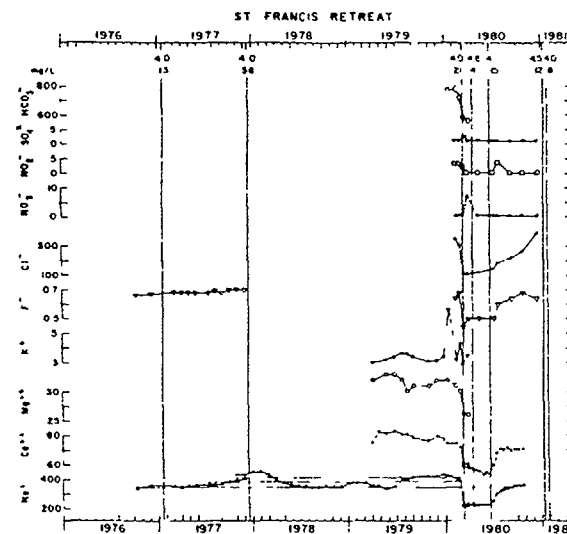
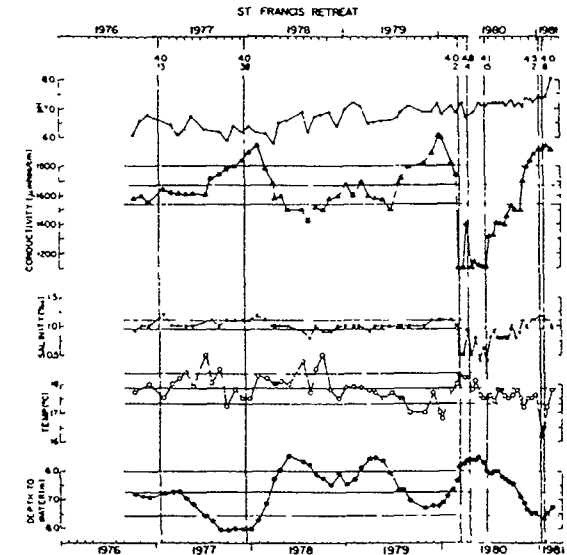


Figure 18. Time series of ion concentrations (mg/L) in water samples from the MFC well.  $\text{NO}_3^-$  are in mg/L N. Symbols as in Figure 16. (After KING et al., 1981.)<sup>16)</sup>

the western Nagano Prefecture of central Honshu, Japan. Sugisaki and Sugiura (1986)<sup>24)</sup> observed conspicuous gas anomalies at a fumarole and three springs about 1–3 months before the earthquake. Figure 23 shows the  $\text{He}/\text{Ar}$ ,  $\text{N}_2/\text{Ar}$ , and  $\text{CH}_4/\text{Ar}$  concentration ratios in bubble gases from a mineral spring (Byakko) on an active fault about 50 km from the epicenter. They attributed the anomalies to changes in the emission rate of some deep-seated gas due to earthquake-related changes in pore pressure. The gas bubbles also showed some anomalous increases in hydrogen concentration beginning about one month before the earthquake. The  $\text{H}_2$  anomaly was attributed to reaction between ground water and newly formed crack surfaces in the rocks. Sano et al. (1986)<sup>20)</sup> observed some post-earthquake increases (compared with values obtained in November 1981) of  $^3\text{He}/^4\text{He}$  ratios in bubble gases from several hot springs located less than 10 km from a fault that



was possibly formed at the time of the earthquake. They suggested that the earthquake was triggered by an upward migration of some  $^3\text{He}$ -rich fluids associated with magma intrusion beneath the source region. *Katoh et al.* (1986)<sup>10</sup> observed anomalous increases of radon concentration in soil gas (superposed on some apparently seasonal changes) at several monitoring stations located on three active faults about 25 to 100 km away from the epicenter, beginning about 1 to 2 years before the earthquake (Figure 24). These anomalies coincided with coda-wave duration anomalies observed by *Sato* (1988)<sup>21</sup>. They are similar in shape to soil-gas radon anomalies recorded elsewhere (see *e.g.*, *King*, 1978)<sup>11</sup>.



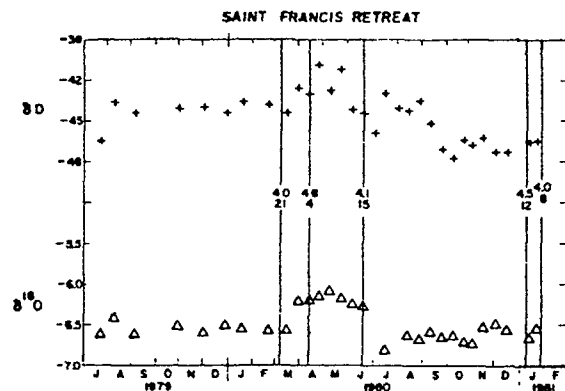


Figure 22. Time series of  $\delta D$  and  $\delta^{18}O$  in water samples from the SFR well. Symbols as in Figure 16. (After O'NEIL and KING, 1981.)<sup>19)</sup>

#### POSSIBLE MECHANISMS FOR EARTHQUAKE-RELATED GAS-GEOCHEMICAL ANOMALIES

Several possible mechanisms have been postulated by various investigators to explain the earthquake-related gas anomalies, most involving tectonically induced movement of crustal fluids of different concentrations or enhanced water/rock reaction at newly created rock surfaces. They include increased upward flow of deep-seated fluids to the monitored aquifer or holes, gas-rich pore fluids being squeezed out of rock matrix into the aquifer, mixing of water from another aquifer through tectonically created cracks in the intervenient aquiclude, increased water/rock interactions, and increased gas emanation by or from newly created cracks in the rocks to the pore fluids. Some of these possibilities have been tested in laboratory experiments. For example, *Holub and Brady* (1981)<sup>5)</sup> monitored radon emanation and microcracking activity in a uranium-bearing granite sample under uniaxial loading. They observed an initial decrease in emanation possibly associated with closure of pre-existing cracks in the rock and then significant increases in both the emanation and microcracking activity at a load of about one-half of the ultimate strength (Figure 25). Such increases were observed repeatedly until larger increases occurred at time of fracture. *Kita et al.* (1982)<sup>17)</sup> crushed granite and quartz samples under moist conditions at temperature of 25°–270°C, and found increased  $H_2$  release with temperature up to about 200°C; at higher temperatures the release decreased with temperature (see Figure 26 for granite). They attributed the  $H_2$  generation to chemical reaction between water and Si and Si-O radicals on the fresh surfaces of the crushed rocks.

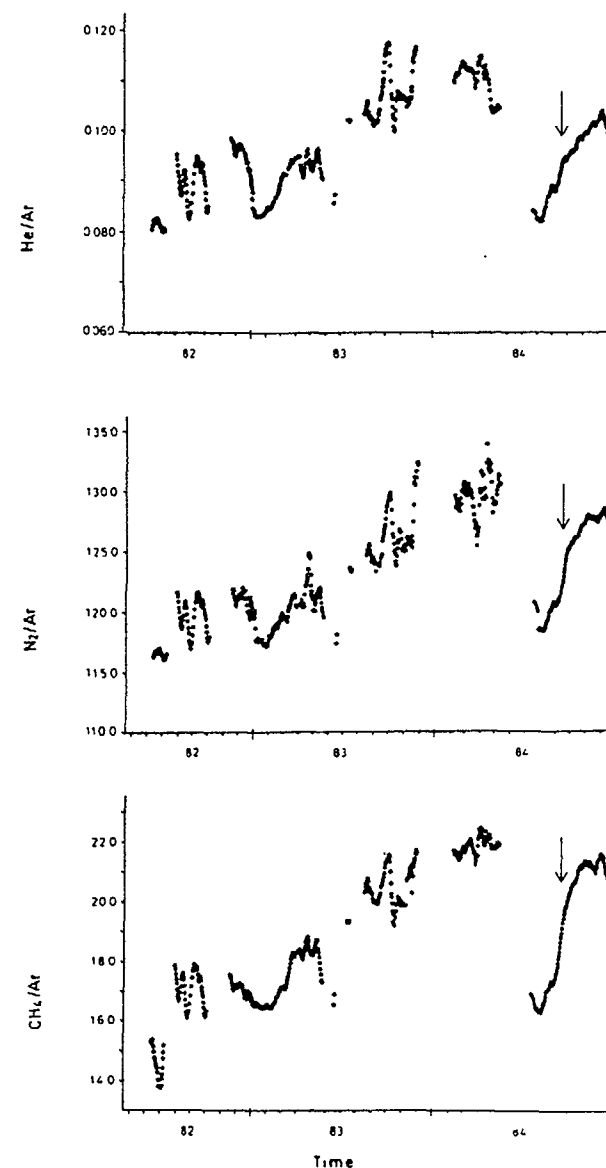


Figure 23. Time series of  $He/Ar$ ,  $N_2/Ar$ ,  $CH_4/Ar$  concentration ratios (daily average values smoothed with a sliding 10-day window) in bubble gases at the Byakko Spring, Japan. Arrows indicate the occurrence of the magnitude 6.8 Western Nagano earthquake in 1984. (After SUGISAKI and SUGIURA, 1986.)<sup>24)</sup>

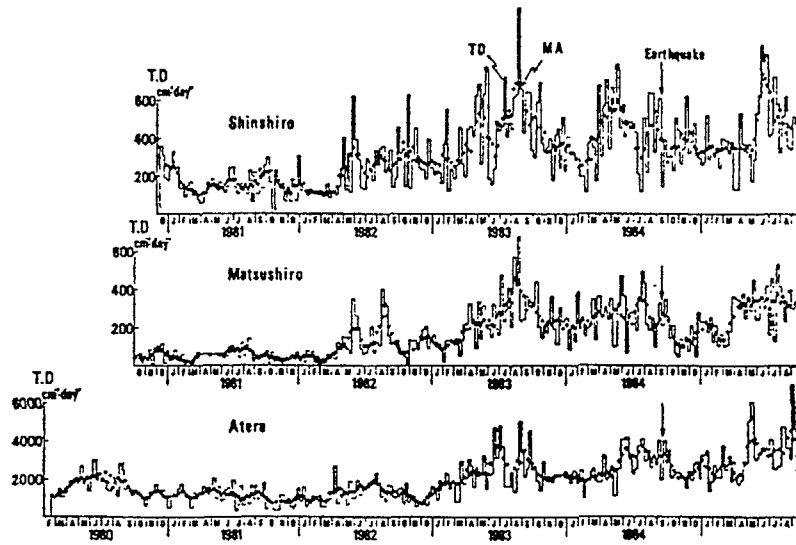


Figure 24. Time series of radon concentration in soil gas (TD:  $\alpha$ -particle track density in weekly exposed cellulose nitrate film; MA: moving average) at three sites located on the Median Tectonic Line, the Matsushiro fault, and the Atera fault, which are, respectively, 100, 100, and 25 km away from the 1984 Western Nagano prefecture earthquake. (After KATOH et al., 1986.)<sup>10)</sup>

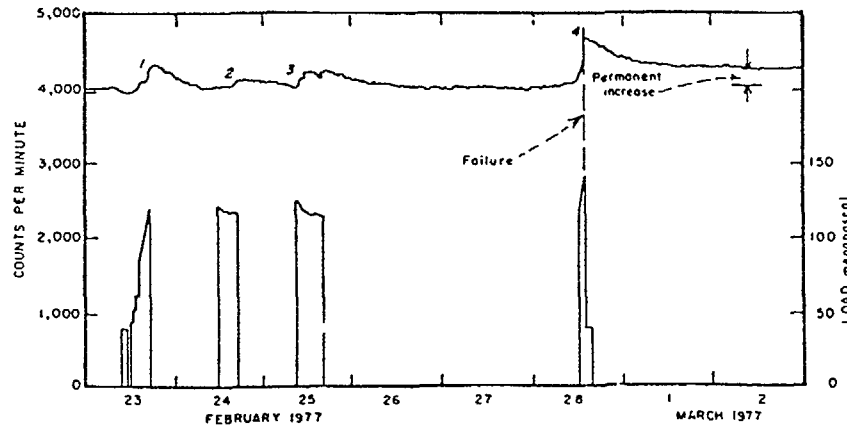


Figure 25. Radon emanation (upper curve) from a uranium-bearing granitic rock under uniaxial stress (lower curves). (After HOLUB and BRADY, 1981.)<sup>5)</sup>

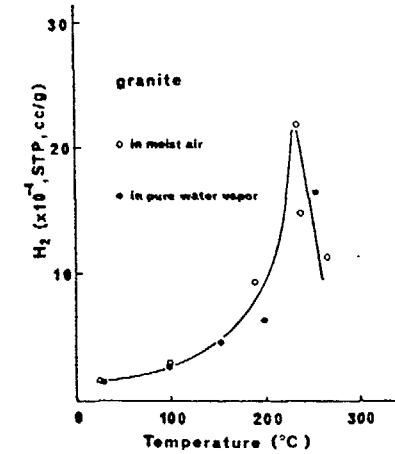


Figure 26. Amount of  $H_2$  release from crushed granitic rocks at various temperatures and in two different atmospheres. (After KITA et al., 1982.)<sup>17)</sup>

King (1978)<sup>11)</sup> invoked a tectonically-induced vertical flow of crustal gases to explain soil-gas radon anomalies recorded along the San Andreas fault in central California. As shown schematically in Figure 27, radon concentration generally decreases slowly with height in near-surface atmosphere, and increases rapidly (by 3 orders of magnitude) with depth in near-surface soil gas, approaching a maximum at a depth of several meters. Because of the high subsurface concentration gradient, a small upward/downward flow can significantly increase/decrease the radon value monitored at a fixed shallow depth of about 1/2 m. King considered a one-dimensional model in which the soil is treated as a homogeneous porous half-space with uniform radon production rate. On the assumption that radon migrates by molecular diffusion governed by Fick's law and by flow governed by Darcy's law and that the radon concentration is negligibly small at the surface, it was shown that the steady-state concentration  $C$  is a function of depth  $-z$  as follows (e.g., , Clements, 1974)<sup>2)</sup>:

$$C = \frac{\phi}{\lambda} 1 - \exp\left[\gamma\left(\frac{\epsilon\lambda}{D}\right)^{1/2}z\right] \quad (1)$$

where

$$\gamma = \frac{v}{2(\epsilon\lambda D)^{1/2}} + \left(\frac{v^2}{4\epsilon\lambda D} + 1\right)^{1/2} \quad (2)$$

$\phi$  is radon production rate,  $\lambda$  is its decay constant,  $\epsilon$  is soil porosity,  $D$  is molecular diffusion coefficient of radon in the soil, and  $v$  is apparent soil-gas flow velocity

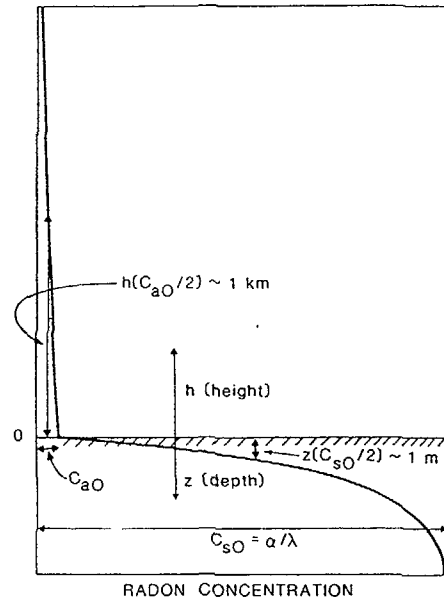


Figure 27. Schematic diagram of radon concentration in atmosphere and soil near the ground surface as a function of elevation and depth.  $C_{a0}$  is concentration in undisturbed soil air at great depth;  $C_{a0}$ , concentration at surface. (After JUNG, 1963.)<sup>9)</sup>

(volume of flow per unit time per unit geometric area). Figure 28 shows this result for five different flow velocities ( $0, \pm 3 \times 10^{-4}, \pm 10^{-3} \text{ cm s}^{-1}$ ) and for some material constants appropriate for typical dry soils. It is evident that a small upward/downward gas flow ( $3 \times 10^{-4} \text{ cm s}^{-1}$ ) can significantly increase/decrease the subsurface radon concentration at shallow depths (by a factor of 2 at a depth of 0.7 m). Note that much larger increases in upward gas velocity do not produce much larger increases in radon concentration; this result may explain why amplitudes of observed radon anomalies are not correlated significantly with earthquake magnitudes and epicentral distances.

King and Slater (1978)<sup>14)</sup> compared the soil-gas radon data recorded at two sites along the Calaveras fault in Hollister, California, with crustal strain data recorded on a two-color laser geodetic meter in the same area; they found periods of higher radon emanation to be coincided (with slight delay) with periods of crustal compression (in north-south direction), as expected from King's model, with the cross-correlation coefficient being 0.67 (Figure 29). The variations in both data sets may be partly seasonal in nature. Nevertheless, the high radon

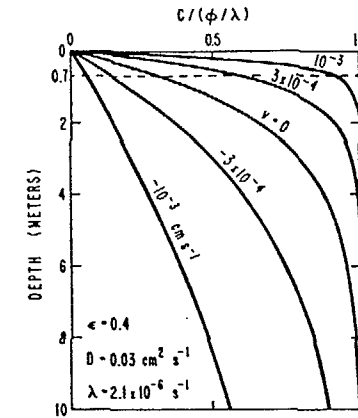


Figure 28. Radon concentration as a function of depth in a homogeneous, porous half-space with uniform radon production rate for five different vertical gas flow velocities. (Modified from KING, 1978<sup>11)</sup>.)

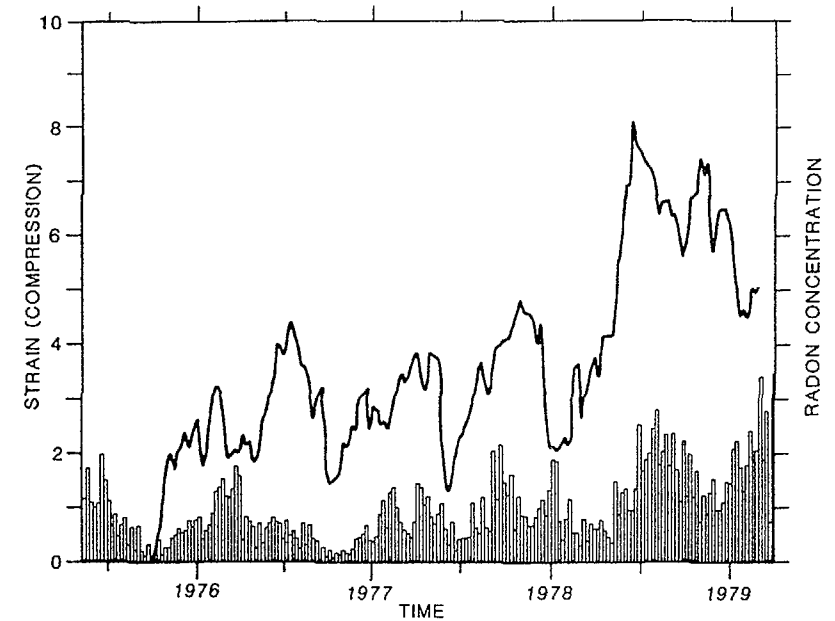


Figure 29. Comparison of average soil-gas radon-concentration data (lower bar graph) recorded at two stations on the Calaveras fault north of Hollister with average distance changes along two lines of 2-color geodetic measurement covering the same area (in arbitrary units).

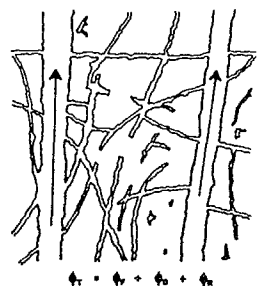


Figure 30. Schematic representation of flow pores ( $\phi_F$ ), diffusion pores ( $\phi_D$ ), and residual pores ( $\phi_R$ ) in rock. Fluid usually flows through the flow pores but not the diffusion or residual pores, unless the rock is significantly stressed. (After NORTON and KNAPP, 1977.)<sup>18)</sup>

values in 1979 may be partly related to the magnitude 5.9 Coyote Lake earthquake on August 6, 1979 about 27 km away on the same fault.

Similar models may explain earthquake related anomalies in other soil-gas components (He, H<sub>2</sub>, Hg, etc.) that have similar concentration-versus-depth profiles. Concentration gradients may also exist in wall rocks of aquifers, which may be considered as consisting of networks of "flow pores" (Figure 30; see Norton and Knapp, 1977)<sup>18)</sup> that transport meteoric waters from recharge areas to the monitored springs or wells. Since ground water in the flow pores usually has shorter residence time in the ground and less reaction with rocks, it contains less dissolved terrestrial gas (and other chemical substances) than the fluids in the "diffusion" and "residual" pores in the wall rocks (Figure 30). Thus the tectonically induced flow from the normally diffusive and isolated pores to the flow pores is expected to introduce waters of anomalously high gas and ion content.

The same models may explain the results of some large-scale pumping tests conducted in China, where the radon contents in the pumped wells tended to increase, whereas those in the surrounding observation wells to decrease (see King, 1985)<sup>12)</sup>.

### STRAIN FIELD RESPONSIBLE FOR EARTHQUAKES AND ANOMALIES

The general observation that gas-geochemical (and other) anomalies are widely spread in space but confined mostly to active fault zones suggests that they (and the associated earthquakes) are possibly incidental results of some

broad-scale episodic strain changes in the crust (King, 1986)<sup>13)</sup>. Such changes can be produced by a number of processes, including magma intrusion and episodic fault-creep events below seismogenic depths. The amplitudes of change need not be very large ( $> 10^{-8}$ ), but may be greatly amplified along pre-existing fault zones and especially at their intersections and bends. The local strain increases at such places, when combined with sufficient pre-existing strains, may reach critical levels (above half fracture strengths) to generate the observed tectonic and physical anomalies (as defined by Ishibashi)<sup>7)</sup> and earthquakes. The anomalies may disappear before or after the earthquakes for a variety of reasons, including stress relaxation associated with the earthquakes, healing of the fault zone, and exhaustion of gas supply (in the case of gas anomalies). The concept of multiple-point concentration of a broad-scale episodic strain change may also explain why earthquakes and the various anomalies sometimes occur in distinct yet apparently related clusters in space and time along the same or different faults, why it seems difficult to predict earthquake location with reasonable precision, why there is a lack of detectable seismic-wave velocity anomalies (the dilatant zones may be too thin compared with seismic wave lengths and too widely distributed), and why there is a lack of observed one-to-one correspondence between earthquake and anomaly occurrences.

One piece of evidence supporting the possibility of strain amplification along a fault zone is coseismic steps recorded on creepmeters along the San Andreas fault (King et al., 1977)<sup>14)</sup>. If interpreted as strain steps (see example in Figure 31),

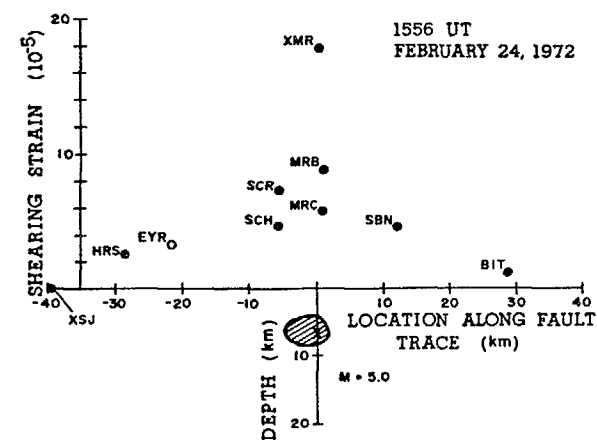


Figure 31. Spatial distribution of coseismic shear strain steps from creepmeter recordings along the San Andreas fault for the magnitude 5.0 Melendy earthquake in 1972. Dots represent data from creepmeters spanning the fault; circle, not spanning. The lower half of the figure shows the hypocenter of the earthquake (cross) and aftershock area (shaded area) projected on the fault plane. (After KING et al., 1977.)<sup>14)</sup>

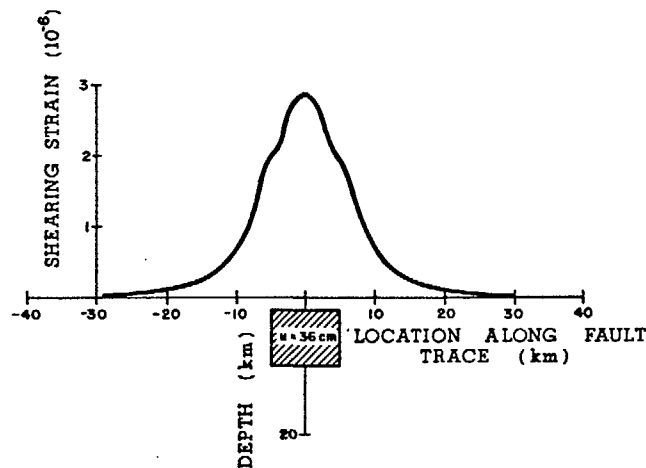


Figure 32. Theoretical shear strain steps along the surface trace of a vertical strike-slip fault in a uniform half-space caused by a uniform offset of 16 cm over a rectangular fault area 10 km long and 2 to 10 km in depth range. (After KING et al., 1977.)<sup>14)</sup>

their amplitudes are about 2 orders of magnitude larger than expected for the strain field of the associated earthquake, based on a dislocation model on the assumption of a homogeneous crust (Figure 32).

#### Acknowledgements

This paper benefitted from reviews by W.P. Irwin, J.C. Savage and especially W.R. Thatcher.

#### REFERENCES

- Chung, Y., Radon Variation at Arrowhead and Murrieta Springs: Continuous and Discrete Measurements, *PAGEOPH*, **122**, 294-308, 1985.
- Clements, W.E., The effect of atmospheric pressure variation on the transport of  $^{222}\text{Rn}$  from the soil to the atmosphere, Ph.D. thesis, New Mexico Inst. Mining Technol., 1974.
- E, X., and Yang, Y., Characteristics of radon anomalies before large earthquakes, in *Collected Reports in Seismo-Hydrogeochemistry*, pp. 93-107, State Seismological Bureau, Division of Scientific Research, Beijing (in Chinese), 1978.
- Hauksson, E., Radon content of groundwater as an earthquake precursor: Evaluation of worldwide data and physical basis, *J. Geophys. Res.*, **86**, 9397-9410, 1981.
- Holub, R.F., and Brady, B.T., The effect of stress on radon emanation, *J. Geophys. Res.*, **86**, 1776-1784, 1981.
- Irwin, W.P., and Barnes, I., Tectonic relations of carbon dioxide discharges and earthquakes, *J. Geophys. Res.*, **85**, 3115-3121, 1980.
- Ishibashi, K., Two categories of earthquakes precursors, physical and tectonic, and their roles in intermediate-term earthquake prediction, *PAGEOPH*, **126**, 687-700, 1988.
- Isreal, H., and Björnsson, S., Radon ( $\text{Rn-222}$ ) and Thoron ( $\text{Rn-220}$ ) in soil air over faults, *Z. Geophys.*, **33**, 48-64, 1967.
- Junge, C.E., Air chemistry and radiochemistry, Academic Press, New York and London, 1963.
- Katoh, K., Takahashi, M., and Yoshikawa, K., Anomalous increase of radon concentration as precursor on some active faults near epicenter of the western Nagano prefecture earthquake, 1984 using cellulose nitrate film, *Zisin* (in Japanese) **39**, 47-55, 1986.
- King, C.-Y., Radon emanation on San Andreas fault, *Nature*, **271**, 516-519, 1978.
- King, C.-Y., Radon monitoring for earthquake prediction in China, *Earthquake Prediction Research*, **3**, 47-68, 1985.
- King, C.-Y., Gas geochemistry applied to earthquake prediction: An overview, *J. Geophys. Res.*, **91**, 12,269-12,281, 1986.
- King, C.-Y., and Slater, L.E., A comparison of soil-gas radon and crustal strain data (abstract), *Earthquake Notes*, **49**(4), 44, 1978.
- King, C.-Y., Nason, R.D., and Burford, R.O., Coseismic steps recorded on creepmeters along the San Andreas fault, *J. Geophys. Res.*, **83**, 1655-1662, 1977.
- King, C.-Y., Evans, W.C., Presser, T., and Husk, R.H., Anomalous chemical changes in well waters and possible relation to earthquakes, *Geophys. Res. Lett.*, **8**, 425-428, 1981.
- Kita, I., Matsuo, S., and Wakita, H.,  $\text{H}_2$  generation by reaction between  $\text{H}_2\text{O}$  and crushed rock: An experimental study on  $\text{H}_2$  degassing from the active fault zone, *J. Geophys. Res.*, **87**, 10,789-10,795, 1982.
- Norton, D., and Knapp, R., Transport phenomena in hydrothermal systems: The nature of porosity, *Am. J. Science*, **77**, 913-916, 1977.
- O'Neil, J.R., and King, C.-Y., Variations in stable isotope ratios of groundwaters in seismically active regions of California, *Geophys. Res. Lett.*, **8**, 429-432, 1981.
- Sano, Y., Nakamura, Y., Wakita, H., Notsu, K., and Kobayashi, Y.,  $^3\text{He}/^4\text{He}$  ratio anomalies associated with the 1984 western Nagano earthquake: possibly induced by a diapiric magma, *J. Geophys. Res.*, **91**, 12291-12295, 1986.



21. Sato, H., Temporal change in scattering and attenuation associated with the earthquake occurrence – A review of recent studies on Coda waves, *PAGEOPH*, 126, 465–497, 1988.
22. Shapiro, M.H., Rice, A., Mendenhall, M.H., Melvin, J.D., and Tombrello, T.A., Recognition of environmentally caused variations in radon time series, *PAGEOPH*, 122, 309–326, 1985.
23. Sugisaki, R., Deep-seated gas emission induced by the earth tide: A basic observation for geochemical earthquake prediction, *Science*, 212, 1264–1266, 1981.
24. Sugisaki, R., and Sugiura, T., Gas anomalies at three mineral springs and a fumarole before an inland earthquake, central Japan, *J. Geophys. Res.*, 91, 12,296–12,304, 1986.
25. Teng, T., and Sun, L.-F., Research on groundwater radon as a fluid phase precursor to earthquakes, *J. Geophys. Res.*, 91, 12,305–12,313, 1986.
26. Wollenberg, H.A., Straume, T., Smith, A.R., and King, C.-Y., Variation of Radon 222 in soil and ground water at the Nevada Test Site, Lawrence Berkeley Lab. Rep. LBL-5905, 1977.
27. Yang, Y., Mu, S., and E, X., Spike-like ground-water radon changes prior to earthquakes, *Ti Chen K'o Hsueh Yen Chiu* (Seismological Res.), no. 1, 34–38 (in Chinese), 1982.
28. Yanitskiy, I.N., Borobeynik, V.M., and Sozinova, T.V., Expression of crustal faults in helium field, *Geotectonics*, 9, 378–384, 1975.
29. Ying, H., Song, G., and Zhen, Y., Fundamental characteristics of ground-water radon anomalies associated with the Tangshan, Haicheng and Bohai earthquakes, in *Collected reports in Seismo-hydrogeochemistry*, pp. 17–41, State Seismological Bureau, Division of Scientific Research, Beijing (in Chinese), 1978.
30. Ying, H., E, X., Leu, H., and Ying, S., Preliminary analysis of the characteristics of ground-water radon changes before the Tangshan earthquake, in *Surveys and studies of Tangshan earthquake*, pp. 149–156, State Seismological Bureau, Division of Scientific Research, Earthquake Publisher, Beijing (in Chinese), 1981.

## RADON MEASUREMENTS IN AUSTRIA AND SOME BASIC PROBLEMS IN EARTHQUAKE PREDICTION RESEARCH

H. FRIEDMANN

Institut für Radiumforschung und Kernphysik,  
Vienna, Austria

### Abstract

Some basic problems in earthquake prediction research are discussed in connection with the analysis of spring water radon ( $^{222}\text{Rn}$ ) measurements in Austria. Two possibilities for the definition of an anomaly are proposed. In the analysed data two periods of outstanding radon concentration could be observed. The data were carefully analyzed using different methods but the extreme radon concentrations could not be explained by an influence of vadose water or by meteorological effects or other non-tectonic disturbances. These two periods were identified as anomalies when using the proposed definition of anomaly. Contingency table tests give high probabilities (>90%) for a correlation between certain earthquakes and the observed radon anomalies. The investigations result in the following hypothesis: The probability for the occurrence of an earthquake in the area  $42^{\circ}\text{N} \leq \varphi \leq 47.5^{\circ}\text{N}$ ,  $13^{\circ}\text{E} \leq \lambda \leq 20^{\circ}\text{E}$ , Friuli area excluded, with a magnitude  $M$  greater as a certain well defined level, increases during the time of an anomaly in the radon concentration of the Freibadquelle by about a factor of ten. To test this hypothesis a new set of radon data is necessary. However this new set of radon data is still not large enough to reach a sufficient statistical proof.

Finally some recommendations are given in order to improve the possibilities for comparing and judging predictions.

### 1 INTRODUCTION

From earlier investigations it is known that the behaviour of the radon ( $^{222}\text{Rn}$ ) concentration in the water of springs can show quite different characteristics. There are springs with fluctuations in the radon concentration of less than 5% over many years, but others show changes in the radon content of more than 100%. Most of these large fluctuations are due to meteorological effects. But sometimes earthquakes seem to be correlated to such anomalies (see e.g. Wakita 1978, Teng 1980, Hauksson 1981, Wakita 1988), or even to anomalies in the radon content in soil gases (King 1980, 1986). A few years ago many scientists were very optimistic concerning future earthquake predictions because of many different observed precursory effects. Meanwhile this first optimism decreased a little bit because neither has any single type of precursor effect been observed before all earthquakes, nor has any single anomaly always successarily been followed by an earthquake. Therefore we have to realize that earthquake prediction will need a rather long time of scientific research with elaborated statistical tests instead of unique predictions based on single anomalies.

However before predicting an earthquake we have to detect earthquake precursors. One of the most critical questions is what can be regarded as an earthquake precursor. The IASPEI sub-commission on Earthquake Prediction defines an precursor 'as a quantitatively measurable change in an environmental parameter that occurs before mainshocks, and that is thought to be linked to the preparation process for this mainshock' (Wyss 1991). To fulfil this definition we have to solve two main problems:

The first concerns the change in the measurable environmental parameter. How can we distinguish between non tectonic influences on such a parameter which in nearly every case causes background fluctuations, from influences which precede earthquakes - We are looking for anomalies, however how do we define an anomaly?

The second problem is to relate a detected anomaly to a certain earthquake. Because earthquakes and its precursors cannot be repeated as in a laboratory experiment, we need either a set of data which gives a statistically satisfactory probability for a correlation between observed effect and subsequent earthquake or a good theory which explains such effects and which may be verified in a certain sense in small scale laboratory experiments

Here some of these problems shall be discussed in relation to radon measurements in Austria

## 2 MEASUREMENTS

From earlier investigations (Friedmann 1984) the radon concentration of more than 100 springs in Austria and their response to different influences is known. With this experience 5 springs were selected which seemed to give the best chance for detecting tectonic effects. The radon concentration of these 5 springs was then continuously monitored. This was done by a system as described by Friedmann et al (1978) and Friedmann (1983). Four of these springs were found to be not suitable for further investigations because of either very constant radon concentration over years, or strong fluctuations correlated to meteorological effects or certain human activities like pumping etc. The remaining spring was the 'Freibadquelle' of Warmbad Villach (46°6'N/13°8'E). It is situated on a lateral fault of the 'Periadriatische Naht', a fault zone system in W-E direction near the Austrian-Italian border (Kahler 1983, Stiny 1937). The temperature of the water varies between 25°C and 27°C. Investigations concerning stable light isotopes as well as tritium measurements show a slight influence of surface water in the spring (Zoyer 1980). The measured radon concentration in the spring since 1977 can be seen from fig 1 (dotted lines are extrapolated data).

The Freibadquelle is one of several springs lying close together and showing the same hydrogeological and chemical behaviour. These springs have all similar radon concentrations and all carry with the water a small amount of spring gas with a radon concentration which is about four times the radon concentration in the water. This means an equilibrium distribution between the radon in the gas and in the water.

From fig 1 we find two periods of extreme radon concentration. First we have to search for possible influences of non tectonic effects. The most interesting parameters which may influence the radon concentration in the spring are meteorological effects like precipitation and air pressure and influences of vadose water, especially temperature and level.

In a first step it was checked if vadose water may have caused the very high radon concentrations. There are several wells around the Freibadquelle with a water level just a few meters below the surface. This water is either pure rain water or has sometimes only a very small component of ground water. The level and the temperature are weekly recorded by the 'Hydrographischer Dienst', however there are some data missing. For this reason and because all the wells show very similar behaviour the mean of the temperature and the mean of the level of these wells (within a distance of 500 m around the spring) are compared with the radon concentration in the Freibadquelle. Water temperature and water level show typically seasonal effects but no apparent anomaly (fig 2). More detailed cross correlation analyses between the well water temperature and the radon data show clear one year periods. This means that the very high radon concentrations in the spring fits nearly equally well to the well water data shifted for one or more years. In other words: no significant deviation from

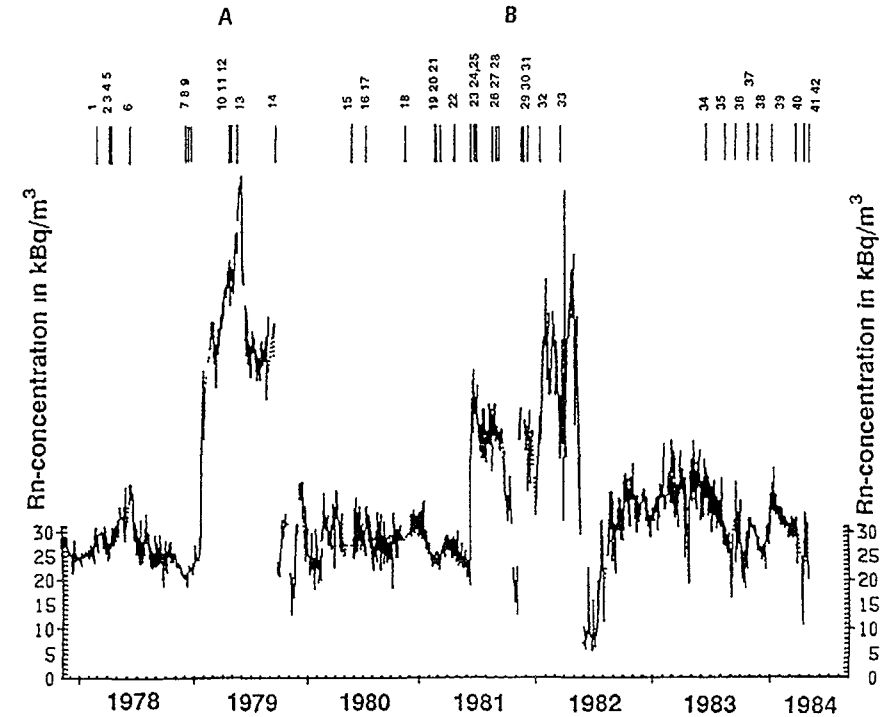


Fig 1 Radon concentration in the spring of Warmbad Villach (Freibadquelle)

seasonal effects could be detected in the well-water temperature. In the case of the well water level, the one year period in the correlation coefficients cannot be seen so clearly. The reason is a broader variation in the well-water level as a consequence of variations in the precipitation. Comparing fig 1 and fig 2 we see that first period of extreme radon concentration (marked 'A' in fig 1) corresponds to a relatively high well-water level, while the second period of extreme radon concentration (marked 'B' in fig 1) occurred during a mean (or even lower) well-water level. So the value of the unshifted correlation coefficient (fig 3) is mainly caused by period A while period B contributes only marginally. When shifting the data sets in such a way that period B correlates to a high well-water level, then period A nearly does not contribute to the correlation coefficient. In any case no shifting is possible so that both periods contribute substantially to the corresponding correlation coefficient without cancelling mutually. We have to conclude that there does not exist any simple correlation between well-water data and the observed extreme radon data. However, this does not mean that vadose water has no effect on the radon concentration in the spring, it only means that vadose water is not responsible for the very high radon concentration.

The same type of correlation analyses was done for the atmospheric pressure. There are no indications of an influence from the atmospheric pressure on the radon concentration in the

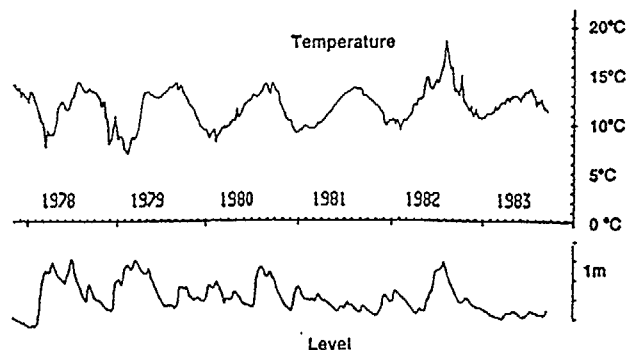


Fig.2: Well-water temperature and well-water level around the spring of Warmbad Villach (mean of several wells).

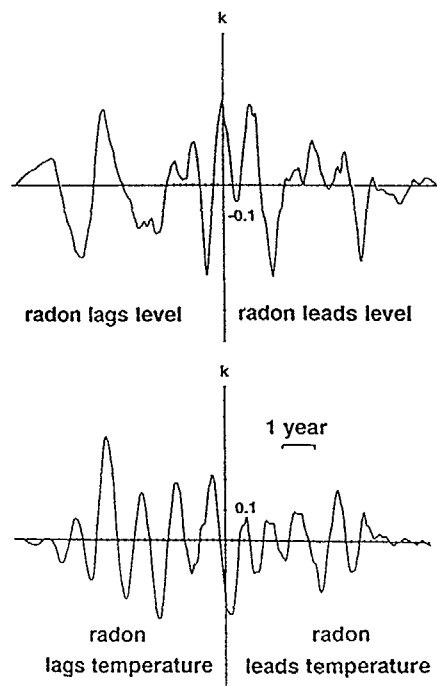


Fig.3: Cross correlation well-water level versus radon and cross correlation well-water temperature versus radon.

spring either in the case of the anomalies or during the 'normal' concentration. This result is consistent with these on hydrogen and carbon dioxide from Sugisaki et al. (1983) for deeper, and especially confined aquifers. The fact that the radon concentration in the spring is not significantly affected by meteorological parameters is in welcome contrast to the radon concentration in soil gas which is often strongly correlated to the time derivation of the atmospheric pressure.

Precipitation may also create radon anomalies. However analyses of these data, as well as analyses of air temperature data did not show any anomalous behaviour prior to or during the radon anomalies. Therefore we conclude that the observed anomalies cannot be attributed to meteorological effects. Nevertheless Fourier analyses of the radon data show typical one year periods, so a small influence of meteorological effects is very probable, which is in agreement with investigations by Zojer (1980) who indicated an influence of surface water in the spring.

No artificial disturbances of the aquifer like pumping, drilling etc. could be identified during or before period A. But there was a pumping test in a newly drilled bore-hole from June 9 to 12, 1981, just prior to period B. The bore-hole has a depth of 268 m and is situated about 100 m away from the observed spring. The proximity to the spring and the correspondence in time (anomaly B started on June 13, 1981, at about 23.30 h) suggests a causal connection between pumping and the high radon concentration. However, it seems very unlikely that this relatively short pumping test can cause an one-and-a-half-year anomaly. There is a second, even stronger argument that this pumping test was not the reason for the high radon concentration. From April 18 to May 5, 1983 there was another pumping test with nearly equal pumping rates without any succeeding high radon data. These arguments negate a connection between the extreme radon concentration during period B and the pumping test.

No influence could be found which may have caused the observed high radon concentrations. Therefore we cannot correct our data for such influences. Of course the one-year period can be eliminated from the data however the applied analysis is not influenced very much by such a correction. So we used the original radon data for our analysis.

In the next step we have to ask if the extreme radon concentrations are anomalies or only random fluctuations. In our case it seems to be clear, however in some papers it is often not clear why certain data are claimed to be an anomaly and other data are assumed as statistical fluctuations (noise). Let us define an anomaly as a statistical significant deviation from the normal value. Thus we must explain what is the 'normal' value and what means 'statistical significant'.

To find the 'normal' value the frequency distribution of the radon data is computed (fig. 4). Under the assumption that anomalies are rather rare events the radon concentration shall be distributed around a mean concentration. Therefore if a main peak in the frequency distribution can clearly be seen then the maximum of this peak should be called 'normal' value. If this peak is approximately Gauss shaped a standard deviation can be derived. In our case the 'normal' value is  $26 \text{ kBq/m}^3$  ( $0.70 \text{ nCi/l}$ ) and the standard deviation is  $4 \text{ kBq/m}^3$  ( $0.11 \text{ nCi/l}$ ). This value is in reasonably good agreement with earlier measurements - 1908:  $0.73 \text{ nCi/l}$  (Österr. Bäderbuch 1928); 1929:  $0.62 \text{ nCi/l}$  (Mayer 1929); 1959:  $0.36 \text{ nCi/l}$  (Komma et al. 1962); 1965:  $0.50 \text{ nCi/l}$  (Scheminzky et al. 1966); 1976:  $0.75 \text{ nCi/l}$  (Friedmann et al. 1977).

To find a criteria for 'statistical significant' is a much more complicated problem. The radon data are strongly correlated within time intervals which primarily are not known. So the value and the duration of an outstanding radon concentration can be used as criteria for statistical significance only in connection with the total time of observation. This means with an increasing time of observation decreases the relative duration of the extreme radon concentration and finally the value and the duration of such a period will fall within the expectation limits of an adopted unconfined distribution (in most cases a normal distribution will be appropriate). If we know the time  $\tau$  between two radon data which guarantees mutual

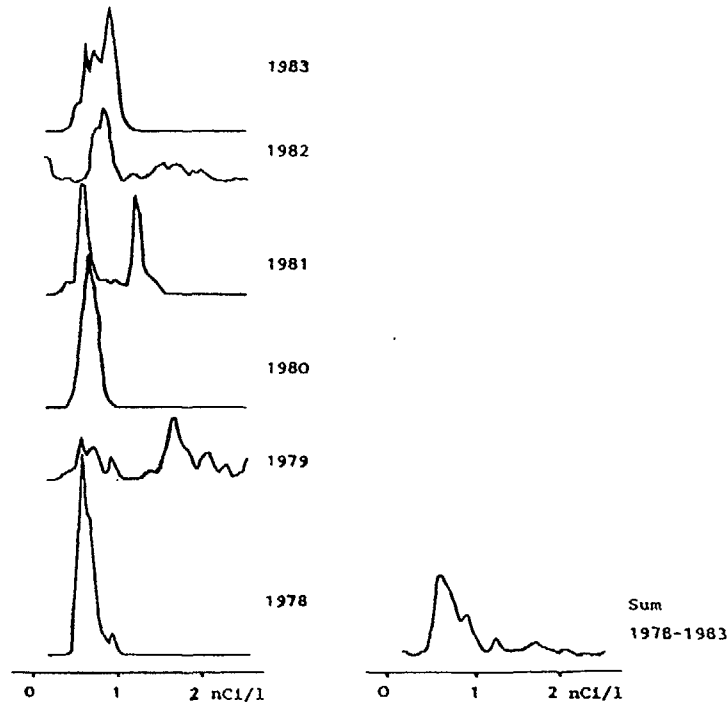


Fig.4: Radon frequency distribution in arbitrary units (1978-1983).

independence we can calculate the probability  $W(R,T)$  for an radon concentration of an amplitude  $R$  and a duration  $T$  under the assumption of a probability density function  $p(R)$  or a distribution function

$$P(R) = \int_{-\infty}^R p(r) \cdot dr. \quad (1)$$

The probability for measuring a value greater or equal  $R$  is  $1-P(R)$ . The probability for measuring successively a value greater or equal  $R$  in time intervals  $\tau$  for a time  $T$  becomes

$$W(R,T) = [1-P(R)]^{T/\tau} \quad (2)$$

Then an observed radon concentration with a level  $R$  and a duration  $T$  is declared as an anomaly if its probability is below a certain predefined limit.

One shortcoming of such a definition is the exponent  $T/\tau$ . The problem concerns the estimation of  $\tau$ . From short time fluctuation one can assume  $\tau$  to be in the order of about a

day. For very short outstanding radon concentrations and if only one observed value has an extreme amplitude (time intervals between subsequent measurements greater than  $\tau$ )  $T/\tau = 1$  must be taken.

The other shortcoming is a possible non stochastic background which could not be eliminated by a preceding mathematical treatment of the measured data. Such a non stochastic background would shift the 'normal' value and lead to a false derivations of the 'normal' value resulting in false probabilities for the deviations from the normal value.

Finally an on-line analysis of radon data with this type of anomaly definition may suffer from a certain delay in detecting an anomaly.

So we tried to apply another definition of anomaly which has not such a clear mathematical basis, however which seems more convenient for the user. First the 'normal' value is determined as described before. Then the data are smoothed by a type of low pass filter with a time constant of about a year. A long term anomaly is defined as a deviation of the smoothed radon data from the 'normal' value by more than 3 times the standard deviation and a short term anomaly is defined by a deviation of the actual radon data from the smoothed data by more than 3 standard deviations.

In 1979 and in 1981/82 the values and the durations of the deviations from the 'normal' radon concentration were far beyond statistical limits, therefore these two periods can be identified as periods of abnormal radon concentration. According to the definition of anomalies the abnormal radon concentration in 1981/82 must be regarded as two separate anomalies. For simplification these anomalies were treated as only one anomaly. This will not have any consequences in the subsequent data analysis.

Repeated tests of the apparatus were performed during and after the anomalies, so there is no question about the reliability of the data. For technical reasons, it could not be determined if the observed radon anomalies are due to a higher radon concentration in the water or due to an increase in the total gas content of the water.

### 3. RADON AND EARTHQUAKES

In the next step earthquakes were examined as possible reasons for the radon anomalies. First it was to decide which earthquakes must be taken into consideration. If the maximum possible distance  $D$  between the epicentre of a forthcoming earthquake and the spring which can be influenced by this earthquake is proportional to the volume of the pre-stressed lithosphere or to the energy of the earthquake respectively, a relation of the form

$$M = a \cdot \log(D) + b \quad a, b = \text{const.} \quad (3)$$

must hold. From known relations between magnitude  $M$  and the volume of the focal zone the  $a$ -value can be determined to about 2. More sophisticated analyses were done by Fleischer (1981) and especially by Dobrowolsky et al. (1979). Both found relations of the form (3). By collecting and analyzing radon anomaly data Hauksson et al. (1981) found a similar relation. It is most important that all these relations do not differ by more than 30% in  $D$  for  $M \geq 4$ . Hauksson's parameter result in the greatest  $D$ -values for  $M \geq 4$ . For this reason these parameters were used but modified by 0.3 to allow for uncertainties in the determination of  $M$ .

$$M \geq M_{\min} = 2.4 \cdot \log(D) - 0.43 - 0.3 \quad (4)$$

In this way all earthquakes which may have caused the radon anomalies should be found. They are listed in tab.1

Table 1. All earthquakes between Nov. 1977 and April 1984 which fulfill relation (4). Earthquakes in the Friuli area are marked by an asterisk. The characters on the left margin indicate earthquakes within the time of the radon anomalies A resp. B.

Earthquake	Date	N/E	M	d(km)	M <sub>min</sub>
#1	78 02 20	46.45/13.33	4.0	39.6 *	3.4
#2	78 04 02	46.27/13.35	3.5	50.2 *	3.7
#3	78 04 03	46.16/13.19	4.2	67.6 *	4.0
#4	78 04 06	46.28/13.31	3.4	51.6 *	3.7
#5	78 04 30	46.22/13.21	3.8	61.8 *	3.9
#6	78 06 20	40.74/23.23	6.8	998.0	6.8
#7	78 12 06	46.32/13.25	3.5	52.4 *	3.7
#8	78 12 12	46.13/12.71	4.4	89.5 *	4.3
#9	78 12 17	46.11/14.11	3.9	59.4 *	3.8
A #10	79 04 15	42.09/19.20	6.9	659.5	6.3
A #11	79 04 15	42.32/18.68	6.3	612.9	6.3
A #12	79 04 18	46.31/13.25	4.8	53.0 *	3.7
A #13	79 05 24	42.26/18.75	6.8	621.7	6.3
A #14	79 09 19	42.81/13.06	5.8	425.2	5.9
#15	80 05 18	43.29/20.84	6.4	664.3	6.3
#16	80 07 09	39.27/23.04	7.0	1106.9	6.9
#17	80 07 09	39.26/22.56	6.7	1081.8	6.9
#18	80 11 23	40.91/15.37	6.5	644.7	6.3
#19	81 02 24	38.22/22.93	7.1	1193.4	7.0
#20	81 02 25	38.12/23.14	6.8	1213.2	7.0
#21	81 03 04	38.21/23.29	7.0	1212.9	7.0
#22	81 04 23	46.34/13.28	3.5	49.2 *	3.6
#23	81 06 10	46.43/13.31	3.6	41.9 *	3.5
B #24	81 06 15	47.06/14.69	3.9	84.8	4.2
B #25	81 06 28	46.47/12.93	3.8	68.0 *	4.0
B #26	81 08 13	44.82/17.26	5.8	333.4	5.6
B #27	81 08 30	46.36/13.29	4.3	47.3 *	3.6
B #28	81 08 31	46.33/13.35	3.4	45.6 *	3.6
B #29	81 12 03	46.35/13.63	2.9	30.6 *	3.1
B #30	81 12 05	46.32/12.69	4.4	90.5 *	4.3
B #31	81 12 19	39.37/25.25	6.9	1227.3	7.0
B #32	82 01 18	39.97/24.41	7.0	1129.3	6.9
B #33	82 03 16	46.15/16.13	4.7	185.5	5.0
#34	83 06 17	46.33/12.93	5.0	73.0 *	4.0
#35	83 08 06	40.14/24.79	6.7	1139.8	6.9
#36	83 08 31	46.77/10.49	5.1	253.0	5.3
#37	83 10 18	46.69/13.90	3.1	12.8 *	2.2
#38	83 11 09	44.70/10.30	5.5	344.2	5.7
#39	83 12 20	46.33/13.33	3.5	46.8 *	3.6
#40	84 03 11	45.88/15.49	4.5	152.5	4.8
#41	84 04 15	47.68/15.87	4.8	197.2	5.1
#42	84 04 29	43.23/12.48	5.7	388.6	5.8

During anomaly A (fig. 5) the maximum of the radon concentration coincides with the catastrophic earthquakes ( $M_{\max} = 6.9$ ) in Montenegro (Nos. 10, 11, 13; distance about 600 km). The radon concentration returns to its normal value just at the time of a  $M = 5.8$  earthquake in Central Italy. Compared to anomaly A, anomaly B (fig. 6) shows quite another behaviour. The anomaly started with a much faster increase and did not show such a homogeneity as anomaly A. Just a day after the first increase of the radon concentration a  $M = 3.9$  earthquake occurred in a distance of 85 km to the spring (No. 24 in tab. 1 and figs. 1 and 6). In the second part of the anomaly an addition spike in the radon concentration can be found, but no earthquake fulfilling (4) could be identified at this time. The only earthquake which may be of interest has a magnitude below 3 and a distance of 92 km, so it does not fulfil relation (4).

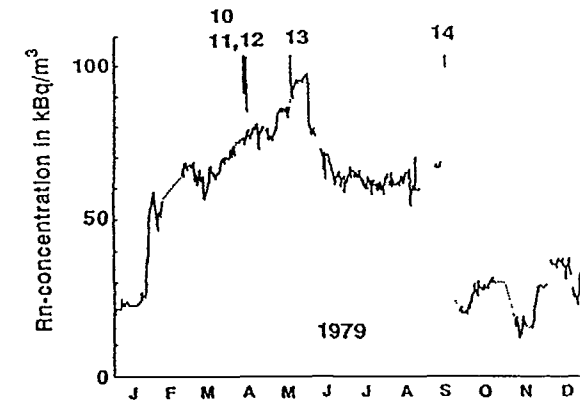


Fig.5: Radon concentration during radon anomaly A. Earthquakes fulfilling relation (2) are indicated by lines. The numbers correspond with the numbers in tab.1.

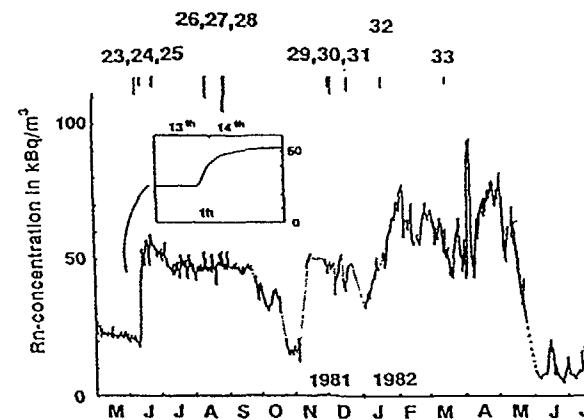


Fig.6: Radon concentration during radon anomaly B. Earthquakes fulfilling relation (2) are indicated by lines. The numbers correspond with the numbers in tab.1.

To check for a correlation between earthquakes and the observed radon anomalies we test if the earthquakes are randomly distributed in time or if the earthquakes occurred mainly during the anomalies. If the probability for the occurrence of an earthquake fulfilling (4) in a certain time interval is proportional to the length of this interval and the earthquakes are mutually independent (random distribution), the time intervals between two earthquakes are exponentially distributed. If the earthquakes are randomly distributed the probability for the occurrence of an earthquake is constant for any given time interval. This can be tested by a 2x2 contingency table. The observed time interval is 2367 days with 564 days of anomalous radon concentration. Distinguishing days with and without 'relation (4)'-earthquakes, we get the following scheme:

Days with	quake	no quake	Sum
Rn anomaly	14	550	564
no Rn anomaly	26	1777	1803
Sum	40	2327	2367

The 2x2 contingency table test gives a  $\chi^2=2.8$  which means a 95% probability for a non-random distribution (Woolf test:  $G=2.6$ , 94% significance; Fisher test: 93% significance).

Many earthquakes from tab. 1 do not coincidence with radon anomalies. Obviously we cannot assume a global earthquake sensitivity of the spring for all the different earthquake areas. However, it can be supposed that earthquakes with about the same magnitude, same depth and from the same area will influence the water system of the observed spring in the same way. For instance many earthquakes in the Friuli area (marked by an asterisk in tab. 1) do not coincide with radon anomalies. In consequence the observed radon anomalies can not be related to the coincident Friuli earthquakes. Using the same argument earthquakes in Greece and in South Italy cannot be responsible for the radon anomalies. In contrast to that one may assume an influence of the northern Balkan region to the spring because of the direction of the main faults and the tectonic stress distribution (Ritsema, 1974). Therefore it would be interesting to check this area separately.

Restricting to the earthquakes in the region  $42^\circ N \leq \varphi \leq 47.5^\circ N$ ,  $13^\circ E \leq \lambda \leq 20^\circ E$ , Friuli area excluded, we get the following table:

Days with	quake	no quake	Sum
Rn anomaly	7	557	564
no Rn anomaly	2	1801	1803
Sum	9	2358	2367

The computed  $\chi^2=14.5$  excludes a random distribution between earthquakes and radon anomalies on a >99% level (Woolf test:  $G=11.7$ , >99% significance; Fisher test: >99% significance). The same test for all earthquakes except those in the selected region, including the Friuli area, gives a probability of 87% for a random distribution. In consequence we conclude that the probability for the occurrence of an earthquake during an anomaly in the selected region is significant different from those during the time of a normal radon concentration.

The anomalies start before the earthquakes (especially anomaly A and the second part of anomaly B, see figs. 1,5,6 and tab.1). Therefore the radon anomalies could not be caused by transient strains from the seismic waves of the earthquakes. Such an effect would be useless for earthquake predictions.

If the occurrence of earthquakes is randomly distributed during the time of the normal radon concentration and also randomly distributed during the time of the anomalies, but with another (constant) probability, we can compute this probability. The probability for the occurrence of an earthquake is the number of days with an earthquake divided by the number of observation days. Applied on all earthquakes fulfilling relation (4) we get an earthquake-probability for the time of normal radon concentration of  $W_{n1} = 0.014 \pm 0.003$  per day and for the time of an anomaly  $W_{a1} = 0.028 \pm 0.007$ . The quoted error represents one standard deviation and is derived from the square root of the number of quakes. Restricting to the selected region ( $42^\circ N \leq \varphi \leq 47.5^\circ N$ ,  $13^\circ E \leq \lambda \leq 20^\circ E$ , Friuli area excluded) there were only two earthquakes during 1803 days without a radon anomaly. This means an earthquake probability of  $w_{n1} = 0.0011 \pm 0.0007$  per day. For the time of radon anomalies we get a probability of  $w_{a1} = 0.011 \pm 0.004$  per day which means an increase of a factor of ten. The uncertainties are relatively large but this is due to the small number of earthquakes during the time of investigation.

The probability for the occurrence of an earthquake within k days can be computed to

$$w_k = 1 - (1 - w_1)^k \quad (4)$$

and the standard uncertainty becomes

$$\delta w_k = k \cdot (1 - w_1)^{k-1} \cdot \delta w_1 \quad (5)$$

This means for a 20 day period during a normal radon concentration a 2% ( $w_{n20} = 0.022 \pm 0.014$ ) probability for an earthquake in the selected region with a magnitude according to relation (4) and for a 20 day period during an anomalous radon concentration a 20% ( $w_{a20} = 0.20 \pm 0.06$ ) probability for an earthquake.

#### 4 CONCLUSION

In most cases it is difficult or even impossible to relate a radon anomaly to a certain earthquake. This makes the interpretation of anomalies sometimes obscure. To avoid these problems a statistical approach was tried. A statistically significant increase in the number of earthquakes which fulfil relation (4) could be observed during the time of radon anomalies in the observed spring of Warmbad Villach. The correlation to the radon anomalies was even stronger for the earthquakes in the region  $42^\circ N \leq \varphi \leq 47.5^\circ N$ ,  $13^\circ E \leq \lambda \leq 20^\circ E$ , Friuli area excluded. For the time of a radon anomaly a substantial increase (factor of 10) in the probability for the occurrence of an earthquake could be found.

At this time the results of our investigations have to be taken as a hypothesis because the assumed sensitivity of the Freibadquelle must be proved by another, different set of data. Today this new set of radon data is still not large enough to reach a sufficient statistical proof.

#### 5 RECOMMENDATIONS

In many papers on earthquake prediction research is a lack of exact mathematical treatment of the data. This concerns many parts of the investigations. First there is often no definition of an anomaly and the definition of a precursor is not given. Even the definition of prediction is not always clear (a prediction is a conclusion derived from several precursors and adequate theory). In the case of an earthquake prediction (even for a 'a posteriori' prediction) the

increase in the probability for the occurrence of an earthquake in a certain time, magnitude and location window after a certain precursor is a key value and should always be given. It would also be interesting to compare different predictions. Perhaps this may be done by introducing a quality factor which is a function of the predicted entrance windows for the quake, the probability and the mean recurrence periods of earthquakes in the considered area. If the predicted probability for an earthquake is near to one we can ask for the reliability of the prediction. The reliability of a prediction is not directly related to the probability for the occurrence of an earthquake because it does not include only the probability for false alarms but also the probability for not predicting some quakes. Finally the two anticorrelated quantities quality and reliability should be combined as a measure for the scientific value of an earthquake prediction.

Many researchers do not agree to such a strict mathematical treatment. They argue that e.g. precursors based on strange behaviour of animals etc. cannot be treated as some measured data like radon concentrations. I agree to that, however I do not agree to the declaration that there is no way to deduce some measurable data which afterwards can be used for statistical analyses.

To make predictions more transparent and to help avoiding predictions with insufficient statistical proof the complete measured data sets and the methods for evaluating the data should be available for all researchers in the field of earthquake prediction.

Concluding the previous statements the following recommendations are given:

- a) All supposed earthquake forerunners should be described in full detail, but also some quantitative data should be derived, which allows anyone to use the data for statistical tests.
- b) Anomalies and precursors should be defined in a mathematical exact way.
- c) Predictions should include time, magnitude and location windows as well as a computed increase in the probability for the occurrence of an earthquake compared to the probability which can be derived from historic data (earthquake catalogues - a priori probability).
- d) A quality factor should be introduced to compare predictions with different entrance windows and different a priori earthquake probabilities.
- e) For predicted earthquake probabilities near to one a measure for the reliability of an earthquake prediction as a function of false alarms and missed quakes should be introduced.
- f) The scientific value of a prediction should be deducible from the combination of the quality factor and the reliability factor and perhaps some additional parameters.
- g) Data and evaluation methods should be available for researchers who are specially interested in the field. Maybe an international organisation like the IAEA can manage the exchange of data and codes.

## REFERENCES

- Dobrowolsky, I.P., S.I. Zubkov, V.I. Mjachkin 1979. Estimation of the size of earthquake preparation zones. *Pure Appl. Geophys.* 117: 1025.
- Fleischer, R.L. 1981. Dislocation model for radon response to distant earthquakes. *Geophys. Res. Lett.* 8: 477.
- Friedmann, H., F. Hernegger 1977. *Gutachten über den Radon- und Radiumgehalt von Freibad Quelle, Neuer Quelle, Zillerbad Quelle und Tschamer Quelle in Warmbad Villach. (Report to the administration of the spa).*
- Friedmann, H., F. Hernegger 1978. A method of continuous measurement of radon in water of springs for earthquake prediction. *Geophys. Res. Lett.* 5: 565.
- Friedmann, H. 1983. A portable radonmeter. *Rad. Prot. Dos.* 4, No. 2: 119.
- Friedmann, H. 1984. A portable continuously working radon measurement system. *Rad. Prot. Dos.* 7, Nos. 1-4: 531.
- Friedmann H. 1984/85. A theoretical model for the change of shape of spring water radon anomalies with epicentral distance. *Pure and Appl. Geophys.* 122, Nos. 2-4: 531.
- Hauksson, E. 1981. Radon content of groundwater as an earthquake precursor: Evaluation of worldwide data and physical basis. *J. Geophys. Res.* 86, No. B10: 9397.
- Hauksson, E., J.G. Goddard 1981. Radon earthquake precursor studies in Iceland. *J. Geophys. Res.* 86, No. B8: 7037.
- Kahler, F., A. Fritz, H. Janschek, R. Köberl 1983. Beobachtungen und Probleme im Thermalgebiet von Warmbad Villach. *20. Jahrbuch des Stadtmuseums Villach, Neues aus Alt-Villach*, Villach (Austria).
- King, C.-Y. 1980. Episode radon changes in subsurface soil gas along active faults and possible relation to earthquakes. *J. Geophys. Res.* 85: 3065.
- King, C.-Y. 1986. Gas geochemistry applied to earthquake prediction: an overview. *J. Geophys. Res.* 91: 12269.
- Komma, E.G., F. Scheminzy 1962. Untersuchung und balneotherapeutische Beurteilung der Therme von Warmbad Villach. *Techn. Versuchsanstalt am Forschungsinstitut Gastein*, Unters. Prot. Nr. 563/59-566/59, Gastein (Austria).
- Mayer, S. 1929. *Bericht über die Untersuchung der Quellen von Warmbad Villach auf ihren Gehalt an Radium-Emanation. (Report to the administration of the spa).*
- Österr. Bäderbuch 1928. *Offizielles Handbuch der Mineralquellen, Kurorte und Kuranstalten Österreichs.* Volksgesundheitsamt im Bundesministerium für soziale Verwaltung, Österreichische Staatsdruckerei, Wien (Austria).
- Ritsema, A.R. 1974. *The earthquake mechanism of the Balkan region.* UNDP Rem 70/172 UNESCO, de Bilt.
- Scheminzy, F., E.G. Komma 1966. Neue Analyse der Villacher Therme und Kontrolluntersuchungen an deren Nutzungsorten, *Techn. Versuchsanstalt am Forschungsinstitut Gastein*, Unters. Prot. Nr. 804/65-807/65, Gastein (Austria).
- Stiny, J. 1937. Zur Geologie der Umgebung von Warmbad Villach. *Jb. Geol. Bundesanst.* 87, H1/2: 57.
- Sugisaki, R., M. Ido, H. Takeda, Y. Isobe, Y. Hayashi, N. Nakamura, H. Satake, Y. Mizutani 1983. Origin of hydrogen and carbon dioxide in fault gases and its relation to fault activity. *J. Geol.* 91: 239.
- Teng, T. 1980. Some recent studies on groundwater radon content as an earthquake precursor. *J. Geophys. Res.* 85: 3089.
- Wakita, H. 1978. Earthquake prediction and geochemical studies in China. *Chinese Geophys.* 1(2): 443.
- Wakita, H., Y. Nakamura, Y. Sano 1988. Short-term and intermediate-term geochemical precursors. *Pure Appl. Geophys.* 126, Nos. 2-4: 267.
- Wyss, M. (ed.) 1991. Evaluation of proposed earthquake precursors. (IASPEI sub-commission on earthquake prediction). *American Geophysical Union*, Washington D.C.
- Zojer, H. 1980. Beiträge zur Kenntnis der Thermalwässer von Warmbad Villach. *Steirische Beiträge zur Hydrogeologie* 32, Graz (Austria).

## GEOCHEMICAL PRECURSORS OF EARTHQUAKES — EXPERIENCE IN ITALY

M. VALENZA

Istituto di Geochemica dei Fluidi (CNR)

P.M. NUCCIO

Istituto di Mineralogia, Petrografia e Geochemica,  
Università di Palermo

Palermo, Italy

### Abstract

Herewith are presented the results of geochemical observations carried out in Italy over the last years referring to volcanic and seismic areas ( Vulcano, Etna, Eastern Sicily ). The results indicate that some geological parameters can be used as effective precursors of earthquakes; however, the choice of those parameters is strictly related to the geochemical properties of each area. To accomplish the goal of earthquake prediction a multi-disciplinary and methodologically homogeneous approach is here suggested which should be carried out in different areas of the world.

### Introduction

Earthquake prediction is a new subject which has only been studied in the last 20-25 years. Inspite of the fact that this is a very short period of time, abundant information regarding this scientific concept has been acquired. A review of literature, concerning precursors of earthquakes, suggests that many geochemical parameters can be usefully used as indicators of an impending earthquake. In table 1 a summary of geochemical parameters reported as earthquake precursors is shown.

An examination of the behavior of each of these parameters, in different areas, indicate that some important

considerations should be made:

The changes observed in each area before an earthquake are not always the same, both in terms of intensity and type. Some parameters, which can be considered as being precursors in one area, do not show any such change in another area. The time of the appearance of a given precursor, cannot be univocally determined as it is related to the characteristics of each area. These considerations suggest that in order to consider geochemical changes in some parameters as being precursors of an earthquake, it is necessary that the following be known for each area:

- The origin of the fluids

Table 1 - Fluid Geochemical Precursors\*

- a) physical parameters: temp., press., flow rate, water level of wells;
- b) chemical-physical parameters: Eh, pH, conductivity
- c) total amount of gases, vapor-gase and water-gase ratios;
- d) partial pressure of  $H_2$ , He, Rn,  $CO_2$ , Ar,  $H_2S$ , CO,  $CH_4$ ,  $O_2$ ,  $N_2$ ;
- e) concentration in water of the gases mentioned in d) and of Na, K, Ca, Mg,  $NH_4$ , Hg, Si, B, F, Cl,  $SO_4$ ,  $HCO_3$ , radioactive elements;
- f) isotopic ratios of  $^3He/^4He$ ,  $^{13}C/^{12}C$ , -

\* From Carapezza, Nuccio & Valenza (1981)

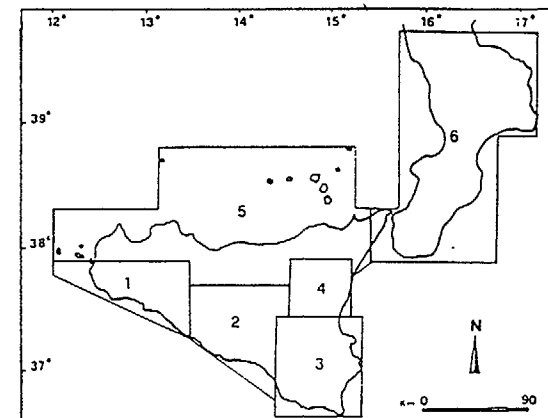


Figure 1 - Seismic zoning of Sicily and Calabria (Italy). From Cosentino M- (1987).

- The circulation mechanism of the fluids  
The interaction between different geochemical spheres (lithosphere, hydrosphere, atmosphere etc.). In other words, it is necessary to elaborate a "geochemical model" of the area to be investigated.

### Some Experiences in Italy

It is well known that almost all the Italian peninsula is subject to seismic risk; however the southeast regions, more than the others, showing the highest seismic risk are Calabria and Sicily. Over the last fifteen years some work, focused towards the geochemical prevision of earthquakes, has been done in these regions of Italy.

Based on the records regarding seismic activity and also taking into consideration the structural properties of the mentioned areas, we can recognize within them six main sub-areas (fig.1) (Cosentino M., 1987). In each of these areas geochemical investigations regarding natural fluids (springs, water wells, gaseous manifestations, soil degassing etc.), have been carried out in order to clarify the origin of these fluids and the mechanism of

their circulation. Then, the time dependence of some major parameters has been investigated in some selected points, in order to establish the background of each system and possibly to reveal anomalous variations in time. In one of the investigated areas, a continuous and automatic system which monitors the temperature and reducing capacity of the fumarolic gases has been installed since 1978 in order to evaluate the high frequency variations in relation to both the volcanic and the seismic activity. (Carapezza et.al. 1981).

We will briefly summarize the results obtained in the investigated areas: Vulcano, Mount Etna and the South-Eastern part of Sicily (areas numbers are, respectively: 5; 4; 3; in fig. 1).

### Vulcano

Vulcano is one of the seven islands that constitute the Aeolian archipelago, which is located off the northern part of the Sicilian coast. Since its last eruption (1888-90) the volcanic activity on the island has been characterized by solfataric activity in the crater area and diffuse



manifestations (thermal waters, sub-marine fumaroles, diffuse soil degassing ). Geochemical observations were intensified (Carapezza et al. 1981), in 1977, when the fumarolic activity increased significantly both in terms of output and maximum temperature.

Starting in the summer of 1978, we began to monitor, on a continuous basis, the reducing capacity (R.C.) of the fumarolic gases.

The reduced gases in the fumaroles are mainly  $H_2$ ,  $H_2S$ ,  $CO$ ,  $SO_2$  which are able to give electrons to the surrounding medium (eg. rocks, waters, gases) thus increasing their oxidation number(?).

A special fuel cell designed by Sato (1975), was used to monitor the R.C. of the fumarolic gases (fig. 2 from Carapezza et al. 1981). Several peaks in the R.C. output were registered in the period August-September 1978. Within 30-40 hours from each peak, earthquakes occurred (fig. 3). The epicenters of these earthquakes were located in the Aeolian area (fig. 4 Carapezza et al. 1981).

The peaks in the R.C. activity were interpreted as having been caused by an increase in the hydrogen release as a consequence of the pore pressure drop in the confining rocks. Similar relationships between R.C. and seismic activity have been recorded in the same area in different periods ( Badalamenti et al. 1986 ).

#### Mount Etna

Mt. Etna, the largest and most active volcano in Europe, is located along the Eastern coast of Sicily in a very complex geodynamic context.

Although predominantly effusive, the volcanic activity ranges over a large spectrum of eruptive styles from central to eccentric eruptions (Romano, 1982; Chester et al;

1985). Historical records and descriptions of the seismic activity of Mt. Etna are well reported in several catalogues e.g. (Catalogo ENEL, 1977). An analysis of these data clearly indicate that Mt. Etna's seismicity is mainly located along the

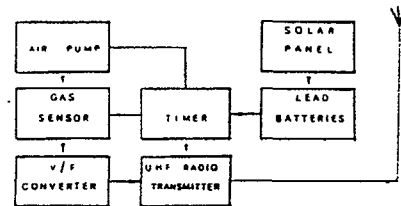


Figure 2a - Scheme of the R.C. automatic monitoring station at Vulcano.

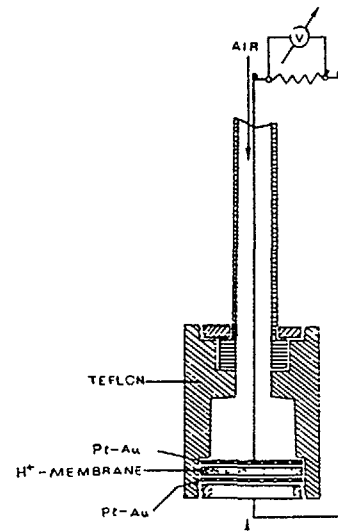


Figure 2b-Design of the reducing capacity sensor. The reduced fumarolic gases (e.g.  $H_2$ ,  $CO$ ,  $H_2S$ ) in contact with the external surface of the sensor are oxidized leaving electrons that flow throughout a resistance; the voltage measured across this resistance is a function of the concentration of the reacting gases (Sato 1975).

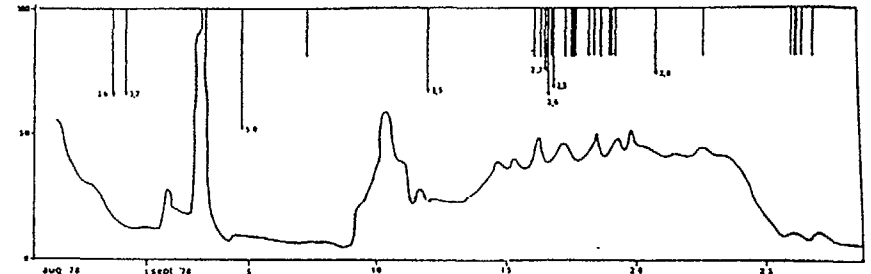


Figure 3 - The R.C. (reducing capacity) variations of the fumarolic gases at Vulcano. Earthquakes (left part of the figure) occurred 30-40 hours after the R.C. peaks. Earthquakes having a magnitude higher than 2 are indicated by arrows. (from Carapezza et al. 1981)

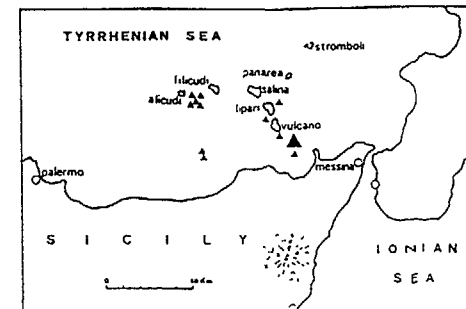


Fig. 4 - The triangles show the position of the epicenters of the earthquakes. The larger triangle indicates the location of the main shock of 16th April 1978.

Eastern flank of the volcano, where highest intensity earthquakes took place (1911-1914, Barbano et al. 1980) and where many tectonic structures are evident. Since 1987 extensive geochemical studies regarding:

- Chemical and isotopic composition of waters (wells, rain, snow)
- chemical and isotopic composition of gaseous manifestations (fumaroles, mofettes)
- Soil  $CO_2$  and Radon degassing have been carried out. ( Anzà et al. 1989).

The main results of these extensive studies can be summarized as follows:

- 1 - The main factor controlling the composition of the waters of the etnean complex is the interaction of rain water with basalts and the principal factor in the chemical watering of volcanites is the supply of  $CO_2$ .
- 2 - The isotopic composition of the interacting  $CO_2$  with waters, point to a primarily magmatic origin of the carbon dioxide ( $\delta^{13}C = -3 \div -4 \text{ ‰}$ ) ( Anzà et al. 1989)

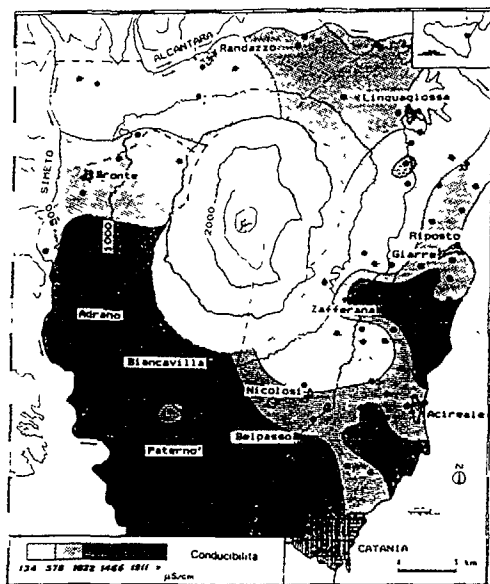


Figure 5 - Spatial distribution of the conductivity of the natural waters of Etna volcano. The higher values are mainly located in the areas of Zafferana and Paternò. (from Anzà et al. 1989)).

3 - The most anomalous area of widespread  $\text{CO}_2$  degassing, as well as total dissolved ions in waters are in the Southern and Eastern part of the volcano (Paternò, Zafferana) fig. 5.

4 - There is a strict relationship between soil degassing and active tectonic structures. The two areas of Zafferana and Paternò are characterized both by the highest diffused soil degassing and by the highest seismicity of the Etnean area. Systematic measurements of soil  $\text{CO}_2$  degassing in these two areas have been effected over the last two years. The method of measurement used is described in another work (Gurrieri and Valenza, 1988), to which readers are referred for further details

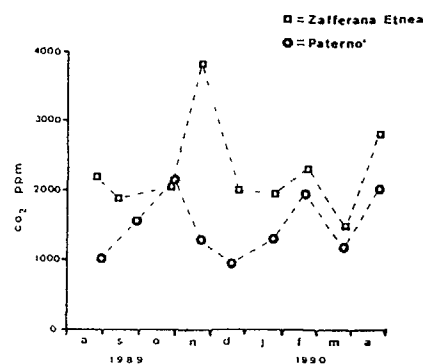


Figure 6 - Variations of soil  $\text{CO}_2$  concentration versus time in the two areas of Zafferana and Paternò. Each point is the average of about 100 points of measurement

Field measurements for each area were based on a sampling grid of about 100 points distributed quite homogeneously over an area of 25  $\text{Km}^2$ , (Giammanco and Valenza 1991 in press).

The two examined areas exhibit a synchronous variation in the average dynamic  $\text{CO}_2$  concentrations.

Furthermore, the variations of the  $\text{CO}_2$  concentrations in 20 selected points seem to be related to the seismic activity of the area.

The time lag (AT) between a minimum  $\text{CO}_2$  concentration and a seismic event seems to be related to the magnitude (M). The best linear fit of the log AT and M is given by the following relationship (fig. 7):  $\log \text{AT} = 2.5 M - 6.6$ .

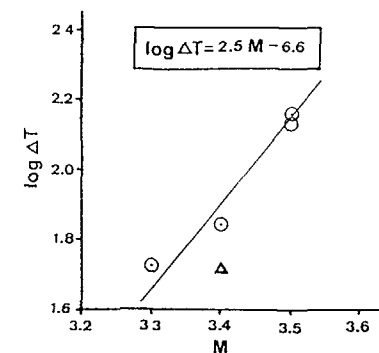


Figure 7 - Time lag between minimum  $\text{CO}_2$  concentrations in 20 selected points of the Zafferana area and occurrence of earthquake versus the magnitude of the seismic events.

#### Eastern Sicily

The Eastern part of Sicily ( area number 3 in fig 1 ) is one of the areas having the highest seismic risk in Italy.

According to the historical record of the seismicity in this area a seismic gap exists. (Purcaru and Berkhemer 1982; Mulargia et al. 1985). The most dangerous earthquake

which has ever hit this area occurred in January, 1693, and had an estimated magnitude of 7.5. Many towns were severely damaged or even totally destroyed and 60.000 people died.

During the night of December 13, 1990, an earthquake of magnitude 5.4 with its epicenter located in the sea at a few

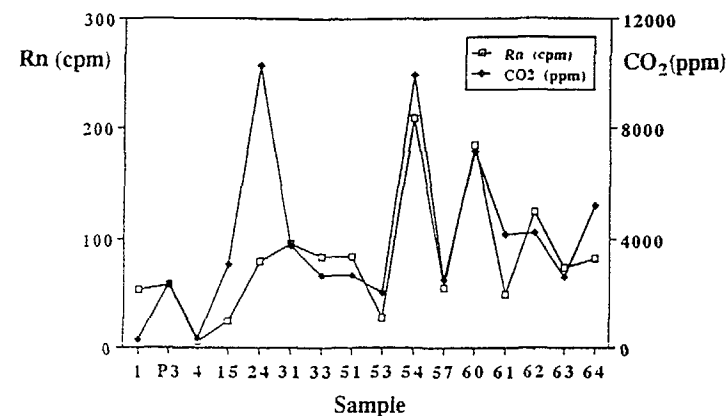


Figure 8 - Diagram of  $\text{CO}_2$  and Rn values in the soils. The trend of the two parameters are very similar suggesting that the  $\text{CO}_2$  acts as carrier for Rn.

kilometers from the coast of Augusta occurred. The towns of Carlentini and Augusta were seriously damaged and a few human casualties were reported. Following the earthquake, geochemical investigations in the area were intensified with the aim of collecting data regarding the possible short-term repetition of earthquakes having a comparable or higher magnitude. Chemical compositions and Radon contents were examined in the waters of springs and wells of the mesoseismic area.  $\text{CO}_2$ , He and Rn from this area were sampled and analyzed. As pointed out by Bonfanti et al (1991 in press) an excellent correlation exists between  $\text{CO}_2$  and Rn both in waters as well as in soil degassing (fig 5). The area having the highest gas flow corresponds to those areas having the greatest density of structural liniments (fig 8). Furthermore the He and  $\text{CH}_4$  contents, measured in some natural gas manifestations (Salinelle and Paternò) at the border of the area interested by seismic activity (fig 10) show anomalous

variations in coincidence with the earthquake occurrence. In the two areas the temporal variations of He and  $\text{CH}_4$  before the earthquake are different (He and  $\text{CH}_4$  decrease in the Salinelle Stadio and increase instead, in the Salinelle Simeto), in coincidence with the earthquake a positive peak in both parameters was recorded (fig 11). Bonfanti et al (1991) demonstrated that the ratio  $\text{He}/\text{CH}_4$ , at a given time, is constant for all gaseous manifestations, but changes before and during earthquake events.

#### Conclusive remarks

Geochemical observations carried out in different parts of the world indicate that some geological parameters can be usefully used as precursors of impending earthquakes. The experiences gained in Italy in the last years, in areas characterized by volcanic and/or seismic activity is best accomplished according to the following steps:

1 - Knowledge of the history of the seismic activity

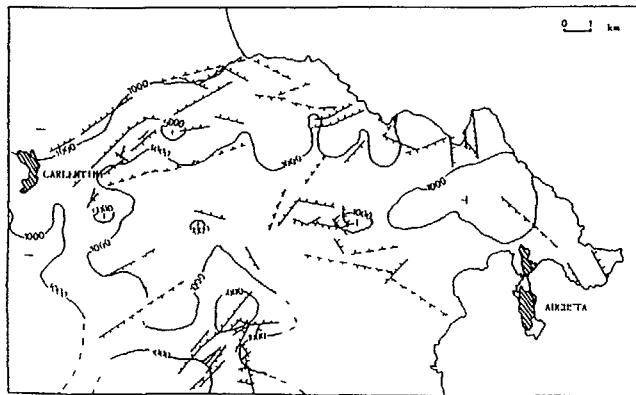


Figure 9 - Spatial distribution of  $\text{CO}_2$  concentration in the soil gases. The higher  $\text{CO}_2$  contents are in the areas with higher density of tectonic lines.

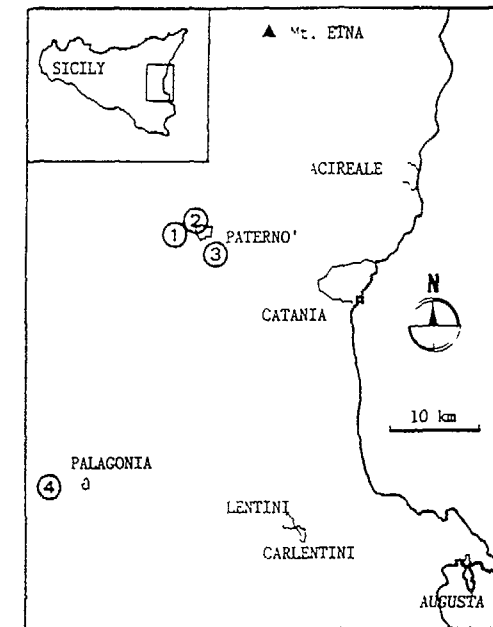


Figure 10 - Location of the natural gas sampling points: 1) Paternò 1 (Simeto); 2) Paternò 2 (Stadio), 3) Paternò 3 (Vallone salato), 4) Mofeta dei Palici.

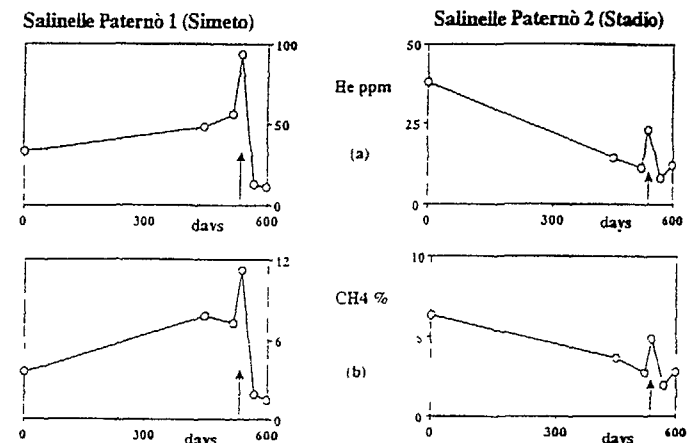


Figure 11 - Time trends of He and  $\text{CH}_4$  values measured at the Salinelle. The arrow indicates the earthquake of December 13, 1990.

- 2 - Knowledge of the seismo-tectonic properties
- 3 - Knowledge of the local geology and hydrogeology
- 4 - Inventory of the natural fluid manifestations ( water wells, springs, gases, soil degassing etc.)
- 5 - Geochemical characterization of the previously mentioned fluids in order to define their origin, circulation mechanism, interactions etc.
- 6 - Definition of the natural variations in time (background of the system ) so as to be able to formulate a geochemical model capable of explaining the chemical/physical behavior of the system.
- 7 - Choice of each area of the sites, the parameters and the frequency of observation.

This approach, if applied to different areas of the world and integrated with geophysical observations, could give powerful results which would bring us much closer to the goal of earthquake prediction. This objective can only be reached through an international cooperative program.

#### References

- ANZA' S., DONGARRA' G., GIAMMANCO S., GOTTINI V., HAUSER S., VALENZA M., (1989) - *Geochimica dei Fluidi dell'Etna. Le acque sotterranee*. - Miner. Petrogr. Acta, Vol. XXXII, pp. 231-251.
- BADALAMENTI B., FALSAPERLA S., NERI G., NUCCIO P.M., VALENZA M., (1986b). Confronto preliminare tra dati sismici e geochimici tra Lipari e Vulcano. Boll. GNV, 2, 37-47.
- BARBANO M.S., COSENTINO M., LOMBARDO G., PATANE' G., (1980) Isoseismal maps of Calabria and Sicily earthquakes (Southern Sicily) C.N.R. P.F. Geodinamica, G. L. "Catalogo dei Terremoti", Pubbl. 341,316.
- BONFANTI P., CARAPEZZA M.L., D'ALESSANDRO W., DE DOMENICO R., DI LIBERTO I.S., GIAMMANCO S.S., GURRIERI S., PARELLO F., VALENZA M., (1991). Earthquakes of 12/13/1990 in Eastern Sicily: some geochemical investigations. (in press)
- CARAPEZZA M., NUCCIO P.M., VALENZA M. (1981). Genesis and evolution of the fumaroles of Vulcano (Aeolian Islands, Italy): a geochemical model. Bull. Volcanol., 44, 547-564.
- CHESTER D.K., DUNCAN A.M., GUEST J.E., KILBURN C.R.J. (1985). Mount Etna; The Anatomy of a volcano. Chapman and hall, London 404 pp.
- COSENTINO M., (1987). Valutazione su una prima zonazione sismica della Sicilia e della Calabria in: *Aree sismogenetiche e rischio sismico in Italia*. Edit. G. Galilei - Lausanne.
- ENEL (1987) Catalogo dei Terremoti avvenuti in Italia dall'anno 1000 al 1975. Geotecneco S.P.A. San Lorenzo in Campo.
- GURRIERI S., VALENZA M., (1988). Gas transport in natural porous mediums: a method for measuring CO<sub>2</sub> flows from the ground in volcanic and geothermal areas. S.I.M.P. Carapezza M. memorial volume 1151-1158.
- MULARGIA F., TUTTI S., GASPERINI P. (1985). Cataloghi sismici e previsione dei terremoti. In "I Terremoti", Quaderni de Le Scienze, 24.
- PURCARU G., BERKHEMER H. (1982). Regularity patterns and zones of seismic potential for future large earthquakes in the Mediterranean region, Tectonophysics, 85 1-30.
- ROMANO R. (1982). Succession of the volcanic activity in the Etnean area. Mem. Soc. Geol. It., 233-27-48.
- SATO M., MALONE D.S., MOXAM R.M., MC LANE J.E. (1975) A.G.U. Annual Spring meeting.(abstracts volume)

## FLUIDODYNAMICAL AND CHEMICAL FEATURES OF RADON 222 RELATED TO TOTAL GASES: IMPLICATIONS FOR EARTHQUAKE PREDICTIONS

G. MARTINELLI

Servizio Informativo e Statistica,  
Regione Emilia Romagna,  
Bologna, Italy

### Abstract

During the earthquake preparation a zone of cracked rocks is formed in the area of future earthquake focal zone under the influence of tectonic stresses. The area of preparation of the seismic event is characterized by the occurrence of many precursory phenomena with particular reference to Radon 222. The main geochemical and geophysical relations useful in understanding Radon occurrences in deep fluids have been discussed with the help of some Italian case histories. Experiments have been carried out to test the reliability of some precursors related equations. Geochemical and geophysical characters of the above mentioned fluids are discussed with the aim of making a contribution towards understanding the relations among Radon 222 anomalies and other precursory related fluids.

### Introduction

The role of deep seated fluids in Radon generating anomalies has been widely described in recent scientific contributions (i.e. Barsukov et Al., 1979 ; Gold and Soter, 1984/85). It is a matter of fact that monitoring deep originated fluids has been succesful with respect to shallow seated fluid evidences in earthquake prediction monitoring experiments (Sultankhodzhaev, 1984). The complex relations among physical constrain factor and chemical evidences will be subsequently described with the help of some case histories.

### 1 - Historical features

A strong help in understanding earthquake precursory phenomena came from the methodologies set up for the reconstruction of past earthquakes damages scenarios, where cross-correlating hystorical information really improved the knowledge in statistic prediction studies (Postpischl, 1985; Gurpinar, 1987).

During the reconstruction of the Ligurian earthquake of 1887 (Ferrari and Martinelli, 1988; Ferrari, 1991) many precursory phenomena were recognized. Because of the ancient age the recognized pattern must be considered as anthropogenic noise free. The sketch in fig.1 shows in particular that deep originated fluids like CO<sub>2</sub> and deep groundwaters have had strong variations in the stress-strained area. The assumption that deep fluids are strongly affected by pre-earthquakes preparatory phenomena with respect to the shallow ones drove the attention in the last decade towards potentially earth-strain sensitive areas where geothermal fluids or deep seated gases had the capability to reach the surface bringing information from the deep environment.

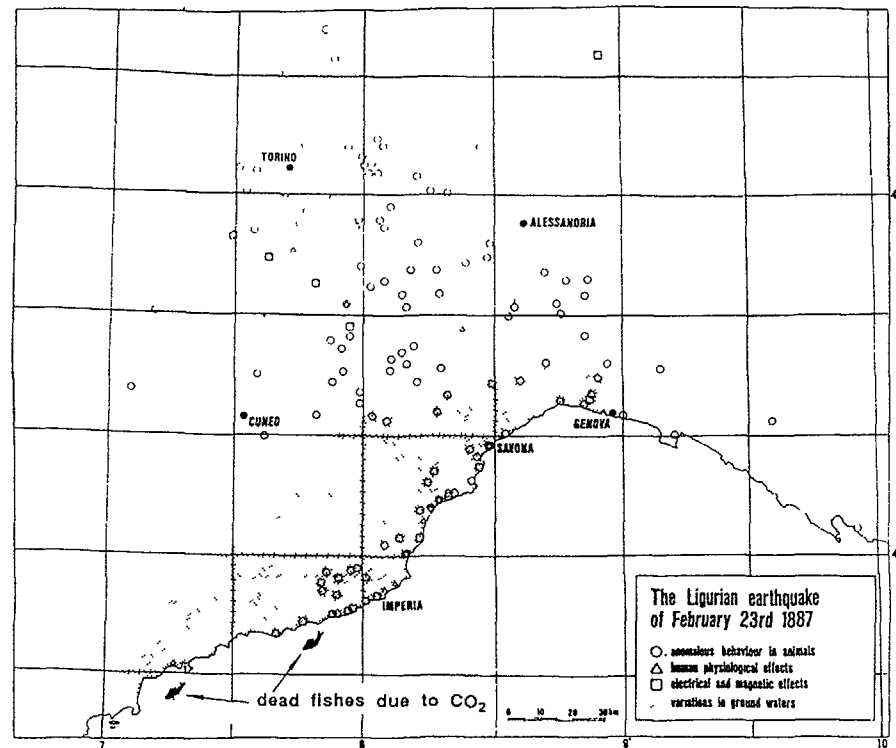


Fig. 1 Reconstruction from historical sources of precursory phenomena occurred before the Ligurian earthquake of February 23rd, 1887.

## 2 - The physical framework

Dobrovolsky et Al. in 1979 have strongly contributed in the calculation of the size and shape of the earthquake preparation zone, where precursory phenomena are also investigated by Myachin et Al. in 1975: the dilatancy-diffusion model (DD) developed mainly in U.S.A. and the crack-avalanche (CA) model (named also IPE, Institute of Physics of the Earth, Moscow) developed mainly in U.S.S.R.

According to the DD model a porous cracked saturated rock constitutes the initial medium. With the increase of the tectonic stresses the cracks extend as well and disengagement cracks appear near the pores, the favourably oriented cracks being opened. Water flows into the opened cracks drying the rock near each pore. This results in a decrease of pore pressure in the total preparation zone and water diffusion into the zone from the surrounding medium. The return of pore pressure and crack increase bring about a main rupture at the end of the diffusion period.

According to the CA model the process is as follows; a cracked focal rock zone is formed by the increasing tectonic stresses. The shape and volume of this focal zone change slowly with time.

A complicated process of crack birth, growth, healing and redistribution proceeds within the zone. At a certain stage in the focal zone volume crack concentration and size reach such values that the whole focal zone becomes unstable. The cracks quickly concentrate near the fault surface where the main rupture has passed. A complete review about the two approaches has been published by Sobolev (1984) and by Barsukov et Al. (1984) who underlined the CA suitability model for any kind of geochemical anomalies being more adapted in understanding fluid's physical and chemical phenomena.

Anyway, after comparing both theories we can recognize a common principle: at a certain preparation stage a region with many cracks is formed and the surrounding medium perceives the focal region as a "solid soft inclusion".

An approximate quantification of the "solid soft inclusion" has been given by Dobrovolsky and Miachkin (1976) and by Dobrovolsky et Al. (1979). According to the above mentioned authors three considerations are the key for a correct comprehension of the phenomena:

- 1) the deformations are the tensor components and the tilts are the vector components. Therefore these values may be connected with the the direction towards the epicentre;

2) the mechanical processes of earthquakes preparation are always accompanied by deformations. The precursors of another physical nature often require, for their manifestation, a complex of specific natural conditions;

3) apparently the deformations are the primary phenomena, but many reports show a very complex picture in which short-term, medium-term and long-term precursory phenomena may be recognized (Rikitake 1989; Hamada, 1990; Wiss 1991).

Because precursory phenomena appear not to be observed beyond the distance  $D$  (Dobrovolsky et Al., 1979; Fleischer, 1981) to estimate roughly the radius of the effective precursory manifestation zone it is possible to use the formula

$$D = 10 \exp 0.43 M \quad (1)$$

where  $D$  is in Kms. and  $M$  is the magnitude of the earthquake. It means, in practice, that a magnitude 5 earthquake will be detected by mean of precursory phenomena at a distance not greater than 142 Kms. Successive observations (Sadovsky et Al., 1984) demonstrate the Dobrovolsky approach is theoretically correct but too much cautelative.

Being anisotrope the rheological behaviour of the earth's crust (Crampin, 1991) the above mentioned law can be modified according to the effective sensitivity to impending earthquake, and the theoretical radius of the ideal circle can be interpreted in terms of the minor and major radii of an ellipse (elongated, as an example, along the major fault) or characterized by shadow areas where no precursory phenomena are observable. Thus empirical relations which consider the theoretical physical constrain factors (as described by Dobrovolsky) and experimental field data have been set up (Hauksson and Goddard, 1981; Friedmann, 1991). Observational data and previous works allow us to consider as satisfactory the relation for which

$$M = 2.4 \log D - 0.43 \quad (2)$$

(Hauksson and Goddard, 1981). Regarding the case histories recorded in the Italian Peninsula and taking into account the characteristics of the crustal structure in Italy the relation may be modified as follows :

$$M = 2.4 \log D - 0.43 - 0.4 \quad (3)$$

as similarly proposed by Friedmann (1991), for the evaluation of earthquake's precursors in Austria.

On the basis of the data on variations in concentrations of the gaseous components recorded in a seismically active area in Central Asia in the period 1974-1980 an empirical formula relating precursor time  $T$  (in days) to magnitude  $M$  and epicentral distance  $D$  (in Kms) has been satisfactorily experimented by Sultankhodzhaev et Al. (1980) :

$$\log DT = 0.63 M + (-) 0.15 \quad (4)$$

Intense gaseous upsettings occur in the identified area of a forthcoming earthquake and a continuous gas monitoring may add further informations. Long term series analyses have revealed a relation between the amplitude and duration of the gaseous anomaly and the Magnitude of the expected earthquake (Barsukov et Al., 1984) :

$$M = K\sqrt{S} \quad (5)$$

where  $M$  is the Magnitude,  $K$  is a correction factor and  $S$  is the area of the detected peak anomaly. As a consequence the shape of the peak (and not only the amplitude) is a diagnostic parameter for the forthcoming seismic event as underlined by Friedmann (1988/89), after the check of all the published data on pre-earthquake Radon anomalies. It must be underlined that evidences of fluids/rock interactions are practically the only signatures of ongoing deep processes we are allowed to detect through fluid's composition monitoring.

Thus the knowledge of the main geochemical and geophysical features which govern the occurrence of deep gases become essential in understanding Radon precursory phenomena.

### 3 - The chemical framework and the geochemical consequences

A set of gases such as CO<sub>2</sub>-H<sub>2</sub>S-CH<sub>4</sub>-H<sub>2</sub>-N is practically always present in or near geothermal areas (D'Amore and Panichi, 1980) and detailed studies on the chemical and isotopic composition of gas samples suggest that their relative amounts can be formulated as a function of temperature and used as a tool in geothermal exploration. It's possible to derive a suitable geochemical model of natural hydrothermal systems in which gas-water-rocks equilibrium reactions occur (Giggenbach and Matsuo, 1991; Marini, 1991).

The knowledge of these reactions is useful in evaluating the deep geothermal temperatures using surface data of gas samples and in earthquakes prediction researches, being the gas mix pattern influenced by deep physical and chemical processes.

Because of the depth of hypocentres and the frictional heating generated during the earthquakes, seismic events are to be considered as "hot events" which strongly affect pore-fluid pressure and deep thermodynamic conditions (Mase and Smith, 1984/85). Thus the knowledge of the exact origin of deep seated gases becomes of decisive importance in the evaluation of experimental data in earthquake prediction research studies.

The origin of methane in some geothermal localities can be explained by considering the so called Fisher-Tropsch (Biloen and Sachtle, 1981) reaction:  $\text{CO}_2 + 4\text{H}_2 = \text{CH}_4 + 2\text{H}_2\text{O}$ , but part of  $\text{CH}_4$  could derive from reaction synthesis between carbonious material and molecular hydrogen or by organic processes. Meanwhile, carbon dioxide seems to be particularly interesting because  $\text{CO}_2$  manifestation has been found to be related to the seismicity in test areas, suggesting that the  $\text{CO}_2$  production is practically everywhere related to present day tectonic activity (Irwin and Barnes, 1980).

Thermometamorphism, which chiefly characterizes the earthquake's deep chemistry, is the main process responsible for the ubiquitous occurrence of  $\text{CO}_2$  in thermal areas, although mantle derived, magmatic and organic processes may locally give a significant contribution to the total discharge of  $\text{CO}_2$  (Ferrara et Al., 1963; Colombo et Al., 1966; Gianelli, 1985). On the other hand  $\text{H}_2\text{S}$ ,  $\text{H}_2$ ,  $\text{N}_2$  and  $\text{CH}_4$  may have both organic and inorganic origin being subjected to a continuous reworking in the earth's crust.

This set of gases can be considered according to their reactivity under geothermal conditions, taking into account that the three main factors controlling the distribution of gaseous constituents in geothermal discharge are temperature, pressure and the partitions coefficients in distribution of gases between fluids (Giggenbach, 1976, 1979). The effect of the last factor can provide important information on the underground kinetic reservoir situation.

On the basis of the above mentioned considerations, subterrestrial fluids can be classified in three main groups according to their chemical reactivity in response to changes in temperature and/or pressure conditions before or during an earthquake.

In particular :

Group 1  $\text{H}_2\text{O}-\text{CO}_2-\text{H}_2\text{S}-\text{NH}_3-\text{H}_2-\text{N}_2$  is considered to be highly active species

Group 2  $\text{CH}_4$ -Upper Hydrocarbons is considered to be relatively unaffected by chemical equilibration processes

Group 3 Noble gases-He-Radon is considered inert or poorly affected by chemical equilibration processes, and often considered in earthquake's prediction researches because of the high mobility characteristics, the high natural production rate and relatively low-price of automatic monitoring analytic equipments.

Group 3 always accompanies Group 1 and 2.

According to the experiences gained with geothermal and oil prospection,  $\text{CO}_2$  and  $\text{CH}_4$  can be considered gas carriers (Kawabe, 1984/85; Locardi, 1991) diluting the gases formed in geothermal environments while poorly reactive noble gases and high mobile elements like Hg, As, Sb, and Bi may be regarded as tracers useful in estimating deep kinetic processes (Brondi and Dall'Aglio, 1989). Many other gas molecules at trace level concentration have been detected in deep fluids by means of particular analytical equipment such as the so called "soft-ionization mass spectrometry". As a matter of curiosity the molecule of  $\text{CF}_4$  has also been clearly recognized but the above mentioned classification is to be considered exhaustive for earthquake's prediction purposes (for a more comprehensive tractation see Federer et Al., 1990 and Locardi, 1991).

The transport phenomena relative to noble gases and to high mobile elements characterize mainly the particular features of the earthquake's shallow chemistry, while the deep chemical phenomena are mainly driven by fluid-rocks interactions related to the thermodynamical conditions.

Gas carrier fluid-dynamic in the earth's crust is subject to the rules which describe the gas motion as well observed in artificial systems, such as diffusion, effusion, combination of both, but non-linear phenomena may occur in natural system and the physical-mathematical tractation could be particularly complex (Nikolaevskij, 1990; Gurrieri and Valenza, 1988).

#### 4 - Radon behaviour

Noble gases may form unstable hydrates (Haissinsky, 1957). Radon in particular forms a metastable clathrate-hydrate with water:  $\text{Rn} \cdot 6\text{H}_2\text{O}$ , while other compounds with nonpolar solvents

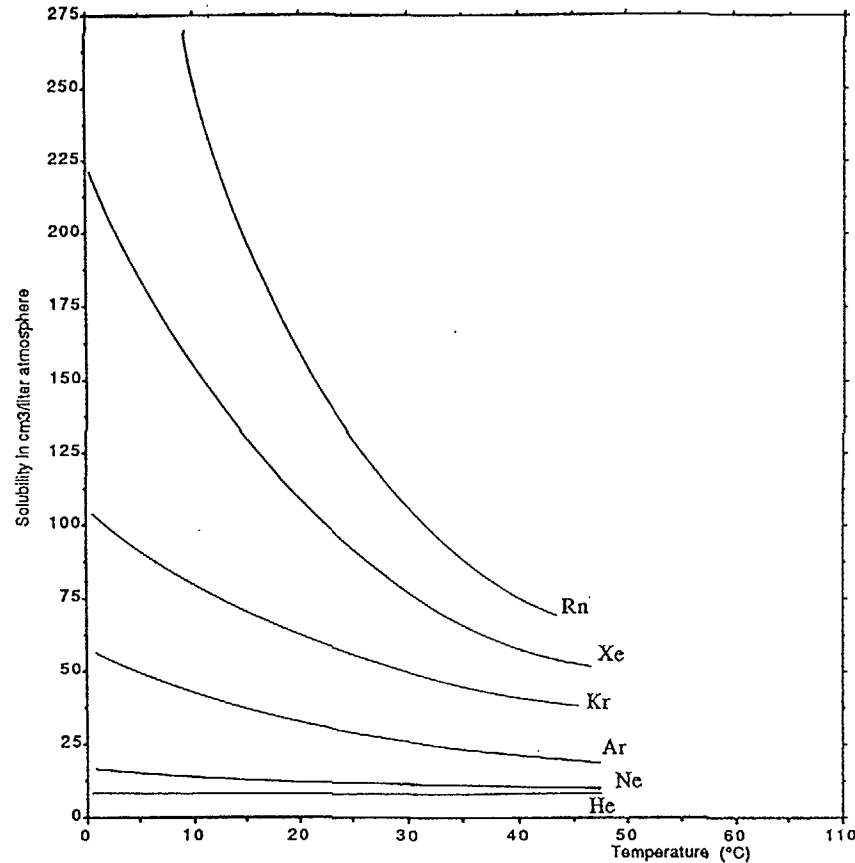


Fig. 2 Solubility of Noble Gases in pure water.

have been studied and reported (Nesmeyanov, 1974). According to the Clathrates behaviour, the solubility of noble gases increases rapidly with atomic weight. The solubility of each noble gas decreases with temperature but the temperature dependence is much stronger for the heavier gases. This effect is illustrated in fig. 2.

Noble gases have been analyzed in springs and hydrothermal areas, and two main characteristics of these elements have been recognized: the noble gases occur in about the same proportions, in the hydrothermal areas and in the atmosphere; the noble gas

content in the waters is significantly below saturation for any possible recharge infiltration temperatures; radiogenic noble gases patterns may give information on the kinetics of the reservoir. The chemical and physical characteristics of Helium and Radon which appear at the extremes of fig. 2 are particularly useful in monitoring tectonically active areas. In particular Helium is characterized by a particular high fugacity value and Radon is continuously produced by Uranium series decay which occur widely in many crustal rocks formations. The alpha particles produced by the natural radioactive decay of Radon become Helium nuclei, so the gases naturally linked are often analyzed together in order to detect subterrestrial fluid dynamic changes. The actual amount of Helium and Radon in the geological environments depends on many factors. The most important ones are the amount of parent nuclide present and the emanation rate at which the gases are released from its sources. The gas flux can be defined as the amount of gas crossing the soil-atmosphere boundary per unit time.

For Helium, which does not decay, both crustal (mainly Helium 4) and mantle (mainly Helium 3) generated gas can contribute to the flux. For Radon the half-time life reduces the volume of material that can deliver gas to the flux because of the limited distance the atom can migrate before it decays. Diffusion and transport are influenced by local geology, rock types, joints, fractures, hydrology, porosity, permeability and presence of other long distance gas carriers.

The rate of emanation not only depends on material type and crystalline structure but also varies in response to changes in physical forces such as pressure and stress. This latter response has strictly linked Radon and Helium analysis to earthquake prediction researches.

The dependence of the Radon released from a Radon-emanating source and its specific surface area was quantitatively discussed by Andrews and Wood (1972). Andrews (1977) calculated the percentage of Radon 222 generated by Radium 226 decay, released from grain-sized rock particles into water as follows :

$$\log (\% \text{ Rn release}) = 0,5 \log D + C \quad (6)$$

where  $D$  is the diameter of the grain and  $C$  is a constant. Most sedimentary materials with uniform composition (e. g. limestone, shales, etc.) were experimentally found to adhere this equation.

The distribution of the Radon released at rock-water interface into the water flowing through the intergranular spaces depends on



its diffusion in the fluid and on the water flow rate. As a result of the slowness of this process, diffusion presumably does not affect Radon distribution, while water movement seems to be of primary importance in determining the dispersion of Radon into large volumes of water, in particular in the case of primary high-permeability aquifers where flow velocity is presumed to be reasonably high. According to Andrews (1977), the Radon concentration in water passing through a porous Radon-emanating rock is :

$$R_n = (A d R_a / f) (1 - \exp(-x/v)) \exp(-x'/v') \quad (\text{pCi/l}) \quad (7)$$

where  $R_a$  is the Radium (or Uranium) activity content of the rock,  $d$  is the rock density and  $f$  its fractional pore space ;  $v$  ,  $v'$  are the transport velocities of water within the aquifer and after leaving it, respectively ; and  $x$  ,  $x'$  are the distance covered within the aquifer and after leaving it, respectively. Factor  $A$  is the ratio of Radon released into water against the Radon generated within the rock and depends on the pore-size distribution and mineral composition of the rock. This equation was found to satisfactorily estimate the Radon content in fluids in common aquifers if the hydrodynamic parameters were adequately known (Gorgoni et Al., 1982; Martinelli, 1985).

Hence Radon transport models have been developed for many fluid phases while helium transport models have been similarly set up (Andrews and Hussain, 1989).

In the past unusual natural phenomena such as groundwaters well-level changes, turbidity of groundwaters, bubbling of gases in groundwater, chemical changes in spring or well waters, unusual gas exhalations, have been correlated in a general way to the occurrence of earthquakes (Roeloffs, 1988). The above mentioned phenomena and other physical events have affected the behaviour and the sensorial perception of people and all the biosphere involved in earthquakes . This has driven the attention of researchers on earthquake's precursor phenomena to Radon and connected nuclides.

## CASE HISTORIES

### 5 - Mud volcanoes : physical models and fluid dynamic anomalies

The rate of emanation not only depends on material type and crystalline structure but also varies in response to changes in physical forces such as fluid pore-pressure and stress (Zschau and

Ergunay, 1989) . These changes are also responsible for other reported geophysical precursors such as electric signals, magnetic signals and related effects being driven from transient variations in the deep permeability and porosity conditions mainly connected to electrokinetic processes ( Fitterman, 1979 ; Dobrovolsky et Al., 1989 ; Patella et Al., 1991).

Precursory changes in crustal permeability may be easily observed in natural systems characterized by physical insulation with respect to meteorological environment. From this point of view some peculiar natural occurrences named mud volcanoes have been chosen. They are deep confined fluid reservoirs and behave like natural strain-meters (Bodvarsson, 1970) capable of transmitting physical and chemical signals to the surface (Martinelli and Ferrari, 1991). Understanding the chemical signals require some recalls in the knowledge of Radon transport models. As previously remembered, some Radon Transport models have been developed in hydrology or in geothermal engineering. Among them the most suitable one for the studied system seemed to be the equation of Stoker and Kruger (1975) :

$$C / E = (1 / p) \left( 1 - \exp \left( \frac{-\pi p h \lambda}{Q} (R_e^2 - R_w^2) \right) \right) \quad (8)$$

where  $C$  (pCi/cm<sup>3</sup>) is the activity ratio of Radon per cubic centimeter of fluid,  $E$  (pCi/cm<sup>3</sup>) is the Radon emanating from the rock,  $\lambda$  is the decay constant of Radon 222,  $R_w$  (cm) is the Radius of the cylindrical fracture of height  $h$  (cm), within a rock of given porosity  $p$ , finally  $R_e$  (cm) is the radius of the circular ring of rock from which Radon diffuses into the fracture and  $Q$  (cm<sup>3</sup>/sec.) is the flow rate. This relation is also useful to systematize a large amount of analysis carried out during many other earthquake prediction studies . In particular, according to Gasparini and Mantovani ( 1978) who discussed the application of Stoker-Kruger equation to the duct of volcanic type, it results that the essential condition to detect Radon at great distance is a high gas-carrier flow rate. In mud volcanoes this condition is widely satisfied because the measured gas flow rate of 15-30 l/h corresponds to a velocity of about 150-300 m/day (fig.3,4).

Along the duct the velocity is highly variable and different in comparison to the values measured at the out flow mouth ; anyway it results from measurements that in general the behaviour of the Radon concentration is inversely proportional to that of the flow rate.

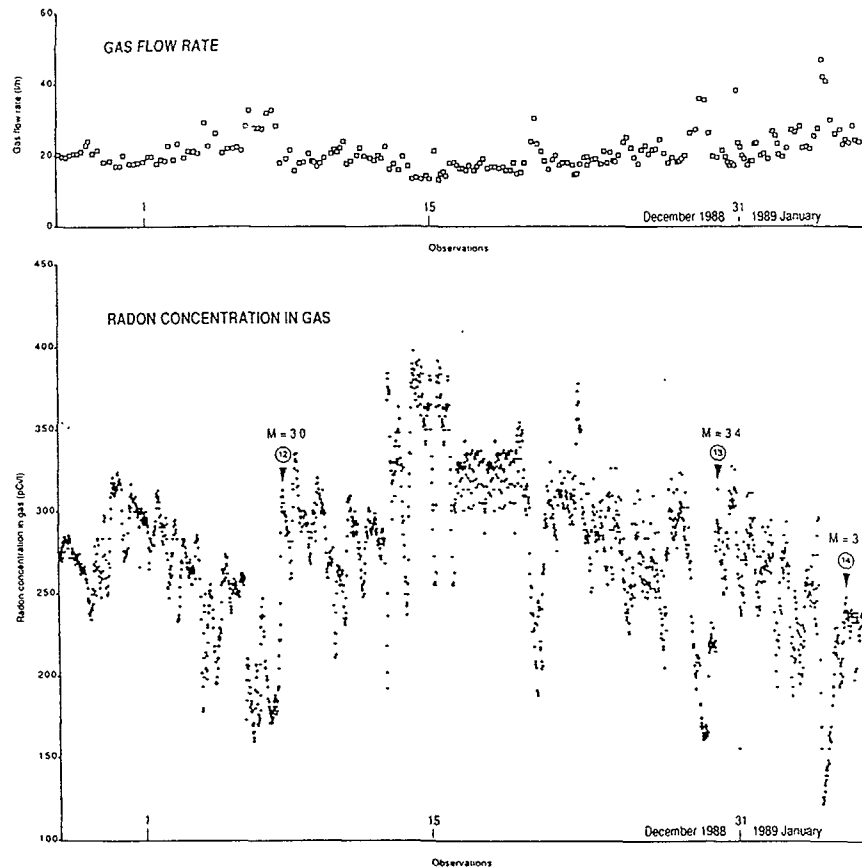


Fig. 3 The dots represent a typical record of the automatic monitoring system of Radon 222 in the gas phase erupted from a Northern Apennine mud volcano. The squares represent total gases flow rate measurements. It can be observed that the plot of the gas flow rate is in general inversely proportional to that of Radon 222 concentration. The listed earthquakes satisfy eq. 3 and have been preceded by a marked gas upsetting. Other anomalies may be related to tidal effects.

These assumptions seem particularly reasonable in the light of the large amount of evidence concerning the physical and chemical variations observed in the fluids of hydrocarbon deposits or together with them, connected with dynamic artificial pressures

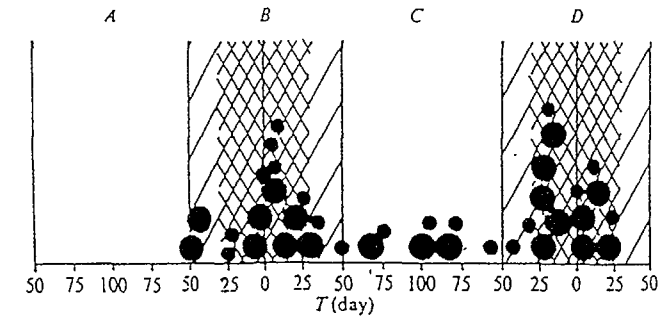


Fig. 4 Eruptions of gaseous mud volcanoes and the cosmic conditions of the Earth. Large circles denote strong eruptions, and small circles denote slight eruptions (volcanic eruptions of East Transcaucasia and the adjoining part of the Caspian Sea are related to the period 1948-1970). The time (day) between the moment when the syzygy and apse lines coincide and the eruption day is shown in the horizontal axis. The time during which the apse line is in the quadrature of lunar phases has been left clear. The apse line is in the following zones of lunar phases: A, first quarter; B, new moon; C, last quarter; D, full moon.

(exploitations) or natural ones (earthquakes) (Wu, 1975; Ariei and Merzer, 1974; Wakita et Al., 1990). It is useful to remember that a relatively high concentration of Ra-226 is present in the scales of the waters in oil wells (E. and P. Forum, 1988; Bassignani et Al., 1988). The measurements confirm that the gases that bubble in the water, continuously gather Radon from the radium-enriched clay sediments. Similar mechanisms of Radon-222-enrichment have already been observed in previous researches on the natural behaviour of Radon (Zagin and Saskina, 1966; D'Amore et Al., 1978-79). Taking into account the fact that the flow rate of the liquid phase in mud volcanoes is 1-5 l/day, while that of the gases has been measured as 15-30 l/hour, it is possible to deduce that the anomalous values in waters and gases found in pre-earthquake phases are determined by the dynamics of the fluids present, with particular reference to the gas carrier, in this case methane in a proportion of over 90% (Mattavelli and Novelli, 1988). In the case studied it is therefore possible to make the hypothesis that there are many Radon sources along the entire course of the duct, but among these, the most important is logically the "local" one close to the surface, being Radon from a deep origin much more subject to decay (Tidjani et Al., 1990). On the other hand, it is confirmed on the basis

of present knowledge (Mattavelli and Novelli, 1988) that gases carrier are deep originated.

The water present in the mud volcano ducts enables Radon (Fleischer, 1983, 1987) to be released from sediments rich in Radon-226, whereas the gas carrier is constantly enriched through bubbling with water or through direct contact with the sediments. Other slight geochemical anomalies can take place at the same time as these processes, in accordance with the mechanisms hypothesized by Gorgoni et Al. (1988). The bubbling gases then easily yield Radon to the water until a virtually steady state is reached (Martinelli, 1989 ; Martinelli et Al., 1989) . This stationary state in concentration levels can practically only be disrupted by an increase in temperature (Rogers, 1958; Dubinchuk, 1991), by variations of pH (Bergamo et Al., 1985), or by variations in the gaseous dynamics (taking into account that the aqueous phase is little more than negligible). As already mentioned, it was not noted that there were any significant temperature variations in the waters that could modify the partition coefficient of Radon between the gaseous and aqueous phase, as the emissions studied were of a cold nature and because the waters of deep origin constantly re-equilibrate their temperature during their slow ascent to the surface. Similarly, variations in pH were not noted ( Ferrari and Vianello, 1985). Therefore, the particular dynamics of gases, being more subject to sudden accelerations and decelerations, is more likely to be responsible for the variations that were observed. In general, the physical behaviour of gases with respect to that of liquids, is responsible for the greater velocity with which they are ejected from the subsoil if compared with the aqueous phase. If the difference of the gas ejection velocity with respect to the waters and the mud remains constant in time, a steady state is reached in which there is only a transfer of Radon between the gas carrier and the liquids involved. In this case, no anomalies are noted in the liquid phase or in the gaseous phase. On the other hand, if the relative difference of ejection velocity suddenly increases or decreases, it is possible to verify considerable anomalies in the concentration of Radon 222 both in the liquid phase (Martinelli, 1987 ; Gorgoni et Al., 1988) and in the gaseous phase (Martinelli and Ferrari, 1991) in concomitance with seismic events locally occurred and satisfying eq. 3 (fig.3).

According to Tamrazyan (1972), mud volcano main eruptions observed in the Caspian Sea by 1948 to 1970 occur in correspondence of the lunar phases (syzygies), ( fig.4) .

This observation confirms that crustal deformations due to microgravity changes could be clearly emphasized by natural

strainmeters like mud volcanoes, because of their dynamical peculiarities as confined fluids occurrences (ISMES-ATOMENERGOPROJECT, 1991).

The same behaviour was observed in a true volcanic system like Stromboli ( Johnston and Mauk, 1972) . The fact that not all the volcanic systems are subjected to cyclicities suggests that only for particularly critical values of fluid mass and viscosity involved could the above mentioned phenomena be observable ( Agodi et Al., 1990) . It must be pointed out that the lunar-solar tidal effect may influence the seismic activity with particular reference to microearthquakes ( Rykunov and Smirnov, 1985; Rydelek et Al., 1988). The differences in time of the rheological answer of the crust to the tidal effect have been used recently by Westerhaus et Al. ( 1990; 1991) as a precursor index of earthquakes with the supporting proof that pore fluid pressure, that's to say deep gases, is responsible for the observed phenomena. As a consequence deep fluid analysis is confirmed to be a very promising system in monitoring crustal deformations phenomena, not always detectable by tiltmeters and strainmeters.

On the other hand also daily variations in deep seated rare gases emissions induced by earth tides have been reported by Sugisaki (1980), who observed He/Ar changes in a thermal spring near Kyoto. The above mentioned examples demonstrate that in some critical physical emergences long term and short term microgravitational changes cause crustal deformations able to extrude deep seated fluids to the earth's surface ( Sugisaki, 1981; Toutain et Al., 1992).

Crustal deformations induced by astrophysical phenomena have an order of magnitude (in term of energy) smaller or equal to the one generated by little earthquakes. If so, deep fluids in particular conditions (Nikolaevskii, 1991) could be sensitive to pre-earthquakes crustal deformations and Radon 222, used as a tracer, contained in such "magic" emergences located in tectonically active-crust degassing areas (Wood and King, in press ; Facchini et Al., 1991) confirms its particular role in monitoring strategies oriented to earthquake prediction researches.

#### 6 - Bubbles and sensitive fluids

It has been previously shown that bubbling of gases in liquids has a significant role in anomaly generation . In particular the relative difference in velocity of the gas phase with respect to the liquid phase is responsible for many observed anomalous phenomena. Further details may be added in order to explain better what

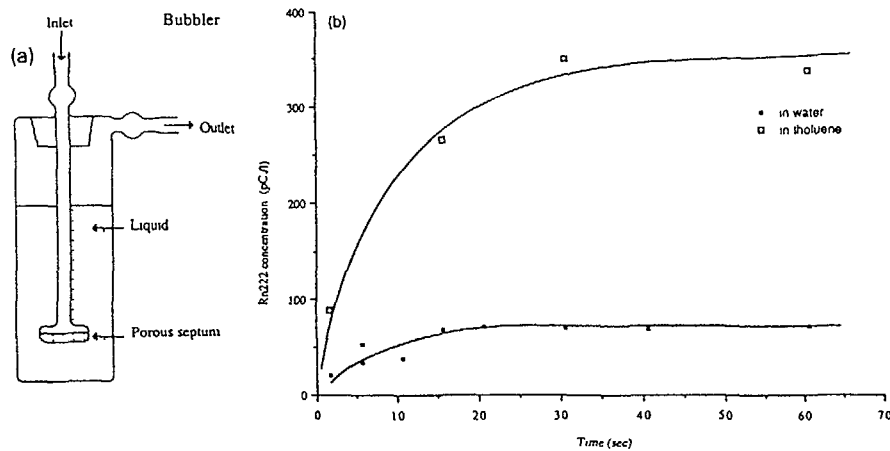


Fig. 5 a) Experimental apparatus and b) the relation between the bubbling time and the concentration of Radon detected in distilled water and tholune.

happens during bubbling. In fig. 5 it is shown how gas bubbling in water may generate artificial Radon rich water starting from zero until reaching the saturation level. In this case bubbles are Radon-donor because they are Radon-rich and very small. If great bubble Radon-free begins to travel within the liquid the Radon degassing of the liquid phase takes place as described by Zagin and Saskina (1966). The nucleation process and the migration play a decisive role in Radon dynamic. Nucleation processes occur generally on the wall of the ducts filled with liquids: this is due to absorption phenomena and because the fluids exerts pressure on the bubble walls which is inversely proportional to the bubble radius (Bodsvort and Bell, 1972; Rice, 1985). In this case Radon generated at rock surface enters in the bubble. Until the bubble is not great enough to travel absorption phenomena makes the bubble link with the surface possible. Having reached a critical value of radius it begins to travel and catch Radon from the liquid phase and not from rocks. This is the why the liquid phase is so poor in Radon if strong bubbling takes place.

In fig. 6 it is shown how a bubble increases in radius after nucleation during its travel in liquid fluid (Shafer and Zare, 1991). The bubble radius increases because of the different density among gas and fluid. Such a different density compells the bubble to travel in the direction towards the pressure drop and during the

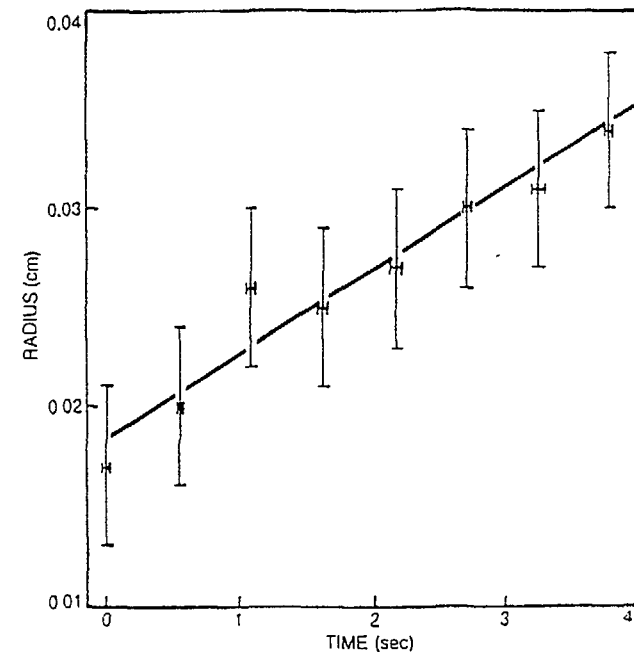


Fig. 6 Radius of a rising fluid bubble changes as a function of time.

travel act as a Radon-acceptor taking Radon from the liquid phase. The above mentioned physical factors make it possible to accept the observations made by Sugisaki (1981) and by Sugisaki and Sugiura (1986), and confirm the particular role of bubbles in fluids subjected to pressure variations induced by pre-earthquake's crustal stresses.

## 6 - Geothermal systems and conclusions

Geothermal systems are subjected to the mentioned phenomena and could act in particular conditions as natural strainmeters. Macroscopic anomalies in the behaviour of a geothermal field are reported by Fournier (1989) in a monographic study on Yellowstone, where a  $M = 7.3$  earthquake generated anomalies in the flow rate and other physical parameters, and confirm similar observations reported by Rinehart (1970) for the same area during the earthquake's occurrences.

Kruger et Al. (1977) talk about Radon anomalies observed in a geothermal field connected with local earthquakes. Wakita et Al. (1990) has observed anomalous values in  $\text{He}^3/\text{He}^4$  and  $\text{He}^4/\text{Ne}^{20}$  in deep fluids collected in gas fields in Japan. The authors have related the anomalous values to a  $M = 7.7$  earthquake which occurred in Central Japan on May 26, 1983 with epicentre located 150 kms. far from the wells.

Once accepted that all gases are involved in the fluid-rocks interaction (see chs. 3 and 4), we could compare noble gases anomalies to Radon preseismic or coseismic anomalies, obviously considering their different origin.

A similar case occurred in Central Italy near Larderello in a geothermal productive well in 1982 during a monitoring period performed by Hooker et Al. (1985). The well showed slight

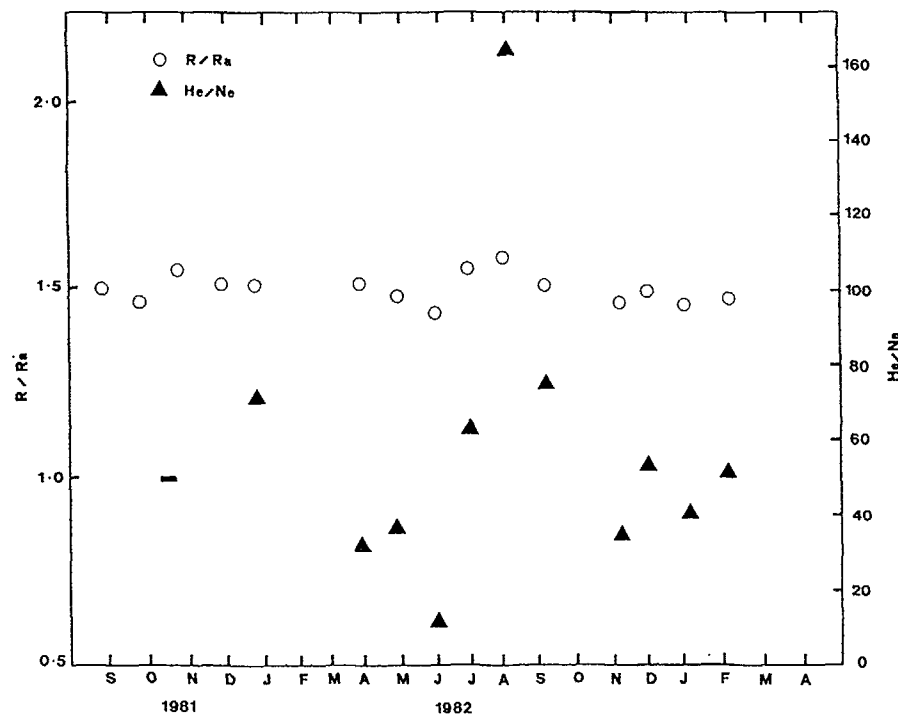


Fig. 7 Variation of  $R/Ra$  (dots) and  $\text{He}/\text{Ne}$  (triangles) values in samples of steam from a well in the Larderello area between September 1981 and February 1983.

variations in the  $R/Ra$  Helium ratio and strong variations in the  $\text{He}/\text{Ne}$  ratio. The observed anomaly was very sharp (less than two months, see fig. 7) and the geothermal field dimensions and recharge modalities didn't allow an explanation for the phenomena in terms of sudden variation in recharge or meteorological noise (see Panichi and Gonfiantini, 1978). If we list all the earthquakes that occurred in the area able to satisfy the relation

$$M = 2.4 \log. D - 0.43 - 0.4 \quad (\text{eq. 3})$$

we may observe that a  $M = 3.2$  earthquake occurred on July 28 1982 (I.N.G. Seismological Report, 1982). The preseismic and/or coseismic stress field variation occurred has probably changed the values of crustal permeability allowing the anomaly to occur as observed by Bertrami et Al. (1990) in Latium (Central Italy) during an earthquake's swarm. The low enthalpy systems behaviour doesn't seem to be too much different, but the presence of  $\text{CO}_2$  seems to drive the phenomena as observed in thermal springs in Central Italy.

In fig. 8 Radon data coming from some thermal springs of Central Italy characterized by long circulation pathflows and stability in chemical composition are shown (Battaglia et Al., 1991; Panichi, 1982; Barazzuoli et Al., 1987). In spite of the lack of a set of data collected continuously some comments are possible. In particular spring n.1 didn't change significantly the Radon concentration during the period of monitoring while springs n.2 and n.3 have shown large variations. During the period of monitoring more than 100 earthquakes with  $M \geq 3$  occurred in Central Italy (I. N. G. Seismological Report, 1985, 1986, 1987) and changes in crustal permeability almost certainly occurred, but the low frequency of sampling limit definitive considerations about precursory phenomena; meanwhile the observed different behaviour suggests that deep originated gas carrier could have affected the Radon concentrations. According to Panichi (1982), spring n.2 and n.3 are characterized by clear  $\text{CO}_2$  bubbling while spring n.1 doesn't show  $\text{CO}_2$  bubbling and is characterized by a low  $\text{CO}_2$  partial pressure. A possible explanation of the observed phenomena is that  $\text{CO}_2$  deep originated acted as Radon carrier as observed by Bella and Pettinelli (1990) in a similar spring located in Latium (Central Italy) where a continuous Radon monitoring system was set up. A first classification of the Italian springs based on the  $\text{CO}_2$  concentration has been attempted by Minissale (1990) on the basis of the available chemical composition of waters. Facchini et Al. (1991) have recently attempted some experiments in earthquake

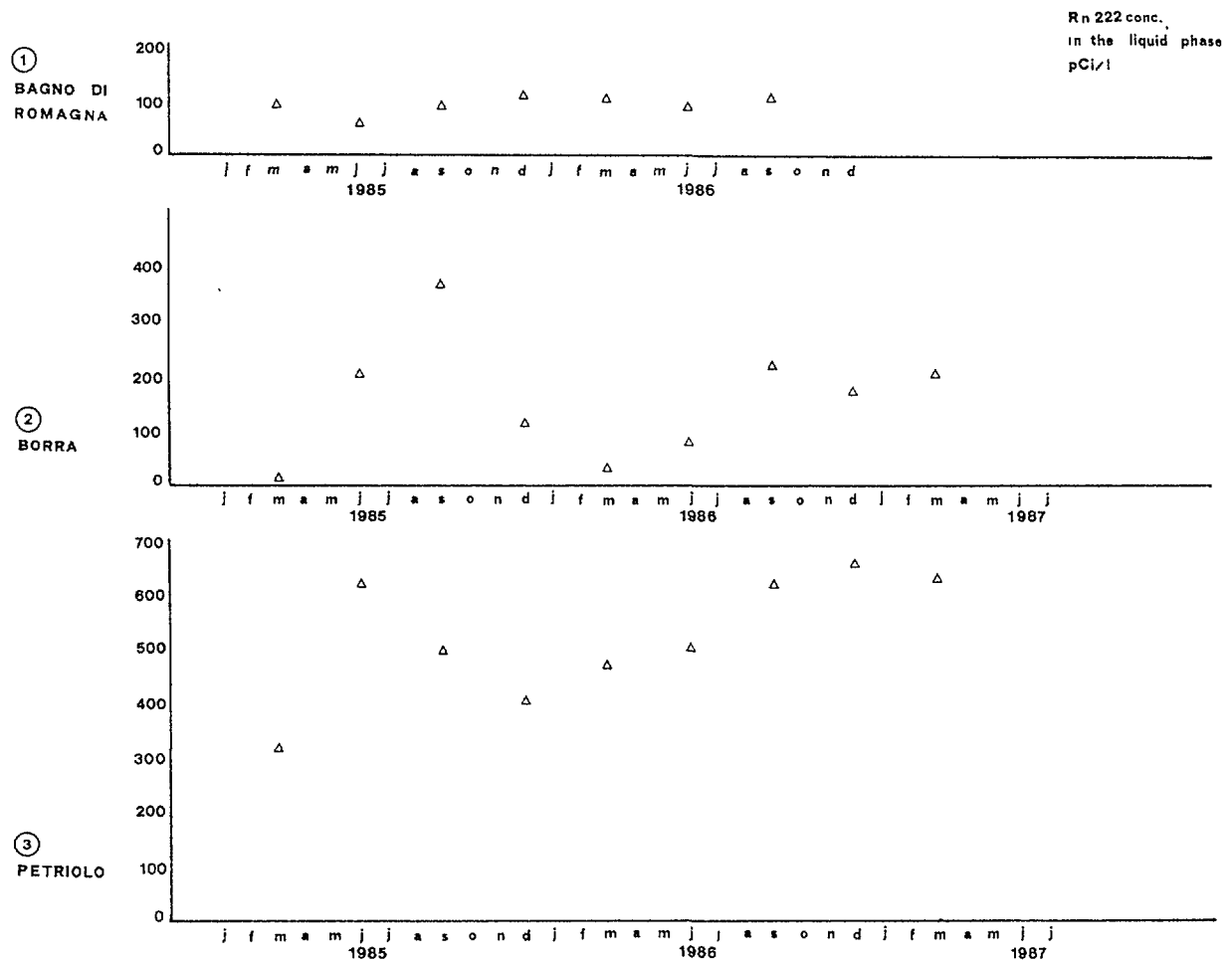


Fig. 8 Radon concentration in thermal waters from selected springs of Central Italy. The springs bargain to different hydrological circuits. The apparent similitude in the behaviour of spring 2 and 3 is not related to meteorological effects (courtesy of Meteorological Service- Tuscan Region) and is probably due to the movements of a regional hydrogeodeformation front able to trigger strong CO<sub>2</sub> activity.

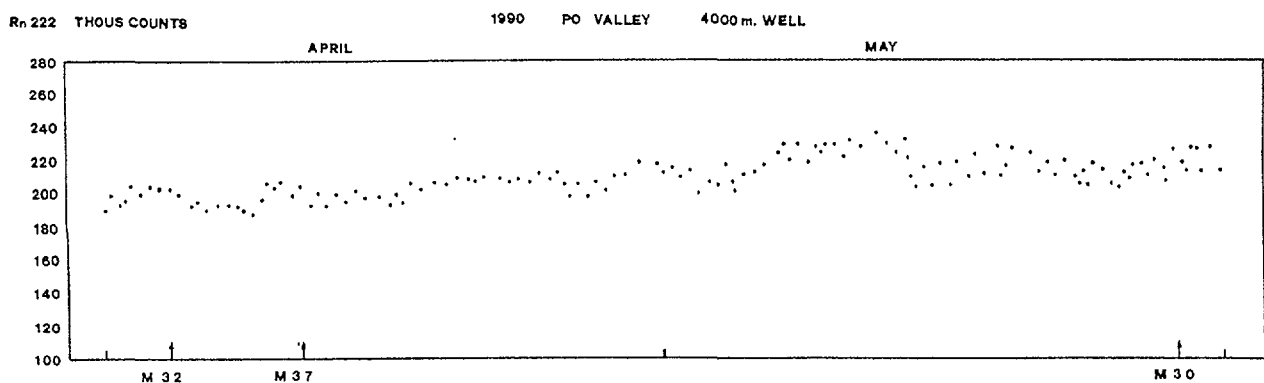


Fig. 9 Plot of Radon 222 countings recorded from an automatic station located on a 4000 mts. depth well in the Po Valley. The listed earthquakes satisfy eq.3 and have been preceded by slight anomalies. Other anomalies may be attributed to short-term and long-term tidal effects.

prediction researches utilizing a 4000 m. depth well located near Mantova (Po Valley), (fig.9), equipped with a Na I continuous Radon monitor. The water is characterized by a 80 m<sup>3</sup> / h spontaneous constant outflow, stable temperature at 59 °C, dO18 = -10.1 ‰, TDS = 0.89 g/l and absence of CO<sub>2</sub> free gas. A tidal effect in Radon is daily recognizable ( Breitenberg and Zadro, 1991) , due to the mechanisms discussed in ch.5 but poor is the sensitivity to earthquakes. In fig. 8 a two months Radon record is showed jointly with earthquakes able to satisfy eq.3 in the same period. The absence of clear spike-like signals in Radon is probably related to the absence of a deep gas component and inhibit the utilization of the well as an earthquake sensitive emergence ( Wakita et Al., 1988). Other Authors have studied the behaviour of selected thermal springs during the occurrence of earthquakes (Albarelo et Al., 1990 ; King and Wood, 1992) and thermal springs characterized by high CO<sub>2</sub> partial pressure showed to be particularly sensitive to impending earthquakes confirming the link among CO<sub>2</sub> and seismic activity as underlined by Irwing and Barnes (1981) and by Bredehoeft and Ingebritsen (1990). Other thermal springs have been continuously monitored in the Tuscan area for other hydrologic researches (Grassi et Al., 1990), but no CO<sub>2</sub> strong activity was detected and the observed seasonal variations can be related only to meteorologic noise so CO<sub>2</sub> is confirmed as a diagnostic parameter in selecting sensitive springs suitable for earthquake prediction researches purposes. As above mentioned this kind of occurrence is particularly frequent in Central and Southern Italy, where the occurrence of strong earthquakes is also most probable ( Petrini, 1980; Mulargia and Gasperini, 1991 ) ; we conclude that earthquake prediction future researches should be concentrated in the mentioned areas and should be characterized by a particular attention to Radon related to the whole geochemical and isotopic context.

### Acknowledgements

Thanks are due to Dr. R. Scandiffio, ENEL (Unità Nazionale Geotermica) for his useful remarks during the preparation of this report.

### REFERENCES

Agodi, A , Frasca, A , Imposi, S , Ripepi, C , Patane, G , 1990 Maree gravitazionali ed eruzioni vulcaniche : un tentativo di correlazione tra le due fenomenologie durante l'eruzione del 1983 In Atti del 7° Convegno del C.N.R. , Gruppo Nazionale di Geofisica della Terra Solida pp 1659-1669

Albarelo , D , Ferrari, G , Martinelli, G and Mucciarelli, M , 1991 Well level variation as a possible seismic precursor : a statistical assessment from Italian historical data In M. Weiss (Editor), Earthquake Prediction Tectonophysics, 193 385-395

Andrews J. N., 1977 Radiogenic and inert gases in groundwaters In H. Paquet and Y. Tardy (Editors), Proc. 2nd Int. Symp. on Water-Rock Interaction, Strasbourg Inst. Geol. Univ. L. Pasteur, Paris 334-342

Andrews, J. N., and Hussain, N., 1989 Radon and helium modelling of an HDR geothermal reservoir In Miles D. L. (Editor), Water Rock Interaction , WRI 6, Rotterdam 19-22

Andrews, J. N., and Wood, D. F., 1972 Mechanism of radon release in rock matrices and entry in ground waters Trans. Int. Min. Metall., 81 B197-B209

Arieh, E. and Merzer, A. M., 1974 Fluctuations in oil before and after earthquakes Nature, 247 534-535

Barazzuoli, P., Costantini, A., Grassi, S., Lazzarotto, A., Micheluccini, M., Piantelli, F., Salleolini, M., Sandrelli, F., Squarci, P., Taffi, L., Veronesi, G., 1987 L'energia geotermica in Provincia di Siena, Siena, 1988, pp. 1-201

Barsukov, V. L., Serebrennikov, V. S., Varshal, G. M., and Garanin, A. V., 1979 Geochemical methods of predicting earthquakes Geochemistry International, 16, n. 2 1-13

Barsukov, V. L., Varshal, G. M., Garanin, A. B., and Serebrennikov, V. S., 1984 Hydrochemical Precursors of Earthquakes In Earthquake Prediction, UNESCO, Paris 169-180

Bassignani, A., Finazzi, P. B., Fracchetta, V. and Sartorio, C., 1988 Misure di radioattività sugli "scale" nel settore SESI Istituto di Radioprotezione AGIP RAD, Milano, pp. 1-14

Battaglia, A., Ceccarelli, A., Ridolfi, A., Froelich, K. and Panichi, C., 1991 Radium isotopes in geothermal fluids in Central Italy In Int. Symp. on the uses of Isotopes Techniques for water resources development, IAEA, Vienna . 1-26

Bella, F., and Pettinelli, E., 1990 Radon monitoring aimed to study seismic precursors In Tommasino L., Furlan, G., Khan, H. A., and Monnin, M. (Editors), Radon Monitoring in Radioprotection, Environmental Radioactivity and Earth Sciences , Proc. 1° Int. Workshop ICTP, Trieste, 1989, Singapore 275-294

Bergamo, R., Gasparini, P. and Veltri, C., 1985 Studies on radon anomalies related to earthquakes Proc. Int. Conf. Geochemical Earthquake Prediction, Palermo

Bertrami, R., Buonasorte, G., Ceccarelli, A., Pieri, S., Scandiffio, G., and Lombardi, S., 1991 Soil gases in geothermal prospecting : two case histories (Sabatini Volcanoes and Alban Hills, Latium, Central Italy) J. Geophys. Res., 95 . 21 415-421, 481

Biloen, P. and Sachtler, W. M. H., 1981 Mechanism of hydrocarbon synthesis over Fischer-Tropsch catalysts Adv. Catalyses, 30 165-216

Bodsworth, C. and Bell, H. B., 1972 Physical chemistry of Iron and Steel manufacture, London

Bodvarsson, G., 1970 Confined fluid as strain-meters J. Geophys. Res., 75 2711-2718

- Bredehoeft, J D and Ingebritsen, S E., 1990 Degassing of Carbon Dioxide as a possible source of high pore pressures in the Crust In *The Role of Fluids in Crustal Processes* Washington 158-164
- Breitenberg, C, and Zadro, M 1991 Personal communication Istituto di Geodesia e Geofisica, Trieste
- Brondi, M, and Dall'Aglia, M, 1989 Mercury, arsenic, antimony, radon and helium in ground waters and fumaroles from the Vulcano Island In Miles D L., (Editor) *Water Rock Interaction*, WRI-6, Rotterdam 117-120
- Colombo, U, Gazzarrini, F, Gonfiantini, R, Sironi, G and Tongiorgi, E, 1966 Measurements of C 13 / C 12 isotope ratios on Italian natural gases and their geochemical interpretation In *Proc Int. Meeting in Rueil Malmaison, Advances in organic Geochemistry* 279-292
- Crampin, S, 1991 Monitoring changes of stress before earthquakes possibilities for deterministic prediction In *Int Conf on Earthquake prediction State-of the-Art (preprints)* 305-308
- D'Amore, F, and Panichi, C, 1980 Evaluation of deep temperatures of hydrothermal systems by a new gas geothermometer *Geochim Cosmochim Acta*, 44 549-556
- D'Amore, F, Sabroux, J C, and Zettwoog, P, 1978-79 Determination of characteristic of steam reservoirs by radon 222 measurements in geothermal fluids *Pure Appl Geophys*, 117 253-261
- Dobrovolsky, I P, Gershenzon, N I, and Gokhberg, M B, 1989 Theory of electrokinetic effects occurring at the final stage in the preparation of a tectonic earthquake *Physics of the Earth and Plan Inter*, 57 144-156
- Dobrovolsky, I P, Kubkov, S I, and Miachkin, V I, 1979 Estimation of the Size of earthquake Preparation Zones *Pure Appl Geophys*, 117 1025-1044
- Dubinchuck, V T, 1991 The role of intrinsic relaxation characteristics of hydrogeochemical systems in formation of isotopic and chemical precursors of earthquakes (Radon as a precursor of earthquakes) In *Int. Conf on Earthquake prediction State-of-the Art (preprints)* 195-232
- E and P Forum 1988 Low specific activity Radio Active Scale origin, Treatment and disposal The Oil industry international exploration and production Forum Rep n° 6 6, 43 pp
- Facchini, U, Cantadori, M, Magnoni, S, Verdiani, G, Sordelli, C, and Benato, B, 1991 La stazione di monitoraggio Radon al pozzo geotermico di Rodigo In *Geothermal-District Heating Workshop, Commission of the European Communities* 1-25
- Federer, W, 1990 Evaluation of soil gas compositions in the area of Caldara and Monterano by mobile on-line mass spectrometry In V & F Analyse und Messtechnik Ges M B H (technical report), Absam (Austria)
- Ferrara, G C, Ferrara, G, and Gonfiantini, R, 1963 Carbon isotopic composition of carbon dioxide and methane from steam jets of Tuscany In Tongiorgi, E, (Editor), *Nuclear Geology on geothermal areas*, C N R, Pisa 277-284
- Ferrari, C, and Vianello, G 1985 *Le saline dell'Emilia-Romagna. Regione Emilia Romagna* Bologna, 151 pp
- Ferrari G 1991 The 1887 Ligurian earthquake a detailed study from contemporary scientific observations *Tectonophysics*, 193 131-139
- Ferrari, G, and Martinelli, G, 1988 Historical earthquake and premonitory related phenomena data base as a strategy to geophysical and geochemical monitoring of a seismic area. EGS XIII General Assembly, abstract in *Annales Geophysicae*, special issue
- Fitterman, D V, 1979 Theory of electrokinetic-magnetic anomalies in a faulted half space *J geophys Res*, 84 (B12) 6031-6040
- Fleischer, R L, 1981 Dislocation model for Radon response to distant earthquakes *Geoph Res Letters*, 8, n° 5 477-480
- Fleischer, D V, 1983 Theory of alpha recoil effects on Radon release and isotopic disequilibrium *Geochim Cosmochim Acta*, 47 779-784
- Fleischer, R L 1987 Moisture and 222 Rn emanation *Health Phys* 52 797-799
- Friedmann, H, 1991 Continuous spring water Radon measurements in Austria and possible relations to earthquakes In *Int conf on Earthquake prediction State-of the Art (preprints)* 233-240
- Friedmann, H, 1988-89 Untersuchung über die Ursachen von Radonkonzentrationschwankungen in Quellwassern unter besonderer Berücksichtigung der Seismizität *Sitzungser Ost Akad Wiss Math Natur Kl Abt. II*, 197, Bd 5 bis 10 Heft
- Fournier R O, 1989 Geochemistry and dynamics of the Yellowstone national park hydrothermal system *Ann Rev Earth Planet Sci*, 17 13-53
- Gasparini, P, and Mantovani, M S, 1978 Radon anomalies and volcanic eruptions *J Volcanol Geotherm Res*, 3 325-341
- Gianelli, G, 1985 On the origin of geothermal CO2 by metamorphic processes *Boll Soc Geol It* 104 575-584
- Giggenbach, W F, 1979 The Chemistry of Geothermal gases Chemistry Division DSIR Petone (New Zealand)
- Giggenbach W F, and Matsuo, S 1991 Evaluation of results from Second and Third IAVCEI Field Workshops on Volcanic Gases, Mt Usu, Japan, and White Island, New Zealand *Applied Geochemistry* 6 125-141
- Gold T and Soter S 1984/85 Fluid ascent through the Solid Lithosphere and its Relation to Earthquakes *Pure Appl Geophys*, 122 492-530



Gorgoni, C, Bonori, O, Lombardi S, Martinelli, G, and Sighinolfi, G P 1988 Radon and Helium anomalies in mud volcanoes from Northern Apennines a tool for earthquake prediction *Geoch J*, 22 265-273

Gorgoni C Martinelli, G, and Sighinolfi, G P, 1982 Radon distribution in groundwater of the Po sedimentary Basin (Italy) *Chem Geol* 35 297-309

Grassi, S, Squarci P Celati, R, Calore, C, Perusini, P, and Taffi, L, 1990 Nuove conoscenze sul sistema idrotermale di Campiglia Marittima (Livorno) *Boll Soc Geol It* 109 693-706

Gurpinar, A 1987 The IAEA Interregional Project on Seismic Data for Nuclear Power Plant Siting (INT/9/066) In Margottini, C, and Serva, L (Editors) Workshop on historical seismicity of Central Eastern Mediterranean region ENEA, IAEA, Rome

Gurrieri, S, and Valenza, M, 1988 Gas transport in natural porous mediums a method for measuring CO<sub>2</sub> flows from the ground in volcanic and geothermal areas *Rend Soc It Min Petr*, 43 1151-1158

Haussinsky M, 1957 *La chimie nucleaire et ses applications*, Paris

Hamada, K, 1990 Classification of Earthquake Precursor and regularity of precursor appearance In US Japan Earthquake Prediction Seminar (USGS open file report)

Hauksson, E, and Goddard, J G, 1981 Radon Earthquake Precursor Studies in Iceland *J Geophys Res* 86 (B8) 7037-7054

Hooker, P J Bertrami, R, Lombardi, S, O'Nions, R K, and Oxburgh, E R, 1985 Helium 3 anomalies and crust-mantle interaction in Italy *Geochim et Cosmochim Acta*, 49 2505-2513

Irwin, W P, and Barnes, I, 1980 Tectonic Relations of Carbon Dioxide Discharges and Earthquakes *J Geophys Res*, 85 (B6) 3115-3121

ISMES-ATOMENERGOPROJECT, 1991 Evaluation of operating and design earthquakes for the Crimea Nuclear Power Plant Site RAT-CGA-0285 (technical report), 84 pp Rome

ING Istituto Nazionale di Geofisica Seismological Report, Roma, 1981 - 1991

Johnston, M J S and Mauk, F J, 1972 Earth Tides and the Triggering of Eruptions from Mt Stromboli, Italy *Nature*, 239 266-267

Kavabe, I, 1984/85 Anomalous changes of CH<sub>4</sub>/Ar Ratio in Subsurface Gas Bubbles as Seismogeochemical precursors at Matsuyama, Japan *Pure and Appl Geophys*, 122 194-214

Kruger, P Stoker A, and Umana, A, 1977 Radon in geothermal reservoir engineering *Geothermics* 5 13-19

Locardi E, 1991 Minerogenesi di origine mantellica nell'Appennino *Rend Fis Acc Lincei* 2

Marini, L 1991 Geochemistry applied to volcanic surveillance In Second Workshop on Radon Monitoring in Radioprotection, Environmental and/or Earth Sciences, ICTP, IAEA UNESCO pp 24 in press

Mase, C W, and Smith, L 1984/85 Pore Fluid Pressures and Frictional Heating on a Fault Surface *Pure and Appl Geophys* 122 583-607

Mattavelli, L, and Novelli, L 1988 Geochemistry and habitat of natural gases in Italy In Mattavelli, L, and Novelli, L (Editors), *Advances in Organic Geochemistry*, I 1-13

Martinelli, G, 1985 Geochemistry of Groundwaters of the Po Sedimentary Basin (Northern Italy) In Proc 2nd Int Symp on Geochemistry of Natural Waters Leningrad 325-345 (in Russian)

Martinelli, G, 1987 Geochimica dei precursori sismici con particolare riferimento al Radon esperienze della Regione Emilia Romagna Atti del 6° Convegno, CNR, GNGTS, Rome, I 63-71

Martinelli, G, 1992 Geochemistry and fluid dynamics of subterrestrial precursory gases In Earthquake Prediction International School of Solid Earth Geophysics "Ettore Majorana Centre for Scientific Culture", Ence

Martinelli, G, Bassignani, A, Ferrari, G, and Finazzi, P B, 1989 Predicting earthquakes in Northern Apennines recent developments in monitoring of Radon 222 Proc 4th Int Symp Analysis of Seismicity and Seismic Risk, Bechyne Castle

Martinelli, G, and Ferrari, G, 1991 Earthquake forerunners in a selected area of Northern Italy recent developments in automatic geochemical monitoring *Tectonophysics*, 193 397-410

Minissale, A, 1991 Thermal springs in Italy their relation to recent tectonics *Applied Geochemistry*, 6 201-212

Mulargia, F and Gasperini, P, 1991 La previsione statistica dei terremoti *Le Scienze Quaderni*, 59 60-63

Nesmeyanov, An N, 1974 *Radiochemistry*, Moscow, 644 pp

Nikolaevskij, V. N, 1990 *Mechanics of Porous and Fractured Media*, Singapore, 489 pp

Nikolaevskij, V N, 1991 Extraterrestrial induced Multi Years Cyclicality in Geophysical, Geochemical and Biological Parameters In Second Workshop on Radon Monitoring in Radioprotection, Environmental and/or Earth Sciences, ICTP, IAEA UNESCO, pp 19, in press

Panichi, C, 1982 Aspetti geochimici delle acque termali In Il Graben di Siena, CNR PFE 61-72, Roma.

Panichi C, and Gonfiantini, R, 1978 Environmental isotopes in geothermal studies *Geothermics*, 6 143-161

Patella, D, Tramacere, A and Di Maio R 1990 Self-potential Anomalies In Mt. Etna the 1989 eruption, CNR 58-61 Pisa

Petrini V (coord) et Al, 1980 Proposte di riclassificazione sismica del territorio nazionale CNR, PFG, Roma

Postpischl D (Editor) 1985 Catalogo dei terremoti italiani dall'anno 1000 al 1980

- Rice, A., 1985 The Mechanism of the Mt. St. Helens eruption and speculations regarding *sorter effects* in planetary dynamics. *Geophys. Surveys*, 7, 303-384.
- Rikitake, T., 1982 Earthquake forecasting and warning. Tokyo, 402 pp.
- Rinehart, J.S., 1970 Effect of Earth Strain on Geyser Activity. *Geothermics* (special issue) 2, part 2, 1297-1301.
- Roeloffs, E.A., 1988 Hydrologic precursor to earthquakes: a review. *Pure Appl. Geophys.*, 126, 177-209.
- Rogers, A.S., 1958 Physical behaviour and geological control of Radon in mountain streams. *U.S. Geol. Surv. Bull.*, 1952E, 187-211.
- Rydelek, P.A., Davis, P.M., and Koyanagi, R.Y., 1988 Tidal Triggering of Earthquake Swarms at Kilauea Volcano, Hawaii. *J. Geophys. Res.*, 93 (B5), 4401-4411.
- Rykunov, A.L., and Smirnov, V.B., 1985 Variations in Seismicity under the influences of Lunar Solar Tidal deformations. *Izvestiya, Physics of the Solid Earth*, 21, 1, 71-75.
- Sadovskii, M.A., Monakhov, F.I., Kissin, I.G., and Shirokov, B.D., 1984 Short-Term Hydrogeodynamic Precursors of Earthquakes. In *Earthquake Prediction*, UNESCO, Paris, 233-241.
- Shafer, N.E., and Zare, R.N., 1991 Through a beer glass darkly. *Physics Today*, 44, n° 10, 48-52.
- Sobolev, G.A., 1984 Physical processes during the Earthquake Preparation Period. Experiment and Theory. In *Earthquake Prediction*, UNESCO, Paris, 281-310.
- Sugisaki, R., 1981 Deep-seated gas emission induced by the earth tide: a basic observation for geochemical earthquake prediction. *Science* 212, 1264-1266.
- Sugisaki, R., and Sugiura, T., 1986 Gas anomalies at three mineral springs and a fumarole before and inland earthquake. Central Japan. *J. Geophys. Res.* 91, 12296-12304.
- Sultankhodzhaev, A.N., 1984 Hydrogeoseismic Precursors to Earthquakes. In *Earthquake Prediction*, UNESCO, Paris, 181-191.
- Sultankhodzhaev, A.N., Latipov, S.U., Zakirov, T.Z., and Zigan, F.G., 1980 Dependence of Hydrogeoseismological Anomalies on Energy and epicentral Distance of Earthquakes. *Dokl. A.N. Uzb. SSR*, 5, 57-59.
- Tamrazyan, G.P., 1972 Peculiarities in the Manifestation of Gaseous-Mud Volcanoes. *Nature*, 240, 406-408.
- Tidjani, A., Monnin, M., and Seidel, J.L., 1990 Enhancement of radon signals in geophysical studies with the track technique. *Pure Appl. Geophys.*, 132, 495-504.
- Toutain, J.-P., Baubron, J.-C., Le Bronec, J., Allard, P., Briole, P., Marty, B., Miele, G., Tedesco, D., and Luongo, G., 1992 Continuous monitoring of distal gas emanations at Vulcano, southern Italy. *Bull. Volcanol.* 54, 147-155.
- Wakita, H., Nakamura, Y., and Sano, Y., 1988 Short-term and intermediate term geochemical precursors. *Pure Appl. Geophys.* 126, 267-278.
- Wakita, H., Sano, Y., Urabe, A., and Nakamura, Y., 1990 Origin of methane rich natural gas in Japan: formation of gas fields due to large scale submarine volcanism. *Applied Geochemistry*, 5, 263-278.
- Westerhaus, M., Welle, W., Buyukose, N., and Zschau, J., 1991 Temporal variations of crustal properties in the Mudurnu Valley, Turkey: an indication for regional effects of local asperities? In *Int. Conf. on Earthquake Prediction: State-of-the-Art*, Strasbourg (preprints), 272-281.
- Westerhaus, M., Zschau, J., and Welle, W., 1990 Tidal tilt modification related to earthquakes. In *ESC XXII General Assembly, European Seismological Commission, (Programme and Abstracts)* Barcelona, 199.
- Wood, R.M., and King, G.C.P., 1991 Hydrological Signatures of Earthquake Strain, 69 pp, in press.
- Woith, H., Pekdeger, A., and Zschau, J., 1991 Groundwater Radon anomalies in space and time: a contribution to the joint Turkish-German earthquake prediction research project. In *Int. Conf. on Earthquake prediction: State-of-the-Art*, Strasbourg (preprints), 282-283.
- Wyss, M., (Editor), 1991 Evaluation of Proposed Earthquake Precursors, American Geophysical Union, 94 pp.
- Zagin, B.P., and Saskina, N.N., 1966 Transfert du Radon dans la chambre d'emanation a l'aide du gaz carbonique. *Radiochimie*, 8, 125-126 (unabridged translation of Radiokhimiya, original in Russian).
- Zongjin, M., Zhengxiang, F., Yingzhen, Z., Chengmin, W., Guomin, Z., and Defu, L., 1990 Earthquake Prediction: Nine Major Earthquakes in China (1966-1976), Beijing, 332 pp.
- Zschau, J., and Ergunay, O., 1989 Turkish-German Earthquake Research Project, Istanbul, 211 pp.

# SOME ISOTOPIC AND GEOCHEMICAL ANOMALIES OBSERVED IN MEXICO PRIOR TO LARGE SCALE EARTHQUAKES AND VOLCANIC ERUPTIONS

S. DE LA CRUZ-REYNA\*, M.A. ARMIENTA-HERNANDEZ

Instituto de Geofísica,

Universidad Nacional Autónoma de México

N. SEGOVIA

Instituto Nacional de Investigaciones Nucleares

Mexico City, Mexico

## Abstract

A brief account of some experiences obtained in Mexico, related with the identification of geochemical precursors of volcanic eruptions and isotopic precursors of earthquakes and volcanic activity is given. The cases of three recent events of volcanic activity and one large earthquake are discussed in the context of an active geological environment. The positive results in the identification of some geochemical precursors that helped to evaluate the eruptive potential during two volcanic crises (Tacaná 1986 and Colima 1991), and the significant radon-in-soil anomalies observed during a volcanic catastrophic eruption (El Chichón, 1982) and prior to a major earthquake (Michoacán, 1985) are critically analyzed.

## 1. INTRODUCTION

Mexico is a country with significant rates of seismic and volcanic activity. Analysis of seismic gaps and recurrence periods of large, shallow interplate earthquakes along the Mexican subduction zone, marking the boundary between the Cocos and the North American plate, shows that the average repeat times of large earthquakes ( $M_s \approx 7.4$ ) in 6 Pacific regions (East, Central and West Oaxaca, Petatlán and Colima) are between 32 to 56 years. Most of the seismic moment (or, equivalently, seismic energy) release since the beginning of the 19th century appears to occur for 15 years followed by relative quiescence in the next 15 years (Singh et al., 1981).

On the other hand, an analysis of the historical volcanic activity shows that since the 16th century, the rate of (significant size) eruptions is in the order of 15 per year. In this case many types and sizes of eruptions have been taken into account and, in contrast with the seismic analyses in which the size of earthquakes can be measured in a rather well defined way, the classification of eruptions by size is a problem that has not been solved.

It is therefore clear that the risk associated to such levels of seismic and volcanic activity in Mexico can not be overlooked, and some ways to mitigate it must be looked for. One of the ways of reducing the

risk is improving the estimate of the probability of occurrence of a given event. This can be done by statistical methods involving the analysis of the past activity, or by "real time" methods, requiring close monitoring of the regions prone to produce an earthquake or an eruption. The latter involves a developed capability of recognizing the precursors of significant events.

In this report we attempt to describe the experiences obtained in Mexico over more than 10 years in the recognition of geochemical and isotopic precursors of earthquakes and volcanic eruptions.

## 2. TECTONICS OF MEXICO, EARTHQUAKES AND VOLCANOES

### 2.1. SEISMICITY

The large earthquakes ( $M_s \approx 7$ ) in Mexico are mostly caused by the subduction of the Cocos and Rivera oceanic plates under the North American plate (Figure 2.1). The relatively small Rivera plate, subducts under the state of Jalisco at a relative velocity of about 2.5 cm/y. The relative velocity of Cocos plate respect to the continent varies from about 5 cm/y near Manzanillo to about 8 cm/y in Tehuantepec, Oaxaca.

The largest 20th century earthquake in Mexico (known as the Jalisco earthquake,  $M_s=8.2$ , June 3, 1932) occurred on the interface between the small Rivera and the North American plates, showing in this way that young, small plates, with a relatively low subduction velocities can produce large earthquakes (Singh et al., 1985), and the destructive Michoacán earthquake of September 19, 1985 (causing over 20000 victims

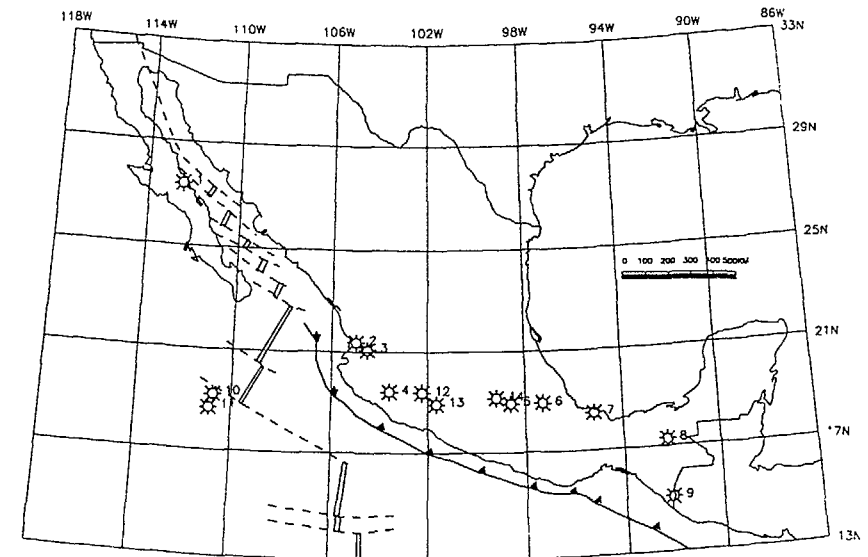


Figure 2.1 Map of Mexico showing its main tectonic features

\* Consultant to the National Center for Disaster Prevention (CENAPRED), Av. Delfín Madrigal 665, Mexico, D.F., Mexico.

in Mexico City) was originated in the Michoacan gap, one of the quiescence regions along the boundary between Cocos and North American plates.

Some large earthquakes also occur under the continent at depths near 60 km. These earthquakes are usually produced by normal faulting associated with the breaking of the subducting lithosphere. Although this type of events is rather infrequent, they can be very destructive like those of Oaxaca (01-15-1931,  $M_s=7.8$ ), Orizaba (08-23-1973,  $m_b=7.3$ ) and Huajuapán de León (10-24-1980,  $m_b=7.0$ ).

Even less frequent are the interplate continental earthquakes. Although their magnitudes are usually less or equal to 7.0, they can be very destructive too, as it was the case of the Jalapa earthquake (01-03-1920,  $M_s=6.4$ ), or the Acambay earthquake (11-19-1912,  $M_s=7.0$ ).

## 2.2. ACTIVE VOLCANISM

Most of the holocenic volcanism occurs along the Mexican Volcanic Belt (MVB), a somewhat anomalous feature, for it runs unparallel to the subduction zone. There are also active volcanic centers in the Baja California Peninsula in northwestern Mexico and in the state of Chiapas (southeastern Mexico).

The Mexican Volcanic Belt is a complex continental arc extending more than 1200 km from the Pacific coast, to near the Gulf of Mexico. Other important volcanic centers are Tres Virgenes volcano, located in the middle of Baja California Peninsula, Los Tuxtlas volcanic massif, the active volcanoes of Chiapas: El Chichón and Tacaná, and the Revillagigedo island volcanoes.

MVB volcanism is believed to be related to the 80-100 km depth contour of the subduction of the Cocos plate, which varies in a similar way as the relative velocity between Cocos and North America. This means that this depth contour may be far away from the trench at the SE end of the Mexican portion of the Middle America Trench. The complex structure of the MVB is characterized by a large diversity of volcanic types. The most common is the monogenetic volcano, which clusters in extensive fields like that of Michoacan-Guanajuato, containing more than 1000 cones, or the Chichinautzin monogenetic field, south of Mexico City, containing nearly 200 cones. There are also large active andesitic composite volcanoes like Colima (about 4000 msl), Popocatepetl (5450 msl), or Pico de Orizaba (5700 msl). Off the MVB are important active centers, the most recent of which is El Chichón, that produced one of the most destructive eruptions in the history of Mexico, in 1982.

Appendix 1 shows a summary of the recent seismic activity, while Appendix 2 gives a brief account of the historical volcanic activity in Mexico.

## 3. THE MEXICAN EXPERIENCE WITH GEOCHEMICAL PRECURSORS OF THE VOLCANIC AND SEISMIC ACTIVITY

Geochemical precursors research is rather new in Mexico, and most of its development can be found during the last few years. In that time there have been two cases of volcanic crises in which geochemical methods have been used with some success. To the knowledge of the authors, no work on identification of geochemical precursors of tectonic earthquakes has been done. The reason of this becomes evident after examination of Figure 2.1, or the table in Appendix 1. Most of the large

scale seismicity occurs along the subduction zone, over 1200 km long, and with many of the important earthquakes having their epicenters in the sea, making very difficult to have a sampling program that could cover all the regions of higher probability of occurrence (zones of relative quiescence).

However, the volcanic crises mentioned above were mostly related to seismic swarm crises, and several of the observed geochemical precursors have been associated to the seismic component of the volcanic activity.

The two cases in which geochemical methods have been used to identify precursors, the 1986 Tacaná volcano seismic crisis and phreatic explosion (3.1) and the 1991 Colima volcano seismic crisis and effusive eruption (3.2), are described next.

### 3.1 CHEMICAL CHANGES OBSERVED IN SPRING WATERS AT TACANÁ VOLCANO, CHIAPAS, MEXICO: A POSSIBLE PRECURSOR OF THE MAY 1986 SEISMIC CRISIS AND PHREATIC EXPLOSION

#### 3.1.1 INTRODUCTION

(This case is described in detail in De la Cruz-Reyna et al., 1989). Tacaná volcano ( $15.13^{\circ}\text{N}$ ,  $92.10^{\circ}\text{W}$ ) marks the north-western end of the active Middle America volcanic belt. Its summit serves as one of the benchmarks of the Mexico-Guatemala border line.

Starting in late December 1985, local earthquakes accompanied by rumble noises were reported. The earthquakes continued through January 1986, when a portable seismic network was installed around the volcano. At the same time, sampling and chemical analysis of the only known thermal spring of the volcano, Agua Caliente, was initiated. The largest single earthquake occurred on February 3 1986, producing some damage in adobe constructions in the town of Ixchiguan, Department of San Marcos, Guatemala, about 25 km ENE of the Tacaná summit. Afterwards the seismic activity declined and persisted at lower levels for about seven weeks. All of this time the epicenters were confined to an area between 15 and 25 km E and ENE of the volcano.

However, around April 20, 1986, earthquakes started to be felt and heard stronger in the immediate volcano area, and the seismic network located them in a volume below the volcanic deposits of the W and SW flanks of the mountain. This new activity steadily increased until May 7, when an earthquake swarm caused panic among the population. On May 8, when earthquakes were felt at a rate of 2 or more per minute, a small phreatic explosion opened a craterlet in the northwestern flank of the volcano at 3600 m, and almost exactly on the Mexico-Guatemala border line. The approximate craterlet dimensions were 20 x 10 meters, and a white steam column rose approximately 1000 meters, when unperturbed by winds. Afterwards seismicity declined steadily returning to the pre-April levels two days later. However the fumarole has persisted with little change to the present time.

An interesting feature of the seismicity is that both, the activity prior to April 20 1986, concentrated between 15 and 25 km E - ENE from the volcano summit, and the after-April 20, seismicity, below the volcano, including the May 7-9 swarm, had essentially the same waveform features: well defined impulsive P and S phases and a dominant high frequency content. This activity developed within the high background seismicity of a region of high tectonic activity. North America, Cocos and the Caribbean plates interact in complex ways and local interplate earthquakes of magnitude 6 or higher are not uncommon. However the

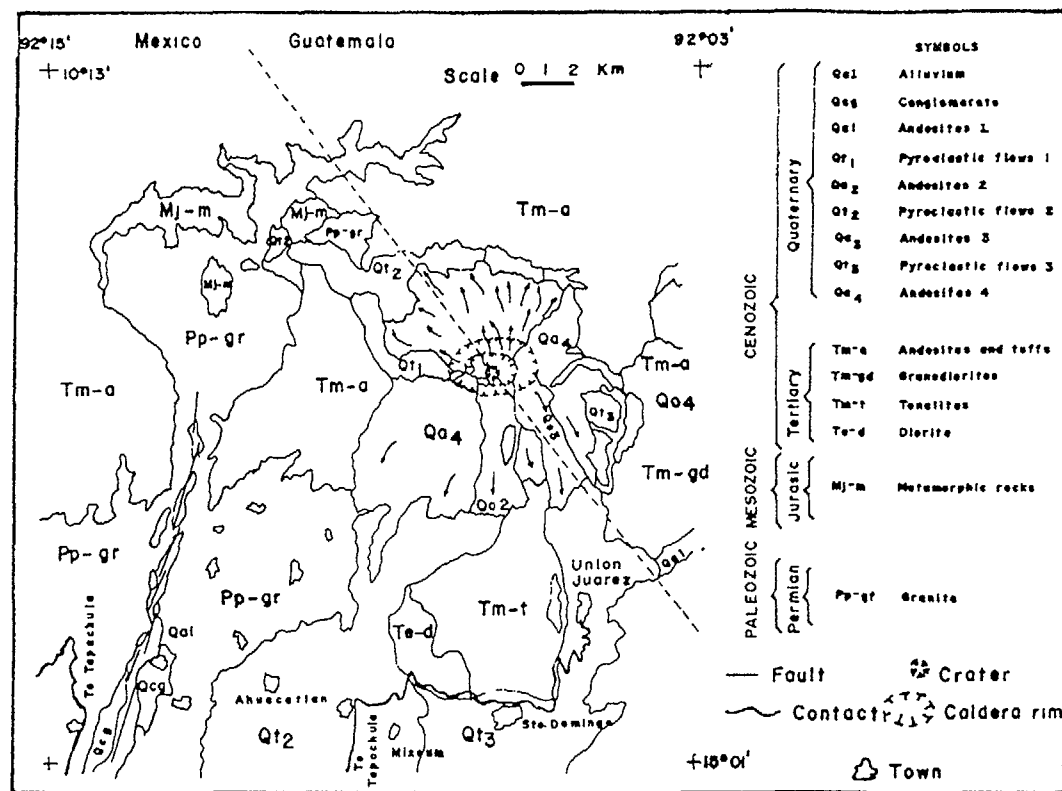


Figure 3.1.1. Schematic geological map of the Tacana area (after De la Cruz M. V. and Hernandez, 1985).

waveform of these larger interplate earthquakes is rather different to that mentioned above.

### 3.1.2 LOCAL GEOLOGY

A large crystalline rock massif forming a horst structure of granitic and granodioritic rocks of Cambrian to Permian age is the dominant structure underlying the volcano. This granitic basement outcrops at the base of the volcano at heights up to 2000 meters above sea level. The Tacana volcanic products intrude and overlie this basement forming stratified layers of variable thickness. At least four major recent events can be recognized (De la Cruz V. and Hernandez, 1985). In all of them the composition is hornblende-biotite andesite. The stratigraphy of deposits suggest a repetitive process: a major pyroclastic eruption including massive laharic flows is followed by a dome implant and effusion of lava flows. The oldest of these events is dated at ca. 40000 ybp (Espindola and Medina, 1988). No relevant evolution in lava composition has been reported and the volume of the

ejecta has decreased persistently. Fig. 3.1.1 schematically summarizes the geology of Tacana volcano.

### 3.1.3 SAMPLING AND CHEMICAL ANALYSIS

Sampling of the Agua Caliente thermal waters proved to be rather difficult due to problems of access to the area. For this reason sampling dates were conditioned to field opportunities to access the zone. During the collection of the water samples, temperature was measured and discharge of the spring was estimated from the depth of the small pool it formed. During the entire sampling period, no changes in temperature greater than 1° C, nor flow rate changes greater than a few percent were observed. Temperature of the spring water still remains at 50° C.

Chemical analyses were performed by different methods. Sulfates were determined by a modified turbidimetric technique. Bicarbonates were measured by titration using a mixture of methyl red and bromocresol green

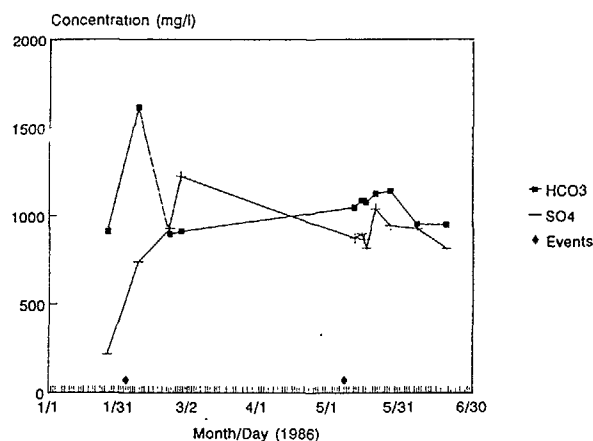


Figure 3.1.2. Plot of the Sulfate and Bicarbonate concentrations in the Agua Caliente spring waters vs. time.

as indicator, and heating the sample at the end of the titration for a more accurate end point. Iron was determined using the phenanthroline method. The transmittances were measured using a Carl Zeiss PM2 DL spectrophotometer with 1 cm optical path. Magnesium and calcium concentrations were obtained through the complexometric titration with EDTA. Boron was colorimetrically measured through its reaction with carminic acid. Chloride and fluoride ion concentrations were determined with selective electrodes.  $\text{Na}^+$  and  $\text{K}^+$  were directly measured with a flame photometer. Finally,  $\text{SiO}_2$  concentration was colorimetrically obtained by the molybdosilicate method.

#### 3.1.4. OBSERVED CHEMICAL CHANGES IN HOT-SPRING WATERS: IDENTIFICATION OF PRECURSORS

Figure 3.1.2 shows the variation of sulfate concentration with time. The most important feature that can be recognized, is the large increase in dissolved  $\text{SO}_4^{2-}$ , two months prior to the seismic crisis and phreatic explosion. The sulfate ion concentration increases steadily since January 26, when it measured 218 mg/l to February 27, when it rose to 1225 mg/l. Two days after the May 8 event, the samples show a significant decrease to 875 mg/l, maintaining similar values until May 20, when it increases again. After that, the sulfate concentration slowly decreases back to the 800 mg/l range maintaining similar values afterwards. Table 3.1. lists the concentrations read on different dates.

Bicarbonate ion concentration shows a behavior which is somewhat anticorrelated with that of sulfate. The bicarbonate concentration is relatively stable over the period from mid-February to early May, as is the sulfate concentration. However, large changes in sulfate concentration occur simultaneously with important changes in the opposite direction for bicarbonate (Fig. 3.1.2). Total iron ( $\text{Fe}_{\text{tot}}$ ) also shows important variations. The third column in Table 3.1.1 lists concentration changes which roughly correlate with the sulfate behavior. These data are plotted in Fig. 3.1.3.

TABLE 3.1.1 Concentrations of different species in spring water samples of Tacana volcano, expressed in mg/l.

Date of Sampling	$\text{SO}_4^{2-}$	$\text{HCO}_3^-$	Fe	$\text{Mg}^{++}$	B
01-26-1986	218	911	---	146.9	2.51
02-08-1986	740	1615	8.8	151.8	2.02
02-22-1986	928	897	2.6	157.2	2.97
02-27-1986	1225	912	9.6	152.0	2.62
05-11-1986	875	1051	3.6	283.9	3.53
05-14-1986	900	1088	9.0	212.2	2.04
05-15-1986	867	1091	---	212.2	2.61
05-16-1986	820	1079	7.4	212.2	3.72
05-20-1986	1042	1128	5.0	191.8	2.91
05-26-1986	945	1142	8.2	212.2	1.76
06-06-1986	928	953	---	154.4	3.20
06-18-1986	815	950	---	152.0	2.76

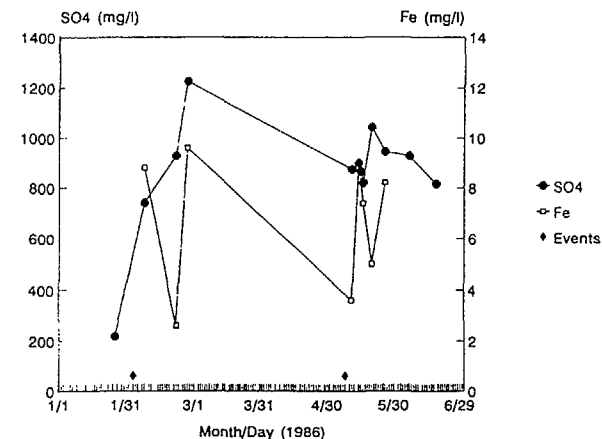


Figure 3.1.3. Iron and sulfate ion variations in time. Agua Caliente.

Other elements which also vary significantly, are magnesium (as  $\text{Mg}^{++}$ ) and boron, as shown in Table 3.1.1, although these changes roughly correlate with the May activity rather than with the sulfate variations (Fig 3.1.4). Our chemical analyses included determinations of  $\text{Cl}^-$ ,  $\text{F}^-$ ,  $\text{Ca}^{++}$ ,  $\text{Na}^+$ ,  $\text{K}^+$ , and  $\text{SiO}_2$ , but no significant variations of their concentrations, compared with the above mentioned, were found during the sampling period.

#### 3.1.5. GEOCHEMICAL MECHANISMS

The large increase in  $\text{SO}_4^{2-}$  concentration in Agua Caliente thermal spring water, detected nearly two months before the seismic swarm crisis and phreatic explosion, may be attributed to the dissolution of  $\text{SO}_2$  from

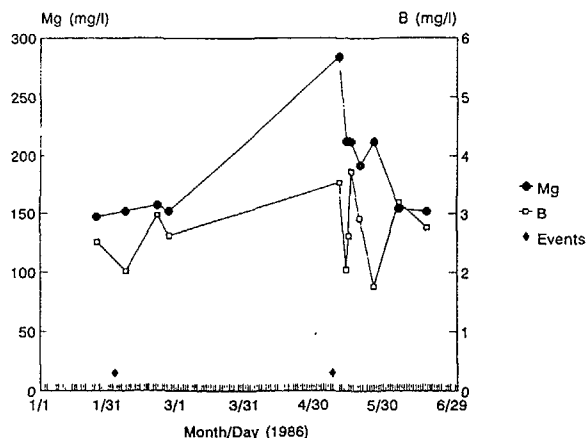
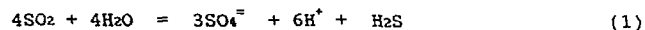
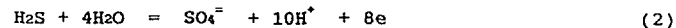


Figure 3.1.4. Magnesium ion and boron concentrations in Tacana spring waters.

a deep magma source into shallow groundwaters, which together with other magmatic gases, found its way to the surface by a mechanism discussed below. Increasing emissions of  $\text{SO}_2$  prior to eruptions have been reported by many authors (see for instance Malinconico, 1987). The amount of these ascending gases was probably not very large, but sufficient to significantly increase  $\text{SO}_4^{2-}$  through the following reaction:

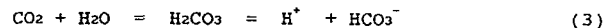


It is also possible that the  $\text{SO}_4^{2-}$  concentration anomaly in the spring waters may have a contribution from a secondary process, in which a somewhat larger amount of magmatic gases dissolves in intermediate or deeper groundwaters and by the above reaction liberates significant amounts of  $\text{H}_2\text{S}$ , which reacts with shallower waters through:



From the available data it is not possible to ascertain which proportion of the above  $\text{H}_2\text{S}$  comes from reaction (1) occurring in a deep water body or directly from a magma source.

The above reactions may influence the carbonate equilibrium enhancing the carbonic acid formation by the release of  $\text{H}^+$  as follows:



This would produce an inverse relationship between sulfate and bicarbonate ions, since increasing hydrogen ions should produce higher concentrations of carbonic acid at the expense of bicarbonate.

A steep rise of  $\text{HCO}_3^-$  apparently preceded the increase in  $\text{SO}_4^{2-}$ . This suggests an earlier discharge of  $\text{CO}_2$  at about the time of the

Ixchiguan earthquakes. This may be explained in terms of the lower solubility of  $\text{CO}_2$  in silicate melts, compared with that of sulfur. Thus, when new fracturing allows the gas passage,  $\text{HCO}_3^-$  is the ion expected to rise its concentration first in the water. Iron may be subject to redox reactions exchanging electrons with sulfur or oxygen.  $\text{Fe(II)}$  is more soluble in water than  $\text{Fe(III)}$ ; thus an increased amount of iron in solution could be related to the release of electrons through reaction (2). In this way, increasing oxidation of sulfide should produce higher iron values. We do not have a clear explanation for the magnesium variations, however it is conceivable that its higher solubility in acidified waters may produce higher concentrations in the spring waters by leaching of the surrounding rock.

Boron, as  $\text{H}_3\text{BO}_3$ , frequently can be found in high concentrations in hot springs (Harder, 1969). Its source could be either magmatic or leaching from country rocks; in this case, the base value (i.e. the values corresponding to the "normal" situation), probably results from country rock leaching. However, the observed anomaly may be attributed to some magmatic gas influence since, without significant changes of temperature of the hot spring water, an important increase in boron concentration can only be explained by an increased discharge of volatile magmatic boron compounds into intermediate or shallow groundwater.

The halogens ( $\text{Cl}^-$ ,  $\text{F}^-$ ) do not vary significantly during the sampling period. Fluorine, which could be considered a magmatic product, probably contributed little to the spring water composition in this case, since the HF content in volcanic gases is generally only 1 to 2 vol-% of the total gases (Koritnig, 1969). These low values are a result of the high solubility of molecular fluorine compounds in magmatic melts, compared to that of water (Martini, 1984). If the amount of magmatic gases affecting the intermediate or shallow water tables in Tacana is not very large, it is likely that most of the fluorine reacts locally leaving little to be transported as an ion to the surface spring water, or perhaps the dissolution of fluorine compounds occurs in deeper groundwaters allowing no important exchanges of fluoride ions with the shallow waters.

The uniform behavior of the silica concentrations reflects no important changes in the temperature of the water source, supporting in this way the idea of a secondary exchange between deeper water and shallower tables from which the spring comes. The apparent correlation of the different ions and compounds with the  $\text{SO}_4^{2-}$  anomaly, or with the seismic swarm and phreatic explosion about two months later is difficult to explain by a single argument.

If one accepts the presence of a magmatic body at an undetermined depth, it is conceivable that the regional seismic activity developing in the area since December 1985 produced significant fracturing of the basement rocks, thus allowing an increased transport of magmatic gases to the surface. The above arguments suggest the existence of two groundwater bodies at different depths, receiving this moderate amount of gases. The most abundant magmatic gases like  $\text{SO}_2$  for instance, would produce effects which could be immediately seen in the spring water through mechanisms like those proposed above. Less abundant volatiles, like boron, would first slowly affect the lower water body and reflect its presence in the shallow waters only when increased gas transport or saturation of deeper waters occur. This may also explain the observed increase of non-magmatic ions like magnesium since higher leaching would correspond to higher acidity of the shallower water body. Unfortunately no *in situ* values of the pH of the spring water could be obtained to corroborate this explanation.

### 3.1.6. MODEL AND CONCLUSIONS

There is little doubt of the relation between the early regional seismic activity, the seismic swarm crisis, the phreatic explosion and the chemical changes observed in the Agua Caliente spring water. The nature of the observed anomalies and the *a posteriori* determined character of the May 8, 1986 phreatic explosion are indicative that the amount of magmatic volatiles in this process is rather small. The changes in the observed concentrations of chemical species suggest the existence of two groundwater bodies at different depths, and some degree of interaction between them. The shallower waters are represented by the Agua Caliente spring samples; the deeper ones may be the source of the phreatic explosion.

It can thus be concluded that the activity observed in May 1986 was of phreatic origin in the sense that the moderate degassing of a quiescent magma body reached shallow depths through the increased fracturing of basement rock, probably produced by regional tectonic stresses. Deeper water underwent direct interaction (both, chemical and thermal) with a moderate amount of the hot magmatic gases ascending through the basement new fractures, process which eventually evolved into the phreatic explosion. The shallower water body supplying the hot spring water interacted chemically but not thermally with products resulting from the deeper primary process, producing the observed changes in the Agua Caliente samples. This allowed a preliminary evaluation of the volcanic risk in the area, fixing the hazard level respect to an important magmatic eruption in the low side, since no significant magmatic volatiles content have been found, nor volcanic B-type earthquakes or harmonic tremors have been so far detected.

## 3.2 GEOCHEMICAL VARIATIONS IN LAKE WATERS CORRELATED WITH THE 1991 SEISMIC AND EFFUSIVE ACTIVITY OF COLIMA VOLCANO

### 3.2.1 INTRODUCTION

Colima Volcano sites in an highly complex tectonic region, where the North American, Pacific, Cocos, and Rivera lithospheric plates interact. Although nominally a part of the Mexican Volcanic Belt, which is pointedly non-parallel to the orientation of the local subduction trench, the Colima- Nevado-Cantaro system appears to be oriented perpendicular to the MVB. These volcanoes, of which the first one is the only active one, are located within a graben structure which trends roughly N-S and connects at its northern end with two other graben structures, the Chapala (trending roughly E-W and including the Primavera caldera) and the Zacoalco (trending roughly NW-SE and including the Tequila, Ceboruco and Sangangüey volcanoes). This arrangement has led some scientists to propose the Colima graben as a spreading center where the Jalisco block separates from the continent (Luhr et al., 1985; Bourgois et al., 1988).

Colima Volcano (19.512°N, 103.617°W), also known as Fuego, is an andesitic stratovolcano raising nearly four kilometers over the sea level, and is indeed the most active volcano in Mexico. The present cone grew within a horseshoe shaped caldera-like structure 4-5 km wide, produced by a large volcanic debris avalanche eruption which destroyed the ancient Paleofuego volcano more than 4,000 years ago. The collapse of this nearly 10 km<sup>2</sup> large volcanic building, produced a massive debris deposit covering a large area 10<sup>3</sup> km<sup>2</sup> south of the volcano (Robin et al., 1987; Luhr & Prestegard, 1988). Currently, about a quarter million people live in the area covered by the resulting avalanche deposits, and a similar event would have catastrophic results, unless appropriate measures are taken.

Historical activity has been reported by eyewitnesses since 1560. Over this time 29 eruptions have been recorded, from which at least 6 have had large magnitudes and intensities (Medina, 1983, 1985; De la Cruz-Reyna, 1991; see Appendix 2). This volcano is indeed the most active in the country and has shown an ample spectrum of eruption types, ranging from the most common block lava, merapien avalanches, to intense pyroclastic explosions, like those of 1585, 1606, 1622, 1818, 1890, and 1913, which produced large pyroclastic flows and intense ash falls over distances hundreds of kilometers away from the crater. Although part of the volcano risk area is a national park, several towns, agricultural and industrial centers have developed in areas that may be vulnerable to large scale pyroclastic activity. Currently Colima Volcano is 3800 m high, has very steep slopes, and a growing block lava dome is plugging the summit crater. The gravitational stability of such a configuration, is a problem which spans both scientific and public defense areas of interest.

Since 1975, block lava flows started to develop from the summit dome, when the crater formed by the 1913 eruption was filled by a slowly rising magma column which overflowed, producing repeated merapien avalanches. This type of activity has been repeated with different degrees of intensity along the past decade. The latest dome growth and lava flow formation episode started in march 1991, and was preceded by evolving patterns of volcanic seismicity. In late 1975, an extrusion event produced block lava flows which poured through the dome, producing a significant increase in the size and number of merapien type avalanches. This type of activity repeated in 1982 and 1985.

On February 1991, a microseismic swarm developed in Colima volcano and persisted with fluctuations in intensity and rate of occurrence until the beginning of March. Contemporary to this, a new scoria-encrusted lobe extruded on the SW sector of the summit block lava dome of the volcano Figure 3.2.1. Increased fumarolic activity had also been present. This lobe grew generating numerous avalanches, first of displaced older dome material and of mixed juvenile and older material later. On April 16 and 18, relatively large amounts of dome and lobe materials produced the largest avalanches ever observed. The amount of dust displaced by these avalanches gave the impression that a large pyroclastic eruption was taking place. However, these "dust flows" can not be called actual pyroclastic flows since the material was powdered by effect of the avalanche rather than by explosions within the volcano. Nevertheless, given the history of this volcano, there was big concern about the possibility of a large scale eruption developing, and all available methods of monitoring were applied.

### 3.2.2. MONITORING OF COLIMA VOLCANO

Small scale monitoring began in 1975, when portable seismic stations were operated there for limited periods, some geodetic baselines were established and a net of radon detectors was implanted around Colima volcano. This type of sporadic observations continued until 1989, when a permanent telemetric seismic network began to be deployed to study the seismic activity (tectonic and volcanic) in the region. Currently, this network consists of 5 close range short period vertical seismometers distributed on and around the volcano and radio linked to a central receiving and processing unit. Another two telemetric stations are located 35 and 40 km south and SW of the volcano to study regional seismicity. This network was purchased by the government of the State of Colima and is operated by the University of Colima. A high stability Blum tiltmeter has also been recently installed in the volcano within a joint Mexico-France program.



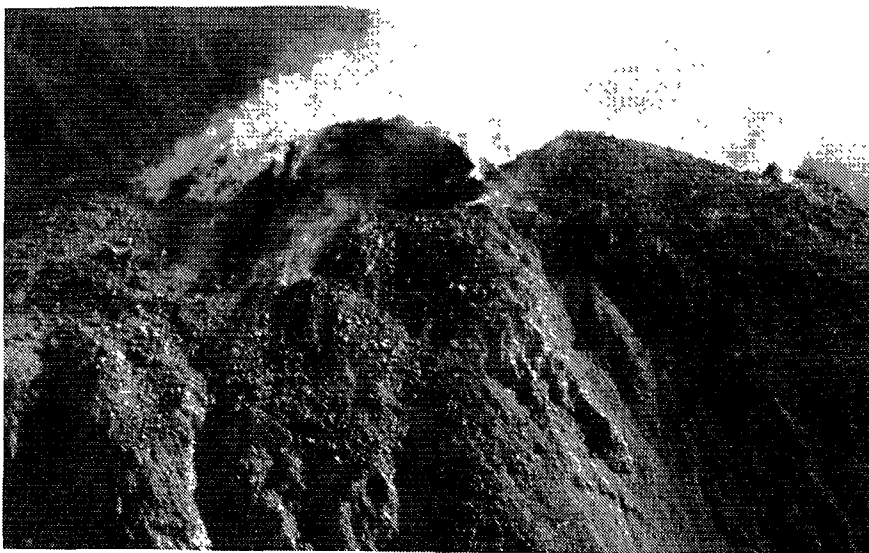


Figure 3.2.1. The recent (March 1991) lobe on Colima volcano summit dome.

Regarding geochemical methods, water samples were taken from the nearby lakes, water streams, and two cold water springs, for geochemical analysis and several airborne COSPEC measurements were made.

### 3.2.3. DESCRIPTION OF THE RECENT ACTIVITY

Steadily increasing fumarolic activity and more frequent small merapian avalanches from the summit crater, preceded the recent activity, which begun on February 14, when seismic activity at Colima Volcano started to increase from a base line level of 1 or 2 very small A-type earthquakes per day to several significantly larger A-type events per hour plus - never before observed, B-type earthquakes - at a rate of about 2 per hour. Within a few hours, the seismic activity increased fivefold. Between February 14, and February 15, more than 110 earthquakes were identified. The seismicity decreased afterwards until February 24, when a new swarm developed producing more than 150 recognizable events per day, for 48 hours. Again A and B type earthquakes were detected and frequent small to medium merapian-like avalanches sled along the flanks of the volcano from the crumbling edges of the summit dome. After February 25 a period of relative quiescence followed, after which seismic activity increased again to a rate of about 130 events per 24 hours. This second micro-seismic crisis began to decrease after February 27 and the number of avalanches increased getting a maximum on March 2. Previously, on March 1, a dome shaped black lobe was observed for the first time, growing on the SW sector of the summit dome. Seismic activity decreased after March 3, but the growth of extrusive lobe towards the southern rim continued, and begun to cover a substantial portion of the dome. Merapian avalanches

continued all the time. On April 12, a new micro-seismic crisis began with about 110 events per day, and lasted until April 13, when the seismicity returned to background level.

On April 16, the merapian avalanche activity increased, and a fairly small part of the lobe, carrying a significant amount of older material from the summit dome, collapsed during a protracted series of avalanches accompanied by medium size earthquakes and large dust clouds. Wind carried most of the dust to the SE, producing light ashfalls on towns in that sector at distances up to 30 km. That night, incandescent blocks were observed in the dome and sliding downhill. Afterwards, a block lava flow started to develop from the SW sector of the summit dome. Frequent small incandescent avalanches issued from the lava front, and occasionally from the top and flanks of the lava flow, particularly the eastern flank. The rock avalanches and associated dust clouds have been repeated with different degrees of intensity up to late 1991. The estimated lava production rate, during the dome growth and lava flow episode is about 5000 - 10000 m<sup>3</sup>/day. Three canyons of the main volcano drainage system towards the SW and S were filled up with avalanche-derived clastic material, most of which is very fine powder. This material had a non-compacted volume of the order of 10<sup>8</sup> m<sup>3</sup>. A lahar warning was issued for the approaching rainy season (which usually begins in middle June). Fortunately, the onset of the rains was slow, and the dust was harmlessly washed away.

### 3.2.4. OBSERVED CHEMICAL ANOMALIES

Some 10.5 km due southwest of the volcano, an important change was observed in the water of a small group of lakes belonging to a private ranch. The caretaker reported on March 7 that the level of the lakes had dropped about 30 cm in 24 hours and that fish were dying at a high rate. A quick analysis of the dying fish showed no evident signals of disease and no other bird or mammal species living around the lakes appeared to be affected.

### 3.2.5. SAMPLING AND CHEMICAL ANALYSIS

Water samples were taken from the lakes in order to determine if there had been any important chemical anomaly in the water composition due to the volcanic activity. Temperature and pH were measured in the field. Chemical analyses included: Na<sup>+</sup>, K<sup>+</sup>, Ca<sup>2+</sup>, Mg<sup>2+</sup>, HCO<sub>3</sub><sup>-</sup>, CO<sub>3</sub><sup>2-</sup>, OH<sup>-</sup>, Cl<sup>-</sup>, SO<sub>4</sub><sup>2-</sup>, A (conductivity), SiO<sub>2</sub>, B, Fe, F<sup>-</sup>, S<sup>2-</sup> and As. Standard wet methods described above were applied. Sodium and potassium by flame photometry. Calcium and magnesium by complexometric titration. Alkalinity by titration with HCl, using bromocresol green and methyl red as indicator. Chloride and fluoride were measured with selective electrodes. The conductivity value was measured with a conductivity cell. For SiO<sub>2</sub> and B the spectrophotometric method was used; silicon by means of the formation of yellow molybdosilicate, and boron through its reaction with carminic acid. Iron was measured with an atomic absorption spectrophotometer. A specific sample treated with sodium carbonate and zinc acetate was taken for the sulfide determination which was performed also colorimetrically by the blue methylene method. Sulfates were obtained by turbidimetry. Finally arsenic was analyzed through the arsine generation and colorimetric determination.

### 3.2.6. OBSERVED CHEMICAL COMPOSITIONS

The pH values were all alkaline ( $\approx$  8.0). This contrasts with the pH measured in water samples of the same area on March 1985 by Martini which were slightly acidic (around 6.0). Hydrogeochemical classification of the waters was done by means of Piper diagrams (Figs.3.2.2 and 3.2.3)

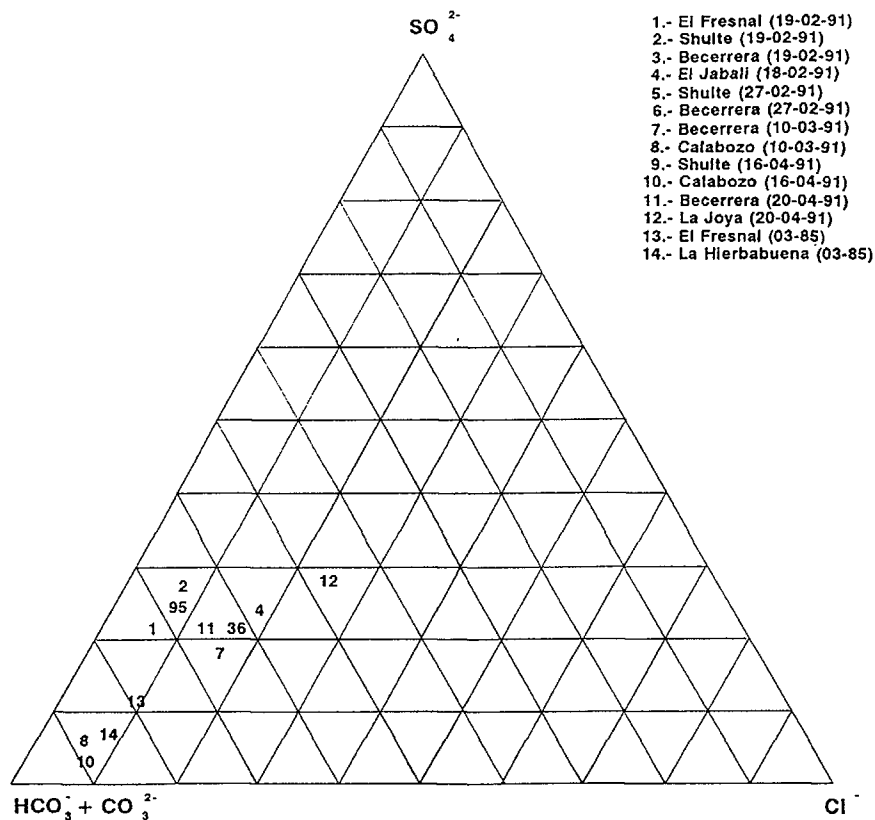


Figure 3.2.2. Anion Piper diagram of Colima water samples.

showing a Bicarbonate mixed type of waters. Another difference with the analyses done by Martini in 1985 (personal communication) which showed a bicarbonate sodium type. Principal ions did not show important concentration variations during the sampling period (February-April 1991) (Figures 3.2.4 and 3.2.5). Bicarbonate concentrations were around 6 times the chloride concentrations and around 4 times the sulfate concentrations. Sulfide or arsenic were not detected in any of the samples. Minor species (boron and iron) did show variations, although not very large. Boron concentration increased in the sample taken around the date of extrusion of the lobe, and iron concentration decreased with time (Figure 3.2.6).

Saturation indexes were obtained for anhydrite, calcite, aragonite, dolomite, gypsum and magnesite. The values were greater than 1 for calcite, dolomite, aragonite and magnesite, indicating an oversaturation of the water for these minerals. Figures 3.2.7 and 3.2.8 show their variation with time. No important changes were observed for the samples

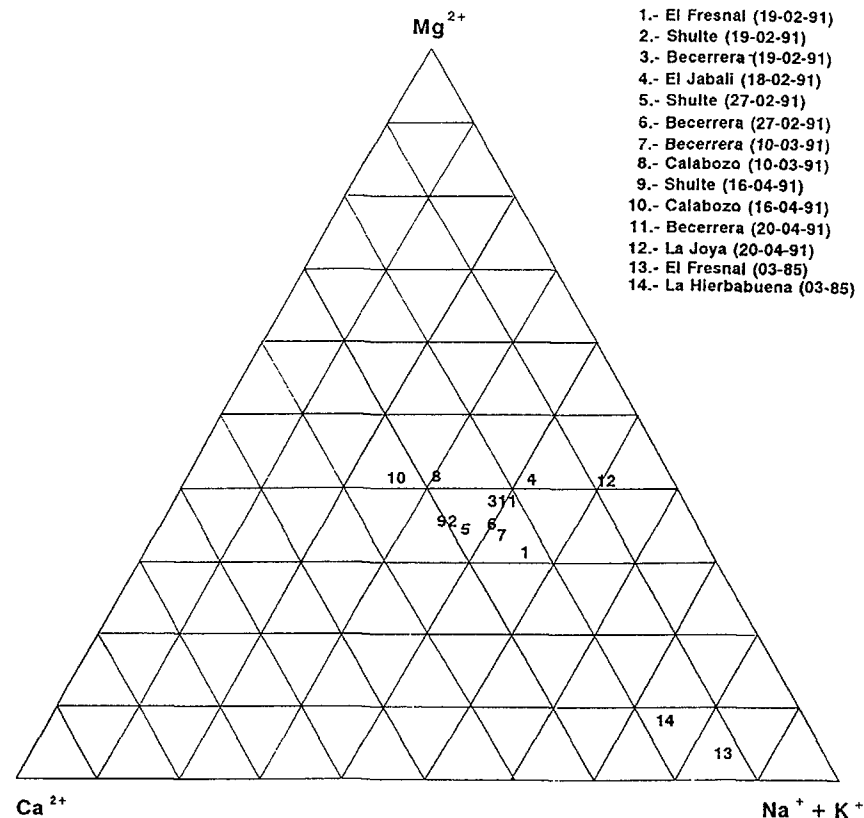
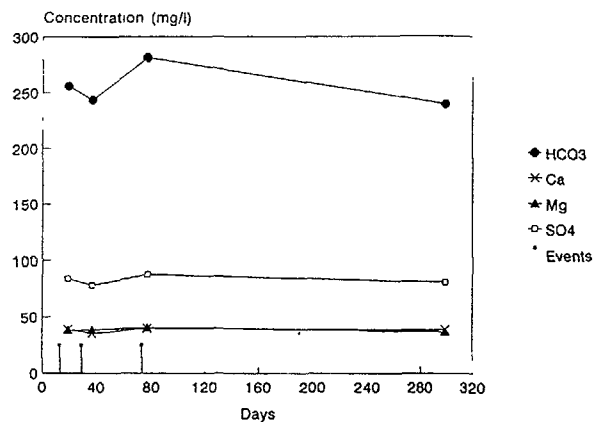


Figure 3.2.3. Cation Piper diagram of Colima water samples.

taken from "La Becerrera". The water from "Schulte" showed some variations, the most remarkable one being the increasing with time of the saturation index for dolomite.

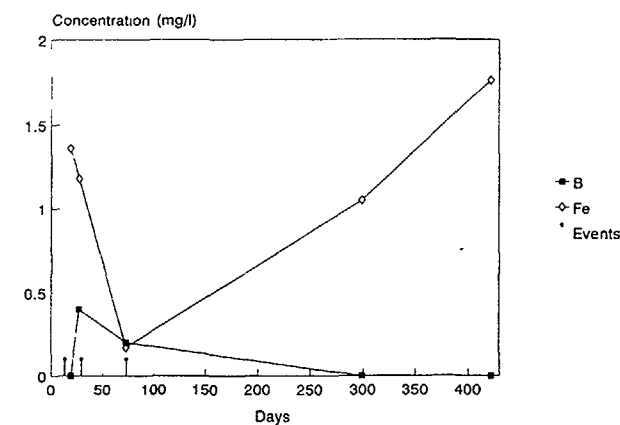
### 3.2.7. MODEL AND CONCLUSIONS

COSPEC (Correlation spectrometry) airborne measurements, were done in collaboration with Dr Stanley Williams of the Louisiana University (Dr. Williams is currently at Arizona State University) started on April 25. They showed SO<sub>2</sub> production rates on the order of 300 - 600 ton/day, similar to those observed in 1982 by Casadevall et al. (1984). These stable low levels are consistent with the relatively low energy released by seismicity and support an interpretation that the present cycle of activity does not yet include important quantities of new magma or magmatic gases. This is apparently inconsistent with the relative high levels of carbonates and bicarbonates relative to the other anions observed in the water samples, which could be attributed to the



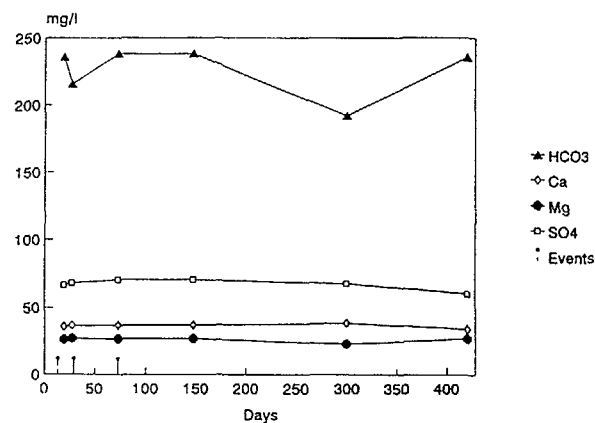
Since February 1st, 1991

Figure 3.2.4. Ion variations at La Becerrera site.



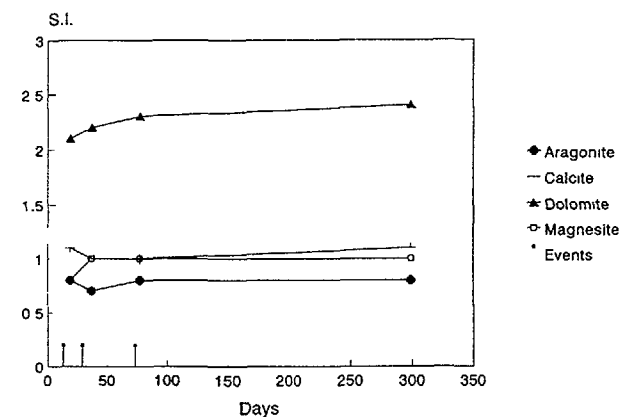
Since February 1st 1991

Figure 3.2.6. B and Fe variations at Schulte site



Since February 1st 1991

Figure 3.2.5. Ion variations at Schulte site



Since February 1st 1991

Figure 3.2.7. Time variations of saturation indexes at La Becerrera site.

dissolution of  $\text{CO}_2$  coming from a magma body. However, one could say that the anomaly observed in the water samples is a rather small contribution, for other magmatic gases did not show any significant increase.

The values of the saturation indexes for the minerals containing magnesium and calcium and the increasing of the dolomite saturation index with time indicates that leaching of country rocks may be the cause of the amount of carbonates and bicarbonates transferred to the

water, together with calcium and magnesium. However the moderate amount of boron which showed some correlation with the activity may indicate some interaction of the water with magmatic gases.

The observed chemical variations led to the conclusion that the effusive activity of the volcano, with its associated shallow seismicity, has modified the groundwater flow patterns by cracking the shallow crust and by changing the stress patterns, allowing an increase

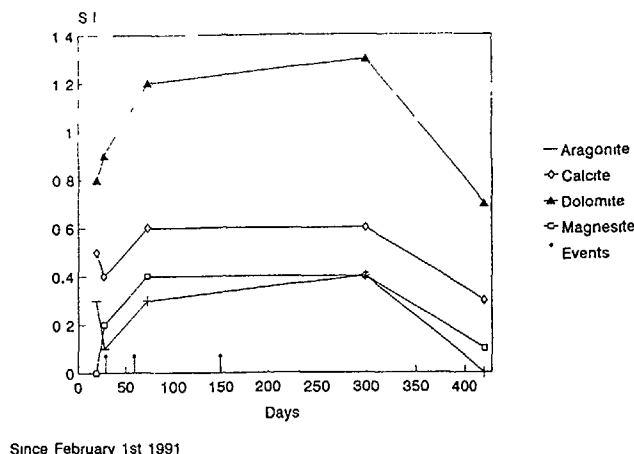


Figure 3.2.8. Time variations of saturation indexes at Schulte site

in the leaching of the country rock, and also the contact with a slightly increased volume of magmatic gases. The observed stable low levels of  $\text{SO}_2$  in the volcanic column, the mixed character of the water sampled anomalies and the absence of significant deep seismicity supported an interpretation that the present cycle of activity does not yet include important new magma or magmatic gases, and the tremors, which have not been repeated since, have been attributed to hydrothermal activity in the dome enhanced by the beginning of the rainy season.

#### 4. THE MEXICAN EXPERIENCE WITH ISOTOPIC PRECURSORS OF THE VOLCANIC AND SEISMIC ACTIVITY

Isotopic methods, mostly radon-in-soil, is also a relatively new development in Mexico. However, it has been used more extensively than geochemical methods due to the relative simplicity of the sampling and its low cost. This method has been used in different sites for different purposes, like seismic and volcanic monitoring (De la Cruz-Reyna et al., 1985; Segovia et al., 1986), studies of environmental radon levels (Segovia et al., 1987, 1988, 1989, 1990), geophysical and geochemical surveying (De la Cruz-Reyna et al., 1986) and it has rendered positive results as (a posteriori) recognizable precursors during large seismic and volcanic events. The analysis of radioactivity levels of volcanic products have also produced some interesting results, as a possible source of information that may help to develop volcanic risk criteria. One case in which a clear correlation between important radon-in soil anomalies were related to a large volcanic eruption is discussed in section 4.1. The results of radioactivity analysis of volcanic eruption products in terms of volcanic potential are described in section 4.1.6. Finally, a case in which a significant radon in soil anomaly may be interpreted as a precursor of a large earthquake is discussed in section 4.2.

#### 4.1. RADON EMANOMETRY IN SOIL GASES

##### 4.1.1 INTRODUCTION

El Chichon Volcano ( $17.36^\circ\text{N}$ ,  $92.23^\circ\text{W}$ ) in the state of Chiapas, Mexico, erupted violently on March 28, 1982. Two major eruptions followed on April 3 and April 4, 1982. The preceding seismic activity was recorded by a seismic network operating at 27 km south of the volcano (Havskov et al., 1983). After the first eruption, more detailed seismic monitoring of the volcano continued using a portable network. At the same time, monitoring of radon content in soil was initiated in order to study the degassing behaviour of the area adjacent to the volcano.

In general, it is conceivable to associate radon concentration variations with changes in flow patterns of diverse fluids within the ground, resultant from modifications in local stress fields of the crust. An easily detectable tracer for gas flows is  $^{222}\text{Rn}$  (radon), a naturally radioactive noble gas emitting 5.48 MeV alpha particles in its decay to  $^{218}\text{Po}$ , with a mean life of 3.825 days. Other naturally occurring Rn isotopes,  $^{220}\text{Rn}$  (thoron) and  $^{219}\text{Rn}$  (actinon) can follow fluid flows in the ground, but their short half lives, 55s, and 3.92 s, do not permit significant transport. Alpha particle track methods allows to detect very low levels of  $^{222}\text{Rn}$ , free from interference from other earth radioactivity (Fleischer and Mogro-Campero, 1978). The evidence that radon concentration in soil gases undergoes significant changes in correlation with volcanic activity is growing rapidly. Reports by Cox et al. (1980), Seidel and Monnin (1982), and others show that anomalies in radon concentrations in soil can lead to a better understanding of the volcanic phenomena and have a significant forecasting value. Positive radon anomalies observed in hot springs (Chirkov, 1975) were correlated with eruptive events. Gasparini and Mantovani (1978) suggest that an increase in radon emission could be produced either from fractured rocks heated by magmatic gases, or by direct emission of radon from magma body reaching shallow depths. Del Pezzo et al. (1981) conclude that radon anomalies might correspond to an increase of magmatic pressure at depth. We report here the variations of radon content in soil following the eruptions of March-April, 1982 at El Chichon Volcano, and the high activity of radon and thoron daughters in its erupted products.

##### 4.1.2. THE VOLCANO SITE AND ACTIVITY

El Chichon is located half-way between the eastern end of the Mexican Volcanic Belt and the northern end of the Central-America volcanic belt, in a region of thick sedimentary rock strata (Fig. 4.1.1). The sedimentary beds are folded, forming a sequence of anticlines trending NW-SE covering an ample area of the central and northern Chiapas. El Chichon intruded through the sediments at a small syncline between the Union anticline (with its axis about 5 km W of the volcano) and Caimba anticline (with its axis 7 km E of the volcano). Descriptions of the geological setting can be found in Canul et al. (1983), and in Duffield et al. (1984). Regional stratigraphy has been described in detail by Santiago-Acevedo (1962) and Lopez-Ortiz (1962).

The oldest formation (Salty Formation or red beds), averaging 800 m thick, of Triassic-Jurassic age, contains oceanic and continental sediments. It underlays a Late-Jurassic-Early Cretaceous evaporite deposits of anhydrite and halite, (Santiago-Acevedo, 1962). Upper-Cretaceous deposits consist of alternate limestone and lutite beds. El Chichon stands on exposed Oligocene and Eocene rocks, that in other regions of "Sierra Madre de Chiapas" form massive deposits up to 5 km thick of alternate lutites, sandstones and conglomerates, with some

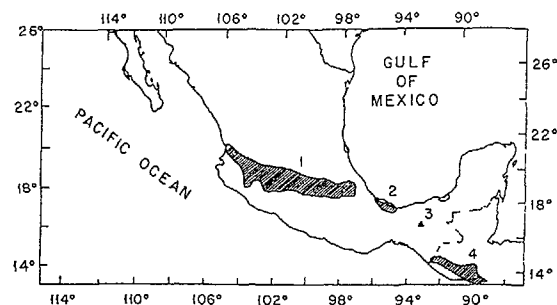


Figure 4.1.1. Location of El Chichon volcano: 1. MVB; 2. Los Tuxtlas volcanic massif; 3. El Chichon volcano; 4. Central America Volcanic Belt

horizons (5-30 cm thick) of volcanic ashes interbedded with the uppermost lutites (Santiago-Acevedo, 1962).

El Chichon is a complex of andesitic domes, talus breccias and pyroclastic and air-fall deposits (Rose et al., 1982). Prior to the 1982 eruptions, its central dome raised nearly 1300 m over sea level. The March-April, 1982 eruptions removed the 1 km diameter central dome producing a crater with the same diameter and 300 m depth. Part of the floor of the crater is now partially covered by an acid, Cl and S rich lake (Casadevall et al., 1984).

The total amount of material ejected by El Chichon during the March-April plinian eruptions was about  $0.54 \text{ km}^3$ , from which  $0.18 \text{ km}^3$  correspond to removed rock debris and  $0.36 \text{ km}^3$  (density normalized to  $2.6 \text{ g/cm}^3$ ) to juvenile material. The three major eruptions were similar in the volume of ejected juvenile material, although the first (March 28) and the third (April 4) produced mostly tephra-fall, while the second (April 3) produced pyroclastic flows, pyroclastic surges and tephra-fall. The composition of the erupted products is the same for the three eruptions, porphyritic trachyandesite, relatively rich in  $\text{SO}_3$  and  $\text{K}_2\text{O}$ , containing phenocrysts of plagioclase, hornblende, augite, anhydrite, titanomagnetite, apatite, sphene, pyrrhotite, and biotite (Luhr et al., 1984; Cocheme and Demant, 1983; Prol et al., 1982); and previous activity dated at about 650 yr BP and 1250 yr BP show no important differences from this composition (Duffield et al., 1984; Tilling et al., 1984; Rose et al., 1984).

Microprobe and neutron activation analyses reported by Luhr et al. (1984) show that fresh pumices of the 1982 eruptions of El Chichon contain a high proportion (2%) of anhydrite, precipitated directly from the melt, accounting for almost all the whole-rock sulfur. Apatite is reported to appear commonly as an inclusion in anhydrite. The uranium and thorium contents found by Luhr et al., in the pumices are 3.2 ppm and 10.3 ppm respectively. These values are high when compared with average values reported for andesites (see for instance Taylor, 1968, who found typical values of 0.69 ppm and 2.2 ppm for U and Th contents in 18 samples of western Pacific andesites). The highest concentrations of U and Th in the mineral separates were found in sphene and anhydrite (mostly through its apatite inclusions). Isotopic analyses by Rye et al.

(1984) suggest that the high values of  $\delta^{34}\text{S}$  for the bulk magma may indicate assimilation of evaporites, although the "normal" (slightly high)  $\delta^{18}\text{O}$  values in crystals, glass and pumices gives no evidence of extensive assimilation of sedimentary rocks. Rye et al. conclude that the sulfur in the El Chichon magma may have two possible non-exclusive origins: assimilation of continental evaporites and partial melting of sulfide deposits in the subducted plate beneath El Chichon. To these peculiarities of El Chichon activity, one more can be added: The high radon and thoron activity induced in the environment by the eruptions.

#### 4.1.3. RADON MONITORING IN SOIL

The experimental set-up for radon monitoring in soil, as described by Seidel and Monnin (1982), is shown in Figure 4.1.2. A shallow hole, 1 m deep, is drilled at each site where radon is to be monitored. The hole is sheathed with a 4 cm diameter, 100 cm long PVC pipe. A smaller tube, 2.2 cm internal diameter and 30 cm long, is inserted inside the pipe and dropped to its bottom. An integrating track detector, cellulose nitrate LR-115 type II, manufactured by Kodak-Pathe, is secured on the top of

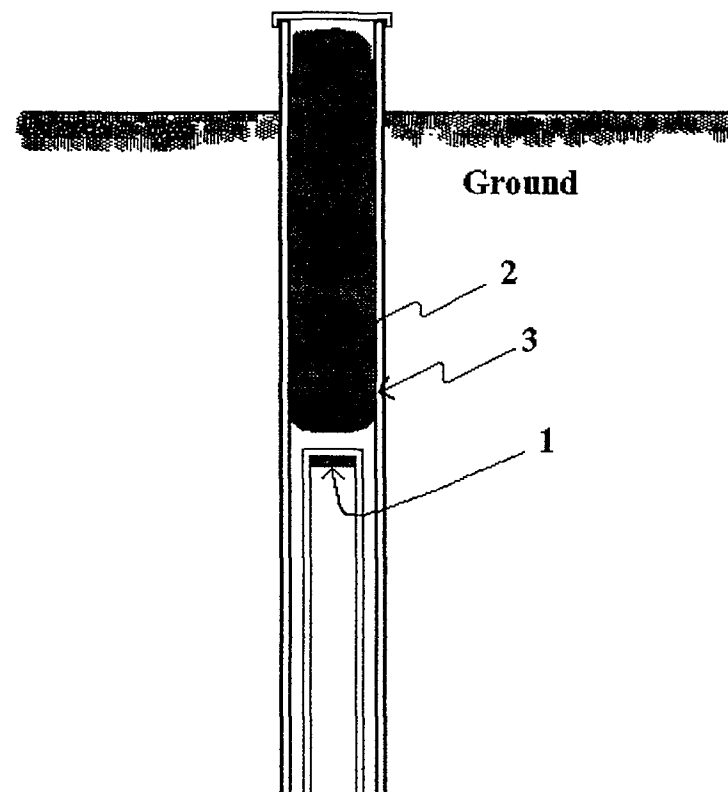


Figure 4.1.2. Radon measuring device: 1. LR-115 plastic detector; 2. Thermal insulator; 3. External tube.

the inner tube, its sensitive surface facing down. Both tubes are closed to minimize atmospheric effects, and the space left between the inner tube and the top of the external pipe is filled with a thermal insulating material. This helps to reduce moisture condensation on the detector surface. The diurnal temperature variations at the depth of the detector are estimated to be no greater than five per cent of the surface variations. Since atmospheric temperature variations in El Chichon latitude are small, (no more than about 15 °C maximum difference between extreme temperatures), cumulative effects of temperature variations on the detectors are neglected.

The position of the detector in the tube is such that only alpha particles from decays occurring within the tube are recorded. The length of the inner tube (30 cm) permits that any thoron gas that may add some unwanted contribution to the radon tracks counting will decay before reaching the detection volume under the detector. After exposure, the detector is chemically etched to enlarge the paths of the alpha particles produced by the decay of radon and its daughters. The etching is performed in a 2.5 N, NaOH solution at 55 °C, to reduce the 12 µm original thickness of the detecting foil to 6 µm.

The evaluation of the number of alpha tracks in each detector is performed with a jumping spark counter (Maldonado et al., 1982). Overall background of detector-measuring system is determined as the number of spark counts on an unexposed detector that has been chemically etched. This number is then subtracted from exposed detectors. Unexposed detectors are stored in sealed polyethylene bags at low temperature to prevent any degradation of the detecting film and to reduce contamination from atmospheric radon. Periodic testing of the detector stock shows that, even for films that have been stored for several months, the background levels are in the range of 3 to 5 tracks/cm<sup>2</sup>, this back-ground level is neglected; otherwise it is systematically subtracted from the measured track counts. Standard deviation of repeated readings on each detector with the spark counter is always less than 3 %.. The number of tracks in field-exposed detectors is proportional to the radon concentration in the detection volume under the detector and is reported in units of tracks per square centimeter per 7 days exposure. According to the range of alpha particles in air and the energy sensitivity range of the LR-115 film detector (0.6-4.4 Mev), and using the geometrical relations reported by Somogyi et al. (1984), an activity equivalent for the detector counts reading is 3.0 tracks/cm<sup>2</sup> week-pCi/l.

#### 4.1.4. RADON MEASUREMENTS AT EL CHICHON VOLCANO

Radon concentrations have been monitored in five fixed stations located on the north region of El Chichon volcano. The sites for these stations are shown in Figure 4.1.3. The exposure time for each detector fluctuated from one to several weeks. At the end of a sampling period, each batch of detector was sealed in a polyethylene bag and given to a central laboratory where it was washed and chemically etched within the next 2 days. After etching, the stability of alpha tracks is very high and no special storing conditions were the required.

Soil samples from the bottom of the radon monitoring sites were taken in order to measure the uranium content of pre-eruption soil. These samples were dried and pulverized. Uranium was extracted with ethylacetate for fluorimetric determinations using the method described by Korkish et al. (1973). The results of uranium content in soils collected at the bottom of radon monitoring stations around El Chichon are shown in Table 4.1.1.



Figure 4.1.3. Distribution of radon stations around El Chichon volcano

Table 4.1.1. Uranium content in soil samples obtained at the bottom of different sites around the northern region of El Chichon volcano.

Location	U (ppm)
Ixtacomitan	2.3
Caimba	1.7
Nicapa	1.7
Ostucan	1.7
Poste Electrico	1.7

#### 4.1.5. TIME EVOLUTION OF RADON ACTIVITY. POSSIBLE CAUSES

The evolution of radon activity in the stations Ixtacomitan, Ostucan, Nicapa, Caimba and Poste Electrico is shown in Figure 4.1.4. In Ixtacomitan and Ostucan, sampling was performed between the eruption time and January, 1983. The remaining stations were lost during the summer of 1982 due to the floods produced by the heavy rainfall and the deposition of tephra in streams. The radon emanation shows a general tendency to decrease with time. However it is particularly noticeable that on 3 stations a significant increase occurred between May and June.

The validity of those results might be questioned. Was it really something happening in depth, or are we dealing with an experimental

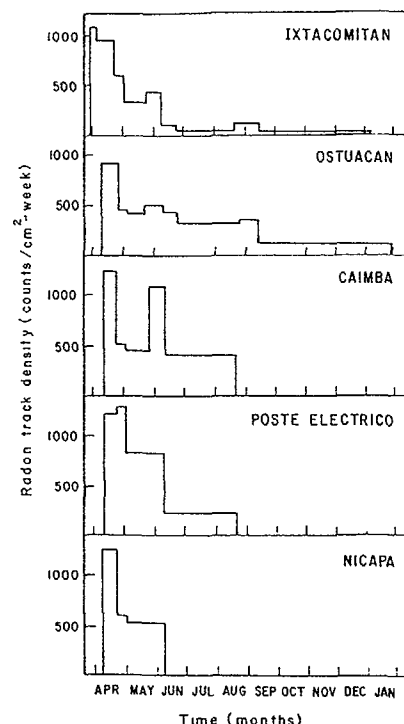


Figure 4.1.4. Radon countings variations with time at different stations.

mishandling or with environmental effects? Let us first discuss the increase exhibited by the May 26-June 10 exposed samples. Since all the detectors from each batch (collected within 3 days) were processed simultaneously, had it been an experimental error they should increase or decrease all alike. In addition the respective variation should be proportional. None of these events occurred: while Ixtacomitan, Ostuacan and Caimba stations showed an increase, Nicapa and Poste Electrico stations showed a constant activity. Mishandling is therefore ruled out. Let us now consider the radon-measurements corresponding to June 10-June 23 exposure time. the rainy season started in the Chiapas state at this time. The direct dependence of radon outflow from soil as a function of rainfall is reported by Seidel (1982). Taking this into account, a cross-correlation analysis has been done on the rainfall data obtained in the Pichucalco meteorological station and the radon readings in Ixtacomitan and Ostuacan. The cross-correlation functions show low values at low and high shifts and a peak at half-year shifts (Figure 4.1.5), suggesting that the initial high values in radon are unrelated to the weather, while the smaller variations in radon counts that follow are strongly conditioned by precipitation.

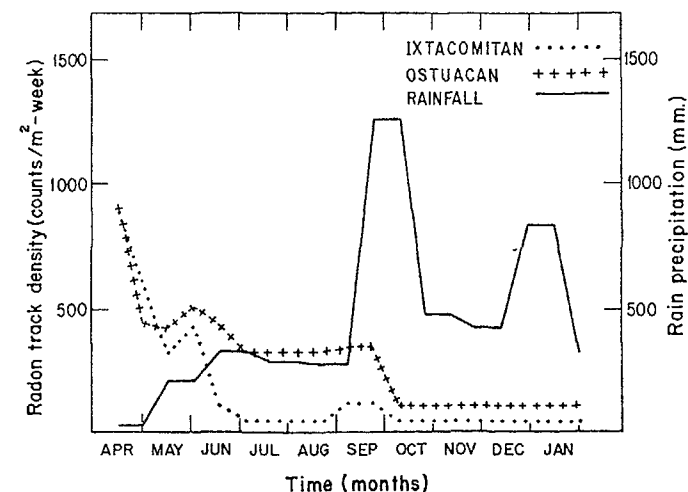


Figure 4.1.5. Radon track densities and rainfall at two sites.

The peaks in radon counts appearing in May could be related with the flood that occurred on May 26, 1982, when a pyroclastic deposit dam on the west flank of the volcano failed and released some  $10^{10}$  m<sup>3</sup> of water and mud along the Magdalena-Ostuacan river course. This phenomenon surely produced an abrupt change in the hydrological regime of the whole region as reflected in the radon peaks of Ixtacomitan and Ostuacan corresponding to these data. These results support the argument that the radon values directly related to the eruptions of March-April 1982 have been decreasing, and variations on this pattern are produced by external factors on the hydrological regime, like rainfall or floods. Figure 4.1.4 shows that about six months after the eruption, the radon track density in Ixtacomitan and Ostuacan remains constant in the levels of 50-100 tracks/cm<sup>2</sup> week. Observations re-started in Ostuacan in October 1983 show no significant departure from this pattern. These levels can therefore be assumed as the steady-state radon output in the vicinity of El Chichon. The one order of magnitude increase in radon activity measured during the eruption is discussed below.

#### 4.1.6. RADIOACTIVITY OF EL CHICHON ASHES. IMPLICATIONS ON THE ERUPTIVE MECHANISMS

All three major 1982 eruptions of El Chichon ejected large tephra columns more than 17 km high, which spread laterally in a short time. For instance, the column of the first eruption was 100 km in diameter 40 minutes after the onset of activity (SEAN, 1982). Ashfall covered an ample area around the volcano. Measurable amounts of ash-fall deposits and falling ash particles could be collected in the "Laboratorio de Monitoreo y Dosimetria Ambiental, Comision Federal de Electricidad", a nuclear power plant in construction at that time in El Farallon (Veracruz), some 450 km NW of the volcano. Sampling was done on March 30 and 31, 1982. The radioactivity of potassium-40 and radon and thoron daughters was measured by gamma-ray spectroscopy with the following results (Heredia-Naal et al., personal communication).

March 30, 1982. Ash-fall deposit sample:

a) Activity of  $^{220}\text{Rn}$  daughters

$^{212}\text{Pb}$ :  $6.93 \pm 0.42$  pC/g

$^{212}\text{Bi}$ :  $7.12 \pm 0.32$  pC/g

Activity ratio  $^{212}\text{Bi}/^{212}\text{Pb} = 1.03$

b) Activity of  $^{222}\text{Rn}$  daughters

$^{214}\text{Pb}$ :  $602 \pm 39$  pC/g

$^{214}\text{Bi}$ :  $1585 \pm 75$  pC/g

Activity ratio  $^{214}\text{Bi}/^{214}\text{Pb} = 2.6$

c) Activity of  $^{40}\text{K}$ :  $28.2 \pm 2.9$  pC/g

March 31, 1982. Sample of particles in air:

a) Activity of  $^{220}\text{Rn}$  daughters

$^{212}\text{Pb}$ :  $2.01 \pm 0.16$  pC/m<sup>3</sup>

$^{212}\text{Bi}$ :  $2.14 \pm 0.14$  pC/m<sup>3</sup>

Activity ratio  $^{212}\text{Bi}/^{212}\text{Pb} = 1.07$

b) Activity of  $^{222}\text{Rn}$  daughters

$^{214}\text{Pb}$ :  $42.8 \pm 2.8$  pC/m<sup>3</sup>

$^{214}\text{Bi}$ :  $124.8 \pm 11$  pC/m<sup>3</sup>

Activity ratio  $^{214}\text{Bi}/^{214}\text{Pb} = 2.9$

Activities of  $^{222}\text{Rn}$  and  $^{220}\text{Rn}$  daughters are much higher than one would expect from the reported values of uranium and thorium content of erupted rocks. However, observed  $^{40}\text{K}$  activity would be consistent with  $4.0 \pm 0.4$  wt. %  $\text{K}_2\text{O}$  concentration (assuming that all the potassium in the rocks is in such form), in reasonable agreement with the reported values of 2.56-3.28 wt. % (Rose et al., 1984), 2.8 wt. % (Pumices) (Lühr et al., 1984), 3.5 wt. % (Ashes) (Varekamp et al., 1984), 2.6-3.6 wt. % (Cocheme and Demant, 1983), and 2.69-3.86 wt. % (Prol et al., 1982) for  $\text{K}_2\text{O}$  concentrations in El Chichon erupted rocks. A possible origin of such high radon and thoron daughters activities is discussed below.

#### 4.1.7. DISCUSSION: MODELS FOR THE RADON-IN-SOIL ANOMALIES AND HIGH RADON DAUGHTERS RADIOACTIVITY IN ASHES

The results presented above can be summarized as follows:

a) During the eruption, radon activity levels observed in soil at distances 6 to 12 km from the volcano showed values one order of magnitude greater than normal. Afterwards, this activity decayed in a crudely exponential way with a half life time of about one month. Departures from this pattern observed during the summer of 1982 were most likely produced by external factors like rainfall and floods.

b) Activity of radon daughters ( $^{214}\text{Pb}$  and  $^{214}\text{Bi}$ ) and activity of thoron daughters ( $^{212}\text{Pb}$  and  $^{212}\text{Bi}$ ) measured some 33 hours after the onset of the first eruption in distal ashfall deposits, showed very high values. If Pb and Bi activities were in equilibrium with the reported U and Th contents in juvenile ejecta of El Chichon, the expected activities

should have been three orders of magnitude smaller than observed for  $^{222}\text{Rn}$  daughters and a factor of about 6 smaller for  $^{220}\text{Rn}$  daughters. Moreover, the parent-daughter activity ratios  $^{212}\text{Bi}/^{212}\text{Pb}$  measured on March 30 and March 31, 1982, suggest relative equilibrium between them, and  $^{40}\text{K}$  activity is consistent with reported concentrations of  $\text{K}_2\text{O}$  in juvenile ejecta. On the other hand,  $^{214}\text{Bi}/^{214}\text{Pb}$  activity ratio shows non-equilibrium between those nuclides.

These results are somewhat puzzling, but can be explained looking closely at the half-lives of the involved nuclides (Table 4.1.2). During the eruption it is likely that a large proportion of the radon and thoron contained in the magma body was released due to violent degassing. Since the half-life of thoron is only 54.5 sec, and the half-lives of  $^{218}\text{Po}$  and  $^{214}\text{Po}$  are short as well, it can be said that all the degassed thoron (and subsequently all the  $^{216}\text{Po}$ ), but only a part of the radon decayed in the site of the eruption. Therefore,  $^{212}\text{Bi}$  and  $^{212}\text{Pb}$  were in equilibrium when the ashes were collected some hours after  $^{212}\text{Pb}$  started to decay as if it were a primary parent. According with the radioactive decay laws, the activity ratio between  $^{212}\text{Bi}$  and  $^{212}\text{Pb}$  should be 1.105, a value which is consistent with the observed 1.03 and 1.06 ratios for such activities.

Table 4.1.2. Half-life data of some nuclides found in El Chichon ashes

Uranium Series		Thorium Series	
Nuclide	Half life	Nuclide	Half life
$^{222}\text{Rn}$	3.825 day	$^{220}\text{Rn}$	54.5 sec
$^{218}\text{Po}$	3.05 min	$^{216}\text{Po}$	0.158 sec
$^{214}\text{Pb}$	26.8 min *	$^{212}\text{Pb}$	10.6 hr *
$^{214}\text{Bi}$	19.7 min	$^{212}\text{Bi}$	60.5 min
* in 99.97%		* in 99.987%	

If the hypothesis that most of the thoron gas released at the time of the eruption was coming from the magma is accepted, it is the possible to make an estimate of the volume of magma that underwent substantial decompression. Assuming that prior to the eruption, the U and Th radioactive series were in equilibrium within the magma, the  $^{212}\text{Pb}$  and  $^{212}\text{Bi}$  activities expected to be in equilibrium with the reported 10.3 ppm of thorium (Lühr et al., 1984) should be 1.14 pC/g. But observed values of the activities of those nuclides were about 7 pC/g as measured some 30 hours after the eruption. If from this we subtract the activity in equilibrium from the existing Th, then an "excess" activity of about 5.8 pC/g remains in the ashes. When this value is taken to the time of the eruption, the activity of  $^{212}\text{Pb}$  should have been about 36 times the expected activity to be in equilibrium with the measured content of thorium.

Inasmuch as  $0.36 \text{ km}^2$  of magma was released during the first eruption, one ends with a rough approximation of 13 cubic kilometers of magma having degassed its thorium content, and having it rapidly decay into  $^{212}\text{Pb}$ , during the March 28 eruption. There is, however, no conceivable mechanism which permits an explanation of the very high activities of  $^{214}\text{Pb}$  and  $^{214}\text{Bi}$  from the radon degassed from such volume, at the reported uranium concentrations in El Chichon magma. The expected



activity of each of those nuclides when in equilibrium with 3.2 ppm of uranium is only 1.07 pCi/g. In order to explain the high level of activity of  $^{214}\text{Bi}$  it is proposed that an important amount of the radon contained in the rock surrounding the magma body was transported into it and dissolved in the melt. This argument can be supported from the fact that water above its critical point ( $374^\circ\text{C}$ , 218 bar) and any noble gas would be perfectly miscible (Pray et al., 1952; Mitchell and Terrell, 1984). Supercritical pressure conditions are attained at depths below about 800 m, and the temperature of the very water-rich melt is reported to have been around  $800^\circ\text{C}$  (Lühr et al., 1984).

It is thus likely that an important exchange of soluble gases existed between the surrounding rock and the melt, mainly via supercritical water circulating over distances of several kilometers. This interaction may have actually accounted for some of the shallow seismic activity, types 1 to 3 reported by Havskov et al. (1983), which was distributed over a volume with a typical vertical extension of about 5 km and an horizontal extension of the order of 10 km, as can be observed in the spatial distribution of foci in Havskov's paper. If a significant proportion of the radon contained at a certain time in a volume of surrounding rock, about three orders of magnitude larger than the volume of the melt, was removed by supercritical water and other fluids, it is then possible that large amounts of  $^{222}\text{Rn}$  dissolved in the magma during the eruption, when the release of pressure in the magma chamber made likely the rapid inflow of surrounding fluids into the melt. This effect should have been unimportant for thoron due to its short half-life.

The high values of radon in soil measured at distances of several kilometers from the volcano (Figure 4.1.3) may be related to the above effect in more than one way. The relatively slow decay of the radon activity in soil cannot be produced by normal decay of sources placed near the surface by the eruption, but rather by a decreased release of radon at different depths. The way in which this occurs depends on many unknown factors, like flow patterns of underground fluids, pressure and temperature distributions and their changes at depth, and in general, the whole dynamics of the magma-surrounding rock and fluids system. It is likely however, that one of the dominant factors governing the release of radon towards the surface was decreased uprising of radon rich fluids and (or) their decreased radon content due to the lower solubility resultant from the lower temperatures consequent with the release of large amounts of thermal energy during the eruption.

#### 4.1.8. CONCLUSIONS AND APPLICATIONS

The very high activity of radon and thoron daughters observed during the 1982 eruptive episode of El Chichón volcano, and the high radon outflow from soil measured over a large area around the volcano, during and after the activity, indicates that the transport of radon and thoron during the large eruptions is important both in the melt and in the surrounding rock. The measurement of the activity of thoron daughters  $^{212}\text{Pb}$  and  $^{212}\text{Bi}$  during explosive activity may actually provide the means to estimate the amount of magma undergoing degassing and, after comparison with the ejected volume at some stage of the eruptive episode, give some indication about the possibility of further eruptive activity, as the relatively high activity of thoron daughters measured in the products of the March 28 eruption suggested that only a fraction of the available magma had been ejected. The following major eruptions of April 4 and 5 indeed confirmed that.

The large area over which radon anomalies in soil were observed should also be regarded as an indicator of the presence of an important

volume of magma, at high pressure and temperature, capable of producing strong alterations in the underground flow patterns over distances of the order of ten kilometers. The matter of what proportion (if any) of the radon observed in surface stations at such distances could actually proceed from the magma cannot be answered with the available information.

In addition to the anomalies in short-lived radon and thoron daughters discussed here, when eruptive activity actually develops, abnormally high activities in long-lived radon daughters has also been reported in other cases (Polian and Lambert (1979) in Erebus volcano, Lambert et al. (1976) in Etna, Bennett et al. (1982), Le Cloarec et al. (1986a, 1986b) in Mount St. Helens, and Lambert et al. (1979, 1982a, 1982b) in several other volcanoes), suggesting a rupture of the radioactive equilibrium with their respective long-lived parents due to the loss of  $^{220}\text{Rn}$  during the magma degassing associated with the eruption. The relations of such anomalies with the size of the magma reservoir, or rather with the amount of degassed magma, may provide a powerful tool for the evaluation of the explosive potential of an active volcano.

It is therefore recommended that in the event of a large eruption, precautions are taken to closely observe the activity of radon, thoron and their daughters both in juvenile ejecta and surrounding soil and rock, as well as the uranium and thorium contents of the erupted products, in order to determine whether similar patterns of behaviour can be established.

### 4.2. RADON IN SOIL ANOMALY OBSERVED AT LOS AZUFRES GEOTHERMAL FIELD, MICHOACÁN: A POSSIBLE PRECURSOR OF THE 1985 MEXICO EARTHQUAKE ( $M_s=8.1$ )

#### 4.2.1. INTRODUCTION

The use of  $^{222}\text{Rn}$  as a tracer of pore fluid motions has proved useful in the study of possible precursors of earthquakes (Mogro-Campero et al., 1980; King, 1980; Wakita et al., 1980), and fault location and displacement (King, 1985; Tidjani et al., 1987).

Since 1981, we have been operating a radon network in seismic and volcanic areas in Mexico. In addition, since 1985, we have maintained a similar survey in Los Azufres, Michoacán, Mexico, geothermal field, with the intention of studying the evolution of fluid transport in geothermally active faults. We have paid particular attention to the Los Azufres fault itself, systematically monitoring it between May 1985 and December 1986. During this period, a doublet of  $M_s=8.1$  and  $M_s=7.5$  occurred, within 36 hr, with devastating effects on several cities of Mexico, particularly Mexico City, where more than 300 buildings were severely damaged and more than 20000 people were killed or missing. In this chapter, we present the measurements of radon concentration variations and discuss their possible relation with those earthquakes. Further discussions can be found in Segovia et al (1989).

#### 4.2.2. LOCATION OF THE GEOTHERMAL FIELD

The geothermal field of Los Azufres is located in the northern part of the State of Michoacán, between  $19^\circ34'$  and  $19^\circ57'$  N and between  $100^\circ36'$  and  $100^\circ43'$  W. It is a part of the Solfatara region of Sierra de San Andrés in the central part of the Mexican Volcanic Belt. The geothermal field is about 260 km NE from the epicentral area of the  $M_s=8.1$  earthquake that occurred on 19 September 1985 (Figure 4.2.1). The

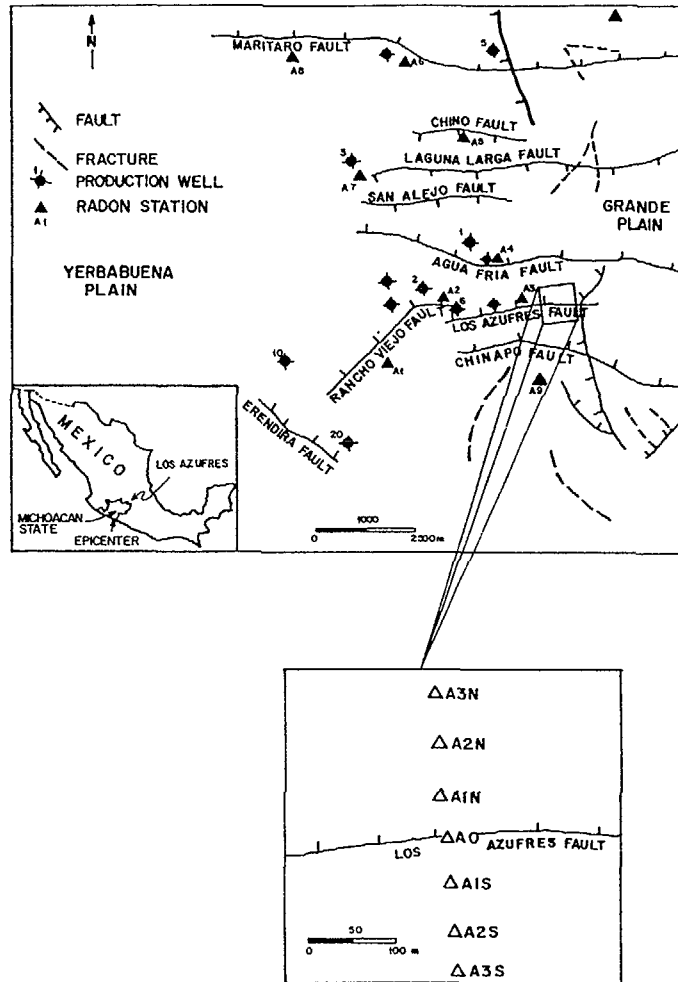


Figure 4.2.1. Fault distribution in Los Azufres Geothermal field: lower right insert shows the distribution of radon detectors across the Los Azufres fault.

Los Azufres fault under study is located in the central part of the geothermal field.

#### 4.2.3 THE 1985 EARTHQUAKES

Two major earthquakes occurred within a period of 36 hr on 19 September ( $M_s=8.1$ ) and 20 September ( $M_s=7.5$ ) of 1985. They broke a segment of the plate boundary between the Cocos and North America plates along the subduction zone known as the Michoacan gap. The first shock broke an area (from aftershock data) of  $170 \times 50 \text{ km}^2$ , and the second 63

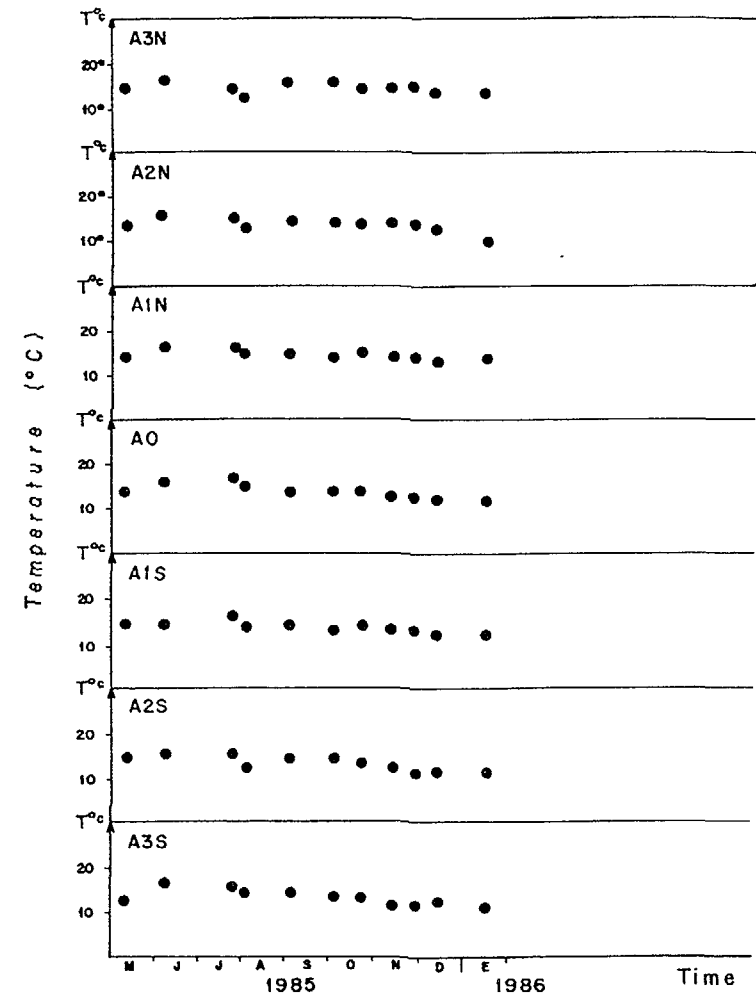


Figure 4.2.2. Temperature variations at the bottom of the 1 m deep radon probes. The arrow shows the occurrence of the earthquake.

$\times 33 \text{ km}^2$ , immediately to the SE of the first, with displacements of 220 and 330 cm, respectively. The overall length of the rupture along the subduction at the depth of about 20 km, was 220 km for the doublet.

#### 4.2.4 RADON ANOMALIES: RECOGNITION OF A POSSIBLE PRECURSOR

Figure 4.2.2, shows the temperature variations obtained at a depth of 1 m below the ground level. It can be seen that only small fluctuations occurred. However a rather good stability of temperature persisted in the detectors during the sampling period. The uranium

Table 4.2.1 Uranium concentration in different sites

Location	U (ppm)
A3N	1.2
A2N	1.5
A1N	1.5
A0	2.6
A1S	2.6
A2S	2.0
A3S	3.6

content of the soil samples is reported in Table 4.2.1. The type of analysis for U content is accurate to within a factor of two. However, the uranium concentration in all soil samples is quite similar, as reflected by the fact that the average radon concentrations are also very similar.

Rain precipitation and raw radon-in-soil data are simultaneously presented as a function of time in Figure 4.2.3. In the area under study, some periodicity in the rainfall regime is well known and can be clearly seen in the diagrams. Rainfall is at its maximum during the months from June to September and the dry season occurs during the months from October to May. In addition, Figure 4.2.4 shows the radon distribution profile across the Los Azufres fault for the different periods of time.

Before any further analysis of the radon data, we would like to draw attention to the fact that the distribution pattern as a function of time for the seven probes is quite similar from one site to another over the year 1986, and the same applies for 1985 if one disregards the central site (0) located right on the fault itself. In addition, a rather consistent relationship between radon output and rainfall can be pointed out. On average, an increase of the rainfall corresponds to a decrease of the radon output and vice versa. As a matter of fact, rainfall is not the only external phenomenon that may influence radon concentration in the soil. Others, such as atmospheric temperature, can do so but, in that particular case, both are intercorrelated and the rainfall parameter alone gives a fair indication of the environmental effects (Segovia et al., 1986).

In the year 1985, about 2 months before the earthquake, an increase in radon concentration was observed at the fault site, whereas a general decrease due to rainfall was observed everywhere else. We consider this apparent contradictory behaviour as a clue for a possible anomaly we would now analyze further. Let us label  $n$  the data recorded for the  $n$ th measure at the given station. Let  $D_n$  be the corresponding raw radon concentration,  $r$  the natural radon component not related to any geophysical perturbation and  $R_n$  the excess of radon due to such a possible perturbation. Environmental effects affect both  $r$  and  $R_n$  by a factor  $P_n$ , since the shallow detection will be influenced by external factors in the same proportion, regardless of the source. Therefore, one can write

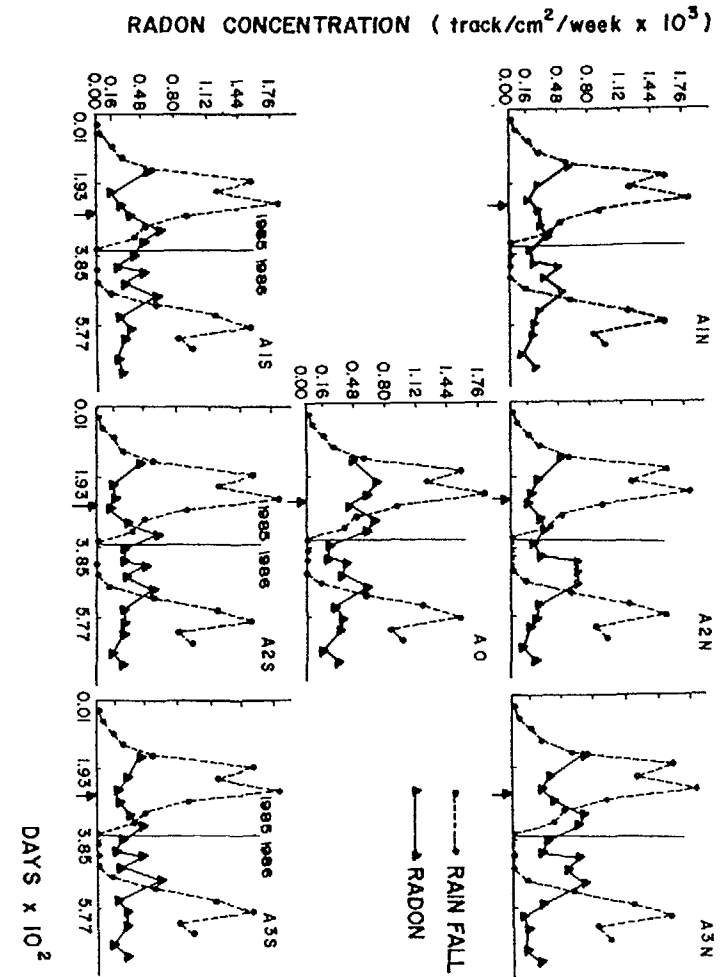
$$D_n = rP_n + R_nP_n = (r + R_n)P_n$$

or

$$D_n = rP_n, \quad \text{when no } R_n \text{ is involved.}$$

Accordingly, one can correct raw data for environmental effects provided the  $P_n$ 's are known. We made the assumption that the radon response to environmental effects is explained through all radon probe

Figure 4.2.3. Raw radon and rainfall data from the detector array crossing the Los Azufres fault.



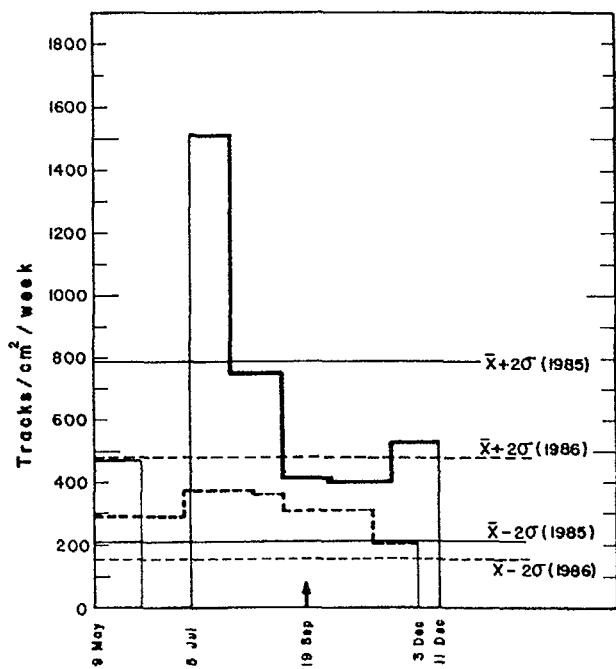


Figure 4.2.5. Radon concentration fluctuations for the central detector in 1985 (solid line) and in 1986 (dashed line). July peak exceeds mean value by more than 7 standard deviations.

data but the central one in 1985 and 1986, regardless of any peculiar radon output due to a deep crustal perturbation. We focused our attention on two periods of time of equal length, namely between May and December, when the environmental parameters are alike. We equaled the  $P_n$ 's to the ratio  $D_n/D_{n-1}$  and corrected the radon data for the central radon probe according to the simple equation given above, both in 1985 and 1986. The corrected results are shown on Figure 5. The dashed histogram shows the radon concentration in 1986. It can be seen that the variation in concentrations are quite small, averaging around 300 tracks  $\text{cm}^{-2} \text{ week}^{-1}$  with an average standard deviation  $\sigma$ -value of 140. This comparison substantiates our initial assumption. Quite obviously, the 1510 peak concentration value for the month of July is well above the  $\bar{x} + 2\sigma$  value usually taken as a sufficient deviation from the background to ascertain a genuine anomaly which, in our case, occurred two months before the earthquake.

Now the question of whether this large anomaly is truly related to the earthquake is rather delicate to answer. To do so, several points can be stressed. The first one is that, to our knowledge, in the Los Azufres region no other phenomenon, outside the scale of the small average fluctuations logged daily by the power company (CFE), occurred at the time of the anomaly that might be linked to it in any way whatsoever. Secondly, the radon concentration observed at the central

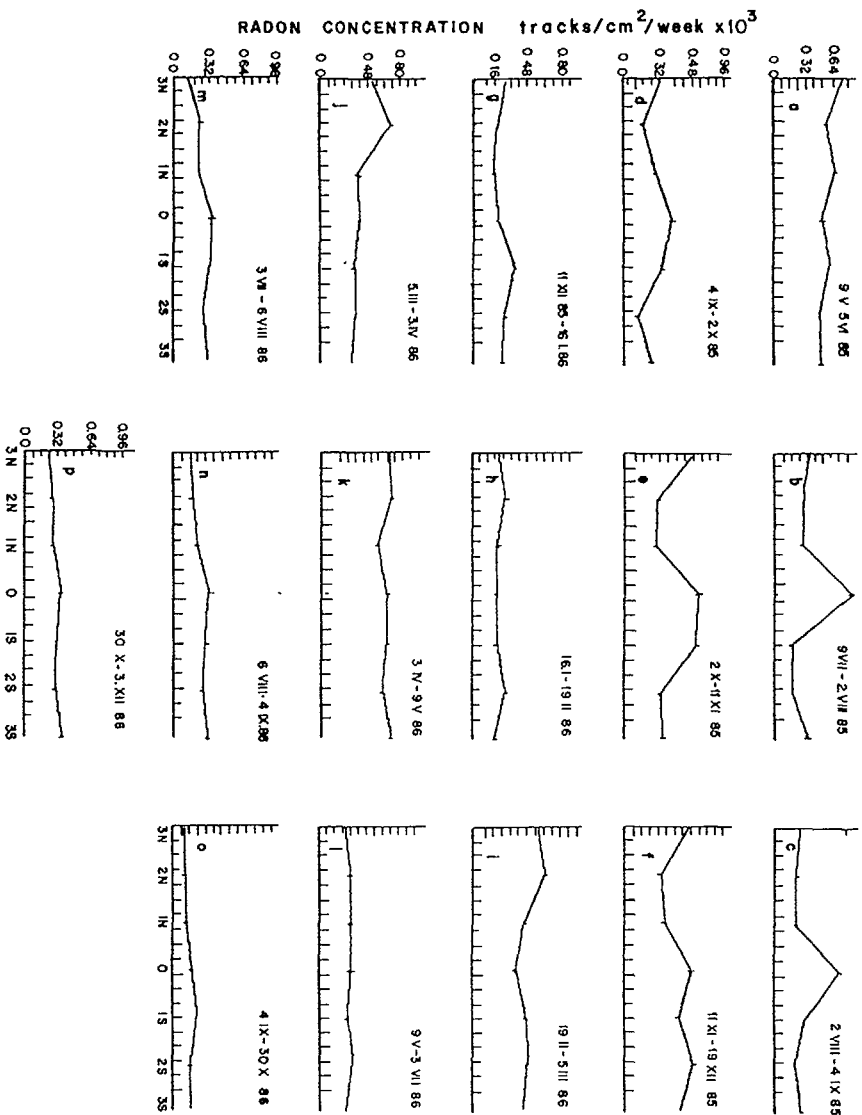


Figure 4.2.4. Radon readings in the seven detectors array for different periods of time. A high level of radon anomaly develops in the central detector in the period July-August, 1985, and persists through the period 2 August to 4 September. Later the anomaly decreases.

site returned to "normal" shortly after the earthquakes; i.e. returned to average values comparable to other sites and comparable to what was measured at the same period of time a year later. Furthermore, not only the N and S probes did not show any peculiar increase in radon, but neither did the other radon measuring stations kept in operation at the Nuclear Center of Salazar (340 km ENE from the epicentral area) in an inactive volcanic area, with no geothermal manifestations. The radon concentration changed only according to the environmental seasonal effects, as it did in the "normal" sites of Los Azufres. Finally, as already mentioned, the central site did not deviate from the normal behaviour of the other probes during the corresponding period of time in 1986, when no geophysical event of particular interest occurred. Therefore, the above mentioned facts lead us to conclude that it is very likely that the September 85 earthquake is in some way related to the observed radon anomaly.

#### 4.2.5. MODEL AND CONCLUSIONS

As mentioned in Section 3, the 1985 earthquake represents one of the largest releases of seismic energy during this century in Mexico. Such energies should have been stored as elastic energy in the seismic gap region, slowly building up to the moment of rupture. Little is known of the build-up process, but it is quite likely that the stress-strain relations describing the behaviour of the region depart from linearity prior to the rupture. Such behaviour is observed in most elastic bodies. It is thus conceivable that when the build-up of elastic energy in the prone area exceeds a certain value, the stress and strain patterns change over shorter time scales prior to the earthquake. These changes are likely to extend over distances at least in the order of the length of the rupture. And, indeed, Los Azufres area is located at a distance from the epicentral region comparable to the earthquake rupture length. But, in such a case, a shallow radon in-soil detector is probably unable to detect small changes in areas where fluid transport is not increased by fractures, since it is known that radon, whose concentration is measured in the soil, does not originate from any great depth (Tidjani et al., 1987). It mostly comes from the U-bearing minerals in the soil, less than 10 m deep, and the variations of its concentration depend upon the motion of other gases that transport it from deeper sources. The outgassing is almost negligible away from the fault and, hence, the absence of anomalous responses in the distal sites. On the contrary, in a fracture zone where active advective transport occurs, an ample cross-section of the crust (about 2km at Los Azufres) is sampled by the detector.

At this point, we shall refer to results reported by Santoyo et al. (1985). They measured concentrations of radon and other gases at the heads of deep-drilled wells in the Los Azufres area before and after the earthquake and report increases of radon, CO<sub>2</sub> and He concentrations before the earthquake at deep wells connected to the steam phase of the geothermal system. Decreases of radon concentrations at the wells connected to the steam-water layer were also reported, which is understandable, since the natural radon partition tends to enrich the vapor phase and, consequently, to deplete the liquid phase. Therefore, according to these data, a strong upward flow of a mixture of gases was generated before the earthquake and it is likely that it found a preferential vertical path through the fault. This gas flow is able to sweep up the radon previously present in the top soil. The amount of radon thus transported upwards is equal to the integrated excess of radon corresponding to the difference between the initial and final steady-state vertical distributions. This transient state produces a needle-like, very intense, radon pulse of short duration which Monnin and Seidel (1988) call a *kloudon*, after a Greek word meaning "wave".

However, since our sampling period is a long, the expected radon enhancement shows up as cumulative high values.

Although the amount of radon data obtained in this event is too small to draw conclusions, a model may be proposed in the light of the observations. Prior to large earthquake, meaning an event which is likely to break several tens of kilometers of crustal rock, the stress build up changes in such a way that may affect the regional stress pattern over distances of at least of the order of the rupture length and probably more. In the present case, an anomaly was observed in a single case out of 17 stations in two sites. The only "uncommon" feature of that station is the fact that it is located on the trace of a fault which shows a significant fluid transport. It is thus conceivable that even a slight change in the regional stress patterns may produce a *kloudon* effect on the fault. The fact that well-head anomalies were observed contemporary to the radon in soil on the fault trace suggest that the changes in stress patterns prior to large earthquakes are small enough so that only a sampling over a significant crustal cross-section may be registered at the surface in the form of radon or other gas anomalies.

The simplicity and low cost of the radon in soil methods and the information available on seismic gaps or regions with high potential for producing a large earthquake, calls for further research in this subject by setting radon detectors in fracture regions near the gaps.

#### 5. GENERAL CONCLUSIONS

From the few cases that have been studied in Mexico, some conclusions may be drawn regarding the analysis of geochemical and isotopic precursors of earthquakes and volcanic eruptions.

The application of geochemical water (hots spring, streams, lakes) monitoring technics to active volcanic areas has proved to be useful and productive, for it has helped to evaluate the eruptive potential of volcanoes in crisis. The relatively straight forward chemical analysis has been sufficient in most cases to obtain valuable information about the nature of ongoing volcanic processes.

Given a modest but good analytical chemistry laboratory, it is possible to perform basic analyses required to obtain fundamental information to substantiate an evaluation of the risk associated to a given volcano. A very important factor is the quality of the sampling itself. It is important to stress the need of the persistent collection of water samples taken with the same method and under conditions as similar as possible. The samples must be analyzed as soon as possible and should be preserved with specific chemicals and kept cold in order to improve reproducibility.

Regarding the isotopic methods, the observations involving the search of radon fluctuations in soil and water associated with minor seismic or volcanic activity is often obscured by anomalies of non-geologic origin, like rainfall, atmospheric pressure fluctuations, hydrological variations induced by rivers, floods, or level changes in dams etc. Segovia et al. (1986) discuss methods for the separation of external factors in the radon time series obtained in three Costa Rican volcanoes and in two sites of high seismicity in Mexico by means of Fourier spectral analysis. In all these cases, the noise level induced by non-volcanic or non-tectonic factors is comparable or even larger than the volcanic or tectonic induced radon anomalies. However, when large volumes of rock are prone to generate a major earthquake with a

large rupture area, or when large volumes of volatile rich magmas accumulate beneath a volcano, the changes of radon levels in soil or water may be well above the environmental radon level fluctuations, much higher than those produced by any other cause, even at considerably long distances from the source of the event. The definition of "minor", "large" or "major" in this context is therefore essential to assign a proper forecasting value to the radon anomalies.

#### APPENDIX 1

Large Earthquakes ( $M_s \geq 7.0$ ) of Mexico (1900 to 1979). Only events between  $15^\circ$  to  $20^\circ$ N and  $94.5^\circ$  to  $105.5^\circ$ W are given. (From Singh et al., 1980; and Singh et al., 1981)

Date	Epicenter		$M_s$	Depth (km)
	Lat. ( $^\circ$ N)	Long. ( $^\circ$ W)		
03-25-1806	18.9	103.8	7.5	
05-31-1818	19.1	103.6	7.7	
05-04-1820	17.2	99.6	7.6	
11-22-1837	20.0	105.0	7.7	
03-09-1845	16.6	97.0	7.5	
04-07-1845	17.3	100.9	7.7	
05-05-1854	16.3	97.6	7.7	
06-19-1858	19.6	101.6	7.5	
10-03-1864	18.7	97.4	7.3	
05-11-1870	15.8	96.7	7.8	
03-27-1872	15.7	96.6	7.4	
03-16-1874	17.7	99.1	7.3	
02-11-1875	21.0	103.8	7.5	
03-09-1875	19.4	104.6	7.4	
05-17-1879	18.6	98.0	7.0	
07-14-1882	17.7	98.2	7.5	
05-03-1887	31.0	109.2	7.3	
05-29-1887	17.2	99.8	7.2	
09-06-1889	17.0	99.7	7.0	
12-02-1890	16.7	98.6	7.2	
11-02-1894	16.5	98.0	7.4	
06-05-1897	16.3	95.4	7.2	
01-24-1899	97.1	100.5	7.9	
01-20-1900	20.0	105.0	7.9	S
05-16-1900	20.0	105.0	7.4	S
01-14-1903	15.0	98.0	8.1	S
04-15-1907	16.7	99.2	8.0	S
03-26-1908	16.7	99.2	8.1	80
03-27-1908	17.0	101.0	7.5	S
07-30-1909	16.8	99.9	7.4	S
06-07-1911	19.7	103.7	7.7	S
12-16-1911	16.9	100.7	7.5	50
11-19-1912	19.9	99.8	7.0	80
06-02-1916	17.5	95.0	7.1	150
12-29-1917	15.0	97.0	7.7	S
03-22-1928	16.2	95.5	7.5	S
06-17-1928	16.3	96.7	7.8	S
08-04-1928	16.8	97.6	7.4	S
10-09-1928	16.3	97.3	7.6	S
01-15-1931	16.1	96.6	7.8	S
06-03-1932	19.8	104.0	8.2	S
06-18-1932	19.5	103.5	7.8	S
11-30-1934	19.0	105.3	7.0	S

#### APPENDIX 1 (continuation)

Date	Epicenter		$M_s$	Depth (km)
	Lat. ( $^\circ$ N)	Long. ( $^\circ$ W)		
07-26-1937	18.5	96.4	7.3	85
12-23-1937	17.1	98.1	7.5	S
04-15-1941	18.9	102.9	7.7	S
02-22-1943	17.6	101.2	7.5	S
01-06-1948	17.0	98.0	7.0	80
12-14-1950	17.2	98.1	7.3	S
07-28-1957	17.1	99.1	7.5	S
05-11-1962	17.3	99.6	7.0	40
05-19-1962	17.1	99.6	7.2	33
07-06-1964	18.3	100.4	7.4	100
08-23-1965	16.3	95.8	7.6	28
08-02-1968	16.6	97.7	7.4	40
01-30-1973	18.4	103.2	7.5	32
08-28-1973	18.3	96.6	7.1	82
11-29-1978	15.8	96.8	7.8	20
03-14-1979	17.3	101.4	7.6	30
10-24-1980	18.0	98.3	7.0	65
10-24-1981	17.8	102.3	7.3	27
06-07-1982	16.4	98.5	7.0	10
09-19-1985	18.2	102.3	8.1	16
09-21-1985	17.8	101.7	7.5	22
04-25-1989	16.5	99.5	7.0	16

(Data of 19th century and early 20th century earthquakes are inferred from isoseismic maps, and are believed to be accurate to within  $\pm 0.3$  unit of magnitude and  $1^\circ$  arc)

#### APPENDIX 2

This appendix lists the Mexican volcanoes that have shown some type of eruptive activity in historical times and some indication of the effects and damages produced is given when applicable, in order to give an idea of the size of the eruptions a VEI value (for definition of the Volcanic Explosivity Index see Newhall and Self, 1982) is also given when possible. This list does not mention other Mexican volcanoes that may be considered active, but have not shown historical activity. It therefore should not be considered as an exhaustive account of the active volcanoes of Mexico, nor a detailed geological catalogue of the volcanism in Mexico. Volcanoes are ordered by region and by type.

#### POLYGENETIC VOLCANOES OF NORTHWESTERN MEXICO

TRES VIRGENES  $27.47^\circ$  N,  $112.58^\circ$  W (B.C.S.)

TYPE: Trachytic Basalt Stratovolcano Height: 2050 m

YEAR	DATE	BRIEF DESCRIPTION OF THE ACTIVITY	VEI
1746		No detailed information available.	
1857		No detailed information available.	

SANGANGUEY 21.45° N, 104.98° W (NAYARIT)

TYPE: Andesitic Stratovolcano Height: 2350 m

YEAR	DATE	BRIEF DESCRIPTION OF THE ACTIVITY	VEI
1742		No detailed information available.	
1859		No detailed information available.	

CEBORUCO 21.15° N, 104.50° W (NAYARIT)

TYPE: Andesitic Stratovolcano Height: 2164 m

YEAR	DATE	BRIEF DESCRIPTION OF THE ACTIVITY	VEI
c. 960		Great Plinian eruption.	5?
1870-1875		Intermediate eruption	3

#### POLYGENETIC VOLCANOES OF WESTERN CENTRAL MEXICO

COLIMA 19.51° N, 103.6° W (JAL-COL)

TYPE: Andesitic Stratovolcano Height: 4000 m

YEAR	DATE	BRIEF DESCRIPTION OF THE ACTIVITY	VEI
1560	-	Eruption reported without details.	2?
1576	-	Large eruption, ashfall. Deaths reported	3
1585	01 10	Very large eruption. Heavy ashfall	4
1590	01 14	Explosive eruption. Ashfall.	3
1606	11 25	Very large explosive eruption. Ashfall	4
1611	04 15	Explosive activity. Abundant ash emissions.	3
1612-13	-	Eruptions and seismicity. No details.	2?
1622	06 08	Very large eruption. Heavy ashfall	4
1690	-	Large explosive eruption. Abundant ashfall.	3
1743	10 22	Seismic activity. Fall of trees	2
1749	-	Eruption and seismicity. No details.	2?
1770	-	Explosion and ash emissions.	2
1771	-	Explosive eruption. Abundant ash emission.	3
1795	-	Eruption with lava emissions.	2
1804	-	Eruption reported without details.	2?
1806	03 25	Block lava avalanche.	-
1807-08	-	Small incandescent avalanches of block lava.	0
1818	02 15	Large eruption. Heavy ashfall. Deaths reported.	4
1869	06 12	Eruption from new crater (El Volcancito)	3
1872	02 26	Explosive eruptions from El Volcancito.	3
1873	01 -	Small eruptions from El Volcancito.	1
1874	-	Minor activity.	1
1877	-	Small explosions.	1
1879	12 23	Minor eruptions.	1
1880	03 31	Minor explosions.	1
1881	03 12	Moderate explosion.	2
1885	12 26	Moderate explosions. Lava flows.	2
1886	01 06	Explosive eruption. Ashfall	3
1889	10 26	Important eruption. Ashfall	3
1890	02 16	Large eruption. Heavy ashfall	4
1891-92	-	Repeated eruptions and ashfall.	2
1893	12 04	Explosion with moderate ash emission	2
1895-1902		Lava flows from summit. Minor explosions	1
1903	02 15	Large explosive eruption. Abundant ash	3
1904-1906		Block lava avalanches probably produced by	-

1908	12 18	Explosive eruption. Ashfall	3
1909	02 04	Explosions with ash emission.	2
1913	01 20	Large explosive eruption. Heavy ashfall	4
1960-70		Growth of summit dome.	1
1975	12 12	Crumbling of dome produces small avalanches	-
1982	-	Episodes of small avalanches of block lava.	0
1985-	-	Similar to 1982.	0
1991-	02 14	Seismic swarms, avalanches block lava.	0

#### POLYGENETIC VOLCANOES OF THE CENTRAL REGION

POPOCATEPETL 19.02° N, 98.62° W (EDOMEX-PUE-MOR)

TYPE: Andesitic-Dacitic Stratovolcano Height: 5450 m

YEAR	DATE	BRIEF DESCRIPTION OF THE ACTIVITY	VEI
1347		Explosive activity. Ashfall	2-3?
1354		Explosive activity. Ashfall	2-3?
1519-1530		Persistent minor activity	2?
1539		Explosive eruption .Ashfall, victims (?)	3
1542-1592		Numerous minor eruptive episodes	1-2?
1664-1667		Numerous minor eruptive episodes	1-2?
1720		Explosive eruption .Ashfall, victims (?)	3
1802-1804		Minor activity	-
1920		Minor activity	-

#### POLYGENETIC VOLCANOES OF THE EASTERN REGION

PICO DE ORIZABA 19.03° N, 97.28° W (VER)

TYPE: Andesitic Stratovolcano Height: 5700 m

YEAR	DATE	BRIEF DESCRIPTION OF THE ACTIVITY	VEI
1537		Eruption reported without details.	2?
1545		Eruption reported without details.	2-3?
1566		Eruption reported without details.	2-3?
1569		Eruption reported without details.	2-3?
1613		Eruption reported without details.	
1630		Eruption reported without details.	2-3?
1687		Eruption reported without details.	2-3?

SAN MARTIN TUXTLA 18.58° N, 95.17° W (VER)

TYPE: Basaltic cone Height: 1550 m

YEAR	DATE	BRIEF DESCRIPTION OF THE ACTIVITY	VEI
1664		Explosive eruption .Ashfall, victims (?)	3
1793	03 02	Large eruptions. Ashfall. Possible victims	4
1794		Minor activity	
1797		Minor activity	

## POLYGENETIC VOLCANOES OF THE SOUTHEAST

EL CHICHON 17.36° N, 92.23° W (CHIAPAS)

TYPE: Andesitic dome complex Height: 1000 m

YEAR	DATE	BRIEF DESCRIPTION OF THE ACTIVITY	VEI
c. 300		Large eruption. Ashfall. Possible victims	4-5?
c. 623		Large eruption. Ashfall. Possible victims	4-5?
c. 1300		Large eruption. Ashfall. Possible victims	4-5?
1982	03 28	Large eruption. Ashfall. Possible victims	4
1982	04 03	Two large explosive eruptions with abundant ashfall and pyroclastic flows. About 2000 victims	
1982	04 04	and 150 km <sup>2</sup> devastated. Great losses	4-5

TACANA 15.13° N, 92.10° W (CHIAPAS)

TYPE: Andesitic Stratovolcano Height: 4060 m

YEAR	DATE	BRIEF DESCRIPTION OF THE ACTIVITY	VEI
1855		Minor phreatic explosion	-
1878		Minor phreatic explosion	-
1903		Minor phreatic explosion	-
1949-1951		Minor phreatic explosion and fumarolic activity	-
1986	05 08	Seismic swarms and moderate phreatic explosion.	-

## VOLCANOES OF THE PACIFIC ISLANDS

BARCENA 19.27° N, 110.80° W

TYPE: Cinder Cone Height: 375 m

YEAR	DATE	BRIEF DESCRIPTION OF THE ACTIVITY	VEI
1952	08 01	Birth volcano in San Benedicto island, Activity continued until March 1953	2

EVERMANN (or SOCORRO) 18.75° N, 110.95° W

TYPE: Shield volcano Height: 1235 m

YEAR	DATE	BRIEF DESCRIPTION OF THE ACTIVITY	VEI
1848		Eruption reported without details.	2?
1896		Eruption reported without details.	2?
1905		Eruption reported without details.	2?
1951	05 22	Eruption reported without details.	2?

## MONOGENETIC VOLCANOES

PARICUTIN 19.48° N, 102.25° W (MICH)

TYPE: Cinder cone Height: 3170 m (about 400 over ground)

1943	02 20	A fissure opens in a corn field. In 12 days a cinder cone reaches over 400 m and produces large amounts of ash and lava	3
------	-------	---	---

JORULLO

19.03° N, 101.67° W (MICH)

TYPE: Scoria cone Height: 1330 m (about 300 over ground)

1759	09 29	A fissure opens, Large amounts of ash and lava were produced. Eruption continued until 1774. Similar to Paricutin	3
------	-------	---	---

XITILE 19.25° N, 99.22° W (D.F)

TYPE: Scoria cone Height: 3120 m

c.470	B.C.	Birth and development similar to those of Paricutin. Lava field covers 72 km <sup>2</sup>	3
-------	------	---	---

## REFERENCES

APHA, 1975. Standard Methods for the Examination of Water and Waste water. American Public Health Association. 13th ed. Washington. 874 pp.

Allan, J. (1986) Geology of the northern Colima and Zacoalco grabens, southwest Mexico: late Cenozoic rifting in the Mexican Volcanic Belt. Geol.Soc.Am.Bull., 97, 473-485.

Barberi F., Blong R., De la Cruz-Reyna S., Hall M., Kamo K., Mothes P., Newhall C., Peterson D., Punongbayan R., Sigvaldasson G., Zana D. (1990) Reducing Volcanic Disasters in the 1990's. Bull. Volcanol. Soc. Japan, ser. 2. 35: 80-95.

Bennett J T, Krishnaswami S, Turekian K K, Melson W G, Hopson C A (1982) The uranium and thorium decay series nuclides in Mt. St. Helens effusives. Earth Planet Sci Lett 60: 61-69.

Bourgeois, J., Renard, D., Auboin, J., Bandy, W., Barrier, E., Calmus, T., Carfantan, J.C., Guerrero, J., Mammerickx, J., Mercier de Lepinay, B., Michaud, F. &amp; R. Sosson (1988) Fragmentation en cours du bord Ouest du Continent Nord Americain: Les frontieres sous-marines du Bloc Jalisco (Mexique) C.R. Acad. Sci. Paris, 307(II), 1121-1133.

Canul R., Razo A. and Rocha V. (1983), Geologia e Historia Volcanologica del Volcan Chichonal, Estado de Chiapas. In: Proceedings of the VI national meeting of the Mexican Geological Society. UNAM: 3-22.

Casadevall T. J., De La Cruz S., Rose W. I., Bagley S., Finnegan D. L., Zoller W. (1984), Volcan El Chichon Mexico: The crater lake and thermal activity, J. Volcanol. Geotherm. Res., 23, 169-191.

Casadevall, T.J., Rose, W.I., Fuller, W.H., Hunt, W.H., Hart, M.A., Moyers, J.L., Woods, D.C., Chuan, R.L., Friend, J.P. (1984) Sulfur dioxide and particles in quiescent volcanic plumes from Poas, Arenal and Colima Volcanos, Costa Rica and Mexico. J. Geophys. Res. 89(D6), 9633-9641.

Chirkov A. M. (1975), Radon as a possible criterium for predicting eruptions as observed at Karymsky volcano. Bull. Volc. XXXVII, 126-131.



Cocheme J. J. and Demant A. (1983), *Naturaleza y composicion del material emitido por el Volcan Chichonal, Chiapas (Marzo-Abril, 1982)*. In. *Proceedings of the National Meeting of the Mexican Geological Society, UNAM: 81-89*

Cox M. E., Cuff K. E., Thomas O. M. 1980, Variations of ground radon concentration with activity of Kilauea Volcano, Hawaii, *Nature*, 288, 74-76.

De la Cruz M.V. and Hernandez Z.R., 1985. Estudio Geologico a semidetalle de la zona geotermica Volcan Tacana, Chis. Informe 41/85, CFE, Mexico.

De la Cruz-Reyna S., Mena M., Segovia N., Chalot J. F., Seidel J. L., Monnin M. (1985) Radon Emanometry in Soil Gases and Activity in Ashes from El Chichon Volcano. *PAGEOPH* 123: 407-421.

De la Cruz-Reyna S., Armienta M.A., Zamora V., Juarez F. (1986) Chemical Changes in Spring Waters at Tacana Volcano, Chiapas, Mexico: A Possible Precursor of the May 1986 Seismic Crisis and Phreatic Explosion. *J. Volcanol. Geotherm. Res.* 38, 345-353.

De la Cruz-Reyna S., Isabelle D.B., Mena M., Monnin M., Romero M., Segovia N., Seidel J. L., Pialoux P., Armienta M.A. (1986) Radon Emanation Related to Geothermal Faults. *Nucl. Tracks. Radiat. Meas.*, 12, Nos. 1-6, 875-878.

De la Cruz-Reyna, S., 1990. Poisson-Distributed Patterns of Explosive Eruptive Activity. Submitted to *Bull. Volcanol.*

Del Pezzo E., Gasparini P., Mantovani M. S., Martini M., Capaldi G., Gomes Y. T. and Pece R. (1981), A case of correlation between Rn anomalies and seismic activity on a volcano (Vulcano Island, Southern Tyrrhenian Sea). *Geophys. Res. Letters*, 8, 962-965.

Duffield W. A., Tilling R. I. and Canul R. (1984), *Geology of El Chichon Volcano, Chiapas, Mexico*. *J. Volcanol. Geotherm. Res.*, 20, 117-132.

Eissler H., Astiz L. and Kanamori H. (1986) Tectonic setting and source parameters of the September 19, 1985, Michoacan, Mexico, earthquake, *Geophys. Res. Lett.* 13, 569-572.

Espindola J. M. and Medina F., 1988. A C-14 Age Determination in the Tacana Volcano Chiapas, Mexico. *Geof. Int.* In press.

Fleischer R. L. and Mogrocampero A. 1978. Mapping of Integrated radon emanation for detection of long distance migration of gases within the earth: Techniques and principles. *J. Geophys. Res.*, 83, 3539-3549.

Gasparini P. and Mantovani M. S. M. 1978, Radon anomalies and volcanic eruptions, *J. Volcanol. Geotherm. res.*, 3, 325-341.

Harder H., 1969 Boron. In K. H. Wedepohl Ed. *Handbook of Geochemistry*, Springer-Verlag Berlin, II-1. 5B1-503.

Havskov J., De La Cruz-Reyna S., Singh S. K., Medina F., and Gutierrez C., 1983 Seismic activity related to the March-April 1982 eruptions of El Chichon Volcano, Chiapas, Mexico. *Geophys. Res. Letters*, 10, 293-296.

King C. Y. (1980) Episodic radon changes in subsurface soil gas active faults and possible relation to earthquakes. *J. Geophys. Res.* 85, 3065.

King C. Y. (1985) Impulsive radon emanation on creeping segment of the San Andreas fault, *Pageoph* 122, 340-351.

Koritnig S., 1969. Fluorine. In. K. H. Wedepohl Ed. *Handbook of Geochemistry*, Springer-Verlag Berlin, II-1: 9B1-904.

Korkish J., Abascal F., Aguilar C. (1973). Fluorimetric determination of microgram amounts of Uranium in Mexican Minerals after preliminary separation by solvent extraction. *revista Latino Americana de Quimica*, Vol. 4/4, 185-189.

Lambert G, Bristeau P, Polian G (1976) Emission and enrichments of radon daughters from Etna volcano magma. *Geophys Res Lett* 3: 724-726

Lambert G, Buisson A, Sanak J, Ardouin B (1979) Modification of the atmospheric polonium-210 to lead-210 ratio by volcanic emissions. *J Geophys Res* 84C: 6980-6986

Lambert G, Ardouin B, Polian G (1982a) Volcanic output of long-lived radon daughters. *J Geophys Res* 84C: 11103-11108

Lambert G, Polian G, Sanak J, Ardouin B, Buisson A, Jegou A, Le Rouley J C (1982b) Cycle du radon et ses descendants. Application s l'etude des echanges troposphere-stratosphere. *Ann Geophys* 38(4): 497-531

Lopez-Ortiz R. (1962) *Geologia y Posibilidades Petroleras de los Sedimentos Cretacicos en la parte Sureste del frente de la Sierra Madre de Chiapas*. *Bol. Asoc. Mexicana Geol. Petrol.* 14, 135-151.

Luhr J. F., Carmichael I. S. E. and Varekamp J. C. (1984) The 1982 eruptions of El Chichon Volcano, Chiapas, Mexico: Mineralogy and Petrology of the Anhydrite-bearing pumices. *J. Volcanol. Geotherm. Res.*, 23, 69-108.

Luhr, J., Nelson, S.A., Allan, J.F. and I.S.E. Carmichael (1985) Active rifting in southwestern Mexico: Manifestations of an incipient eastward spreading-ridge jump. *Geology* 13, 54-57.

Luhr, J. & K.Prestegard (1988) Caldera formation at Volcan Colima, Mexico, by a large holocene volcanic debris avalanche. *J.Volcanol.Geotherm.Res.*, 35, 335-348.

Maldonado, L., Linares R., Morales T., Segovia N. (1982) Desarrollo de un contador de chispa. Informe Tecnico AII-82-19, ININ (MEXICO).

Malinconico Jr., L. L., 1987. On the Variation of SO<sub>2</sub> Emissions from Volcanoes *J Volcanol. Geotherm. Res.*, 33: 231-237.

Martini M., 1984. On the Behavior of Fluorine in Volcanic Processes. *Bull. Volcanol*, 47 (3): 483-489.

Mitchell J. G. and Terrell D. J. (1984) Noble gas solubility in supercritical water: Implications for inert gas studies in geochronology. *Geof Int.*, 23, 483-490.

Medina F. (1983) Analysis of the eruptive history of the Volcan de Colima, Mexico (1560-1980). *Geofis. Int* 22. 157-178.

Medina F (1985) On the volcanic activity and large earthquakes in Colima area, Mexico. *Geofis. Int.* 24: 701-708.

- Mogro-Campero A., Fleisher R. L., and Likis R. S. (1980) Changes in subsurface radon concentration associated with earthquakes, *J. Geophys. Res.*, 85, 3079.
- Monnin M. (1980a) Visualization of latent damage trails, part I, *Nucl. Inst. Meth.* 137, 1-14.
- Monnin M. (1980b) Methods of automatic scanning of SSNTD, part II, *Nucl. Inst. Meth.* 137, 63-72.
- Monnin M. and Seidel J. L. (1988) Sur une hypothetique emission intense de radon avant in evenement geophysique majeur: une analyse theorique. *C. R. Acad. Sci. Paris*, 307, serie II, 1363-1368.
- Newhall, C. G., Self, S., 1982. The Volcanic Explosivity Index (VEI): An estimate of explosive magnitude for historical volcanism. *J. Geophys. Res.*, 87C2: 1231-1238.
- Pray H. A., Schweickert C. E. and Minnich B. H. (1952) Solubility of hydrogen, oxygen, nitrogen and helium in water at elevated temperatures. *Ind. Eng. Chem.*, 44, 1146-1151.
- Polian G and Lambert G (1979) Radon daughters and sulfur output from Erebus volcano, Antarctica. *J. Volcanol. Geotherm. Res.* 6: 125-137
- Prol R. M., Medina F., Choporov D. Y., Frikh D. I., Muravitskaya G. N., Polak B. G., Stephanets M. I. (1982) Preliminary Chemical and petrographic results of the March-April "El Chichon" Volcanics. *Geof. Int.*, 21, 1-10.
- Robin, C., P. Mossand, G. Camus, J. Cantagrel, A. Gourgaud & P. Vincent (1987) Eruptive history of the Colima Volcanic Complex (Mexico). *J. Volcanol. Geotherm. Res.*, 31, 99-113.
- Rose W. I., Bomhorst T. J., Halsor S. P., Capul W. A., Plumley P. S., De la Cruz-Reyna S., Mena M. and Mota R. (1984) Volcan El Chichon, Mexico: pre-1982 S-rich eruptive activity. *J. Volcanol. Geotherm. Res.*, 23: 147-167.
- Rye R. O., Luhr J. F., Wasserman M. D. (1984) Sulfur, and Oxygen isotopic systematics of the 1982 eruptions of El Chichon Volcano, Chiapas, Mexico. *J. Volcanol. Geotherm. Res.*, 23, 109-123.
- Santiago-Acevedo J. (1962) Estructuras de la porcion occidental del frente de la Sierra Madre de Chiapas. *Bol. Asoc. Mexicana Geol. Petrol.* 14, 111-134.
- Santoyo E., Nieva D., Verma S. P., and Portugal- Martin E. (1985) Geochemical earthquake precursors in the Los Azufres geothermal field, *Geos. Bull.* 3, UGM.
- Scientific Event Alert Network (SEAN) Bulletin, 1982. Smithsonian Institution, Washington, D. C., 7, 3, 2-6.
- Seidel J. L. 1982, Radon-emanometrie appliquee a la geophysique interne-These de doctorat de specialite No. 679, Universite Clermont-Ferrand II, (France).
- Seidel J. L. and Monnin M. (1982) Some radon activity measurements of geophysical significance. In: Fowler P. H. and Clapham W. M. editors. *Proceedings of the 11th Int. Conf. Solid State Nuclear Track Detectors*, Pergamon Press: 517-523.
- Somogyi G., Paripas B. and Varga Zc. (1984) Measurement of radon, radon daughters and thoron concentrations by multi-detector devices. *Nucl. Tracks and Rad. Meas.* 8, 423-427.
- SEAN (1987) Colima (Mexico): Large avalanche from summit lava dome; small A-type events, 12(7),2.
- Segovia N., De la Cruz-Reyna S., Mena M., Romero M., Seidel J. L., Monnin M., Malavassi M., Barquero J., Fernandez E., Avila G., Van der Laat R., Ponce L., and Juarez G. (1986) radon variations in active volcanoes and in regions with high seismicity: internal and external factors, *Nuclear Tracks* 12, 1-6, 871-874.
- Segovia N., Seidel J. L., Monnin M. (1987) Variations of Radon in Soils Induced by External Factors. *J. Radioanal. Nucl. Chem. Letters* 119, No. 3, 199-209.
- Segovia N., Seidel J. L., Monnin M., Galle C. (1988) Radon in soils: Intercomparative Studies. *Nucl. Tracks. Radiat. Meas.*, 15, Nos. 1-4, 625-628.
- Segovia N., Gaso M. I., Tejera A., Tamez E. (1989) Environmental Radioactivity Survey in Site Studies. *J. Radioanal. Nucl. Chem. Articles*, 132, No. 2, 339-348.
- Segovia N., De la Cruz-Reyna S., Mena M., Ramos E., Monnin M., Seidel J. L. (1989) Radon in Soil Anomaly Observed at Los Azufres Geothermal Field, Michoacan: a Possible Precursor of the 1985 Mexico Earthquake (Ms = 8.1). *Natural Hazards*, 1, 319-329.
- Segovia N. (1990) Radon Surveys in Mexico. In: Tommasino L., Furlan G., Jhan H. A., Monnin M., Radon Monitoring in Radioprotection Environmental Radioactivity and Earth Sciences. *World Scientific* 1990, 457-462.
- Seidel J. L. (1982) Radon emanometrie appliquee a la geophysique interne. Thesis 679 D. University of Clermont II., France.
- Singh S. K., Guzman M., Castro R. and Novelo D. (1980) A Catalog of Major Nineteenth Century Earthquakes of Mexico. Personal Communication.
- Singh S. K., Astiz L., and Havskov J. (1981) Seismic Gaps and Recurrence Periods of Large Earthquakes Along the Mexican Subduction Zone: A Reexamination. *Bull. Seism. Soc. Am.*, 71 (3), 827-843.
- Singh S. K., Ponce L. and Nishenko S. P. (1985) The Great Jalisco, Mexico Earthquake of 1932: Subduction of the Rivera Plate. *Bull. Seism. Soc. Am.*, 75, 1301-1313.
- Taylor S. R. (1968) "Geochemistry of Andesites". In: Origin and distribution of the elements. Ahrens L. H. editor, Pergamon, Oxford.
- Tilling, R. I., Rubin, M., Sigurdsson, H., Carey, S., Duffield, W., Rose, W. I., 1984. Holocene eruptive activity of El Chichon Volcano, Chiapas, Mexico. *Science* 224: 747-749.

Tilling R. I., Rubin M., Sigurdsson H., Carey S., Duffield W. A. and Rose W. I. (1984) Holocene eruptive activity of El Chichon Volcano (Chiapas, Mexico): Character of the eruptions, ash-fall deposits and gasphase. J. Volcanol. Geotherm. res., 23, 39-68.

UNAM Seismology Group (1986) The september 1985 Michoacan Earthquakes: aftershock distribution and history of rupture, Geophys. Res. Lett. 13, 573-576.

Wakita H., Nakamura Y., Notsu K., Noguchi M., and Asada T. (1980) Radon anomaly. a possible precursor of the 1978 Izu-Oshima-Kinkai earthquake, Science 207, 882-883.

## CONCLUSIONS ON THE POSSIBLE VARIATIONS OF CHEMICAL AND ISOTOPIC COMPOSITION OF GROUNDWATER SYSTEMS IN RESPONSE TO CHANGED HYDRODYNAMIC CONDITIONS *(based on investigations of deep groundwater systems and thermal-mineral waters and brines in tectonic active areas)*

W BALDERER  
Ingenieurgeologie,  
ETH Zurich,  
Zurich, Switzerland

### Abstract

To establish an observation network of possible parameters to be used as precursors of earthquakes or volcanic eruptions it is necessary first to understand the natural conditions of a given groundwater system and the possible variations of groundwater chemistry and isotopic composition. In the presented study three sites within tectonic active areas in Western Turkey were discussed and compared with the situation of the deep groundwaters in Northern Switzerland.

### 1 INTRODUCTION

The aim to be focussed in this study is the use of the composition of the groundwater itself as possible indicator of processes which are related with future earthquakes and volcanic eruptions.

Normally in Isotope Hydrology isotope methods combined with hydrochemical investigations are used to trace back the natural processes which are influencing the groundwater composition within the hydrological cycle from its origin (beginning with the precipitation and successive infiltration, followed by the flow and evolution within the geosphere to the ending point and moment of sampling (BALDERER, 1983).

For this purpose, isotope methods have proved to be the key parameters in hydrogeology e.g. furnishing informations on

- Conditions of recharge (e.g. by the use of infiltration specific parameters as stable isotopes  $^2\text{H}$  and  $^{18}\text{O}$  and noble gases)

- Residence time (radioisotopes e.g.  $^3\text{H}$ ,  $^{14}\text{C}$ ,  $^{39}\text{Ar}$ ,  $^{36}\text{Cl}$ )

-Formation specific origin and flow path (Mineral and reaction specific isotopes as  $^{34}\text{S}$  and  $^{18}\text{O}$  in  $\text{SO}_4$ )

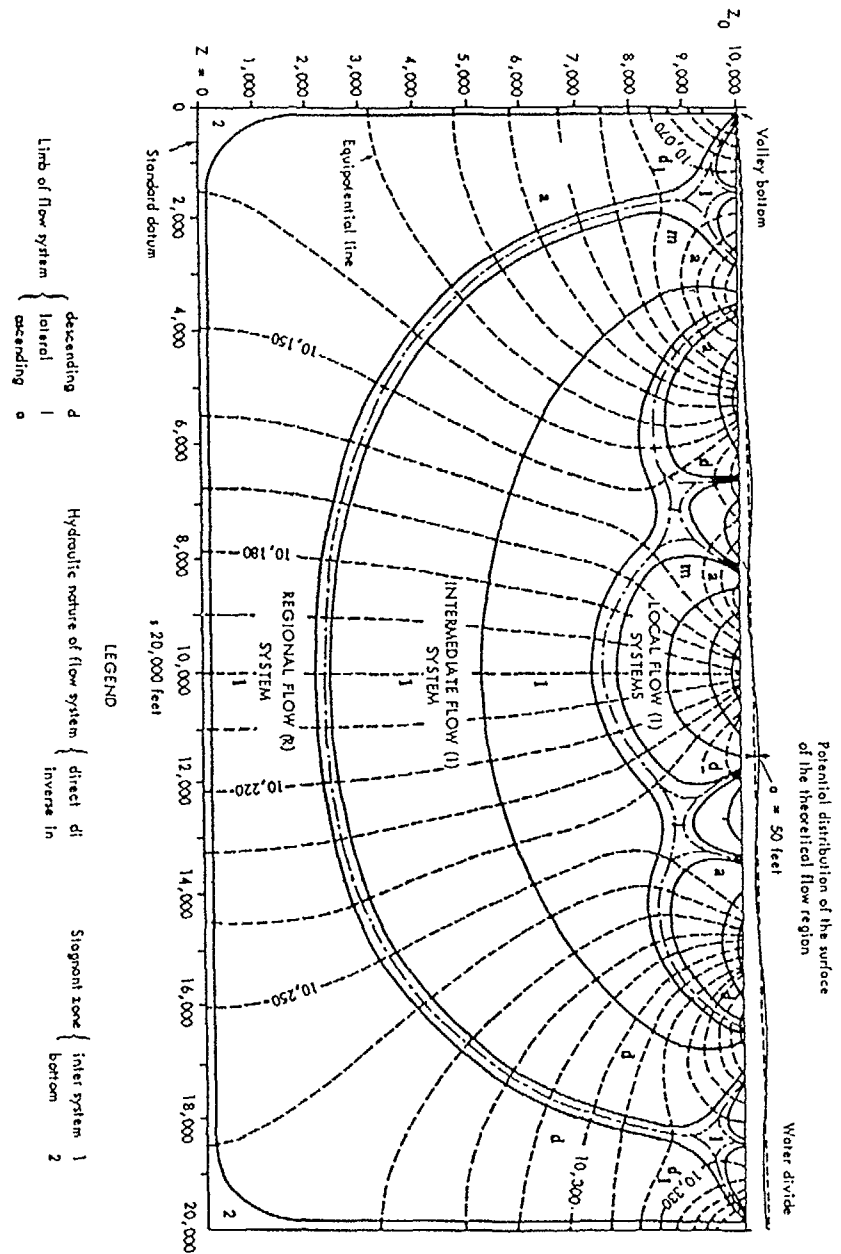
-Evolution by water/rock interaction and underground processes (evolution specific parameters, changing chemical properties)

This informations can then be used to define the investigated hydrogeological system in establishing a conceptual model by adopting the theoretical concept of groundwater flow of the hydrodynamic flow systems (TOTH, 1962, 1963) as represented in Fig.1 to the given hydrogeologic situation (BALDERER, 1984).

This general concept of interpretation applied in isotope hydrology yields the following general characterisation with respect to different the flow systems which can be used as general basic assumptions:

- Short term and seasonal variations are characteristic for Groundwaters originating from local flow systems or containing such mixing components.
- Groundwaters originating from intermediate or regional flow systems are usually not showing any short term fluctuation and are generally considered to present steady state situations.
- Groundwaters in different flow systems (what means also different flow path) present different chemical and isotopic properties (due to different in situ conditions and different residence times). They remain unmixed as long as they are not converging with other flow systems in a naturally occurring outflow zone (what means springs at surface but also tectonic short cuts through hydraulically active fault zones) or boreholes with long screened intake section.

The question now arises if isotope methods could even be of more use in the prediction of unexpected phenomenas of great possible dommages as earthquakes and volcanic eruptions. As until now only very few isotope investigations with this aim (or goal) were undertaken, it must be tried to use existing case studies made with the objective to understand the natural conditions of groundwater flow (e.g. with inclusions of such studies from tectonic active areas) in order to get a first estimate of the potential informations to be expected and looked for with respect to the further use as precursors of earthquakes and volcanic eruptions.



## 2. CAUSE OF POSSIBLE VARIATIONS OF ISOTOPE AND CHEMICAL COMPOSITION AS REVEALED FROM CASE STUDIES: THE QUESTION OF STEADY OR NON - STEADY STATE IN DEEP GROUNDWATER CIRCULATIONS

The way of flow of groundwater depends strongly on the given hydrologic situation and the given tectonic and geological structure. Based on the hydrodynamic principles of groundwater motion (Darcys law, Hubbert's equation respectively) depending on hydraulic head (as a function of recharge) and hydraulic conductivity (and effective porosity) distribution within the rocks of given geological structure the groundwater flow through an entire region can be attributed to local, intermediate and regional hydrodynamic flow systems. This concept also implies hydraulic continuity and is in its representation often applied as a steady state situation, especially for the interpretation of results of isotope investigations. In the presented study three sites within tectonic active areas in Western Turkey were discussed and compared with the now as first presented situation of the deep groundwaters in Northern Switzerland.

### 2.1 INFLUENCE OF LONG TERM FLUCTUATIONS: THE GROUNDWATERS WITHIN THE MOLASSE BASIN OF NORTHEASTERN SWITZERLAND

#### 2.1.1 HYDROGEOLOGICAL SITUATION

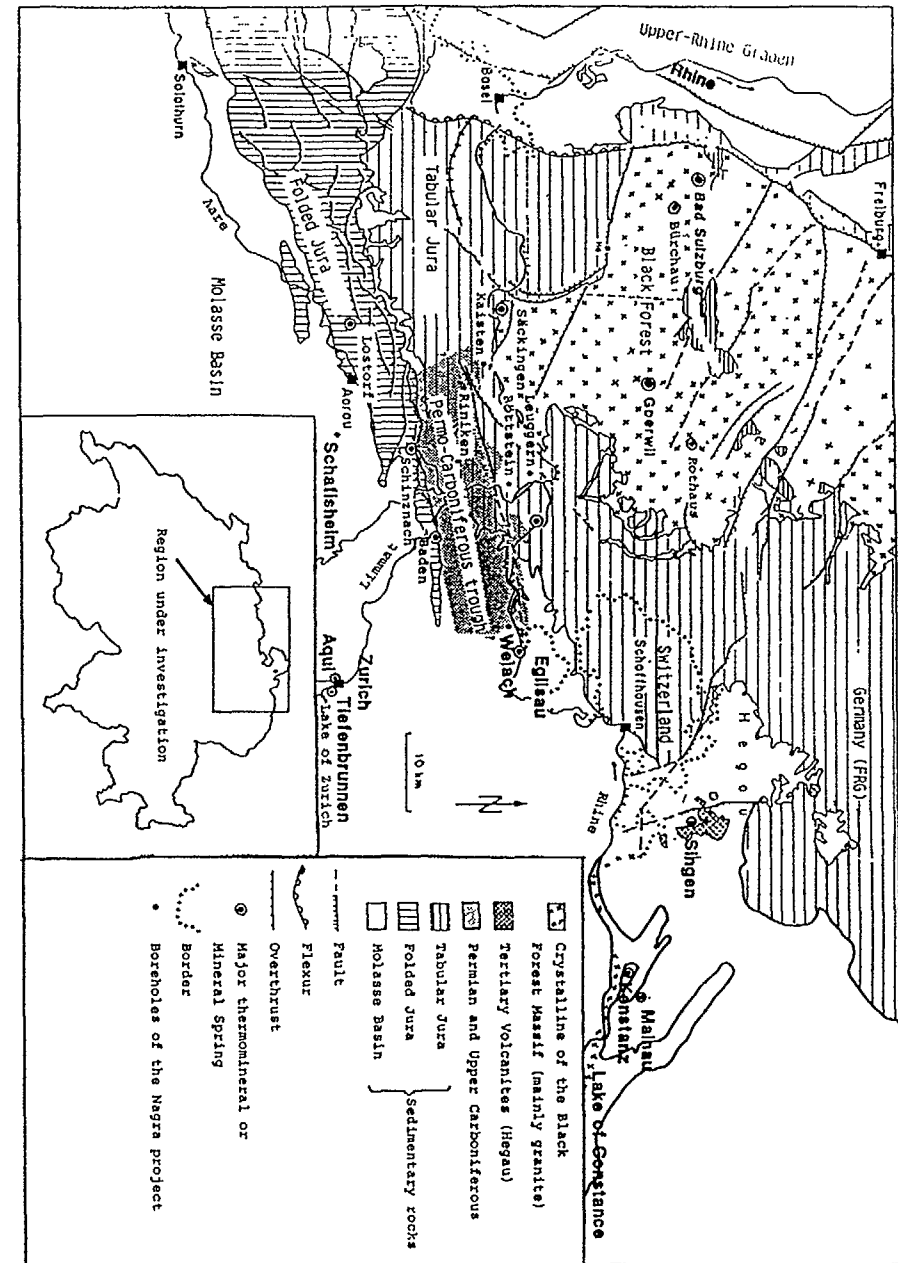
In this case study the situation of the deep groundwaters within the molasse basin of Northeastern Switzerland is considered (Balderer, 1990).

The Tertiary molasse deposits (consisting of clastic consolidated sediments) outcrop in the investigated area of the molasse basin forming the morphology of the region (mostly appearing as hills) if not covered by Quaternary deposits (Fig.2).

These Tertiary deposits, consisting of the formations of the Upper Freshwater Molasse (OSM), the Upper Marine Molasse (OMM), and the Lower Freshwater Molasse (USM) are underlain by the limestones of the Upper Jurassic (Upper Malm/Kimmeridgian). These limestones are karstified. Frequently this karstification is secondary blocked by weathering products (clays of the Siderolithic period). Below these limestones formations of low hydraulic conductivity as the Lower Malm, Dogger and Malm exist.

According to the tectonic structure the formations of the molasse and the underlying jurassic are uprising towards the northern border of Switzerland, towards the Rhine valley (Fig.3, geological cross section) As the morphological base level is decreasing

Fig.2: Main geological elements of the investigated area of Northeastern Switzerland



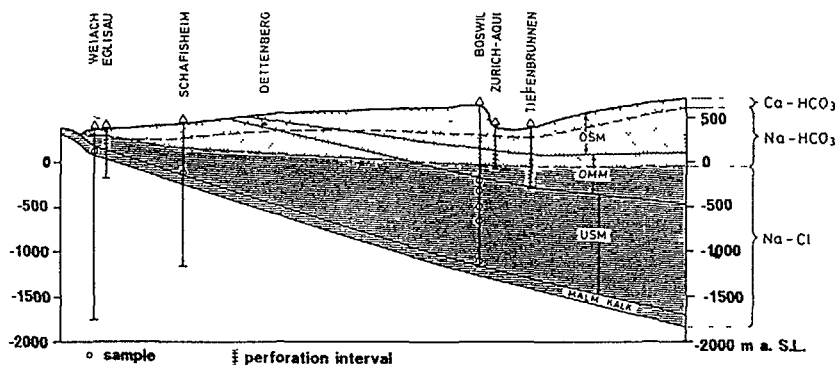


Fig. 4: Schematic representation of the chemical characterisation of the groundwater within the Swiss Molasse Basin

towards the North the molasse formations are outcropping and thinning out towards the Rhine River. (on the northern riverside even outcrops of the underlying Malm are present).

## 2.1.2 CHEMICAL AND ISOTOPIC SIGNATURES OF THE GROUNDWATERS

Within the Molasse deposits and the Limestones of the underlying Upper Malm (where not blocked by weathering products), three different types of groundwaters exist (Fig. 4):

(a) In the region of the morphologically outcropping molasse the water of the outflowing springs is of **Ca-(Mg)-HCO<sub>3</sub>-type** (Balderer, 1985, 1989) with total mineralisation of 5 to 9 meq/l (450-650 mg/l) and contains anthropogenic Tritium (Schmassmann et al. 1984, Schmassmann, 1990). It represents, also with respect to the stable isotopes <sup>2</sup>H and <sup>18</sup>O the conditions of the actual hydrological cycle and is representative for local flow systems (Balderer 1990).

(b) All the groundwaters sampled and analysed from boreholes below the base level of the valleys (in about 150 to 300m depth) within the Upper Marine Molasse (Zürich- Aquif, Konstanz, Manau, Singen) are of **Na-HCO<sub>3</sub>-type** with total mineralisation of 8 to 15 meq/l (0.7-1.5 g/l) and result Tritium- and <sup>14</sup>C- concentrations below detection limit. With respect to their stable isotope values <sup>δ</sup><sup>2</sup>H and <sup>δ</sup><sup>18</sup>O these groundwaters are situated on the meteoric water line but as more depleted in heavy isotopes well below the range of shallow groundwaters reflecting the recent climatic conditions (Fig 5).

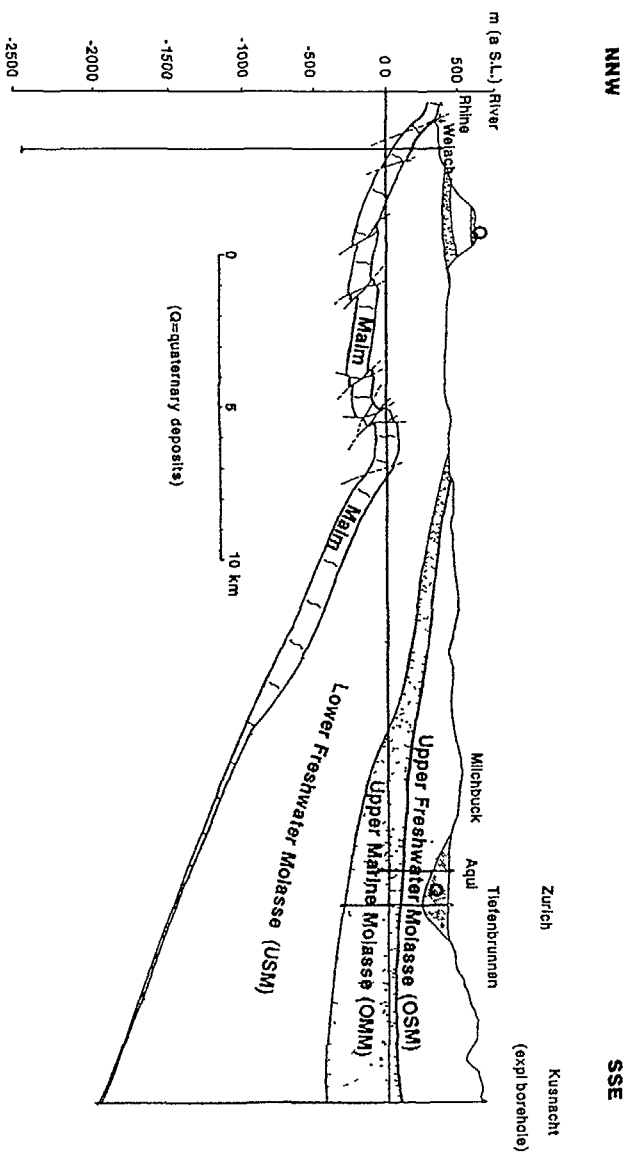


Fig. 3 Geological cross section through the molasse basin of Northeastern Switzerland

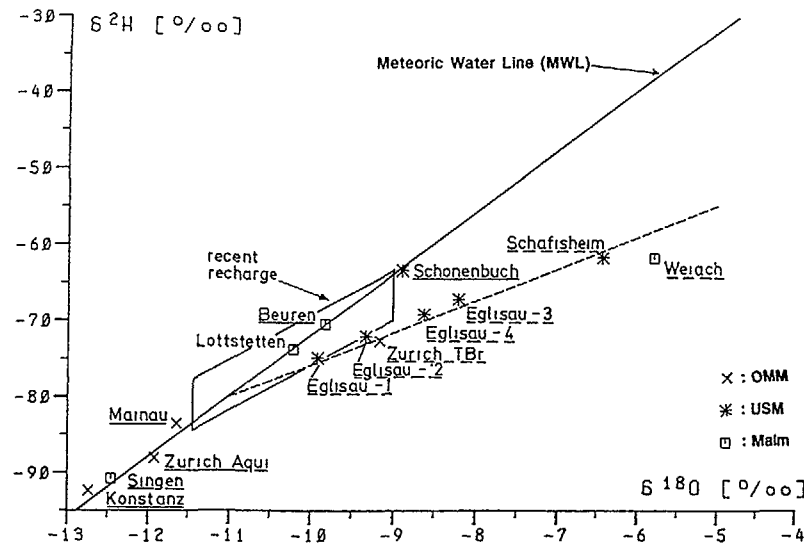


Fig. 5:  $\delta^2\text{H}$ ,  $\delta^{18}\text{O}$ -diagram of the groundwaters within the Molasse and Malm deposits

These deep groundwaters of the Molasse most probably have to be related to recharge during colder climatic conditions, as prevailing during Pleistocene (Schmassmann et al. 1984, Balderer, 1990, Pearson et al. 1991, Schmassmann, 1990). (c) Groundwaters originating from boreholes within the Lower Freshwater Molasse and the hydraulically connected limestones of the Upper Malm (as for the Eglisau 1 to 4 and the first section of the Schafisheim and Weiach boreholes of the Swiss Nagra Project, Balderer, 1985) are with 40 to 150 meq/l (2.4-8.8 g/l) much higher mineralized and of **Na-Cl-type**. These groundwaters result Tritium levels at or below detection limit, but contain  $^{14}\text{C}$  in measurable amounts in a range between 11 l up to 40 46 pmC. According to their  $^2\text{H}$ - and  $^{18}\text{O}$ -contents these groundwaters are situated on the  $\delta^2\text{H}/\delta^{18}\text{O}$ -diagram in Fig 5 below the meteoric waterline on a line with a lower slope which represents according to Bertleff et al., 1987 a mixing line between two endmembers of deep groundwaters. One of them corresponds to an origin during pleistocene conditions and the other to an evolved formation water of probably marine origin (but undergone evaporation and/or water-rock interaction). For this formation water of Na-Cl-type a high residence time outside the range of the radiocarbon has to be assumed. The measured  $^{14}\text{C}$ -concentrations of the analysed Na-

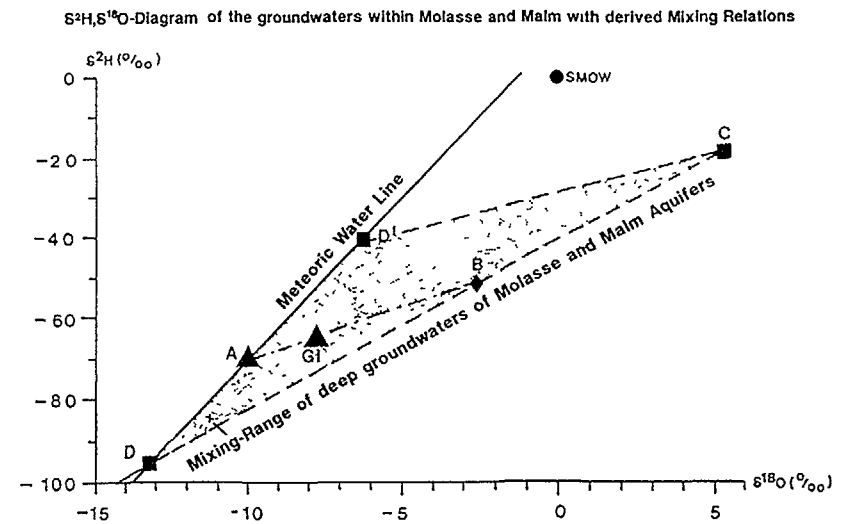


Fig. 6:  $\delta^2\text{H}$ ,  $\delta^{18}\text{O}$ -diagram of the groundwaters within the Molasse and Malm deposits with derived mixing relations

Cl-type waters from the Upper Freshwater Molasse and Malm therefore most probable represent mixing with a third component corresponding to a groundwater of recent recharge but showing no effect of the anthropogenic Tritium release into the water cycle (Balderer, 1990). As shown in Fig 6 according to Balderer (1990) the observed  $\delta^2\text{H}$ - and  $\delta^{18}\text{O}$  values (G1) can be explained by the mixing range due to the different mixing proportions of three endmembers D, D' and C with groundwater of recent recharge (Bertleff et al., 1987).

The observed differentiation with depth, as represented in Fig. 4 for the chemical composition of the groundwaters of the Molasse Basin indicates a very low exchange or communication in vertical direction (Balderer, 1990). Based on the observations of the different boreholes this Fig. 4 shows the fact that the much higher mineralized Na-Cl waters remain within the deeper part of the Molasse deposits and the hydraulically connected Upper Malm and are overlain by low mineralized waters of the Na- $\text{HCO}_3$ -type in the central part and of the Ca-(Mg)- $\text{HCO}_3$ -type near the regional outflow zones of the Rhine resp. Aare river.

The curved shape of the limit between the low and the higher mineralized types of groundwaters with its highest position in vicinity of the regional outflow zones is in

# Conceptual model of the hydrodynamic flow systems within the deposits of the Swiss Molasse Basin

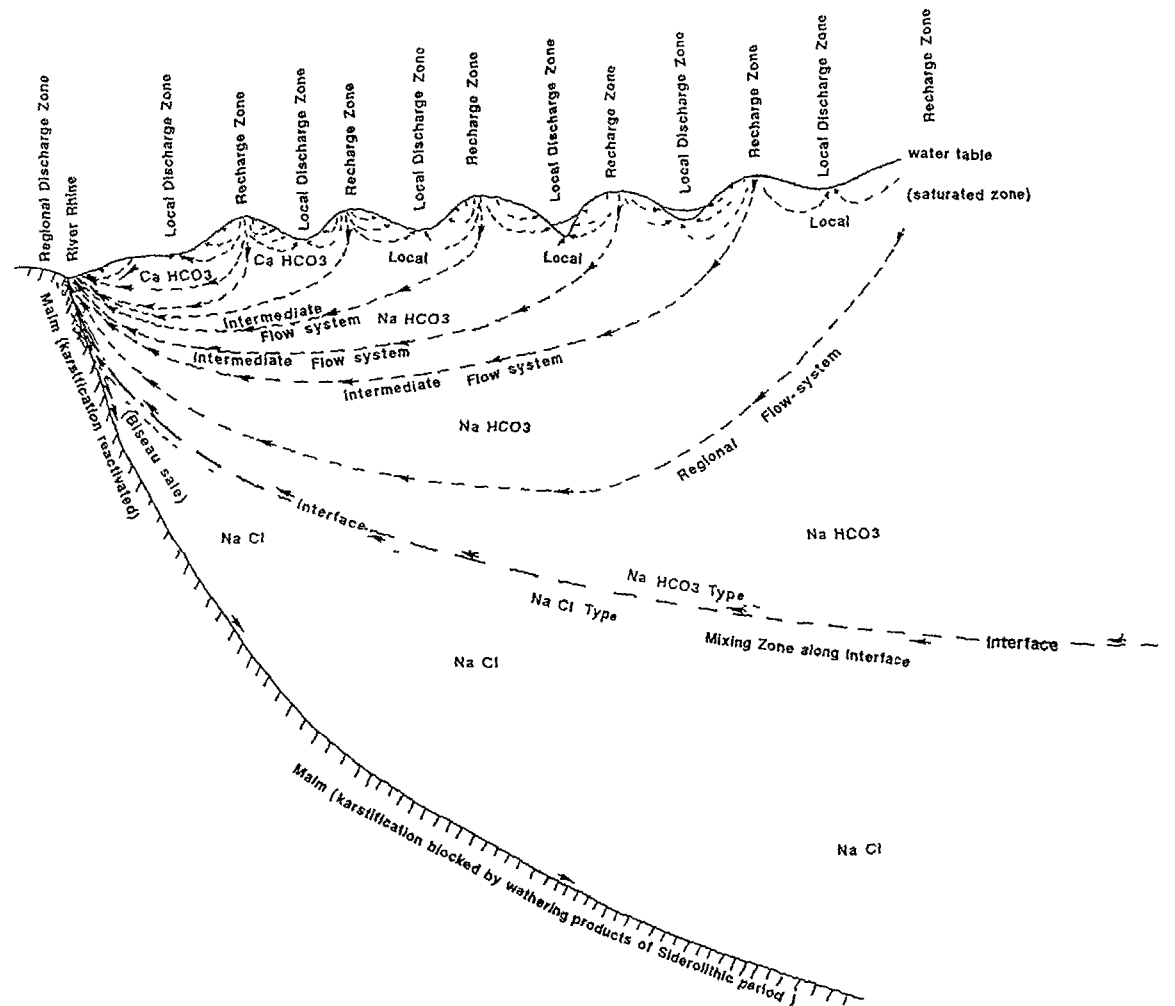


Fig 7 Conceptual model of the hydrodynamic flow systems within the deposits of the Swiss Molasse Basin



ageement with the occurrence of an interface between two liquids of different densities according to the theoretical concepts of Ghyben (1889), Herzberg (1901) and Hubbert (1940). That means that the position of this interface is dependent on the potential (hydraulic head) distribution of the fresh, low mineralized groundwater which correlates (in an attenuated way) to the topographical-morphological relief of the molasse deposits reaching its highest elevation (and maximum value of hydraulic head) within the central part of the Molasse Basin. The limit between the low mineralized **Na-HCO<sub>3</sub>-type** groundwater to the underlying much higher mineralized **Na-Cl-type** water (Fig.4) should therefore if it corresponds to a real interface according to its theoretical definition present a curved shape with its lowest (deepest) position within the central part of the Molasse Basin and rising upwards towards the regional exfiltration zones.

### 2.1.3 DEFINITION OF A CONCEPTUAL MODEL OF THE HYDRODYNAMIC FLOW SYSTEMS

From the hydrogeological structure and the now presented interpretation of the isotopic and hydrochemical data the following conceptual model of the hydrodynamic flow systems can be defined as illustrated by Fig. 7:

(a) Infiltration zones are situated on the topographical heights feeding the local, intermediate and to a small part also the regional flow systems. Most of this infiltrated water is moving to the local discharge zones of springs at the flanks and within the nearby valleys.

(b) During the almost vertical infiltration ionexchange takes place (Ca against Na) in contact with clay minerals containing beds (marls, siltstones).

(c) Along individual flow path starting from recharge zones according to the low and anisotropic hydraulic conductivity (in the nearly horizontally bedded deposits) first the Tritium containing water dies out and further on the <sup>14</sup>C-contents are diminishing. Still further on along flow path (of intermediate or regional flow systems almost parallel to the surface of the water table) a more or less abrupt change is observed with respect to the <sup>2</sup>H- and <sup>18</sup>O-contents characterizing the presence of the pleistocene infiltrated groundwater.

(d) Within the deeper and central part of the Molasse deposits a vertical differentiation or stratification can be observed where the low mineralized Groundwater of **Na-HCO<sub>3</sub>-type** is situated above the strongly mineralized groundwater of **Na-Cl-type** as represented in Fig.4 and 7. As already mentioned the limit between these two types of groundwater probably corresponds to a density related

interface which is rising upwards towards the northern edge of the Molasse basin, towards the regional outflow zones where the Molasse deposits are wedging out and the underlying limestones of the Upper Malm are appearing.

(e) This interface represents also a partitioning boundary with respect to the groundwater flow between the low mineralized water which is floating above the interface to the regional outflow zones (causing a transition zone with active mixing processes as effect of hydrodynamic dispersion) and the more or less stagnant highly mineralized groundwater of the **Na-Cl-type**.

(f) This higher mineralized Na-Cl-type water within the deeper part consists of a formation water of complex origin (probably with marine to brackish or even evaporitic influences). As the regional outflow zones are only connected to freshwater (river and groundwater) this highly mineralized Na-Cl-type water is captured within this deep semi-closed basin and can only outflow to the regional discharge zones as mixing component within the interface transition zone (Fig.8).

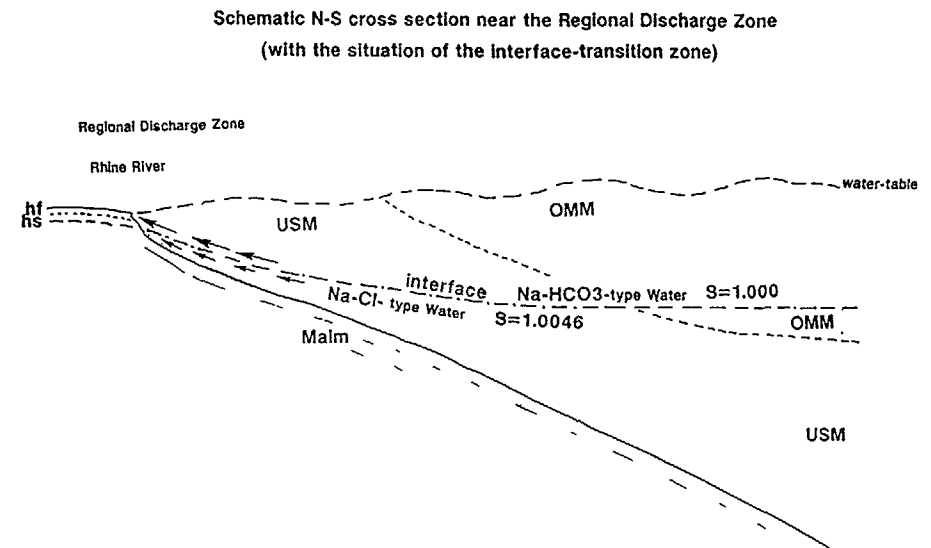


Fig.8: Schematic N-S cross section with the situation of the interface-transition zone near the regional discharge zone

## 2.1.4 RESULTING EVOLUTION OF THE GROUNDWATER WITHIN THE MOLASSE - MALM SYSTEM AS RESPONSE TO CHANGING CLIMATIC AND HYDROLOGIC CONDITIONS

From the now discussed hydrogeological, hydrochemical and isotopic properties adopting the presented conceptual model the following evolution of the groundwaters and flow systems can be deduced:

Primarily it is assumed that already after the end of the deposition of the Upper Marine Molasse a highly mineralized groundwater was present within both formations of Upper Marine and Lower freshwater Molasse as a result of the prevailing marine conditions during the deposition of the Upper Marine Molasse. The further evolution is considered in the following steps with considerably changed hydrodynamic conditions:

**Phase 1:** During and after the deposition of the Upper Freshwater Molasse fresh water containing aquifers were formed (within layers of higher hydraulic conductivity) by infiltration of the precipitation water. Within the saturated part of these Molasse deposits the presence of this second type of groundwater of low mineralisation is provoking the generation of an interface.

**Phase 2:** These processes of the hydrological cycle were also going on during the Pleistocene epoch with its different and extreme climatic conditions (from cold glaciation periods to humid warm interglacial periods). For this epoch it is inferred that the thick overburden by the ice of the glaciers within the largely eroded valleys (producing probably considerable hydrostatic overpressures) together with increased precipitations, reduced evapotranspiration, large river runoffs of meltwater has induced a higher rate of infiltration and therefore a higher amount of recharge also of the groundwaters within the molasse deposits. It can therefore be assumed that during and especially towards the end of this pleistocene epoch the piezometric head of the fresh groundwater had increased resp. the position of the water table was higher than anterior to the pleistocene epoch. As a result of the higher piezometric head of the fresh groundwater the interface moved downwards to a new position probably as down as to the base of Upper Marine Molasse or even deeply into the Lower Freshwater deposits (depending on the local distribution of the piezometric head of the low mineralized fresh groundwater).

**Phase 3:** The global increase in temperature by the climatic change at the end of the last glaciation and beginning of the Holocene epoch provoked the melting of the ice and the retirement of the glaciers to much higher altitudes, leaving behind moraines, valleys filled with fluvio-glacial deposits but also with sediments of low hydraulic

conductivity as drifts and lake sediments. By these processes the imposed pressure of the glaciers was released and also the general rate of infiltration to the molasse sedimentary complex was reduced. These processes led to a lower position of the water table resp. to a decreased piezometric head distribution of the low mineralized groundwater within the molasse deposits. In response to the changed hydraulic conditions a hydrodynamic re-equilibration of the interface was induced which moved upwards to a new, higher position. By this displacement of the interface an intense mixing zone was produced as transition zone of the high mineralized saline formation water of Na-Cl-type and the overlying low mineralized groundwater which mainly corresponds to infiltration during pleistocene conditions.

**Phase 4:** In the actual recent and observable situation the groundwaters originating from recharge by infiltration during the pleistocene epoch are already flushed within the local flow systems, partially still existing within intermediate flow systems but mainly only preserved within the regional flow systems with long, subhorizontal flow path (Fig.7). To such a situation corresponds the groundwater of the producing mineral water well of Aquis-Zürich. In the area of the regional discharge zone (around the Rhine valley) the water of local flow systems is mixed with the groundwater of the intermediate and regional flow systems. Therefore the pleistocene infiltrated groundwater of the Na-HCO<sub>3</sub>-type is nearly completely flushed by the holocene infiltrated water. Probably relicts of these pleistocene infiltrated groundwaters are still present as small mixing components (e.g. as originating from intermediate and regional flow systems within the interface transition zone as evidenced by the <sup>2</sup>H and <sup>18</sup>O contents of the somewhat lower mineralized Na-Cl-type groundwaters of the Eglisau mineral water (wells 1 to 4).

**Phase 5:** From the observed processes and the proposed conceptual interpretation model of the groundwaters within the molasse basin also the future development can be prognosticated: The replacement or flushing of the during the pleistocene epoch infiltrated groundwaters of the Na-HCO<sub>3</sub>-type is continued. These groundwaters will first be further replaced within the intermediate flow systems. This flushing of the low mineralized pleistocene infiltrated is according to Fig.4 most advanced within the regional outflow zone (by the conjunction and mixing with water of local flow systems) and will now further progress moving "backwards" and "downwards" also affect intermediate flow systems of longer flow distances. (For an individual flow system the flushing process starts from the recharge zones and will later on also be affecting the transition zones. Such an intermediate individual flow system will be completely flushed if the postglacial, holocene infiltrated groundwater arrives at the discharge zone). This "flushing" process is going on as evidenced (i) by the presence

of low mineralized Ca-(Mg)-HCO<sub>3</sub>-type waters not only within local flow systems but also within intermediate flow systems in vicinity of the regional discharge zone, and (ii) also by a Na-HCO<sub>3</sub>-type water of postglacial infiltration (according to <sup>14</sup>C, <sup>2</sup>H, and <sup>18</sup>O contents) from a motorway tunnel in Zürich. Along the interface the differential movement of the circulating (outflowing) low mineralized groundwater will lead to a gradually decreasing mineralisation of the underlying quasi stagnant mass of the higher mineralized Na-Cl-type water together with an increase in vertical extend of the transition-mixing zone. In addition it is probable that the reequilibration of the position of the interface as response to the lowered hydraulic head distribution of low mineralized groundwater (caused by the change from pleistocene to the actual holocene climatic conditions is still going on. Probably this process is even intensified in future by the increasing exploitation of these deep groundwaters within the Upper Marine and Lower Freshwater Molasse (beside the traditional use as source for mineral water also the use of the groundwater of this deep aquifer as resource of geothermal energy without reinjecting the water is still more increasing) Especially the intense lowering of the hydraulic head in the vicinity of these exploitation wells will produce with time an upcoming reaction of the interface coupled with an enlargement of the mixing transition zone. This process will therefore intensify the already existing mixing processes between the low mineralized groundwaters of the Na-HCO<sub>3</sub>- resp. the Ca-Mg-HCO<sub>3</sub>-type with the high mineralized groundwater of the Na-Cl-type. Such influences as increasing salinity are already observed in some of the exploitation wells with to high abstraction rate (considering the rather low hydraulic conductivities of about 10<sup>-6</sup> to 10<sup>-7</sup> m/s) and intense lowering of the water table of more than 150 m (N. Sieber pers. comm. 1992). Also some influences of anthropogenic activity as change in water level as by the construction of dams on river Rhine for hydroelectric power generation are provoking local changes of the hydraulic head distribution which also result in newly induced mixing processes (e.g. case of the Eglisau 1 borehole, Balderer, 1990).

## 2.1.5 CONSEQUENCES

As demonstrated by this study, the assumption of a steady state groundwater flow is even for the case of deep circulations at least not true if longterm fluctuations of hydraulic head due to changed recharge conditions (e.g. changed climatic conditions) and/or changes in hydraulic head (e.g. as change of overburden of glaciers resulting in increased pore pressures) are considered

Similar effects as here described for the groundwaters within the Molasse deposits have been evidenced by hydrochemical and isotope investigation for the groundwaters in the deep formations of Lower Triassic (Buntsandstein), Permian (Permocarboniferous trench) and crystalline basement by the Swiss Nagra project (Balderer et al. 1987, Pearson et al. 1991). Due to long-term morphological processes (erosion combined with isostatic uplift) a dilution process by low mineralized waters originating from eroded areas of the outcropping Black Forest Massif as recharge area affecting the tectonically perched high mineralized waters within the deeper crystalline basement and the permocarboniferous trench takes place (Fig.9).

But the evidenced existence of deep groundwaters originating from recharge under different climatic, geological and hydraulic conditions implies very low flow velocities under the today's hydraulic conditions, so the question arises if pressure changes as induced by earthquake processes could result in changes of the groundwater composition of springs or boreholes. This question now will be discussed based on the already existing results of studies in tectonic active areas in

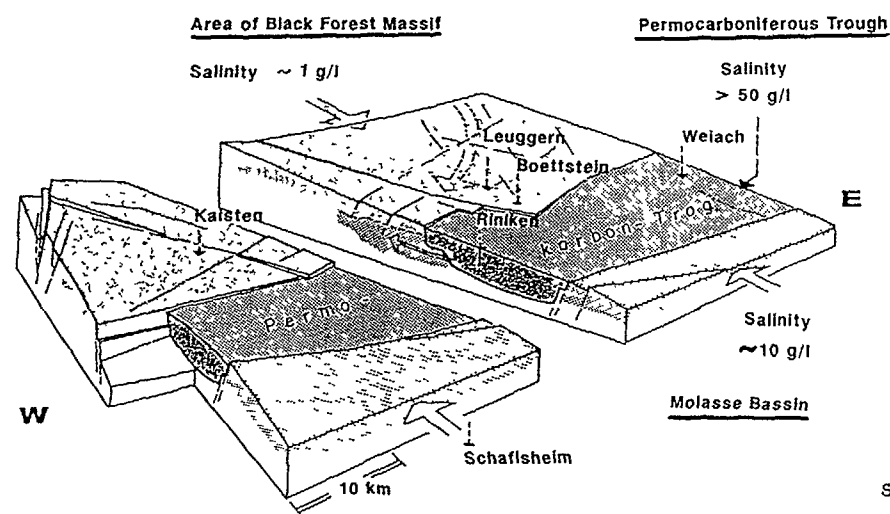


Fig 9 Relation of the groundwaters within the upper part of the crystalline basement and permocarboniferous trench in Northern Switzerland

Western Turkey (studied within the framework of the interdisciplinary research project "Marmara" of ETH-Zurich and Istanbul Technical University ITU, Schindler et al 1992)

### 3 LONG AND SHORT TERM FLUCTUATIONS. INFORMATIONS OF STUDIES FROM TECTONIC ACTIVE AREAS IN NORTH - WESTERN TURKEY

Through its physical properties ground water presents an ideal transport media within the geological underground. But within tectonic active areas the groundwater not only reflects influences of the processes of *recharge/infiltration and flow/migration* (with evolution by water rock-interaction) but also influences of internal processes (with the release of fluids and gases) due to the effects of tectonic activity. Indications for such influences of the earth's interior (of the deeper crust or even the mantle) present the concentration and isotopic composition of the groundwater itself and the contents/isotopic ratios of rare elements and of (reactive and noble) gases (but also of dry exhalations as fumaroles). Such influences, but also the often increased heat flow within tectonic active areas will influence the water - rock interaction and therefore also the evolution of the groundwater. For this reason special applications (tools) have been developed as the chemical and isotopic geothermometers.

#### 3.1 SALINE THERMAL SPRINGS IN THE WESTERN BIGA PENNINSULA

This first studied area is located in the northwestern part of Anatolia on the Biga Peninsula, known in the antiquity as the Troas (Fig 10). Along the western coast, three centers with thermal water discharges occur named **Akçekeçili**, **Kestanbol Kaplıca** (Kaplıca meaning spa) and **Tuzla**. Since classical times these thermal springs were used in spas.

##### 3.1.1 HYDROGEOLOGICAL SITUATION

The small thermal spring of **Akçekeçili** appears on the western limit of a complex of about 100 m thick metamorphic series just before they dip beneath Upper Miocene sediments (Fig 10).

Near **Kestanbol Kaplıca** a larger metamorphic complex is exposed along a NE-SW striking normal dextral faultzone. The two main thermal springs lie on the northern

Geological Scetch of the Western Biga Penninsula  
(Western Turkey)

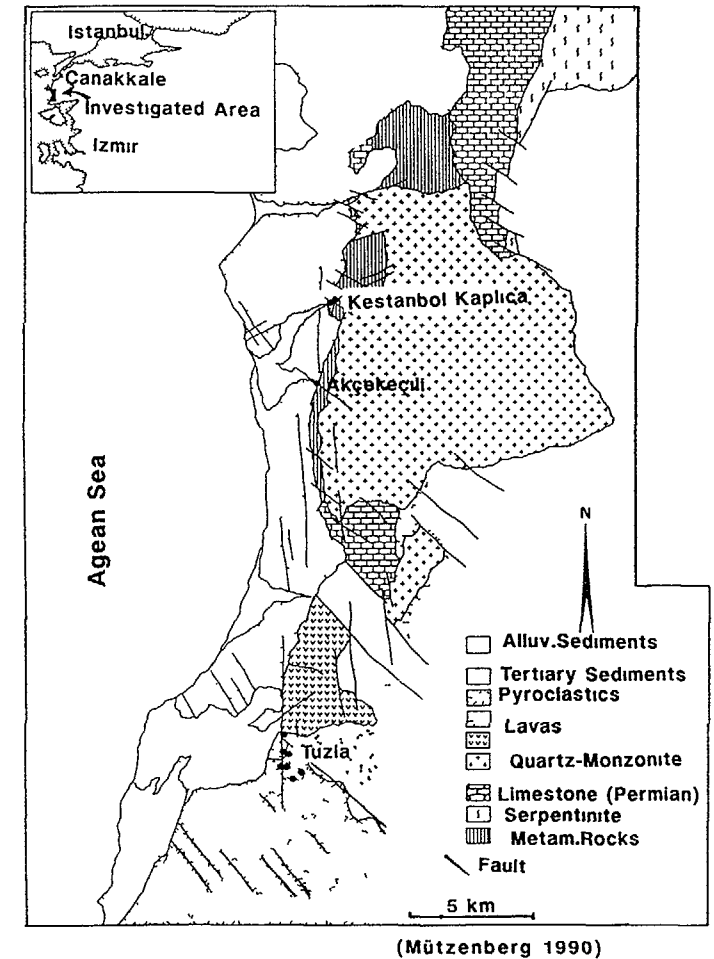


Fig 10 Geological map of the western Biga Penninsula (Mützenber 1990)

flank of the Ilica valley (Fig 11). The intrusive quartz-monzonite type rocks on both sides of the valley are intensively cleft and showing salty exhalations. A 290 m deep drilling (Yurur 1985) has been carried out in 1975 and met thermal water today used for the spa.

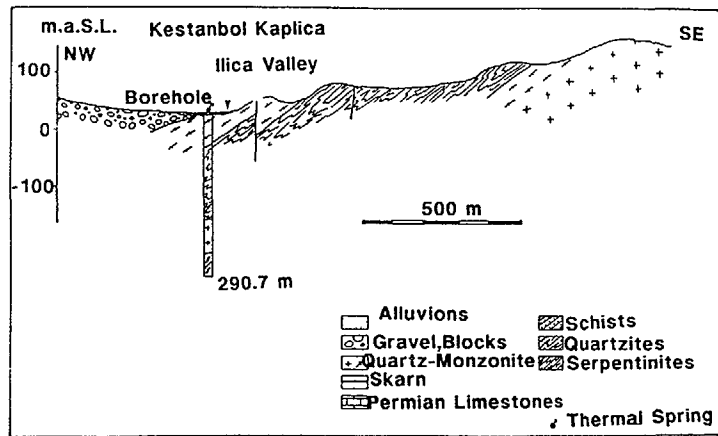


Fig.11: Geological cross section of the Kestanbol Kaplica thermal area

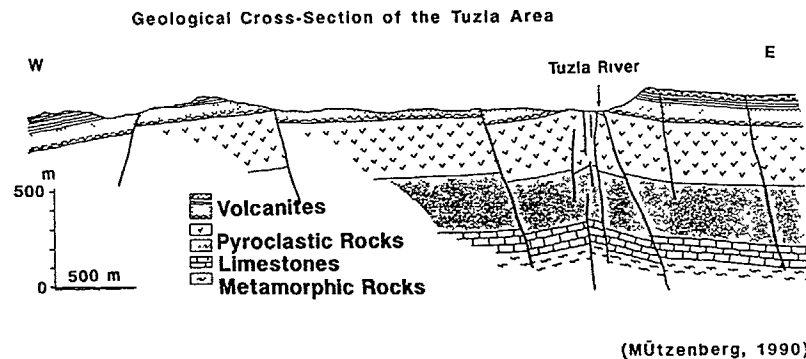


Fig.12: Sections of two drillings in the Tuzla area according to Karmanderesi 1987, in Mützenberg 1990).

The **Tuzla** area is dominated by calcalcaline volcanics and ignimbrites (Fig.10). Below the about 600 m thick volcanic sequence Permian limestones and metamorphic rocks have been encountered in two drillings (Fig.12, according to Karmanderesi 1987, in Mützenberg 1990). The thermal activities around Tuzla cover a surface area of about 1 km<sup>2</sup>. Since Upper Miocene to the Present evidences of at least four thermal phases can be recognized in this area:

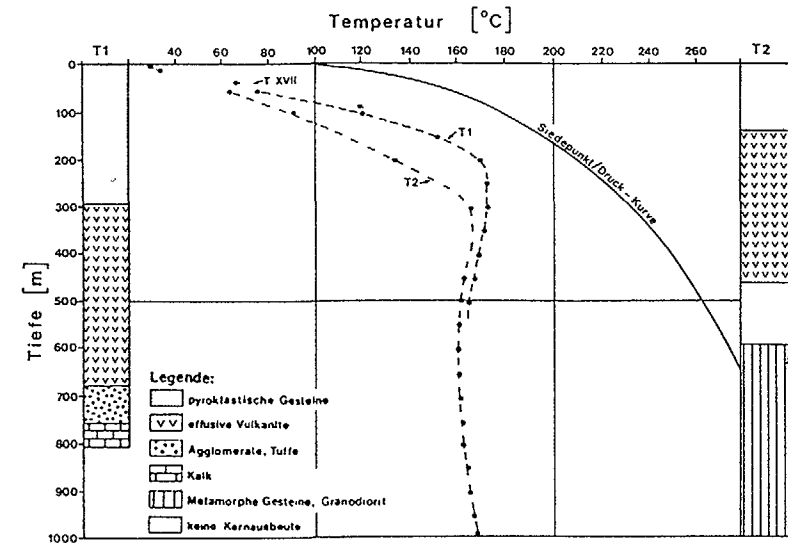


Fig 13: Geological cross section of the Tuzla area (Mützenberg et al 1992)

1. Red and black ferromanganese crusts intercalated in the Upper Miocene sediments with feeders along joint sets;
2. Silicified zones in sedimentary and volcanic rocks, probably associated with N-S striking faults;
3. Travertine terraces as deposits of cooling water rich in carbonate;
4. Outflowing Na-Cl rich hot brines, which characterize the present hydrothermal activity.

Based on the structural pattern of major fault systems (Fig.10) it can be recognized that the origins of the thermal springs within the three investigated areas coincide with the intersection of the following three systems: i) NNE-trending dip-slip fault zones, ii) major NE-SW striking, right lateral strike-slip faults, iii) sets of NW-SE trending joints/faults cutting through all three thermal areas.

From these observation results that due to the resulting increase in vertical permeability the intersection of these three major faults systems represents the actual flow path for the rise of the thermal water from the deep reservoir through the nearly impermeable cover of fine grained Miocene sediments to the spring origins at surface (Fig 13)

The outflow zones of the thermal brines are situated about 20 to 30 m in the Kestanbol and 20 to 80 m above sea level in the Tuzla area.

In both areas springs of low mineralized fresh water at lower temperatures are observed at the same level or at slightly higher altitudes. They represent the outflowing local groundwater recharged and circulating in the fissured rocks of the intrusion of the quartz-monzonite in the Kestanbol, or in layers of increased permeability within the volcanic sediments in the Tuzla area respectively.

### 3.1.2 CHEMICAL AND ISOTOPIC CHARACTERISATION OF THE THERMAL WATERS (BRINES)

During the presented study (Mützenberg, 1990, Mützenberg et al. 1992) the outflow of 14 thermal springs and one artesian borehole were sampled in different seasons from 1987 to 1988. The temperature and total mineralisation of the outflowing thermal water ranges from 33.5 °C and 16 g/l for the spring of Akçekeçili to the boiling point temperature and a maximum value of 65 g/l of total dissolved solids for the highest mineralized spring at Tuzla. Based on the main constituents as presented in Fig.14, the brine can with Na about 80 mval % of total cations and Cl greater than 99 mval % of total anions be characterized as Na-Cl type, with the ratio similar to seawater and with Ca greater than K and low concentrations of Mg, SO<sub>4</sub> and HCO<sub>3</sub>.

The Ca/Cl, K/Cl, and Li/Cl ratios are markedly increased with respect to seawater.

Samples of the thermal waters and of adjacent fresh water springs have also been analyzed for their oxygen-18, deuterium and tritium contents.

The tritium data as represented in Fig.15 versus the chloride concentration reveal that: i) only some of the low mineralized ground water of freshwater springs (with very low chloride concentration) contain anthropogenic tritium; ii) whereas all heavy mineralized thermal waters of the Tuzla and Kestanbol area do not contain any measurable tritium.

Therefore a mixing process between local low mineralized fresh ground water and the deep thermal brine is evidenced for the thermal spring of Akcekeçili by the measured tritium content (3.5±0.7 TU).

The stable isotope contents  $\delta^2\text{H}$  and  $\delta^{18}\text{O}$  are also represented in Figure 5. By this diagram a clear distinction between low mineralized waters of low chloride content and the hot thermal brines is possible.

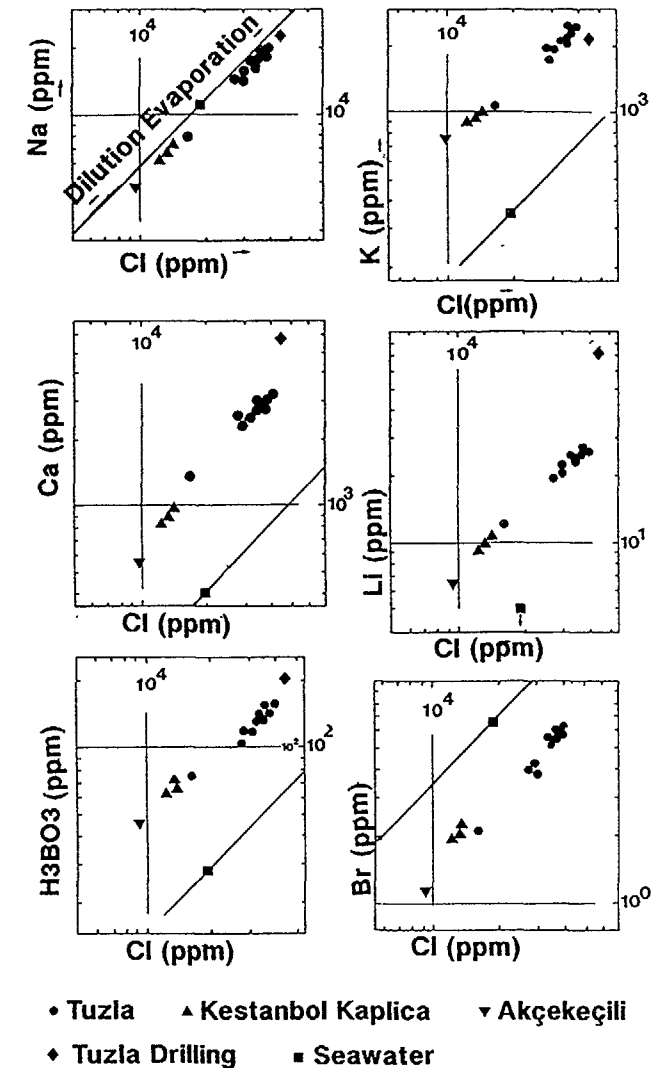


Fig.14: Plots of the dissolved ions versus chloride (in logarithmic scale) of groundwaters of the Tuzla - Kestanbol geothermal area

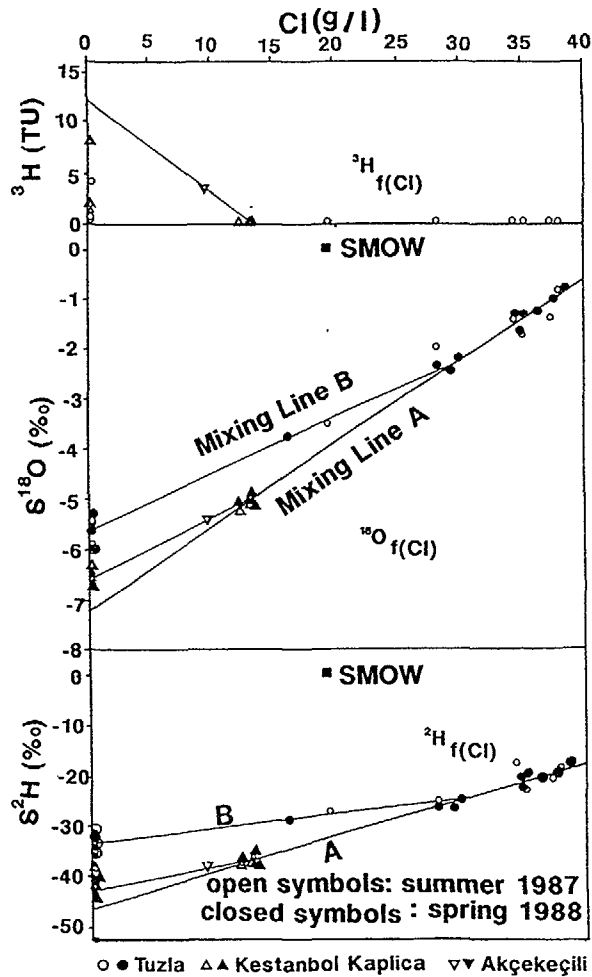


Fig.15: Diagram of isotope contents( $^3\text{H}$ ,  $^2\text{H}$ ,  $^{18}\text{O}$ ) versus Chloride content of groundwaters of the Tuzla - Kestanbol geothermal area

On the  $\delta^2\text{H}$  versus  $\delta^{18}\text{O}$  diagram in Fig.16 the corresponding values of the low mineralized shallow groundwaters with low chloride concentration are situated along the meteoric water line (with values in the range of: -45 to -30 ‰ for  $\delta^2\text{H}$  and -7 to -5 ‰ for  $\delta^{18}\text{O}$ ).

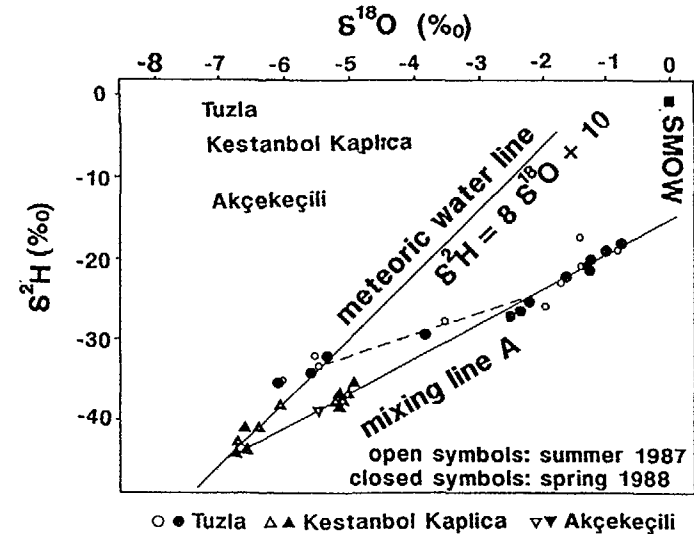


Fig.16:  $\delta^2\text{H}$  versus  $\delta^{18}\text{O}$  diagram of groundwaters of the Tuzla - Kestanbol geothermal area

On the same diagram in Fig.16 the values of the thermal brines are situated below the meteoric water line on a line with lower slope (line A) showing a marked oxygen-18 enrichment.

This line A could be interpreted as mixing line between the low mineralized ground waters and the hot thermal brines, where the most concentrated brine of the Tuzla area represents also the most enriched endmember with respect to its stable isotope contents.

### 3.1.3 RESULTING INTERPRETATION

Based on this presented study the following conclusions can be made:

As the ratios of non-reactive species of the sampled thermal waters differ very little it can be concluded that they evolved from a common saline end-member and represent mixing series with low mineralized fresh groundwater. The last mentioned correspond either to shallow waters (containing anthropogenic tritium) or heated regional ground waters of meteoric origin. For the saline endmember an evolution from a fossil altered seawater (connate water) is suggested based on the similar Na/Cl and only slightly differing Br/Cl and B/Cl ratios (Fig.15).

The high salinity and the observed isotopic signatures can be explained by diagenetic reactions in the sediments (Clayton et al. 1966) and water rock interactions at higher temperatures during circulation in volcanic/ crystalline and metamorphic rocks (also involving oxygen isotope exchange reactions, Savin, 1980, Kharaka and Carothers 1986, Balderer et al. 1991).

Therefore the actual composition of the present day outflowing hot waters of the observed springs can be explained by mixing processes with heated fresh water of regional aquifers and locally with near surface groundwater of meteoric origin up to 85%.

The ascent of the saline thermal water results of the combined effect of (1) deep regional circulation along major fault zones, (2) the high heat flow in this region of active tectonic movements and (3) the dilution effect by mixing with low mineralized hot freshwater of low density which lead the the observed upwelling of the hot brines due to the buoyancy effect along zones of high vertical permeability .

### 3.2 INVESTIGATION OF THE THERMAL AND COLD GROUNDWATERS IN THE BURSA AREA

An apparently also very stable situation even in the active tectonic area along the system of the North Anatolian Fault Zone in Western Turkey present the thermal waters originating within the **Bursa** region (Imbach and Balderer, 1990, Balderer et al.1991, Imbach, 1992, Schindler et al., 1992).

#### 3.2.1 SUMMARY OF THE STUDY AREA AND FIRST RESULTS

In this area thermal springs, used since the Roman-Byzantine period arise within two locations (**Kükürtlü/Bursa** and **Cekirge**) at the northern slope of the **Uludag** massif (with peak altitude of about 2500 m) just above the valley plain (elevation 150m - 200m).

Cold groundwaters with Tritium contents between 10 and 23 tritium units, sampled at altitudes between 100 and 2300 m in the **Bursa** area and on **Mount Uludag**, align with respect to their  $^2\text{H}$ - and  $^{18}\text{O}$ - contents along a local meteoric waterline (Fig. 17) with a deuterium excess of 17.4 ‰.

The outflowing **hot waters** are of **Na-Ca-HCO<sub>3</sub>**- type (with total mineralisation of 1220 mg/l and temperatures of up to 82 °C) in the **Bursa/Kükürtlü** area and of **Ca-Na-HCO<sub>3</sub>**- type (with total mineralisation of 500 mg/l and of temperatures of up to

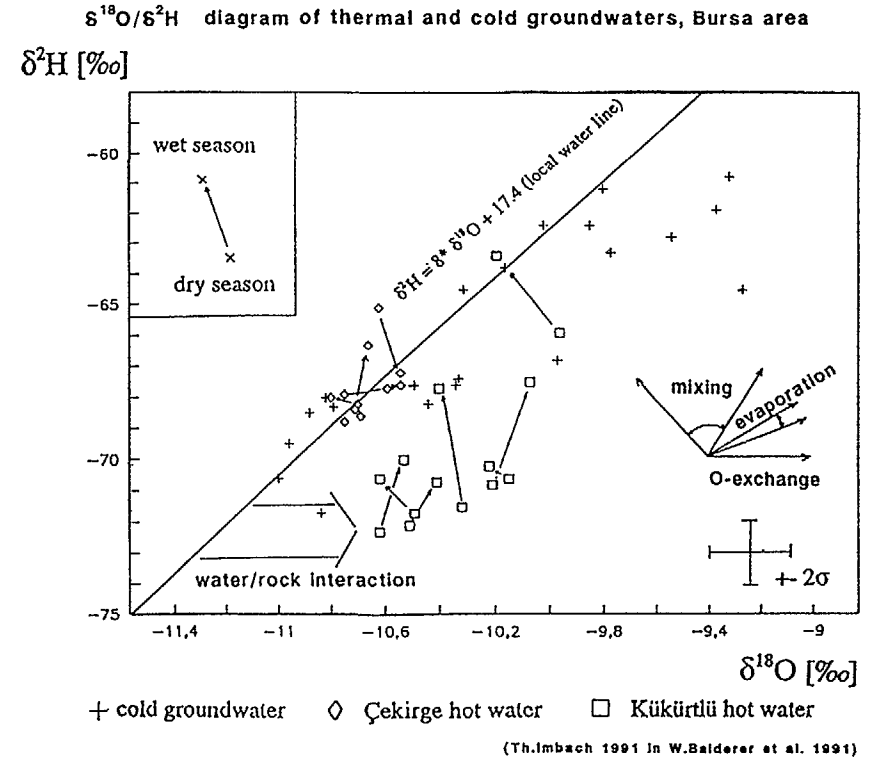


Fig.17:  $\delta^2\text{H}$  versus  $\delta^{18}\text{O}$  diagram of thermal and cold groundwaters of the Bursa area

46 °C) in the **Cekirge** area. The analyzed **Cekirge** thermal waters align with respect to their  $^2\text{H}$  and  $^{18}\text{O}$ - contents also on the defined local meteoric waterline of the cold local groundwaters and reveal tritium concentrations between < 1.3 and 6.3 Tritium units. As shown by Fig.17 some mixing processes occur between waters of dry season and wet season due to mixing in different proportions with local groundwaters. The **Kükürtlü** thermal waters with analyzed tritium values of < 1.3 and 6.7 Tritium units differ from the local meteoric water line (Fig.17) showing an enrichment with respect to  $^{18}\text{O}$  which seems most likely to be attributed to oxygen isotope exchange reactions with rock minerals due to higher temperatures (calculated reservoir temperatures of > 100 °C, according to Imbach, 1992).



### 3.2.2 RESULTING INTERPRETATION

From the observed chemical and isotopic signatures and in consideration of the topographical, geological and also tectonic situation the following interpretation results: The groundwater recharge of the whole area (as well as for cold and hot groundwaters) is concentrated on **Mount Uludag** and dominated by heavy rainfall, snow and snow melt during the winter period. Based on the deuterium contents of the observed thermal waters combined with the deuterium altitude relation of the local cold groundwaters (Imbach 1992) mainly two different recharge areas may be distinguished: The **Kükürtlü** thermal waters would correspond to waters recharged in the altitude range of 1600 to about 2500m up to the highest peaks of Mount Uludag, whereas an altitude range of 300 to 600 m would be adequate for the **Cekirge** thermal waters which coincides with the karstified travertine terraces in the western part of Mount Uludag just above the Cekirge village.

For both cases of **Bursa/Kükürtlü** and **Cekirge**, the outflowing thermal waters represent a actual water circulation system with known recharge and discharge areas. Considering the low mineralisation of these thermal waters a high heat flow or a very rapid ascent from depth is to be assumed.

From the now presented results of isotope, hydrochemical and hydrogeological investigations and in consideration of the historical records (Imbach, 1992) results, that this area of **Bursa** represents an region of a stable thermal system. With recharge in the fissured and partly karstified rocks of the **Uludag** massif, deep vertical circulation due to tectonic structure and high hydraulic gradient what leads together with a higher heat flow to the observed hot waters, naturally occurring at intersections of two fault systems. By the cooling process of the outflowing hot water travertine deposits were formed by calcite precipitation beginning from the upmost springs origins. The fact that the today's used springs are all originating within the altitude range of these these travertine deposits indicates a decrease of hydraulic head with time.

Seasonal variations as shown by the tritium values and the stable isotopes are most probably attributed to mixing processes along flow path inside the aquifer which are induced through change of hydraulic head, increased during recharge period of autumn to spring and decreased in the summer period as mainly dry season.

### 3.3 INVESTIGATION OF THE THERMAL AND MINERAL WATERS OF THE KUZULUK AREA:

Some 40 thermal and mineral waters arise in springs within the subsidence basin of the Kuzuluk area (Greber, 1992). All these waters are dominated by CO<sub>2</sub>-outgassing due to the tectonic activity in the vicinity of the North Anatolian Fault zone.

#### 3.3.1 SUMMARY OF FIRST RESULTS

In this area the mineralized cold and hot waters of outflowing springs are of **Na-(Ca)-(Mg)-HCO<sub>3</sub>-Cl-** type with a total mineralisation up to 3 g/l. At the naturally occurring hot springs (named "central springs") water with temperatures up to about 56°C, resp. of 82°C within the two boreholes of about 160m and 240m depth were observed. The occurring cold mineral waters of the "marginal springs" are higher mineralized of up to 7 g/l. All these mineralized cold and hot waters are characterized by a very high CO<sub>2</sub> contents of up to 1 l per 1kg of water (at surface conditions). But also other evidences of the high CO<sub>2</sub> activity are observed, e.g. higher concentrations at outcropping fault zones, which could even be used as a method of detection of such zones (Greber, 1992). The observed mineralized waters contain generally no anthropogenic tritium in measurable amounts except if some mixing with shallow ground waters occurred. With respect to the  $\delta^2\text{H}$  and  $\delta^{18}\text{O}$  values as represented in Fig.18, a distinct deviation of the cold mineral and thermal waters from the meteoric water line of the local shallow groundwaters can be observed.

#### 3.3.2 RESULTING INTERPRETATION

This deviation of the cold mineral and thermal waters from the meteoric water line of the local shallow groundwaters can with respect to the  $\delta^{18}\text{O}$  values be attributed to water/rock interaction and/or isotopic exchange with the uprising CO<sub>2</sub> (Fig.19).

This interaction with uprising CO<sub>2</sub> which is also influencing the chemical composition of all the observed thermal and cold mineral waters would infer  $\delta^{18}\text{O}$  values of CO<sub>2</sub>(g) in the range of marine carbonates or silica deposits.

$\delta^{18}\text{O}$ -,  $\delta^2\text{H}$ - and  $^3\text{H}$  diagram of shallow groundwater, thermal and cold mineral waters, Kuzuluk/Adapazari

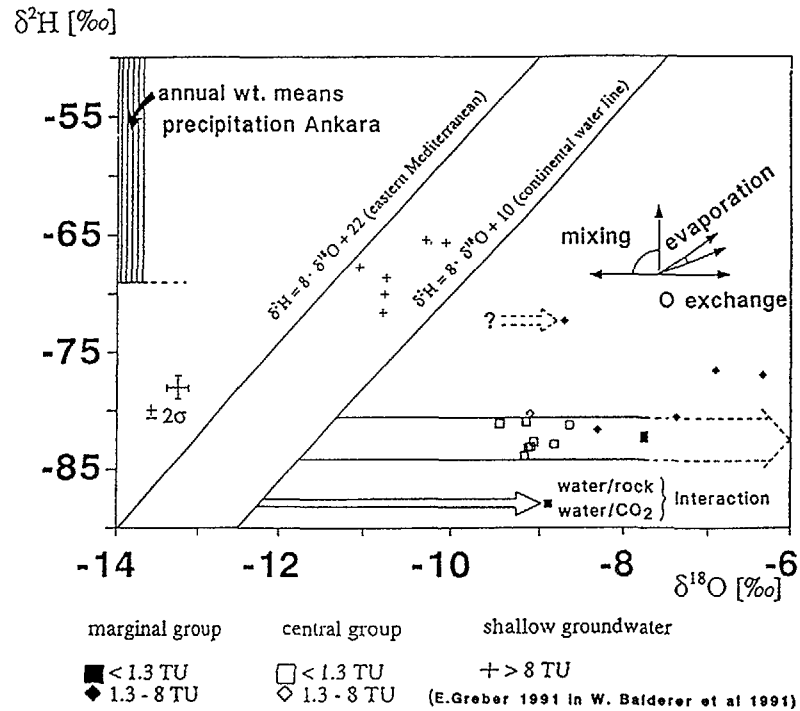


Fig.18:  $\delta^2\text{H}$  versus  $\delta^{18}\text{O}$  diagram of shallow groundwaters, thermal and cold mineral waters of the Kuzuluk/Adapazari area

Additionally the very low  $\delta^2\text{H}$  values of these waters indicate distinct origin not connected with the actual recharge groundwaters. One of the possible explanations could be recharge during a period of cooler climate (e.g. Pleistocene),

#### 4. DISCUSSION OF THE MAIN ASPECTS OF HYDRODYNAMIC INFLUENCES ON GROUNDWATER COMPOSITION AS RESULTING FROM THE PRESENTED STUDY AREAS

In the first presented case study of the **Swiss Molasse Basin** in the same deposits influences of changed climatic and hydrodynamic conditions even in a geological time scale from since Mid Tertiary to today can be observed: (i) in the lowest part a

$\delta^{18}\text{O}$ /dissolved  $\text{CO}_2$  plot ( $\text{CO}_2$  values from field titration), Kuzuluk/Adapazari

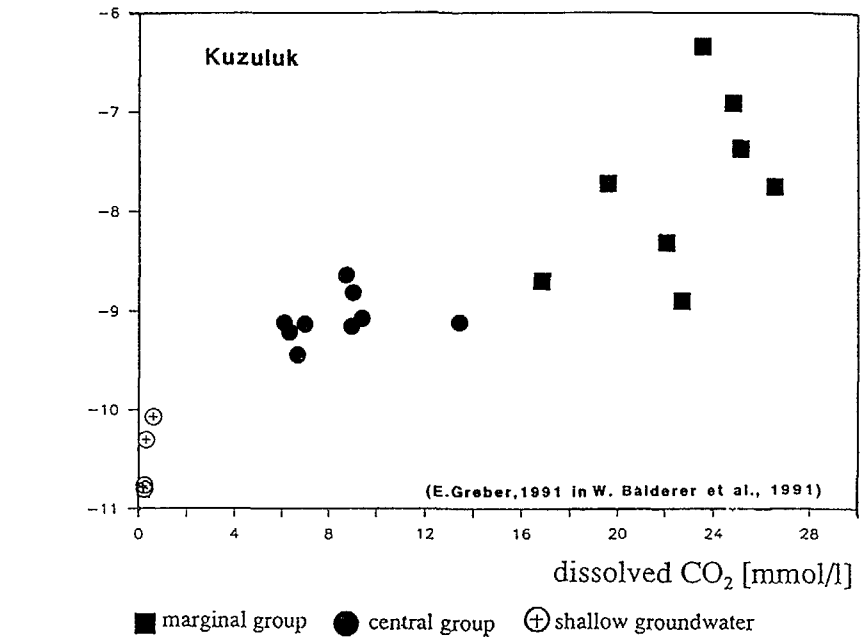


Fig.19:  $\delta^{18}\text{O}$ (water) versus dissolved  $\text{CO}_2$  diagram ( $\text{CO}_2$  values from field titration) of the Kuzuluk/Adapazari area

**Na-Cl- type** water is present which according to the isotopic signatures represents an evolved formation water. (ii) above a density related interface is situated in the upper part a **Na- $\text{HCO}_3$ -type** water of probable origin in the pleistocene time period within regional to intermediate flow systems, and (iii) in the shallower part within local flow systems a water of **Ca-Mg- $\text{HCO}_3$ -type** containing anthropogenic tritium is encountered corresponding to actual recharge conditions. By adopting a model according to the concept of hydrodynamic flow systems the interpretation even of the processes which caused the observed state is possible. (Fig.4 and 7).

In the actual state the recent (post glaciation) water is infiltrating in the recharge area. Due to smaller lateral extent, somewhat faster flow the local flow systems within the shallower morphological part of the deposits contains this recent water.

In the intermediate and regional flow systems the water of the glacial infiltration period (with forced infiltration because of the overpressure effect of the glaciers) is

still present and only partly replaced or mixed within the conjunctive part of the regional discharge zone. The situation is in long term disequilibrium a) with respect to the hydrodynamic state (decrease of hydraulic head, decrease of infiltration rate, reequilibration of the interface causing mixing processes in the regional discharge zones) b) with respect to the information of the water signatures (environmental stable isotopes  $^2\text{H}$  and  $^{18}\text{O}$  serving as natural tracers) the glacial infiltrated water will more and more disappear with time.

In the application of this concept of hydrodynamic flow systems in combination with hydrochemical and isotope methods lies the big advantage for the interpretation with respect to the hydrodynamic conditions. As demonstrated by this example of Northern Switzerland the combined interpretation yields in the reconstruction of a conceptual model of the hydrodynamic flow systems. This conceptual model presents the actual state of the groundwaters within the different flow systems of the investigated area but not only with respect to the chemical properties but also with respect of the water movement itself. It presents the actual situation of the water masses in the underground aquifer system of the given area. It is the state of the flow system representative for the moment of sampling (if it is in steady or insteedy state cannot be judged only by one sampling-) its further evolution -if not in steady state can only be prognosticated in a qualitative way (or by hydrodynamic modeling - if the evolution of the boundary conditions can be estimated from other factors). Normally slow changes can be attributed only as change in recharge, change in abstraction, decrease of hydraulic head. Changes in chemical and/or isotopic composition are only connected with hydrodynamic changes if different water masses are involved or changes in flow velocity will change the mean residence time (e. g. in a karstic aquifer).

In the **Bursa area** the outflowing hot thermal waters can be derived based on the stable isotopes by recharge of precipitation (rain and snow) within two distinct different altitudes ranges on Mount Uludag (and surrounding areas) which evolved in the deeper part of the descending pathways by oxygen isotope exchange as result of the gained higher temperature. This case is well in accordance with the traditional model of regional groundwater flow with the properties needed for geothermal systems: higher heat flow (resp. geothermal gradient) and fast ascendance of the hot fluid by a high conductive regional fault zone (Schindler et al. 1992).

In the **Tuzla - Kestanol area** on the Biga Peninsula the outflowing high concentrated thermal waters can by their chemical and isotopic composition neither directly be derived from infiltrated meteoric water nor from heated sea water. From

the observed chemical and isotopic composition of the water it seems most probable that they are representing mixtures between a deep low mineralized groundwater (containing no anthropogenic produced Tritium) and a deep brine situated as connate water of probable marine origin at even greater depth. The mixed and heated water (also in a region of increased geothermal gradient) is driven to the surface by the buoyancy effect along the hydraulically conductive zones along the intersections of three major fault systems.

For the mineral and thermal waters of the **Kuzuluk** area arising within a topographically well defined subsidence basin are with respect to their stable isotope contents clearly disconnected not only from meteoric waterline showing a marked oxygen shift ( $^{18}\text{O}$ -enrichment probably due to isotope exchange with  $\text{CO}_2$ , Balderer et al., 1991) but also disconnected by their much lower  $\delta^2\text{H}$  values than the local groundwater of recent recharge.

The following different explanations for the origin of this waters are possible (now of big importance for the understanding of the groundwater circulation in this tectonic active area):

(i) the evolution started from normal meteoric water infiltration and in depth within the fault system the waters were heated up and would have undergone oxygen isotope exchange most probably in contact with  $\text{CO}_2$  coming up from depth (Kipfer, 1990, 1991) or produced by thermocatalytic reaction (Wolf et al. 1991) with carbonate rocks in depth (Greber, 1992). If, as usually admitted from experience also in other geothermal areas (Fontes, IAEA ?) no deuterium exchange has to be taken into account, the only explanation for the observed low deuterium contents of these mineral and thermal waters would be that they correspond to the waters infiltrated under different climatic conditions (e.g. the cooler and more humid conditions of the pleistocene epoch).

(ii) The second possibility of also a connection with a process which would lead also to a depletion in the deuterium content e. g. by separation of a steam phase of a deep hot water and condensation in a near surface local meteoric groundwater is unlikely because of the very low tritium contents near or below detection limit. (the oxygen isotope ratio seems in any case to be dominated by the big amount of uprising  $\text{CO}_2$ ).

The now presented isotopic signatures would lead to a conceptual model where a deep seated fluid exist which is disconnected from actual recharge and is outflowing through fractures of the low permeable top layers of volcanic rocks and ignimbrites (Greber, 1992) not because of the usual admitted mechanism of the hydrologic cycle but because of the local tectonic configuration of the pressurizing effect of the uprising  $\text{CO}_2$ . (in the 160 m deep borehole hot thermal water with  $82^\circ\text{C}$  and a hydrostatic

artesian overpressure of 3 bars and additional 2 bars of CO<sub>2</sub> pressure was observed).

In this case not the normal situation of the hydrodynamic flow systems with flow in continuity but the lifting and emptying of a limited reservoir by the effect of upwelling/buoyancy due to the high CO<sub>2</sub>-activity takes place.

## 5. SHORT TERM FLUCTUATIONS, TECTONIC AND SEISMIC INDUCED VARIATIONS: OUTLOOK AND RECOMMENDATIONS FOR FURTHER INVESTIGATIONS

It is now a quite new aspect to investigate the effects of active seismo-tectonic (including volcanic) activity on the groundwater flow and quality (as its chemical and isotopic composition). As such influences are short term perturbations, the possible reactions consists in instationary, extremely time dependent variations, or in abrupt but definitive changes of the observed parameters.

**The most reported known influences of earthquakes on groundwater systems concern changes of the hydrodynamic characteristics** as changes of hydraulic head of wells (mainly artesian) and/or change of flow rate of springs and artesian wells.

For all presented areas such phenomenas are reported:

In **Northern Switzerland** for the thermal spring area of **Baden** (near Zürich) a drop in flow rate was deduced through the analysis of historical records of the periodical flow rate measurements of the observed 18 springs for the **Black Forest** 1901 earthquake by Zorn & Jaffé 1983, and for **Zurzach** strong pressure changes are reported accompaning earthquake events, Aeschbach, pers. comm., 1980.

For the studied areas in **Western Turkey** the following qualitative observations are reported:

For the **Tuzla** area: According to historical records effects of earthquakes as displaced spring sites, but also the disappearance of an ancient geysir (probably caused by a drop in the hydraulic pressure head) in the Tuzla canyon were reported in Mützenberg 1990, for a place where today only some low outflowing hot springs remained.

For the **Bursa** area: No direct information on influences of earthquakes available but most probably influence on hydraulic head and flow rate as spring have displaced downward from the upmost part of ancient occurrence on the hillslope of Mount Uludag more to the valley plain (Imbach, 1992).

For the **Kuzuluk** area: From historical records it is known that ancient spring sites as used for thermal spas have disappeared (as the springs dried up completely) after

strong earthquakes events, respectively were displaced as evidenced by thermal springs yielding at new locations. In the old spa area some zones of high CO<sub>2</sub> emanations have been detected by E. Greber through soil gas measurements (Greber, 1992).

## 5.1 FACTORS OF POSSIBLE INFLUENCE ON CHANGES OF THE GROUNDWATER COMPOSITION

**Short term fluctuations of chemical and isotopic composition of groundwater** other than the well known influence of changing recharge conditions (e.g. due to precipitation events) on shallow groundwater systems as observed in e.g. karstic springs are not yet frequently enough observed. (Imbach 1992, even reports influences of a strong storm event in November 1989 on the conductivity of the thermal waters of the Bursa area which contain no anthropogenic tritium).

But what are the factors that could probably influence or even cause such changes of the composition of the groundwater?

The following factors may influence such phenomenas:

**Constitution of the aquifer rock itself:** Heterogeneous media of secondary (or even so-called double) porosity as especially fractured rocks which are heterogeneous and anisotropic. Relatively small volumes of water are stored within such a rock mass of relatively low average permeability but also uneven distributed within thin spaces e.g. of fracture zones of high hydraulic conductivity.

The generally very low flow velocity of the groundwater in such a rock mass (what means high residence time) favours the individual evolution by water rock interaction leading to a differentiation and therefore also a heterogeneity of the water composition (if not overcome by mixing processes as result of higher flow rates as induced by increased gradients of hydraulic head or pressure).

Heterogeneity also of the **mineralogical - geochemical including isotopic composition of the the rock mass** (e.g. through fracture infillings, through crossing dykes and or hydrothermal veins, e.g. quartz veins, alterations and tectonic shear-, fault- and fracture zones) may further favourite such a differentiation with respect to the resulting water composition.

But all the now mentioned factors only give the necessary predisposition (disponibility) for a sensitive reaction of a aquifer system to the internally or externally caused influences of seismo-tectonic events resulting in short term fluctuations of chemical and isotopic composition of groundwater at a given outflow point.

Furthermore the influences caused by seismo-tectonic events could even mobilize **deep seated fluids** of higher mineralisation and also lead to a addition (injection) of fluids of different origin (e.g. preserved within fluid inclusions over geological time periods or coming from earth interior or of deeper rock masses as thermometamorphic or even magmatic fluids and gases)

Besides the water - rock interaction processes the most probable influence could be exercised by the gases of deep origin. The isotopic composition of each element in gases as  $\text{CO}_2$ ,  $\text{H}_2\text{S}$ ,  $\text{H}_2$ ,  $\text{CH}_4$  are key parameters for the understanding of reactions between fluid phase and gas phase. Then the water in tectonic active areas as in geothermal areas is not longer a water in the sense of pure or mainly meteoric origin but a fluid that contains components which are derived from different reservoirs by different processes and which even may vary in space and time (Balderer & Martinelli, 1992, in prep.)

## 5.2 SENSITIVE PARAMETERS OF SEISMO TECTONIC INDUCED ACTIVITY

But which parameters seem to be promising in reflecting such phenomena? From the above presented approach with respect to isotope and hydrochemical methods the following choice of parameters results

**Evolution specific parameters** Oxygen-18, Deuterium, Carbon-13, chemical and isotope geothermometers (which have to be considered against the natural imprint of the water cycle), changing chemical properties

**Formation specific parameters** (by water/rock interaction and underground processes) Mineral and reaction specific isotopes as  $^{34}\text{S}$  and  $^{18}\text{O}$  in  $\text{SO}_4$  (with respect to minerals, fluid inclusions),  $^{87}\text{Sr}/^{86}\text{Sr}$ ,  $^{35}\text{Cl}/^{37}\text{Cl}$ , etc

**Parameters reflecting the conditions of recharge** infiltration specific parameters as stable isotopes  $^2\text{H}$  and  $^{18}\text{O}$  and atmospheric noble gases

**Process indicating parameters** (including residence time, underground production) radioisotopes e.g.  $^3\text{H}$ ,  $^{14}\text{C}$ ,  $^{39}\text{Ar}$ ,  $^{36}\text{Cl}$ ,  $^{234}\text{U}/^{238}\text{U}$ ,  $^3\text{He}$ ,  $^4\text{He}$ ,  $^{222}\text{Rn}$ , etc

**Indicators of open-/closed- system behaviour:** as reactive and noble gases and their isotopic composition, e.g.  $\text{CH}_4$ ,  $\text{CO}_2$ ,  $\text{H}_2\text{S}$ ,  $\text{NH}_3$ ,  $\text{N}_2$ ,  $\text{Ar}$ ,  $^3\text{He}$ ,  $^4\text{He}$ ,  $^{20}\text{Ne}/^{21}\text{Ne}$ ,  $^{40}\text{Ar}/^{36}\text{Ar}$  etc

## 5.3 POSSIBLE SELECTION OF PARAMETERS FOR CONTINUOUS RECORDING

In order to depict such kind of non systematic and random variations a continuous recording of the parameters to be observed is necessary. For this purpose for the **Kuzuluk** area the following approach is used

-Continuous recording of the hydraulic head of two artesian wells with electrical pressure transducers simultaneously with a seismometer signal

Such a station is already installed and working since spring 1991 at the Kuzuluk site

-As a further step the installation of a station for observations of chemical and physical parameters of the water as electrical conductivity, temperature, eventually also including pH and  $\text{CO}_2$  flux is planned within the **Bursa** area (in the same area a network of microseismic survey was installed within the framework of the coordinated interdisciplinary ETH / ITU Marmara-project in spring 1992, Schundler et al 1992)

## 6 GENERAL CONCLUSIONS AND RECOMMENDATIONS

-Case studies can help for the general understanding of chemical processes of interaction between water, rock and gases

-In further studies all available isotope methods should be applied in order to understand better the meaning of processes and reactions e.g. exchange, isotope-fractionation, mixing, dissolution, precipitation

-Especially new methods as  $^{36}\text{Cl}$ , ev  $^{13}\text{C}$  and  $^{14}\text{C}$  on organic carbon but also more isotope determinations of all elements in gases as  $\text{CO}_2$ ,  $\text{H}_2\text{S}$ ,  $\text{H}_2$ ,  $\text{CH}_4$  should be made because they represent the key parameters for the understanding of reactions between solid phase, fluid phase and gas phase

-The groundwater should in tectonic active areas as in geothermal areas no longer be considered as representing a "normal" water in the sense of pure or mainly meteoric origin within the hydrological cycle but as a fluid that contains components which are derived from different reservoirs by different processes and which even may vary in space and time (Balderer & Martinelli, 1992, in prep.)

In the interpretation of data from stations for continuous recording one has not only to look for and to observe peaks but they have to be related to real processes. Only if anomalies can be explained by real processes one can use the selected methods to try to get a prediction of somewhat related phenomena as earthquakes or volcanic eruptions

-For each region affected by tectonic activity as by earthquakes (or volcanic eruptions) one has therefore first to establish a) the geological, tectonic and hydrogeological situation, b) the state of existing hydrochemical and isotopic properties of groundwaters, rocks (minerals) and gases and to understand the interaction and processes (including the hydrodynamic situation, with respect to flow systems and boundary conditions) and c) based on this whole interpretation try to isolate the most probable sensitive indicators before one can start to explain short term variations of some kind of constituents

Especially for isotope and hydrochemical methods which are dependent on well known reactions and processes one should try to understand this informations and not only to be fixed to enregister and interpret variations in a statistical way only

#### REFERENCES

- Balderer, W, 1983 Bedeutung der Isotopenmethoden bei der hydrogeologischen Charakterisierung potentieller Standorte für hochradioaktive Abfälle -Nagra Techn Bericht NTB83-04, Dezember 1983, Nagra, Baden
- Balderer, W, 1984 To the concept of interpretation of the results of isotope and hydrochemical determinations for the definition and characterisation of the natural conditions in geological formations Bull du Centre d'Hydrogéologie, No 5, University of Neuchâtel, Switzerland
- Balderer, W (1985) Sondierbohrung Bottstein Ergebnisse der Isotopenuntersuchungen zur hydrogeologischen Charakterisierung der Tiefengrundwasser NTB 85-06, Nagra, Baden, Switzerland
- Balderer, W (1985) The Nagra Investigation Project for the Assessment of Repositories for High-Level Radioactive Waste in Geological Formations Mineralogical Magazine, April 1985, Vol 49, pp 281-288
- Balderer, W (1986) Signification de l'âge moyen de l'eau souterraine donné par les isotopes radioactifs Bull du Centre d'Hydrogéologie, No 6, Université de Neuchâtel, Suisse
- Balderer, W (1989) Hydrochemie der Quellen der Oberen Süsswassermolasse im Einzugsgebiet des Aubaches (Schweiz) Steir Beitr z Hydrogeologie, Nr 40, S 49-74, Graz, 1989
- Balderer, W, 1990 Hydrogeologische Charakterisierung der Grundwasservorkommen innerhalb der Molasse der Nordostschweiz aufgrund von Hydrochemischen und Isotopenuntersuchungen Steir Beitr z Hydrogeologie, Nr 41, S 49-74 Graz 1990
- Balderer, W 1990 Paleoclimatic Trends deduced in Groundwaters within Swiss Molasse Basin as Evidence for the Flow Systems Definition Mem 22nd Cong IAH, Vol XXII, pp 731 740, Lausanne, 1990
- Balderer, W, 1990 Past and Future Evolution of Flow systems as Response to Changing Climatic Conditions and Anthropogenic Influences Mem 22nd Cong IAH Vol XXII pp 741 750 Lausanne 1990
- Balderer W Greber E, Imbach, Th Rauert W, Trimborn P, Guler, S, 1991 Environmental Isotope Study of Thermal- Mineral and Normal Groundwater within the Bursa and Kuzuluk/Adapazarı Area North Western Turkey IAEA-SM 319/52P International Atomic Energy Agency, IAEA, Vienna, Austria
- Balderer, W, & Martinelli, G (1992) Environmental and hydrochemical study of the mineral-, thermal- and normal groundwaters in the area affected by the Campania Basilicata earthquake of 23 November 1980, in prep
- Bertleff B W, Goldbrunner, J E, Stuchler, W, Andrews, J N, Darling, G, 1987 Characterisation of Deep Groundwater in South Germany and Upper Austria by means of Isotopic and Hydrochemical Investigations IAEA SM-299/8P, International Atomic Energy Agency, IAEA, Vienna, Austria
- Clayton R N et al 1966 J Geophys Res 71/6
- Ghyben, B W, 1889 Nota in verband met de vorgenommen put boring nabij Amsterdam - Kunst Inst Ing Tijdschrift, Den Haag, 21 pp
- Greber, E, 1992 Das Geothermalfeld von Kuzuluk / Adapazarı (NW-Turkeı) Geologie, aktive Tektonik, Hydrochemie, Isotope und Gase Diss ETH-Zurich, im Druck
- Herzberg A, 1901 Die Wasserversorgung einiger Nordseebäder - Journ Gasbeleuchtung und Wasserversorgung, Vol 44, 815-819
- Hubbert, M K, 1940 Theory of ground-water motion Journ of Geology, Vol 48, Nr 8, pp 785-944
- Imbach, Th, 1992 Geologie, aktive Tektonik, Hydrochemie, Isotope und Gase der Bursa Region (NW-Turkeı) Diss ETH Zurich, im Druck
- Imbach, Th and Balderer, W, 1990 Environmental hydrogeology of a karstic system with thermal and normal groundwaters Examples from the Bursa Region (Turkey) Proc Int Symp and Field Seminar on Hydrogeological Processes in Karstic Terranes, 7-17 October 1990 Antalya, Turkey,
- Kharaka Y K and Carothers W W 1986 In Handbook of Environmental Isotope Geochemistry vol 2 (Fritz, P, Fontes, J Ch, Eds), Elsevier, Amsterdam

Karamandereci M 1987 Hydrothermal alteration in well Tuzla T-2, Canakkale, Turkey MTA Internal Report, Izmir

Kipfer, 1991 Primordiale Edelgase als Tracer für Fluide aus dem Erdmantel Diss ETH Nr 9463, Zurich

Mutzenberg, S, 1989 Westliche Biga - Halbinsel Geologie, Tektonik und Thermalquellen (Canakkale,Turkey) Mitt Geol Inst der ETH und der Universität Zurich Nr 287

Mutzenberg, S Balderer W, and Rauert W 1992 Environmental Isotope Study of Saline Geothermal Systems in Western Anatolia (Canakkale Turkey) Proc of the 7th International Symposium on Water Rock Interaction, Park City, Utah AA Balkema publishers Rotterdam, Netherlands

Pearson, FJ, Balderer, W, Loosli, H H, Lehmann, B E, Matter, A, Peters, Tj, Schmassmann, H, Gautschi, A (1990) Applied Isotope Hydrogeology - A Case Study in Northern Switzerland In Studies in Environmental Science 43, ELSEVIER, Amsterdam, Oxford, New York, Tokyo 1991, 439 p

Pezdic, J, Dolenc, T, Zizek, D, Fritz, P, Wolf, M, 1991 Origin and Transport of CO<sub>2</sub> in the highly mineralized water system of the Pannonian Tertiary Basin (Northeast Slovenia) IAEA-SM-319/58P, International Atomic Energy Agency, IAEA, Vienna, Austria

Savin S 1980 In Handbook of Environmental Isotope Geochemistry vol 1 (Fritz, P, Fontes, J Ch, Eds), Elsevier, Amsterdam,

Schindler, C, Balderer, W, Greber, E, Imbach, Kahle, H G, Marti, U, Straub, C, Aksoy, A, Rybach, L, Pfister, M, Pavoni, N, Mayer-Rosa, D, 1992 The MARMARA Poly-Project Tectonics and recent Crustal Movements Revealed by Space-Geodesy and Their Interaction with the Circulation of Groundwater, Heat Flow and Seismicity in Northwestern Turkey Terra Nova, in press

Schmassmann, H, Balderer, W, Kanz, W, & Pekdeger, A (1984) Beschaffenheit der Tiefengrundwasser in der zentralen Nordschweiz und angrenzenden Gebieten Nagra Technischer Bericht NTB 84-21, Nagra, Baden

Schmassmann, H, 1990 Hydrochemisch Synthese Nordschweiz Tertiär und Malm-Aquifere Nagra Technischer Bericht NTB 88-07, Nagra, Baden

Sieber, N, 1988 Geothermie Bohrung Hohstrasse Kloten-Geol u Hydrogeol Gutachten, unveroff

TOTH, J, 1962 A theory of groundwater motion in small drainage basins in Central Alberta, Canada -Journ of Geophys Res, 67/11,4375-4387

TOTH, J, 1963 A theoretical analysis of groundwater flow in small drainage basins Journ of Geophys Res 68/16,4795-4812

Yurur, T 1985 Diploma thesis ITU, Istanbul

Zorn, A H & Jaffé, F C, 1983 Les variations du débit des sources thermales de Baden (Canton d'Argovie, Suisse) Eclogae Geol Helv Vol 76/2 pp 451-463 Bâle, Suisse

## PRINCIPLES AND METHODS OF VOLCANIC SURVEILLANCE: THE CASE OF VULCANO, ITALY

P.M. NUCCIO

Istituto di Mineralogia, Petrografia e Geochimica,  
Università di Palermo

M. VALENZA

Istituto di Geochimica dei Fluidi (CNR)

Palermo, Italy

### Abstract

This paper is the report presented at the Advisory Group Meeting on the Isotopic and Geochemical Precursors of Earthquakes and Volcanic Eruptions, held from 9 to 12 September 1991 at International Atomic Energy Agency Headquarters in Vienna.

The historical developments of the volcanic surveillance principles, from the empirical identification of a single precursor to the more organic modelistic approaches, are briefly reported. Geochemical methods are reviewed, the volcanic surveillance executed on the Vulcano island is illustrated and the main results reported.

### 1. Introduction

Over the past twenty years man's attitude towards natural calamities has changed considerably. In fact today the idea that the catastrophic consequences of these events can be reduced both by taking precautionary measures and by predicting the events themselves has become a common conviction.

Although there is no appreciable difference in the natural processes that lead to violent eruptions, the consequences can either be negligible or catastrophic depending on the level of urbanization of the area where the eruption occurs.

The notion of volcanic risk has contributed considerably to the rationalization of man's actions in reducing the damages caused by a volcanic eruption.

In fact today competent volcanic surveillance can appreciably mitigate volcanic risk.

Volcanic surveillance is the monitoring of a volcanic system with the aim of evaluating its state of activity so as to be able to estimate whether a volcanic event will occur.

The most important aspects obviously are on one hand the principles and method of volcanic surveillance which determine its correct planning, on the other the technological aspects which increase its reliability.

### 2. Principles on which volcanic surveillance is based

A volcanic eruption is preceded and accompanied by the upward movement of a magmatic mass and by the transfer of fluids and energy towards the surface. Both phreatic explosions and the release of dangerous gases are generally linked to volcanic processes and, although these phenomena do not necessarily imply a magma movement, they are also related to the transfer of fluids towards the surface. These movements cause chemical and physical changes very deep down, which can be recognised at the surface under the form of more or less direct *indicators*.

These *indicators*, once they have been recognised as such, are usually classified as precursors. However the precursors do not always give univocal indications because their sequence in time, their amplitude and their early appearance can assume values and meanings which differ from volcano to volcano, from event to event, and even from one moment to the next during the evolution of an event of one single volcano.

The meaning of precursor is absolutely empirical.

Although some *indicators* or variations habitually precede volcanic events, in actual fact there is no such thing as the *precursor*.

*When possible the variations observed on the surface must be deciphered one by one and interpreted as a whole in a logical sequence: a model.*

The more a model is bound by scientific laws the more the interpretation of the *indicators* will be less ambiguous.

A typical problem that one meets when using this kind of approach is that more than forming a model one tends to explain a set of observations.

In this case it is more practical to group together the various possible models in function of the consequences which would arise so as to be able to evaluate the level of the volcanic activity.

At the same time it is worthwhile selecting the parameters that enable us to evaluate the consistency of the various models.

It is, however, relatively obvious that the higher the number of parameters there are to be considered, the fewer the number of possible models there will be.



Very often work programmes which are formulated lead one to obtain data regarding parameters which could potentially supply indications useful to the selection and better definition of the model. With this in my mind it would be appropriate to apply the principle of *primary process to be kept as simple as possible* although the laws governing it are certainly more or less complex. A model complicated by *ad hoc* processes, having the sole aim of justifying a set of *anomalous* values of a few parameters, is to be considered suspect.

### 3.1 Volcanic surveillance

Although surveillance methods must be supported by a good basis of Volcanology and Petrology they are essentially based on:

- Geophysics;
- Geochemistry.

Obviously good surveillance requires the maximum integration of these methods so as to obtain the most complete monitoring possible. Putting aside the geophysical methods, we will briefly examine the geochemical ones.

### 3.2 Geochemical methods

The basic knowledge of the volcanic system being studied comes from

- History of its past and recent activity;- Surveying and sampling of the surface manifestations;
- Analysis and classification of the latter;
- Preliminary model of the circulation of the fluids;
- Selection of observation points;
- Selection of parameters to be monitored.

### 4.1 Surveillance planning

All the resources available for the surveillance (financial, level of specialisation, number of operators etc.) must be carefully distributed and organised so as to acquire as much useful information possible so as to be able to recognise and monitor the "indicators" coming from deep down.

It is therefore necessary to plan the surveillance so as to be able to select the areas and the parameters to be monitored.

One of the more notable aspects of volcanic surveillance, which differs from that of other scientific researches, is that it is particularly interested in acquiring data regarding the relative variations in time of a given parameter, rather than acquiring extremely accurate data giving only a few values.

An important criterion in the choice of frequency of the sampling operations develops from the following requirement: the sampling frequency must be effected in relation to the frequency of the expected variations of each parameter. Obtaining *on-line* parameters gives a rapid up-date of the situation and allows the evolution of the activity to be followed in real-time.

Anyway the parameters obtained *on-line* generally give basic information regarding current changes taking place deep down and should therefore be followed by measurements of other parameters so as to obtain a complete picture of the changes themselves as quickly as possible.

### 4.2 Intensive and extensive parameters

Apart from recognising the parameters, the modellistic approach aims at interpreting the modifications taking place in the volcanic system.

Researchers' particular interest is generally placed either on evaluating the variations in temperature and pressure occurring deep down, or evaluating the higher magmatic contribution of the gases reaching the surface.

These interests derive from the worry that an accumulation of pressure could cause a freatic explosion or that an increase in the magmatic component could indicate that the magma itself is rising. However at present the current methods used (i.e. evaluation of the variations in the concentration of the chemical components and of their isotopic ratios in both gases and waters) are inadequate. For example, geothermometry and geobarometry are currently applied in geochemical surveillance. Even though evidences of pressure build-up of the fluids can give a good indication of an impending explosion, the information would certainly be more complete if the variations in the energetic output were evaluated and the accumulation of energy deep down estimated. Furthermore, as pointed out by Italiano and Nuccio (1992), any interpretation of the observed variations which is solely based on intensive parameters will be ambiguous and will have a high possibility of being inaccurate if the quantitative variations are not taken into consideration by acquiring extensive values (output of the same components).

### 5.1 Surveillance of Vulcano island

The island of Vulcano is situated in the Aeolian archipelago (Italy). In the past, its volcanic activity was well known and many myths regarding the island were transmitted by ancient races. There are historical reports on its volcanic activity dating back to the 4th century A.C.

A summary was reported in Fustaino (1981) and De Fiore (1925), while the volcanological evolution of the island was published by Keller (1980) and more recently by Frazzetta et al. (1988).

The typically *vulcanian* eruptive activity (Mercalli e Silvestri, 1891) is characterised by explosions when lava rocks, bombs, sand and cinder are launched. Following the last eruption, which took place between 1888 and 1890, the activity on the island has been limited to fumarolic emissions and thermal manifestations on the plain surrounding the active edifice.

Over this century the fumarolic activity has varied somewhat, and was particularly accentuated about 1923 when the temperature of the gas reached 613°C. (fig.1)(Sicardi, 1940).

Over the past twenty years the island has undergone an intense urbanization, which is particularly concentrated at the foot of the edifice of the active volcano. Therefore, when in 1977 the temperature of the fumarolic gas increased from 190 to 280°C, a volcanic surveillance programme was developed.

The surveillance of the activity of Vulcano is effected by various research groups, that are coordinated by G.N.V. (the National Group for Volcanology).

The geophysical surveillance is effected by permanent and mobile seismic systems; measurements of the deformation of the ground are effected by using tiltmeters, trilaterations and levellings.

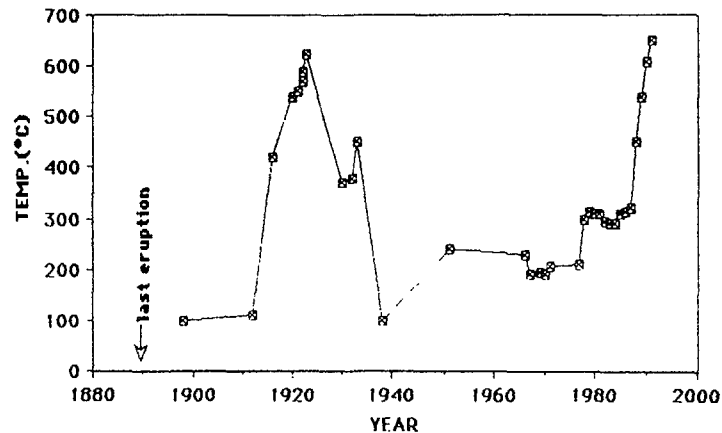


Figure 1. Historical record of the maximum temperature of the fumarolic gases.

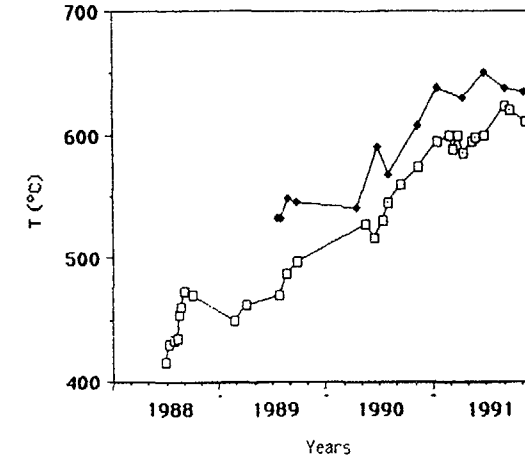


Figure 2. Evolution of the temperature in the crater fumarole FA and FF.

Other measured parameters are generally gravity, and differential magnetometry. Our group is formed by researchers from both the Istituto di Geochimica dei Fluidi of the C.N.R. and the Istituto di Mineralogia, Petrografia e Geochimica of the University of Palermo, who are in the process of performing the following programme of geochemical surveillance.

## 5.2 Intensive parameters

Gas and water sampling is generally carried out monthly, but its frequency is adjusted according to the evolution of the volcanic activity.

- Temperature survey of the fumaroles of the crater (fig. 2);
- Chemical composition of the fumarolic gases of both crater and seaside areas (fig. 3, 4), 1-4 times a month (Badalamenti et al., 1988; Italiano and Nuccio, 1991);
- Chemical and physical parameters of thermal well waters (fig. 5) (Capasso et al., 1989, 1991; Dongarra' et al., 1988);
- Soil gas concentrations ( $\text{CO}_2$ , He and Rn), in the area of Vulcano Porto (fig. 6);
- The following isotopic compositions are also determined:

$\delta\text{D}$  and  $\delta^{18}\text{O}$  in waters and condensates (fig. 7-9) (Carapezza et al., 1983; Carapezza et al., 1988; Capasso et al., 1992);  $\delta^{13}\text{C}$  and  $\delta^{18}\text{O}$  of  $\text{CO}_2$  (Badalamenti et al., 1984; Cannata et al., 1988);  $^3\text{He}/^4\text{He}$  ratio (Sano et al., 1989);

- General survey of underwater exhalations along the coast down to a depth of about 1000 metres (Italiano et al., 1991) (1-3 times a year).

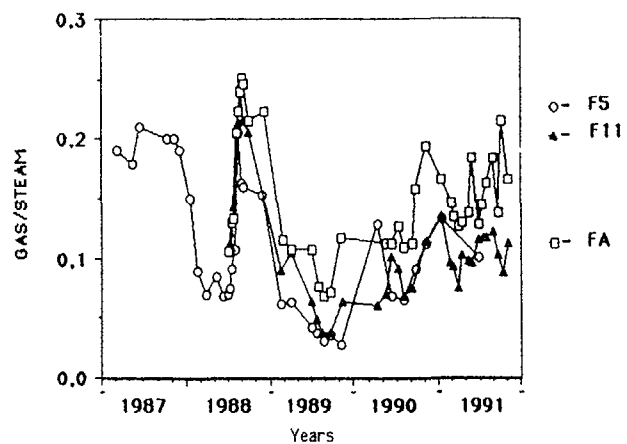


Figure 3 Variation in time of the gas/steam ratio in the fumarolic gases

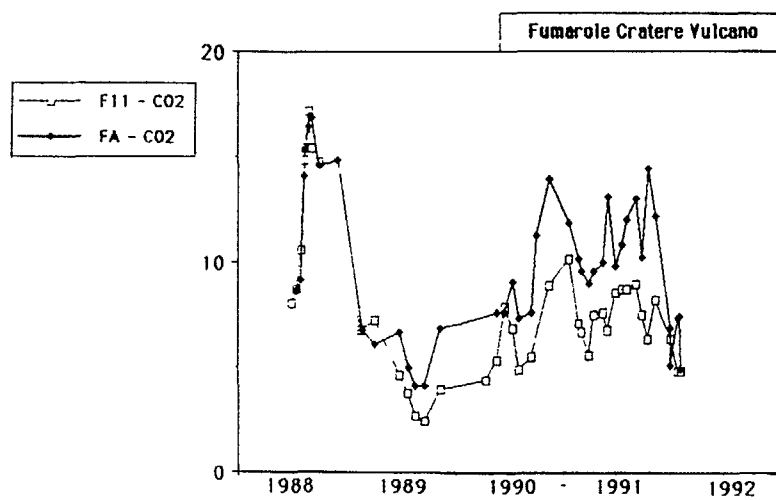


Figure 4 Variation in time of the  $\text{CO}_2$  concentration in fumaroles FA and F11

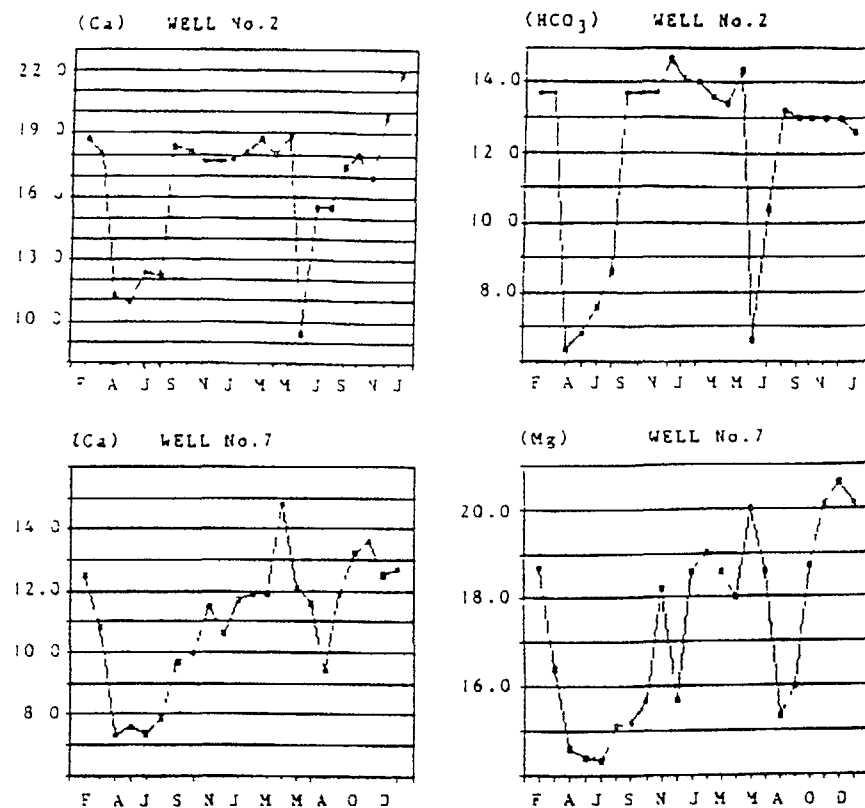


Figure 5 Variations of some chemical parameters of waters in the wells of Vulcano Porto

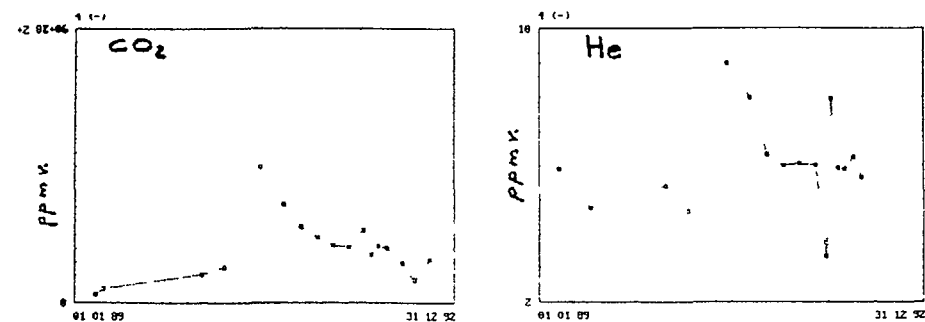


Figure 6 Variations in time of  $\text{CO}_2$  and He concentrations at the sampling point n 4 in soils of Vulcano Porto

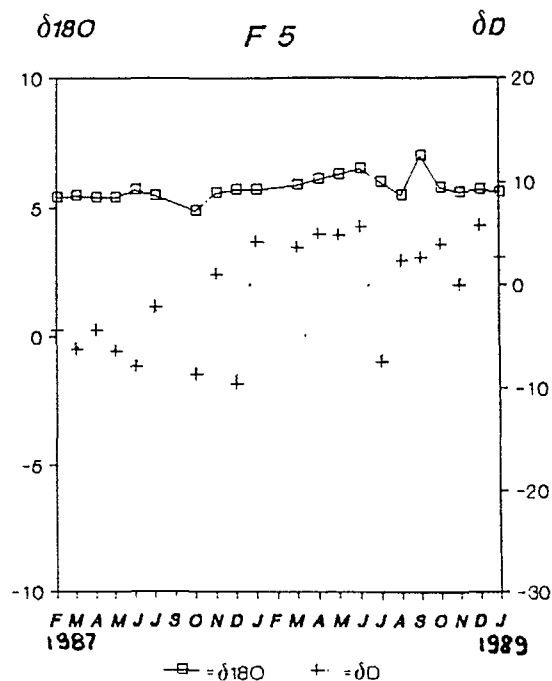


Figure 7. Variation in time of  $\delta^{18}\text{O}$  (square symbols) and  $\delta\text{D}$  (+) in the crater fumarole F5 (After Capasso et. al. 1992).

### 5.3 Extensive parametres

- Output of steam and of the other fumarolic components (Italiano et al., 1984; Italiano and Nuccio, 1992), in the crater area (2-3 times a year) (fig.9);
- Outputs of  $\text{CO}_2$  and steam from underwater fumaroles of Acque Calde (1-3 times a year);
- Convective thermal energy output (Italiano and Nuccio, 1992) (2-3 times a year);
- $\text{CO}_2$  fluxes from the soil, in the area of Vulcano Porto (Gurrieri and Valenza, 1988; Badalamanti et al., 1988; Badalamenti et al., 1991a,b) (monthly) (fig.10).

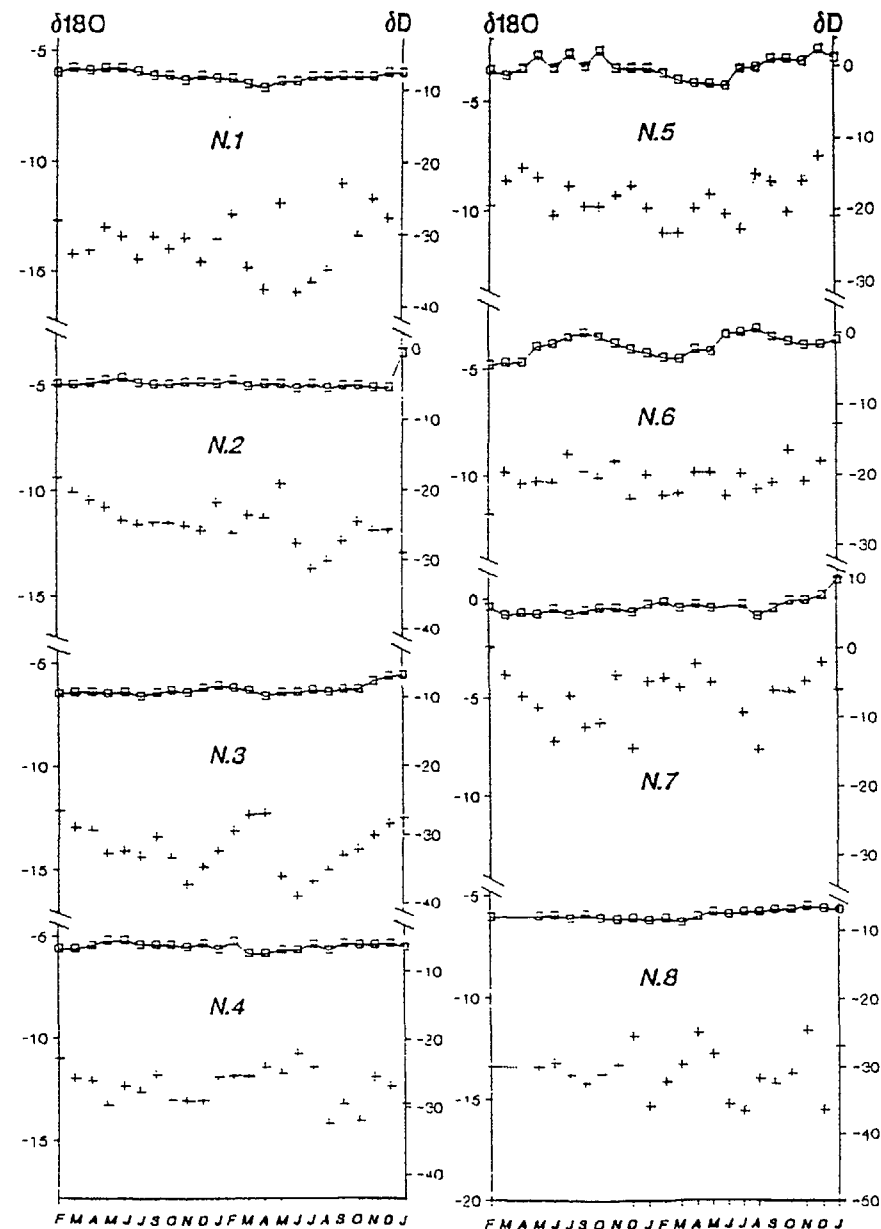


Figure 8. Variation in time of  $\delta^{18}\text{O}$  (squares) and  $\delta\text{D}$  (+) in some wells of Vulcano Porto (After Capasso et al., 1991)

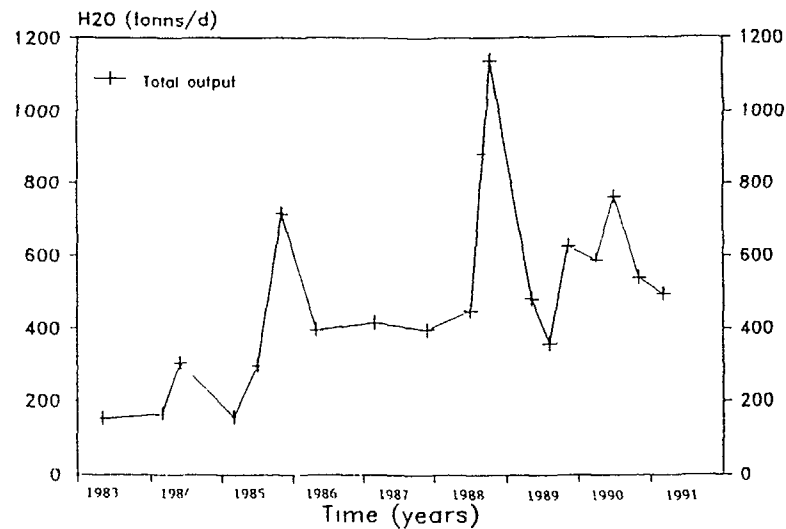


Figure 9 Steam output from the crater fumaroles of Vulcano island

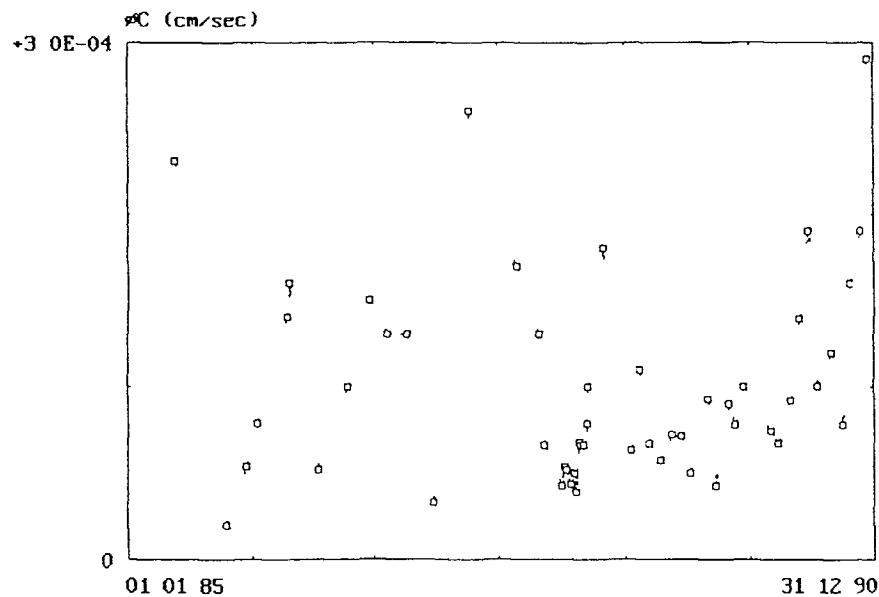


Figure 10 CO<sub>2</sub> fluxes from soils of Vulcano Porto measured during years 1985-1990

#### 5.4 On-line parameters

- Temperatures of selected fumaroles (crater and seaside of Vulcano, and caoline quarry fumaroles of Lipari),
- Reducing Capacity of fumarolic gases (crater and seaside fumaroles of Vulcano, and Caoline quarry fumaroles of Lipari) (fig 11),

CO<sub>2</sub> concentration in the atmosphere of the village of Vulcano Porto (Badalamenti et al 1991b),

CO<sub>2</sub> fluxes from the soil in selected sites of the Vulcano Porto area (Gurrieri et al, 1988, Badalamenti et al, 1991a,b),

- Radon in the soils

#### 6. Results

The first results initially lead us to formulate a geochemical model regarding the genesis of the fumaroles and the geothermal circulation of Vulcano (Carapezza et al, 1981)

The existence of a small geothermal liquid-vapor reservoir at a depth of 1-2 Km. was stated (Italiano et al, 1984) According to the same authors the reservoir was

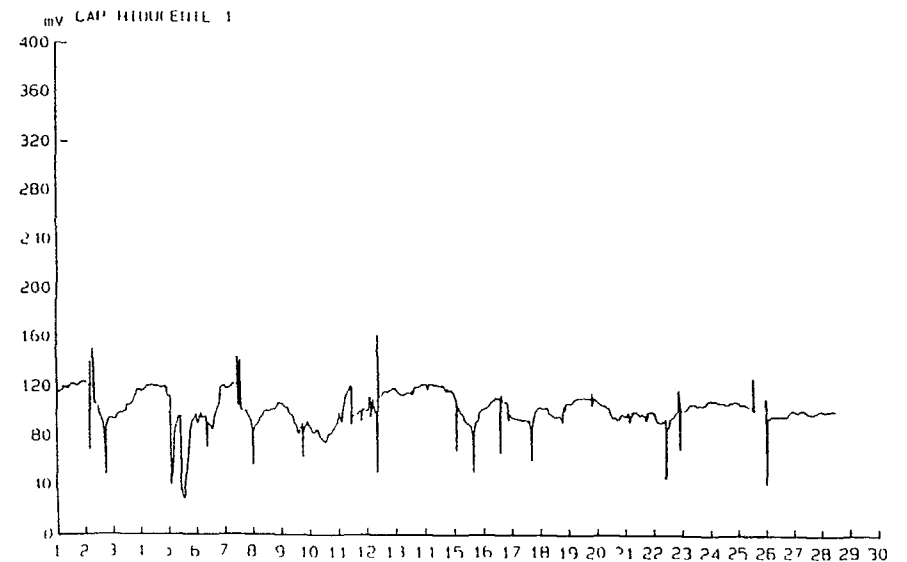


Figure 11 Reducing Capacity of fumarolic gases monitored on line

able to evolve towards a vapor monophasic system, as a consequence of an increased input of thermal energy from the depth.

Over the past ten years Vulcano has undergone several important evolutions which occurred in 1985, in 1988 and from 1990 to date.

Nuccio and Valenza (1990a), on the basis of a theoretical analysis of magma degassing processes, proposed a new model and then interpreted the observed geochemical variations as being the consequence of magma ascent for about one hundred metres (Nuccio and Valenza, 1990b).

### References

Badalamenti B., Gurrieri S., Hauser S., Tonani F., Valenza M. (1984). Considerazioni sulla concentrazione e sulla composizione isotopica della CO<sub>2</sub> presente nelle manifestazioni naturali e nell'atmosfera dell'isola di Vulcano. *Rend. Soc. It. Mineral. Petrol.*, 39, 367-375.

Badalamenti B., Gurrieri S., Hauser S., Parelo F., Valenza M., (1988). Ground CO<sub>2</sub> output in the island of Vulcano during the period 1984-1988 : gas hazard and volcanic activity surveillance implications. *Rend. Soc. It. Mineral. Petrol.*, 43, 893-899.

Badalamenti B., Gurrieri S., Hauser S., Parelo F., Valenza F., (1991a). change in the soil CO<sub>2</sub> output at Vulcano Island during the summer 1988. *Acta Vulcanol.*, 1, 219-222.

Badalamenti B., Gurrieri S., Nuccio P.M., Valenza M., (1991b). Gas hazard on Vulcano island. *Nature*, 350, 7 March 1991, 26-27.

Badalamenti B., Chiodini G., Cioni R., Favara R., Francofonte S., Gurrieri S., Hauser S., Inguaggiato S., Italiano F., Magro G., Nuccio P.M., Parelo F., Pennisi M., Romeo L., Russo M., Sortino F., Valenza M., Vurro F., (1991). Special field Workshop at Vulcano (Aeolian Islands) during summer 1988: geochemical results. *Acta Vulcanol.*, 1, 223-228.

Badalamenti B., Gurrieri S., Hauser S., Parelo F., Valenza M., (1991). Change in the soil CO<sub>2</sub> output at Vulcano island during the summer 1988. *Acta Vulcanol.*, 1, 219-222.

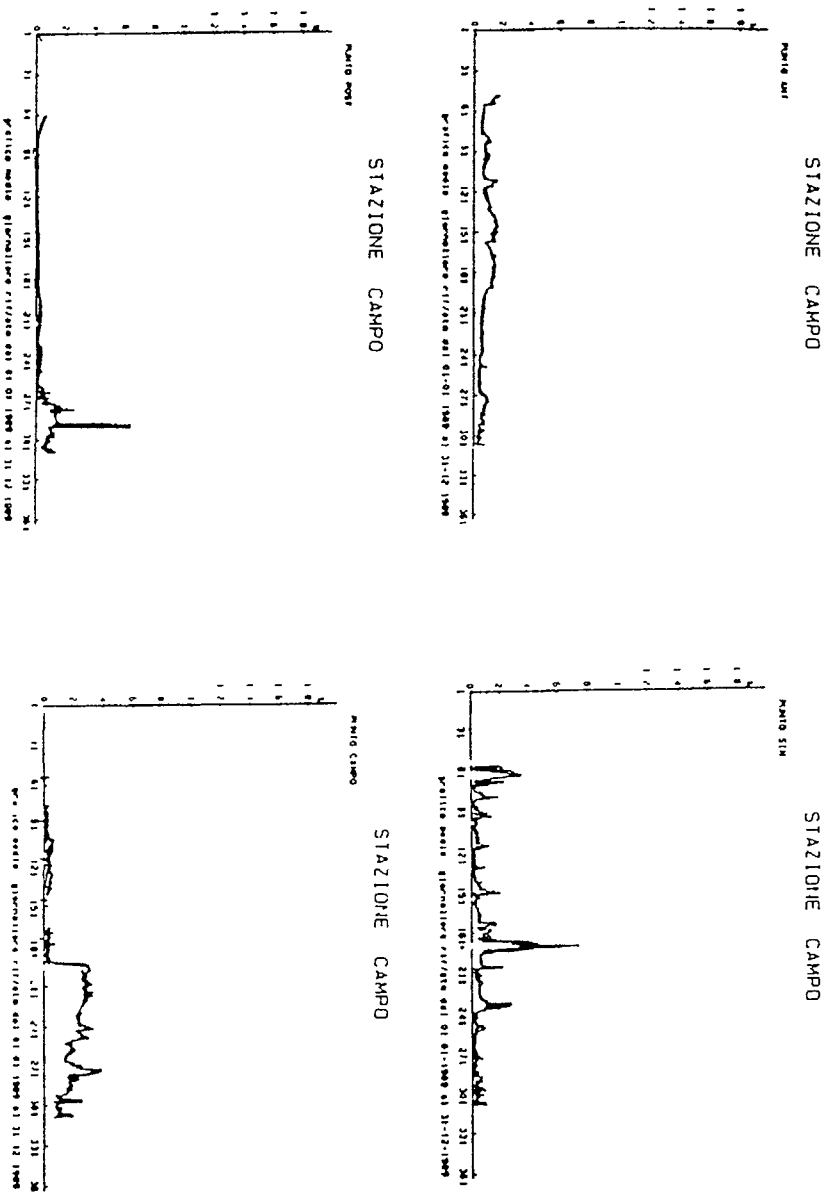


Figure 12. On - line monitoring of the dynamic concentrations of CO<sub>2</sub> in the soils of Vulcano Porto

Cannata S., Hauser S., Parelo F., Valenza M., (1988). Caratterizzazione isotopica della CO<sub>2</sub>, presente nelle manifestazioni gassose dell'isola di Vulcano. Rend. Soc. It. Mineral. Petrol, 43, 153-161.

Capasso G., Dongarra' G., Favara R., Hauser S., Valenza M., (1991). Chemical changes in waters from Vulcano island: an update. Acta Vulcanol., 1, 199-210.

Capasso G., Dongarra' G., Favara R., Hauser S., Valenza M., (1992). Isotope composition of rain water and fumarole steam on the island of Vulcano. J.V.G.R., in press.

Carapezza M., Dongarra' G., Hauser S. and Longinelli A., (1983). Preliminary isotopic investigation on thermal waters from Vulcano island. Italy. Mineral. Petrogr. Acta, 27, 221-232.

Carapezza M., Nuccio P.M. and Valenza M., (1981). Genesis and evolution of the fumaroles of Vulcano (Aeolian islands, Italy): a geochemical model. Bull. Vulcanol., 44, 547-563.

De Fiore G., (1925). Bibliografia delle isole Eolie. Bull. Vulcanol., 3/4, 1-49.

Dongarra' G., Favara R., Hauser S. and Capasso G., (1989). Characteristics of the variations in the water chemistry of some wells from Vulcano island. Rend. Soc. It. Mineral. Petrol, 43, 1123-1131.

Frazzetta G., La Volpe L., Sheridan M.F., (1983). Evolution of the Fossa Cone, Vulcano. J.V.G.R., 17, 329-366.

Fustaino G., (1981). L'attivit  vulcanica dell'isola di Vulcano: ricostruzione storica e fenomeni attuali. Degree thesis, University of Palermo.

Gurrieri S., Valenza M., (1988). Gas transport in natural porous mediums: a method for measuring CO<sub>2</sub> flows from the ground in volcanic and geothermal areas. Rend. Soc. It. Mineral. Petrol, 43, 1151-1158.

Italiano F., P.M. Nuccio, M. Valenza, (1984). Geothermal energy and mass release at Vulcano, Aeolian islands, Italy. Rend. Soc. It. Mineral. Petrol, 39, 379-386.

Italiano F. and Nuccio P.M., (1991). Preliminary investigations on the underwater manifestations of Vulcano and Lipari. Acta Vulcanol., 1, 243-247.

Italiano F. and Nuccio P.M., (1992). Volcanic steam output directly measured in the fumaroles: the observed Variations at Vulcano island, Italy, between 1983-1987. Bull. Vulcanol., in press.

Keller J., (1980). The island of Vulcano. Rend. Soc. It. Mineral. Petrol, 36, 349-414.

Mercalli G., Silvestri O., (1891). Modo di presentarsi e cronologia delle esplosioni eruttive di Vulcano, cominciate il 3 Agosto 1888. Ann. Uff. Centr. meteorol. e geodin., P.IV, vol.10, 72 pgg.

Nuccio P.M. and Valenza M., (1991a). Modello evolutivo del sistema di Vulcano (Eolie). G.N.V.- Rapporto sulla sorveglianza vulcanica in Italia. 5, 2-10.

Nuccio P.M. and Valenza M., (1991b). Interpretazione dell'evoluzione del sistema di Vulcano sulla base del modello di degassamento. G.N.V.- Rapporto sulla sorveglianza vulcanica in Italia. 5, 11-15.

Sicardi L., (1940). Il recente ciclo dell'attivit  fumarolica dell'isola di Vulcano. Bull. Vulcanol., 7, 85-140.

## BUILDUP OF CO<sub>2</sub> IN LAKE NYOS AND EVALUATION OF RECURRENCE OF FUTURE GAS OUTBURSTS

M. KUSAKABE

Institute for the Study of the Earth's Interior,  
Okayama University,  
Misasa, Tottori-ken,  
Japan

### Abstract

On 21 August 1986 an outburst of lethal gas from Lake Nyos, Cameroon, killed about 1700 people. The gas was found to be CO<sub>2</sub> dissolved in the lake; it was suddenly released from the lake to the atmosphere and flowed rapidly down valleys asphyxiating people and animals in its path. Isotopic analyses of carbon ( $\delta^{13}\text{C} = -3.4\text{‰}$ ) and helium ( $^3\text{He}/^4\text{He} = 5.7 R_{\text{atm}}$ ) of the dissolved gases indicate that CO<sub>2</sub> and He are of mantle origin. The conductivity-temperature-depth profiler measurements and chemical analyses of the lake water done during November 1986 and December 1988 revealed that the temperature, total dissolved solid and CO<sub>2</sub> content of the water increased markedly from 160 m to the bottom. This result supports the view that CO<sub>2</sub> is being supplied to the lake bottom in the form of warm, CO<sub>2</sub>-charged, mineralized water favoring the "limnological" hypothesis rather than the "volcanic" one for the cause of the gas bursts in 1986. The heat and CO<sub>2</sub> fluxes at the bottom were estimated to be 0.43 MW and 1.0 Gmol/y, respectively. The CO<sub>2</sub> flux is large enough to saturate the lake's hypolimnion within about 30 years. Considering that the gas release may not require full saturation of the lake, another gas outburst could occur at any time. Regular geochemical and limnological monitoring of the lake is highly desirable in order to prevent future disasters. Remedial measures to remove CO<sub>2</sub> from the bottom water should also be taken.

### 1. Introduction

A huge amount of "toxic" gas was suddenly released from Lake Nyos in the evening of August 21, 1986 with the reported death of more than 1700 people and an uncountable number of animals (Sigvaldason, 1989). Journalists at that time described the disaster "as if a neutron bomb was dropped", because only humans and animals were killed while houses and

trees remained almost undamaged. A very similar event was reported to have taken place just 2 years prior to the Lake Nyos disaster at Lake Monoun which is located only 100 km south of Lake Nyos, although it was much smaller in scale (Sigurdsson et al., 1987). These tragic events constitute a new type of natural disaster that has never been recorded, and has been a subject of international concern. The only natural volcanic gas disaster reported to date was from the Dieng Volcano (Indonesia) in 1979. A flow of carbon dioxide gas engulfed 142 people who were evacuating from the expected eruption of the Dieng volcano (Le Guern et al., 1982). The outburst of gas from Lake Nyos was initially thought to be due to emission of volcanic gases. Later most of the researchers involved in the survey agreed that the toxic gas discharged from Lake Nyos was carbon dioxide. Various lines of evidence, including isotopic signatures, indicate that the carbon dioxide is of magmatic origin. It did not come from a volcanic eruption, but was supplied to the surface from the lake bottom at a measurable rate (Nojiri et al., 1990, Evans et al., 1990, Nojiri et al., 1992). Part of the scientific studies initiated soon after the Lake Nyos disaster has been published in special issues of Journal of Volcanology and Geothermal Research (Le Guern and Sigvaldason, 1989 and 1990).

In order to assess the recurrence of future gas bursts and to mitigate future gas disasters, it is essential to estimate the rate of CO<sub>2</sub> supply to the lake and to understand what is going on in the lake. This report describes the origin of the gas and the rate of CO<sub>2</sub> buildup in Lake Nyos based on the changes in the thermal and chemical structures obtained from our repeated surveys in 1986 and 1988. From such information, the possibility of recurrence of future gas bursts will be evaluated.

### 2. Field survey

Lake Nyos is a deep maar lake which has a surface area of 1.58 km<sup>2</sup>, a flat bottom, and a maximum water depth of 208 m. It is situated on the Cameroon volcanic line which runs southwest to northeast parallel to the Cameroon-Nigeria border in west Africa (Fig. 1). Depth sounding and CTD (electric conductivity-temperature-depth profiler) measurements were made during the field surveys in October 1986 and December 1988. Water and gas samples taken in the field were chemically and isotopically analyzed.



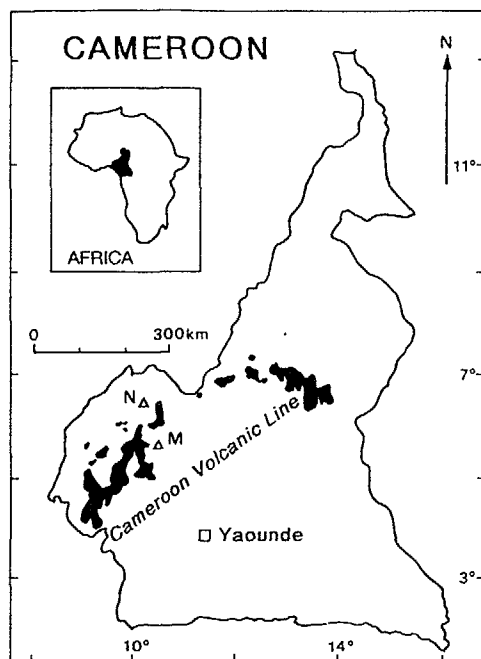


Fig. 1 Map showing locations of the Cameroon volcanic line (black), Lake Nyos (N) and Lake Monoun (M).

Deep water of Lake Nyos is highly charged with free- $\text{CO}_2$  which exsolves when brought near to the surface. Water samples were collected using a 1.4 l PVC Niskin water sampler from which a plastic bag (a capacity of 10 l) was attached to accommodate the exsolved gas (Kusakabe et al., 1989). If a plastic bag was not attached, the high gas pressure that built up inside the sampler forced the sampler lid to open when the sampler was recovered at the lake's surface. Using the above sampling method, the amount of  $\text{CO}_2$  in the plastic bag and in the Niskin sampler was determined to obtain the total  $\text{CO}_2$  concentration in the sample. In the 1988 survey, a newly-designed, simpler  $\text{CO}_2$  sampler was used (Kusakabe et al., 1990). It is a 50 ml plastic syringe in which sits a concentrated caustic soda solution. At a given depth, a messenger weight actuates the syringe to suck water and all of the dissolved  $\text{CO}_2$  is fixed in situ. The amount of a water sample can be calculated from the difference in weight of the syringe before and after sampling.

### 3. Chemical composition

Figure 2 shows the chemistry of Lake Nyos measured in December 1988. The cations are dominated by  $\text{Fe}^{2+}$ ,  $\text{Mg}^{2+}$  and  $\text{Ca}^{2+}$ , while the anions are dominated by  $\text{HCO}_3^-$ . However, the most abundant dissolved species is free- $\text{CO}_2$ . Presence of  $\text{Fe}^{2+}$  indicates that water is anoxic below the surface mixing layer at about 30 m. Most dissolved species (except  $\text{Cl}^-$ ) have similar profiles with depth indicating they are supplied to the lake from a common source. In contrast to normal lakes in a temperate region, temperature at Lake Nyos increases towards the bottom. However, high concentrations of dissolved  $\text{CO}_2$  and other ionic species in the deep water make the water density higher towards the bottom thus forming a stable, stratified structure.

Figure 3 illustrates the results of CTD measurements: the profiles of temperature (Fig. 3a) and electric conductivity (Fig. 3b), and free- $\text{CO}_2$  content (Fig. 3c) of Lake Nyos in December 1988 are compared with the corresponding profiles measured in October and November 1986. Generally speaking, all three items are found to vary in a parallel fashion, showing a gradual increase in the mid-depth followed by a sharp increase near the

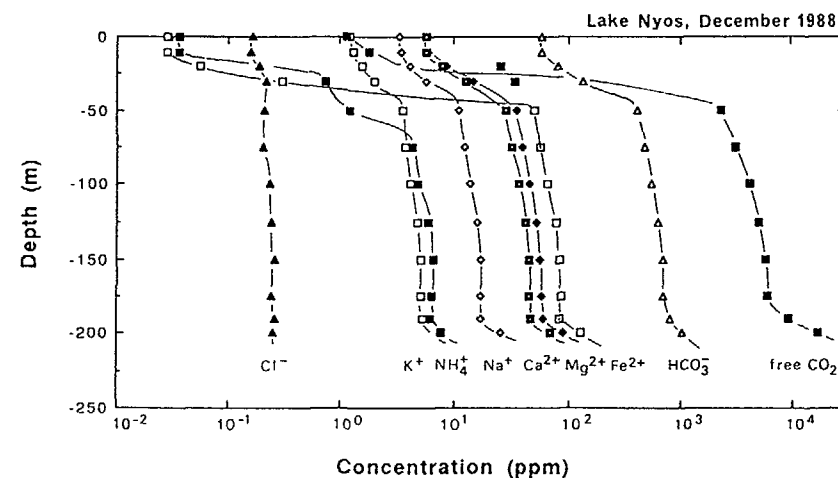


Fig. 2 Chemical composition of water from Lake Nyos as a function of depth (samples collected in December 1988).

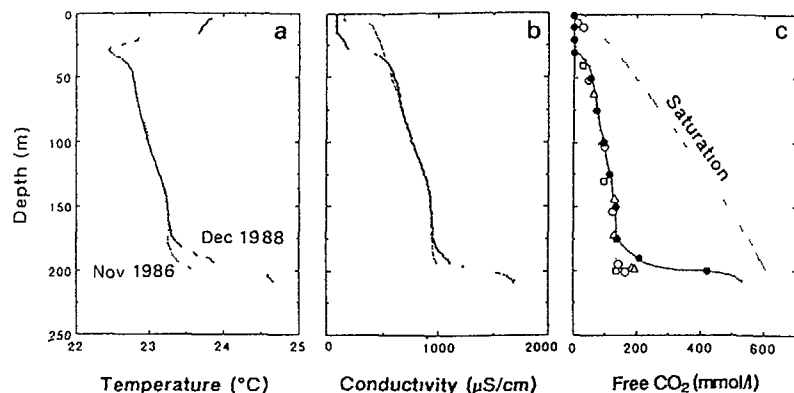


Fig. 3 Profiles of temperature (a), electric conductivity (b) and free CO<sub>2</sub> (c) of Lake Nyos measured in November 1986 (Tietze, 1987) and December 1988. CO<sub>2</sub> data were taken from Kusakabe et al (1989), Tietze (1987), Kling et al. (1989) and Nojiri et al. (1992)

bottom. Decrease in temperature accompanied by decrease in conductivity at depths around 30 m (Fig. 3a and 3b) indicates recent mixing of surface lake water with inflow water. What should be stressed here is that during the period between November 1986 and December 1988, all three items increased significantly at depths below 160 m, while the changes in the mid-depth are almost negligible. This rapid and simultaneous increase in temperature, conductivity and free CO<sub>2</sub> in the bottom water (Fig. 3) supports the view that CO<sub>2</sub> is being supplied to the lake bottom in the form of warm, CO<sub>2</sub>-charged, mineralized water. This conclusion favors the limnological hypothesis for the cause of the 1986 disaster.

#### 4. Heat, TDS and CO<sub>2</sub> fluxes

The increase of heat in the bottom water during the 25 month period (Fig. 3a) was integrated over the whole lake below 165 m to give a heat flux of 0.43 MW (or 3.2 Tcal/y). This value agrees well with the heat flux of 0.39 MW reported recently by Evans et al. (1990). These estimates are much smaller than those usually encountered in active volcanic environments, but they are consistent with the reported heat flow in Crater Lake in Oregon (Williams and Von Herzen, 1983). There is also a significant increase in

electric conductivity near the bottom (Fig. 3b), which is similar to the temperature profiles (Fig. 3a). Electric conductivity of natural water is related to the concentrations of the total dissolved ionic species or the total dissolved solids (TDS); these are calculated from the chemical composition of the water. Figure 4 shows the TDS profiles thus converted from the conductivity profiles. The TDS increment in the bottom water during November 1986 and December 1988 can be estimated by again integrating the TDS profiles over the whole lake below 165 m. This gives the TDS flux of 1100 ton/year. For this calculation, the assumption was made that the relative composition of the dissolved species was constant in the deep water.

The free-CO<sub>2</sub> data are plotted as a function of depth (Fig. 3c). Although the number of data points for CO<sub>2</sub> is much smaller than that for temperature and conductivity, one can still recognize that the CO<sub>2</sub> profiles are similar to the temperature and the conductivity profiles. This indicates that CO<sub>2</sub> in the bottom water has also increased after the 1986 gas event. Some of the 1988 data points below 175 m are not very accurate, because our syringe

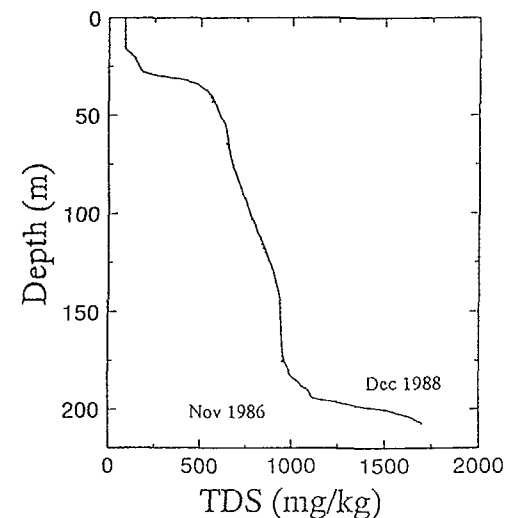


Fig. 4 Estimated TDS profiles in December 1988 (solid curve) and in November 1986 (dotted curve) of Lake Nyos based on the CTD measurement and chemical composition of water. Modified from Nojiri et al (1992)

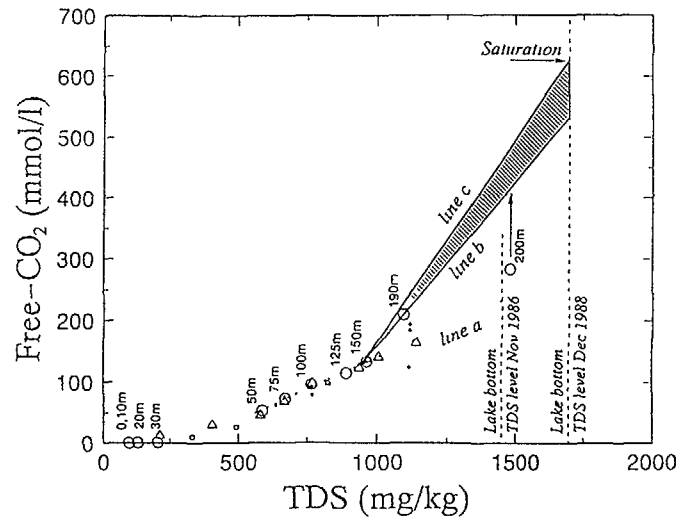


Fig. 5 Relationship between the TDS and free CO<sub>2</sub> concentrations in Lake Nyos. Open circles are for December 1988, small dots for May 1987 (Kling et al., 1989) and triangles for November 1986 (Tietze, 1987). See text for lines *a*, *b* and *c*. Taken from Nojiri et al. (1992).

sampler did not work properly at depths greater than 175 m; the CO<sub>2</sub> concentration there was higher than expected. However, in this region the CO<sub>2</sub> concentration was estimated as described in detail by Nojiri et al. (1992).

Figure 5 shows the relationship between TDS and our free-CO<sub>2</sub> data (Nojiri et al., 1992) together with those available in literature (Tietze 1987, Kusakabe et al. 1989, Kling et al., 1989). There is a linear relationship for the data collected between 50 m and 150 m during the 1986, 1987 and 1988 surveys. It is interesting to note that while the 1986 data lie on extension of line *a* for depths below 150 m, the data points for the deep waters sampled in 1987 and 1988 tend to lie above line *a*. The deep waters sampled in December 1988 are characterized by line *b* (the data point for 200 m in the 1988 samples is a minimum value and the CO<sub>2</sub> concentration there is probably higher as indicated by an arrow.). This may indicate that the CO<sub>2</sub>/TDS ratio in the bottom spring water is higher than that in the present mid-depth water. If the line *b* is extrapolated to the bottom, free-CO<sub>2</sub> concentration at the bottom is estimated to be about 0.53 mol/l, close to the saturation value of 0.63 mol/l.

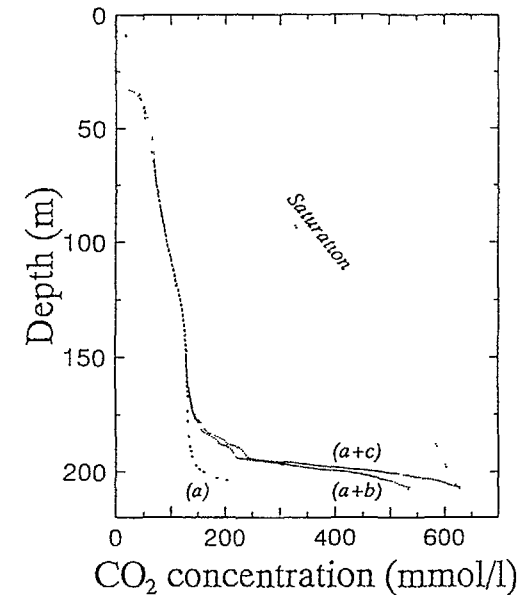


Fig. 6 Estimated profiles of free CO<sub>2</sub> in Lake Nyos in November 1986 and December 1988 (Nojiri et al., 1992). See text for curves *a*, *a+b* and *a+c*. The saturated free CO<sub>2</sub> concentration is derived from Houghton et al. (1957).

Since the maximum CO<sub>2</sub> concentration in the deepest water will be limited by saturation, the highest slope of the mixing line may be restricted by the line *c* which connects the points at 150 m and saturation at the bottom. Thus, the possible TDS-CO<sub>2</sub> relationship for the deep water is fairly well constrained by the lines *b* and *c*. By using the CO<sub>2</sub>-TDS relationships shown in Fig. 5, the free-CO<sub>2</sub> profiles can be drawn through the TDS profiles as shown in Fig. 6.

In Fig. 6, the curve *a* is the CO<sub>2</sub> profile for November 1986 and the curve *(a+b)* for December 1988. The curve *(a+c)* corresponds to the case where saturation is assumed at the bottom. An integration of the CO<sub>2</sub> increment below 165 m during the last 25 months gives a CO<sub>2</sub> flux of  $1.0 \pm 0.1$  Gmol/y. The total amount of CO<sub>2</sub> in Lake Nyos in December 1988 was calculated to be 13 Gmol; this was done by integrating the curve *(a+b)* over the whole lake below the surface mixing layer at 30 m. The maximum amount of CO<sub>2</sub> that the lake can retain would be given by integration of the

saturation curve below 30 m, i.e., 40 Gmol. Thus, the difference between the maximum retainable and the present amounts of CO<sub>2</sub> is 27 Gmol. If the CO<sub>2</sub> flux estimated above remains unchanged and if there is no mixing of CO<sub>2</sub> into surface water, the lake's hypolimnion would be saturated with CO<sub>2</sub> in 27±3 years. It should be noted that the gas outburst from the lake may not require full saturation of CO<sub>2</sub> of the whole lake and that the formation of a gas phase may take place when the CO<sub>2</sub> concentration reaches the saturation curve at any depth. Figure 6 suggests that saturation may be first reached in the deepest water where CO<sub>2</sub> concentration is rapidly increasing. Local saturation of CO<sub>2</sub> may also be reached in a part where density gradient is high as a result of low exchange coefficients of gases, because gas accumulates in such a layer (Tietze, 1987).

Another estimate of CO<sub>2</sub> flux at Lake Nyos was attempted by Sano et al (1990). Their approach was based on a coupled increase of <sup>3</sup>He concentration and temperature of water below 150 m (Fig. 7). The <sup>3</sup>He concentrations were obtained through measurements on <sup>3</sup>He/<sup>4</sup>He ratios and He concentrations. There is a linear relationship between the <sup>3</sup>He concentration and temperature for water deeper than 150 m. Since the slope of the line is the increment of

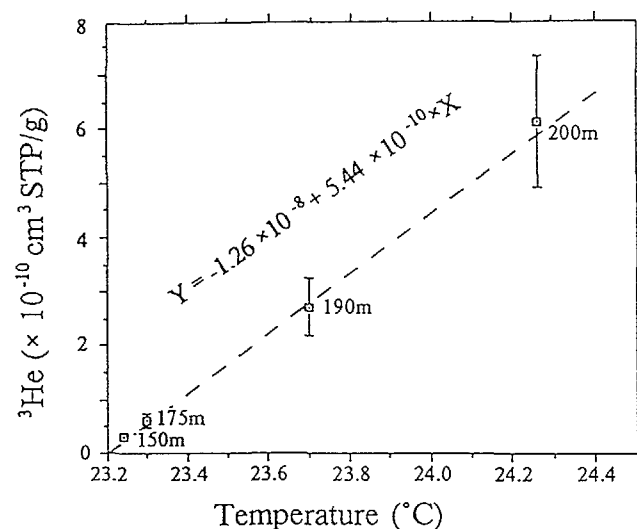


Fig. 7 <sup>3</sup>He concentration versus temperature of deep water of Lake Nyos (Sano et al., 1990).

the amount of <sup>3</sup>He per unit temperature increase per gram of water (the heat supply), the <sup>3</sup>He flux can be calculated as the product of the slope with the thermal flux. By multiplying the observed CO<sub>2</sub>/<sup>3</sup>He ratios of  $3.0 \pm 1.5 \times 10^{10}$ , one can get the CO<sub>2</sub> flux of 2±1 Gmol/yr. The range overlaps the CO<sub>2</sub> flux estimated on the basis of TDS-CO<sub>2</sub> relations. The recharge time then is calculated to be 20±10 years.

Recently, a lower CO<sub>2</sub> flux of 0.2 Gmol/y was estimated by Evans et al. (1990) to explain the increase of dissolved CO<sub>2</sub> after the 1986 gas burst, although their estimate of the heat flux (0.39 MW) is in good agreement with our value of 0.43 MW. Their estimate of the CO<sub>2</sub> flux is about a factor of 5 smaller than ours. This discrepancy is likely due to the lack of CO<sub>2</sub> data in deep water. Collection of more accurate data is required on much more densely sampled waters especially below 160 m where thermal and chemical gradients are high. Comparison of the sampling techniques is also necessary.

## 5. Source of CO<sub>2</sub> in Lake Nyos

Chemical and isotopic compositions of gases exsolved from deep waters of Lake Nyos, sampled in December 1988, are given in Table 1 (Kusakabe and Sano, 1992). The compositions of gas from carbonated mineral springs in the

Table 1 Chemical and isotopic compositions of gases exsolved from deep waters of Lake Nyos and mineral spring gases from North-West Province of Cameroon.

Sample	CO <sub>2</sub> %	N <sub>2</sub> %	Ar %	CH <sub>4</sub> %	He ppm	He/Ne	<sup>3</sup> He/ <sup>4</sup> He R <sub>atm</sub>	δ <sup>13</sup> C <sub>total</sub> ‰	*
Lake Nyos 100 m	99.5	0.10	-	0.40	4.0	1.5	5.68	-3.2	
125 m	99.5	0.0	-	0.46	2.5	36.0	5.65	-3.3	
150 m	99.5	0.12	0.03	0.36	2.0	28.3	5.60	-3.3	
175 m	99.4	0.19	0.01	0.39	2.9	57.0	5.72	-3.2	
190 m	-	-	-	-	6.8	49.6	5.73	-3.4	
200 m	99.5	0.08	0.01	0.37	4.9	113	5.70	-3.7	
Lake Monoun 95 m**	~100	-	-	-	2.6	1.8	3.56	-5.0	
Mineral springs									
Lihuh	99.4	0.53	-	0.02	9.9	72.4	5.91	-4.6	
Gesel	-	-	-	-	0.3	0.4	0.60	-0.5	
Koutaba	-	-	-	-	-	111	1.55	-5.7	
Kunchuantium	97.1	2.82	0.08	0.01	32	52.0	5.39	-2.6	
Boujau	~100	-	-	-	0.7	10.9	3.81	-3.4	
Ndibisi	99.7	0.23	0.02	0.00	0.3	9.1	3.57	-2.8	
Bare	-	-	-	-	0.1	1.1	4.16	-2.8	

All values have been recalculated on air-free basis using N<sub>2</sub>/O<sub>2</sub>=3.73 or N<sub>2</sub>/Ar=84 and He/Ne=0.274 when oxygen was detected in the samples. Raw analytical results have been given in Sano et al. (1990) except δ<sup>13</sup>C values.

\* Total CO<sub>2</sub> fixed *in situ* in an alkaline solution except the Lake Monoun sample.

\*\* Taken from Kusakabe et al. (1989).

North-West Province of Cameroon are also listed in Table 1. The gas compositions were recalculated on air-free basis using  $N_2/O_2=3.73$  (v/v). The dissolved gases in deep waters of the lake are overwhelmingly dominated by  $CO_2$  (99.4-99.5 %) with only a small proportion of the other gases ( $CH_4$ : 0.36-0.46 % and  $N_2$ : 0.1-0.2 %). The  $^3He/^4He$  ratios in Table 1 were also corrected for a slight degree of air contamination using the method in Sano et al. (1990). The  $^3He/^4He$  ratios thus corrected fall in a narrow range from 5.60-5.73  $R_{atm}$  in good agreement with the values reported for the 1986 samples (Sano et al., 1987).  $R_{atm}$  is the atmospheric  $^3He/^4He$  ratio, i.e.,  $1.4 \times 10^{-6}$ . The  $\delta^{13}C$  values are for the total dissolved carbonate, i.e., free- $CO_2$  and  $HCO_3^-$ . They also agree well with  $\delta^{13}C$  values obtained soon after the Lake Nyos disaster of August 1986 (Kling et al., 1987, Freeth et al., 1987, Tietze, 1987, Kusakabe et al., 1989) indicating no significant change with time in carbon isotopic composition.

The isotopic compositions of helium and carbon ( $CO_2$ ) can give constraints on the origin of these gases especially when they are coupled. Figure 8 shows a  $\delta^{13}C$  versus  $^3He/^4He$  plot for the gases from Lakes Nyos and Monoun and the nearby carbonated mineral springs (Kusakabe and Sano, 1992). Mantle helium is characterized by high  $^3He/^4He$  ratios as indicated by MORBs and hot-spots. Carbon from MORBs and hot spots has isotopic compositions ranging from -8 to -3 ‰. In contrast to the mantle helium, crustal helium occurring in a non-volcanic terrain exhibits  $^3He/^4He$  ratios lower than 1  $R_{atm}$  due to predominance of radiogenic  $^4He$ . The accompanying carbon may have distinctly different isotopic compositions depending on the sources: the  $\delta^{13}C$  values for  $CO_2$  which are close to 0 ‰ suggest derivation from limestone while those ranging from -10 to -30 ‰ suggest an organic carbon origin from sedimentary rocks (Hoefs, 1980). The Lake Nyos sample plots very close to the mantle region (Fig. 8) indicating that both He and  $CO_2$  are mostly magmatic (mantle) in origin. The gases from Lake Nyos and most of the carbonated mineral spring are plotted close to a mantle-limestone mixing curve suggesting that high proportions (50 to 80 %) of the mantle components are mixed with smaller proportions of the crustal components except one sample (showing atmospheric contribution). The source of the crustal carbon is likely to be limestone. The  $\delta^{13}C$  value of Lake Monoun is slightly lower than that of Lake Nyos. The deep water of Lake Monoun is rich in dissolved organic carbon (Kusakabe et al., 1989) which exists as humic acids, decomposition products of plankton, soil organic

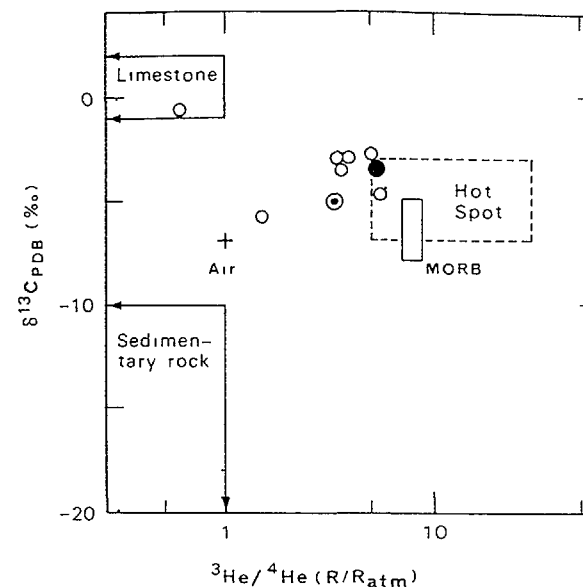


Fig. 8 Relationship between carbon and helium isotopic compositions of gases from Lake Nyos (solid circle), Lake Monoun (double circle) and nearby carbonated springs (open circle). Dotted curves show mixing relations between gases from the mantle and crustal reservoirs (Kusakabe and Sano, 1992).

material and plant leaves. This explains the lower  $\delta^{13}C$  value of Lake Monoun than Lake Nyos.

Hydrogen and oxygen isotopic ratios of waters from Lakes Nyos, Monoun and Wum (a gas-inactive crater lake 30 km west of Lake Nyos) are shown in Fig. 9. They lie on the meteoric water line (Craig, 1961). It is very difficult to recognize any contribution of magmatic water to Lake Nyos even in the deep water collected in 1986 (Kusakabe et al., 1989).

From the foregoing, it is very likely that highly  $CO_2$ -charged, warm spring water is supplied to the bottom of Lake Nyos. The temperature of the spring water before mixing with the bottom lake water has been estimated from the saturation of amorphous silica to be 31°C (Nojiri et al., 1992). It has also been estimated that the deepest water is close to saturation with respect to free- $CO_2$  (see Fig. 6). The bottom spring water may, therefore, be saturated with free- $CO_2$  or a two-phase fluid from underneath. Since the critical temperature is 31.1°C,  $CO_2$  would be in a liquid or supercritical state in the

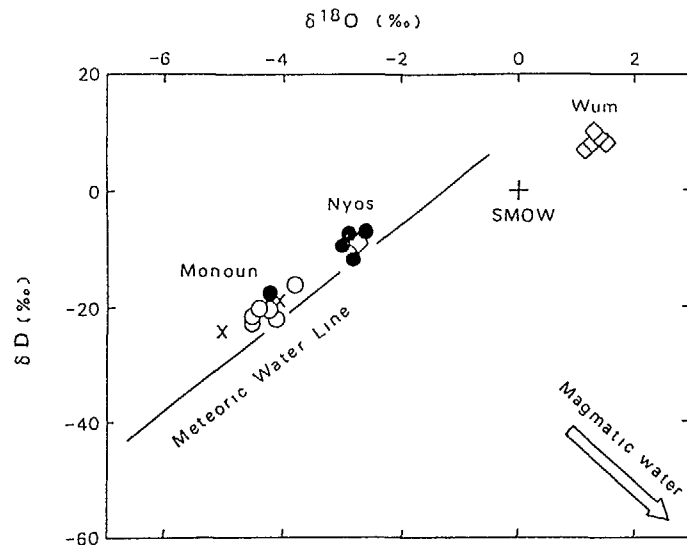


Fig. 9 Hydrogen and oxygen isotopic compositions of waters from Lakes Nyos, Monoun and Wum, and local tap water (Kusakabe et al., 1989).

sediment and basement rocks. Low temperature phase relations for the  $\text{CO}_2$ - $\text{H}_2\text{O}$  system (Takenouchi and Kennedy, 1965) is shown in Fig. 10. A geotherm beneath the lake bottom with a temperature gradient of  $1^\circ\text{C}/100\text{ m}$  could cross the gas-liquid boundary of  $\text{CO}_2$  at a pressure between 45 and 73.4 bar (critical pressure). Therefore, liquid  $\text{CO}_2$  could exist within a few hundred meters of the lake bottom (Fig. 10). In a region of higher temperature gradient (i.e.,  $2^\circ\text{C}/100\text{ m}$  or higher), liquid  $\text{CO}_2$  would no longer be present but would exist as a supercritical fluid.

Accumulation of  $\text{CO}_2$  near the Earth's surface may take place nearby geologically young basaltic volcanoes like Lake Nyos (Lockwood and Rubin, 1989). Such accumulation of  $\text{CO}_2$  results from preferential exsolution of a  $\text{CO}_2$ -rich fluid from an ascending magma due to low solubility of  $\text{CO}_2$  in basaltic melts at low pressure (Stolper and Holloway, 1988). The existence of liquid  $\text{CO}_2$  has been reported in a  $\text{CO}_2$  well drilled on the flank of a young basaltic volcano in southern Australia (Chivas et al., 1987). Also, the emission of liquid  $\text{CO}_2$  to the seafloor has been filmed in the Okinawa Trough hydrothermal area (Sakai et al., 1990). If either liquid  $\text{CO}_2$  or supercritical

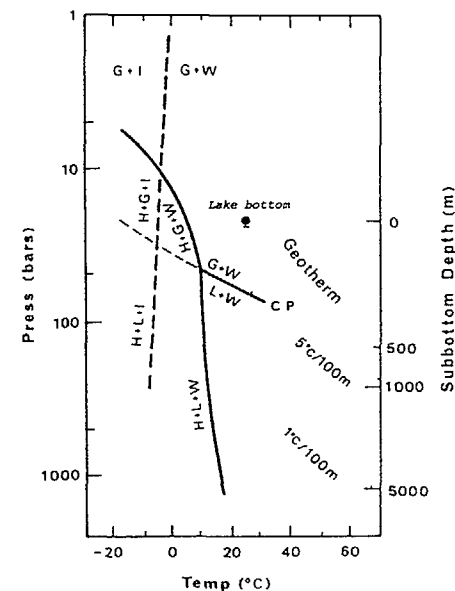


Fig. 10 Phase relations in the  $\text{CO}_2$ - $\text{H}_2\text{O}$  system (Takenouchi and Kennedy, 1965).

H= $\text{CO}_2$  hydrate ( $\text{CO}_2 \cdot 5.75\text{H}_2\text{O}$ , solid), L=liquid  $\text{CO}_2$ , G=gaseous  $\text{CO}_2$ , W=liquid water, and I=ice. C.P. indicates the critical point of  $\text{CO}_2$  ( $31.1^\circ\text{C}$  and 73.4 bar). Geothermal gradients from the lake bottom are shown by dotted curves.

$\text{CO}_2$  meets groundwater, a  $\text{CO}_2$ -saturated aqueous solution would form. Such solution would then react with surrounding basaltic rocks to leach cations like  $\text{Fe}^{2+}$ ,  $\text{Mg}^{2+}$  and  $\text{Ca}^{2+}$  and form an equivalent amount of  $\text{HCO}_3^-$ . It has been estimated that the deepest water of Lake Nyos is almost saturated with free- $\text{CO}_2$  (Fig. 6). Thus, it is conceivable that such a process may be going on beneath Lake Nyos and that a small fraction of the  $\text{CO}_2$ -saturated, mineralized groundwater is continuously supplied to the lake bottom. As a consequence, the concentration of dissolved  $\text{CO}_2$  in Lake Nyos should increase with time especially in deepest part of the lake.

## 6. Conclusions

- (1) The 1986 disaster was caused by a massive release of  $\text{CO}_2$  dissolved in Lake Nyos, and not by a volcanic phreatic explosion.

- (2) Carbon dioxide is being supplied to the bottom Lake Nyos in the form of a warm, CO<sub>2</sub>-charged, mineralized spring. Thermal and CO<sub>2</sub> fluxes to Lake Nyos have been estimated to be 0.43 MW and 1-2 Gmol/yr, respectively.
- (3) If the above CO<sub>2</sub> flux remains unchanged, the hypolimnion of Lake Nyos will be fully saturated with CO<sub>2</sub> in not too distant future (less than 30 years), and there is a high possibility that outburst of gas from Lake Nyos will be repeated.
- (4) Regular geochemical and limnological monitoring of gas-active lakes is highly desirable in order to mitigate the occurrence of the next gas outburst.
- (5) Remedial means to reduce the possibility of gas re-outburst should be taken including artificial pumping of CO<sub>2</sub>-rich bottom water out of the lake (Halbwachs et al., 1990).

The above conclusions constitute an essential part of the agreement reached by the participants of a seminar on the Lake Nyos disaster held on 11 September 1990 at Nancy, France (Freeth et al., 1990).

## References

- Chivas, A. R., I. Barnes, W. C. Evans, J. E. Lupton, and J. O. Stone. 1987. Liquid carbon dioxide of magmatic origin and its role in volcanic eruptions. *Nature*. **326**: 587-589.
- Craig, H. 1961. Isotopic variations in meteoric waters. *Science* **133**: 1702-1703.
- Evans, W. C., G. W. Kling, and M. L. Tuttle. 1990. Ongoing research activities at Lakes Nyos and Monoun, Cameroon, by the U. S. Scientific Team. Abstr. 15th Colloquium of African Geology, p. 128, Universite Nancy 1, September 1990.
- Freeth, S. J., R. L. F. Kay, and P. J. Baxter. 1987. Reports by the British Scientific Mission sent to investigate the Lake Nyos gas disaster. Report to the Disaster Unit of Overseas Development Administration, London, 86 pp.
- Freeth, S. J., G. W. Kling, M. Kusakabe, J. Maley, F. M. Tchoua, and K. Tietze. 1990. Conclusions from Lake Nyos disaster. *Nature* **348**: 201.
- Halbwachs, M., J. Vanedemeulebrouck, J.C. Sabroux, and E. Naah. 1990. Artificial priming of gas-lift on Lakes Nyos and Monoun and its application to CO<sub>2</sub> release prevention. Abstr. 15th Colloquium of African Geology, p. 131, Universite Nancy 1, September 1990.
- Hoefs, J. 1980. *Stable Isotope Geochemistry* (3rd edition), Springer-Verlag, pp. 241.
- Houghton, G., A.M. McLean and P.D. Ritchie. 1957. Compressibility, fugacity, and water-solubility of carbon dioxide in the region 0-36 atm and 0-100°C. *Chem. Eng. Sci.* **6**: 132-137.
- Kling, G. W., M. L. Tuttle, and W. C. Evans. 1989. The evolution of thermal structure and water chemistry in Lake Nyos. *J. Volcanol. Geotherm. Res.* **39**: 151-165.
- Kusakabe, M., T. Ohsumi, and S. Aramaki. 1989. The Lake Nyos gas disaster: chemical and isotopic evidence in water and dissolved gases from three Cameroonian crater lakes, Nyos, Monoun and Wum. *J. Volcanol. Geotherm. Res.* **39**: 167-185.
- Kusakabe, M., Y. Nojiri, and M. Narita. 1990. A simple plastic syringe sampler for *in situ* fixing of the total CO<sub>2</sub> dissolved in lake water. International Working Group on Crater Lakes Newsletter No. 2, 11-14.
- Kusakabe, M., and Y. Sano. 1992. Origin of gases in Lake Nyos, Cameroon, In: *Natural Hazards in West and Central Africa*, International Monograph Series on Interdisciplinary Earth Science Research and Applications, S. J. Freeth, K. M. Onuoha and C. O. Ofoegbu, eds., Friedr. Vieweg and Son, Braunschweig/ Wiesbaden, p. 79-92.
- Le Guern, F., H. Tazieff and R. Faivre-Pierret. An example of health hazard: people killed by gas during a phreatic eruption: Dieng Plateau (Java, Indonesia), February 20th, 1979. *Bull. Volcanol.* **45**: 153-156.
- Le Guern, F. and G.E. Sigvaldason. 1989, 1990. Special issue "The Lake Nyos event and natural CO<sub>2</sub> degassing, I and II". *J. Volcanol. Geotherm. Res.* **39** (2/3) and **42** (4).
- Lockwood, J. P., and M. Rubin. 1989. Origin and age of the Lake Nyos maar, Cameroon. *J. Volcanol. Geotherm. Res.* **39**: 117-124.
- Nojiri, Y., M. Kusakabe, J. Hirabayashi, H. Sato, Y. Sano, H. Shinohara, T. Njine, and G. Tanyileke. 1990. Gas discharge at Lake Nyos. *Nature* **346**: 322-323.
- Nojiri, Y., M. Kusakabe, K. Tietze, J. Hirabayashi, H. Sato, Y. Sano, H. Shinohara, T. Njine, and G. Tanyileke. 1992. An estimate of CO<sub>2</sub> flux in Lake Nyos. *Limnol. Oceanogr.* **37** (in press).
- Sano, Y., H. Wakita, Ohsumi, T. and M. Kusakabe. 1987. Helium isotope ratios of gases from Lake Nyos, Cameroon. *Geophys. Res. Lett.* **14**: 1039-1041.
- Sano, Y., M. Kusakabe, J. Hirabayashi, Y. Nojiri, H. Shinohara, T. Njine, and G. Tanyileke. 1990. Helium and carbon fluxes in Lake Nyos, Cameroon: constraint on next gas burst. *Earth Planet. Sci. Lett.* **99**: 303-314.
- Sigurdsson, H., J. D. Devine, F. M. Tchoua, T. S. Presser, M. K. W. Pringle, and W. C. Evans. 1987. Origin of the lethal gas burst from Lake Monoun, Cameroon. *J. Volcanol. Geotherm. Res.* **31**: 1-16.

- Sigvaldason, G E 1987 *International conference on Lake Nyos disaster*, Yaounde, Cameroon 16-20 March, 1987 Conclusions and recommendations J Volcanol Geotherm Res 39 97-107
- Stolper, E , and J R Holloway 1988 Experimental determination of the solubility of carbon dioxide in molten basalt at low pressure Earth Planet Sci Lett 87 397-408
- Takenouchi, S , and G C Kennedy 1965 Dissociation pressure of the phase  $\text{CO}_2$   $5\frac{3}{4}\text{H}_2\text{O}$  J Geol 73 383-390
- Tietze, K 1987 Results of the German Cameroon research expedition to Lake Nyos (Cameroon), October/November 1986, Interim Report, Federal Institute for Geosciences and Natural Resources, Hannover, 84 pp
- Williams, D L , and R P Von Herzen 1983 On the terrestrial heat flow and physical limnology of Crater Lake Oregon J Geophys Res 88 1094-1104

## THE LAKE NYOS GAS DISASTER: CONCLUSIONS AND PREDICTIONS

S J FREETH

Geological Hazards Research Unit,  
University College of Swansea,  
Swansea, United Kingdom

### Abstract

Lake Nyos is stable under normal circumstances, despite being highly charged with carbon dioxide, as it was both before and, to a lesser extent, after the 1986 disaster which killed an estimated 1700 people. Samples of gas collected from the lake contain mostly carbon dioxide, with a very small amount of methane and a trace of helium. Isotopic evidence for both the carbon dioxide and for the helium points unambiguously towards a primarily 'magmatic', rather than a biogenic, source for the gas.

What disturbed the lake's stable stratification in August 1986 can never be known, for certain, but perhaps the most plausible explanation is that a cold, and therefore slightly dense, metastable surface layer built up during the early part of the wet season (July-August) then sank in the southern part of the lake causing carbon dioxide rich water to rise towards the surface in the north-eastern part of the lake. Whatever initiated circulation within the lake, the consequences would have been the same: once water from depth reached a level at which it was oversaturated, with respect to carbon dioxide, it would have exsolved bubbles of gas which then rose towards the surface increasing the convective flow and leading to runaway degassing of part of the lake.

Lake Nyos is currently being recharged with carbon dioxide at a rate of about 5 million cubic metres per year. Although the amount of gas which was discharged in 1986 is not known for certain, most scientists who have been working on the problem would probably accept a figure of about 100 million cubic metres - which implies that the gas which was lost will only take about 20 years to replace. But perhaps the more important factors controlling the frequency with which major gas releases occur are those which influence the stability of the lake. If this is the case then Lake Nyos may be almost as dangerous now as it was immediately prior to the 1986 disaster.



## Introduction

Within the context of a meeting concerned with "isotopic and geochemical precursors of earthquakes and volcanic eruptions" it is important that all aspects of the subject should be considered. It is therefore with this in mind that I would like to draw attention to the Lake Nyos gas disaster which killed an estimated 1700 people in 1986.

The Lake Nyos disaster, as we now know, was caused not by the direct release of gas from an active volcano but by the slow build-up of gas in a deep lake, situated in the caldera of a long dead volcano, gas which was released when the stable stratification of the lake was disturbed.

Isotopic and chemical evidence has made it possible to determine the origin of the gas. And the gas concentration is currently being monitored in an attempt to forewarn of a dangerous build-up which might lead to a further disaster.

## The disaster

In August 1986 a cloud of toxic gas swept down the valleys to the north of Lake Nyos, in a remote part of the North-West Province of Cameroon, leaving a trail of death and devastation in its wake (Freeth & Kay, 1987; Kling et al., 1987). The disaster occurred late on a Thursday evening; news that something quite horrendous has happened started to circulate the following day and this was confirmed on the Saturday when the market village of Nyos was visited by people from outside the immediate area. On the Sunday, Lake Nyos itself was visited, by two Cameroonian scientists, and by that time news of the disaster was spreading around the world. The horrific nature of the disaster and the high death toll, subsequently estimated at over 1700 people, brought a rapid response from the many Governments which sent both humanitarian assistance and teams of scientists, to help with the investigation.

## Geological setting

Lake Nyos is in an area where there has been extensive volcanic activity in the geologically recent past. It is close to the axis of the

Cameroon Volcanic Line which extends from the Gulf of Guinea islands, for nearly 1900 km, through south-western Cameroon to the shores of Lake Chad, and along the whole length of which there are volcanic rocks that are less than one million years old. It is also a little less than 300km to the north-north-east of Mt Cameroon, which is the most active volcano in the area, having erupted eight times since 1838. The only other active volcano in the area being Pico Basil, on the offshore island of Bioko, which last erupted in 1898. Lake Nyos itself is in the crater of an extinct volcano, which we now know from the age of a lava flow which has solidified against the outside of its ash cone, to be at least 100,000 years old (Freeth, 1988).

## The initial investigation

When news of the disaster broke, the obvious association of Lake Nyos with young volcanic rocks caused many (if not most) geologists to start from the quite reasonable assumption that the disaster had been caused by renewed activity from a dormant volcano (Sigvaldason, 1989). This prior assumption created many problems for the investigation and even now, more than five years after the disaster, there are still some who firmly believe, despite much evidence to the contrary, that hot volcanic gases were released from beneath the lake. Although starting from a misleading presumption caused problems for the subsequent investigation, it also had its advantages since of all geological specialists it is, in my experience, the volcanologists who are most willing to react quickly and most willing to enter a potentially hazardous area - and in any disaster investigation it is of paramount importance that someone should start to collect reliable information (and samples for subsequent analysis) as soon as possible.

## Gas in the lake water

In early September 1986 Lake Nyos was highly charged with carbon dioxide so much so that when the first attempts were made to collect samples of deep water so much gas was released as the unpressurised samplers were brought to the surface that they quite literally exploded (Freeth et al., 1987). Only when the samplers were recovered slowly, with a bleed valve left open, was it possible to collect water samples (minus some of their gas).

Samples of gas from the lake were collected by various teams and they were found to contain mainly carbon dioxide with a very small amount of methane and a minute trace of helium (Freeth et al., 1987; Tuttle et al., 1987). Neither these nor any subsequent samples (Tietze, 1987; Kusakabe et al., 1989) contained chemically detectable quantities of hydrogen cyanide, carbon monoxide, sulphur dioxide or hydrogen sulphide. And even lower limits on the possible presence of either sulphur dioxide or hydrogen sulphide can be inferred from the fact that as the water samples were being collected, gas with no detectable smell was bubbling up through the lake surface.

By combining information from various sources we can be confident that the composition of the gas in Lake Nyos after the disaster was:

CO <sub>2</sub>	99.6%
CH <sub>4</sub>	0.4%
He	2 ppm
HCN	<10 ppm
CO	<5 ppm
SO <sub>2</sub>	<0.5 ppm
H <sub>2</sub> S	<0.2 ppm

Although the composition of the gas in Lake Nyos could be determined from the samples which were collected shortly after the disaster the gas concentration at depth could not be determined, for reasons which are given above. Quantitatively accurate sets of gas samples were collected in November 1986 by Tietze (1987) using equipment which could be sealed at depth and returned to the laboratory under pressure. Subsequent sets were obtained in January and May 1987 by Kling et al. (1989) using pressurised steel cylinders and in December 1988 by Nojiri et al. (1990) using a water sampler with a plastic bag attached to collect exsolved gas. From a depth of about 40 metres down to a depth of about 170 metres the results from all four sets can be fitted to the same curve (Fig. 1). Above 40 metres the samples taken within a year of the disaster all fall on a continuation of the curve which extends down to 170 metres (Fig. 1) whilst the samples taken in December 1988, more than two years after the disaster, have very

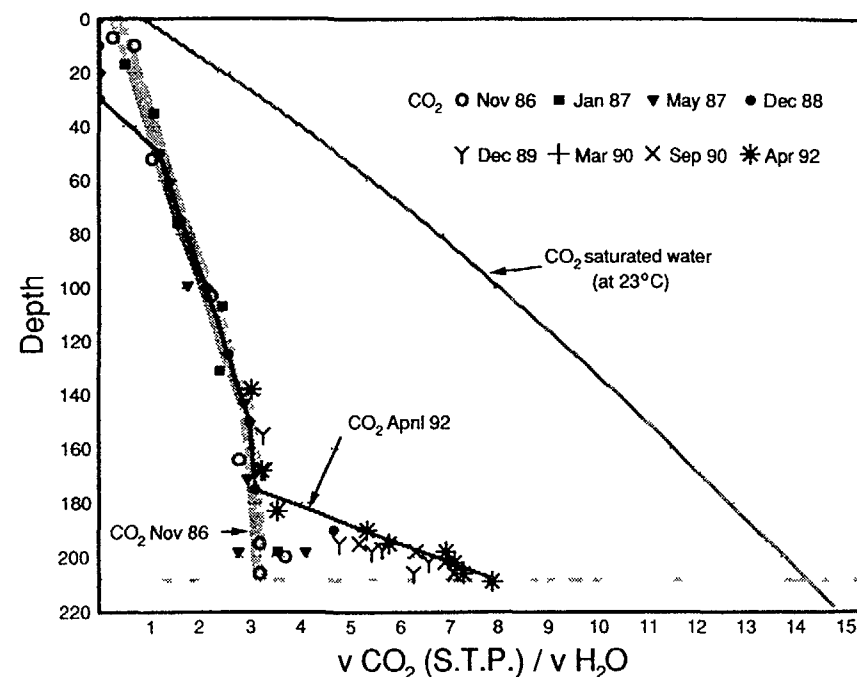


Figure 1: The concentration of dissolved carbon dioxide in Lake Nyos as measured at various times since the disaster in August 1986

low carbon dioxide contents indicating that by that time an oxygenated upper layer, down to at least 30 metres, had been re-established. Below 170 metres the samples collected within a year of the disaster fall more or less on a continuation of the same curve as the samples collected at lesser depths (Fig. 1), though a case could be made out to suggest that the later samples show a slight increase in carbon dioxide content. However, the samples taken in December 1988 not only show a very significant increase in carbon dioxide content at depth but also suggest a rate of increase which would explain much of the apparent scatter of the samples collected shortly after the disaster.

It can be calculated, from the data displayed in Figure 1, that after the disaster Lake Nyos contained approximately 250 million cubic metres (S.T.P.) of carbon dioxide.

### The origin of the gas

The isotopic compositions of the carbon dioxide and of the more abundant inert gases in Lake Nyos have been determined:

$^{14}\text{C}/\text{C}$	0.07	$R/R_{\text{atm}}$
$^3\text{He}/^4\text{He}$	5.68	$R/R_{\text{atm}}$
$^{22}\text{Ne}/^{20}\text{Ne}$	1.01	$R/R_{\text{atm}}$
$^{40}\text{Ar}/^{36}\text{Ar}$	1.02	$R/R_{\text{atm}}$

The ratio of helium-3 to helium-4 (Sano et al., 1987; Kusakabe & Sano, 1992) points unambiguously towards a primarily 'magmatic' origin for the gas. This conclusion is supported by the low level of carbon-14 in the dissolved carbon dioxide (Freeth et al., 1987) equivalent to an apparent radiocarbon age of 20,000 years and indicating very little 'contamination' by atmospheric or biological carbon. The neon and argon isotopic ratios were both determined on a sample which was collected under less than ideal conditions and was contaminated with air (Freeth et al., 1987). The deviation from normal atmospheric ratios presumably being due to production, within the crustal rocks, of radiogenic isotopes; argon-40 from potassium-40 and neon-22 from magnesium-25.

### A model for the Lake Nyos disaster

When all the evidence; not only the chemical evidence from the gas samples but also chemical evidence from the water samples (Giggenbach, 1990), the physical evidence of wave damage around the lake (Freeth & Kay, 1991), the evidence of 'wind' damage in the valleys to the north (Freeth & Kay, 1987), the medical evidence (Baxter & Kapila, 1989; Baxter et al., 1989) and the absence of microseismic activity (Walker et al., 1992) has been put together (Freeth, 1992), it is possible to come up with an entirely self consistent model for the Lake Nyos disaster:-

Prior to the disaster Lake Nyos was highly charged with carbon dioxide. It is not known exactly how much gas was in the lake, since it is not known exactly how much was lost during the disaster. However, the gas concentration shortly after the disaster is known and if this is modified

to take account of the changes near the surface and at depth which have been observed since the disaster, and if account is also taken of the estimated gas loss during the disaster, then a model for the distribution of gas prior to the disaster can be constructed.

During the wet season, the height of which is in August, rain water falls on the catchment and flows down the streams into the southern part of Lake Nyos. The temperature of this water is a little lower than that of the the surface water of the lake and it is therefore slightly denser. However, it forms a separate layer on the lake surface and consequently the stream water flows over the lake and out over the spillway in the north-west corner. As the wet season progresses the thickness of the layer of cold stream water on the lake surface steadily increases, since water is being lost not only over the spillway but also through the pyroclastic deposits which block the valley to the north-east. Under normal circumstances this metastable stratification decays as the surface water warms up at the end of the wet season.

Late on the evening of August 21st 1986 the stably stratified waters of Lake Nyos were disturbed causing bottom water, highly charged with carbon dioxide, to rise towards the surface in the north-eastern part of the lake.

What disturbed the stratification can never be known, for certain. However, at that time of year the prevailing winds are from the north-east and it is possible that in August 1986 they were more steady and more persistent than usual, thus causing the cold surface water to migrate towards the southern part of the lake. If sufficient surface water migrates towards one part of the lake then it will eventually become unstable and sink, thus causing deep, gas charged, water from another part of the lake to rise towards the surface. It has been calculated (Giggenbach, 1990) that the temperature of the surface water, prior to the disaster, was probably about 18.5°C and water at that temperature would have been dense enough to sink to a depth of about 120 m. It would therefore seem entirely possible that sinking surface water could have set off a convective overturn of the upper part of the lake.

Water rising from a depth of about 120 m would be oversaturated with respect to carbon dioxide at depths of less than 30 m and would therefore

start to exsolve bubbles of gas. These bubbles would rise and increase the convective flow thus fuelling the overturn and helping to drag more oversaturated water towards the surface. Exsolution of carbon dioxide is an endothermic reaction and adiabatic expansion of the bubbles would also cool the gas. Therefore the temperature of the gas released at the surface would be well below ambient temperature. Not only would the gas be cold but the water brought to the surface with it would also be cooled and once it had released its gas it would therefore sink thus further fuelling the overturn and leading rapidly to a runaway degassing of part of the lake. And as degassing gathered pace and the rate of gas release increased so the water would be cooled to lower temperatures, and sink to greater depths thus increasing the depth from which water was being drawn. It has been suggested by Tietze (1992) that the process of gas release would generate a fountain of cold water which would then sink forming a cylinder of downward flowing cold water surrounding a rising core of degassing water. This is an interesting possibility since it would be self limiting and could explain why the lake was only partially degassed during the 1986 disaster. It might also explain how stable bottom water was drawn towards the surface and why the composition of the lake water below 150 m was fairly uniform after the disaster.

At the surface the vigorous release of gas generated a wave which swept across the lake and into the valleys to the south.

As the gas was released some of the water accompanying it was transformed into a fine mist, thus generating the cold aerosol of water and carbon dioxide which swept down the valleys to the north of the lake through Nyos and on to Subum, Cha and Fang leaving a terrible toll of death in its wake.

#### Predicting the next Lake Nyos disaster

There are two major factors which need to be considered when seeking to predict the next catastrophic gas release from Lake Nyos: (1) the amount of gas in the lake and (2) the depth to which the stratification is disturbed during a future turnover. Clearly these two factors are interrelated, in that the more gas there is in the lake the less would be the disturbance

needed to trigger a catastrophic gas release, presuming that is that the model set out above is correct.

Lake Nyos contained approximately 250 million cubic metres (S.T.P.) of carbon dioxide after the disaster (Fig. 1).

The rate at which Lake Nyos is being recharged with carbon dioxide can be calculated by comparing the immediately post-disaster gas content with more recent data sets (Fig. 1): collected in December 1988 (Nojiri et al., 1989), December 1989 (Evans et al., 1990; Kling & Evans, 1992), September 1990 and April 1992 (Kling & Evans, 1992). There is also a data set, collected in March 1990, which is in line with the other data sets (pers. comm. Dr.M.Halbwachs), this set has not been included in Figure 1 since the detailed results have not yet been placed in the public domain. Taken together these five data sets indicate a steady increase in gas concentration at depths below 175 metres. Comparison of the most recent (April 1992) data set with the well established post-disaster curve (Fig. 1) would suggest that over a period of five and a half years the gas content at depth has increased by approximately 25 million cubic metres. This corresponds to an annual recharge rate of a little less than 5 million cubic metres of carbon dioxide.

The amount of carbon dioxide which was released during the 1986 disaster is not known for certain, recent estimates (Freeth, 1992; Giggensbach, 1990; Tietze, 1992) have suggested figures from as low as 30 million cubic metres (S.T.P.) to as high as 200 million though most of the people who are working on the problem would probably accept a figure in the region of 100 million as reasonable. If the annual recharge rate were to remain constant at 5 million cubic metres then clearly it would take between six and 40 years to replace the gas which was lost. The low figure is very worrying since it suggests that the gas which was lost has already been replaced whilst even the generally accepted figure of 100 million cubic metres would suggest that the gas will have been replaced by 2006.

Perhaps the more important factors controlling the frequency with which major gas releases occur are those which influence the stability of the lake. If the model set out above is correct then the primary factors are

climatic; large scale disturbance to the lake being related either to temperature or to wind constancy or to a combination of the two. Clearly the more we know about the stability of Lake Nyos the better placed we will be to predict the next major overturn. However there would appear to be little doubt that the more gas there is in the lake the less will be the disturbance needed to trigger a major gas release. And it is generally agreed (Freeth et al., 1990) that there is already quite enough gas in the lake for it to be thoroughly dangerous.

If a further disaster is to be avoided measures which will reduce the amount of gas in Lake Nyos need to be implemented as a matter of urgency.

#### Acknowledgements

The work of the British Scientific Mission which was sent to help investigate the Lake Nyos disaster and on which this study is based was commissioned and funded by the Disaster Unit of the Overseas Development Administration, Foreign and Commonwealth Office.

#### References

- Baxter, P.J. and Kapila, M. 1989. Acute health impact of the gas release at Lake Nyos, Cameroon, 1986. J. Volcanol. Geotherm. Res. 39, 265-275.
- Baxter, P.J., Kapila, M. and Mfonfu, D. 1989. Lake Nyos disaster, Cameroon, 1986: the medical effects of large scale emission of carbon dioxide? Br. Med. J. 298, 1437-1441.
- Evans, W.C., Kling, G.W. and Tuttle, M.L. 1990. Ongoing research activities at Lakes Nyos and Monoun, Cameroon, by the U.S. scientific team. Abstracts, 15th Colloquium of African Geology, CIFEQ Occ. Publ. 1990/20, 128.
- Freeth, S.J. 1988. When the Lake Nyos dam fails there will be serious flooding in Cameroon and Nigeria - but when will it fail? Eos, Trans. Am. geophys. Un. 69, 776-777.
- Freeth, S.J. 1992. The Lake Nyos gas disaster. in: Natural Hazards in West and Central Africa (eds. S.J.Freeth, K.M.Onuoha & C.O.Ofoegbu) pp.63-82 Vieweg, Braunschweig.
- Freeth, S.J. and Kay, R.L.F. 1987. The Lake Nyos gas disaster. Nature 325, 104-105.
- Freeth, S.J. and Kay, R.L.F. 1991. How much water swept over the Lake Nyos dam during the 1986 disaster? Bull. Volcanol. 53, 147-150.
- Freeth, S.J., Kay, R.L.F. and Baxter, P.J. 1987. Reports by the British Scientific Mission sent to investigate the Lake Nyos disaster. Report to the Disaster Unit of the Overseas Development Administration, Foreign and Commonwealth Office (London) 86pp.
- Freeth, S.J., Kling, G.W., Kusakabe, M., Maley, J., Tchoua, F.M. and Tietze, K. 1990. Conclusions from Lake Nyos disaster. Nature 348, 201.
- Giggenbach, W.F. 1990. Water and gas chemistry of Lake Nyos and its bearing on the eruptive process. J. Volcanol. Geotherm. Res. 42, 337-362.
- Kling, G.W., Clark, M.A., Compton, H.R., Devine, J.D. Evans, W.C., Humphrey, A.M., Koenigsberg, E.J., Lockwood, J.P. Tuttle, M.L. and Wagner, G.N. 1987. The Lake Nyos gas disaster in Cameroon, West Africa. Science 236, 169-175.
- Kling, G.W. and Evans, W.C. 1992. Scientific investigation of Lakes Nyos and Monoun: preliminary report. [Report to the Ministry of Mines, Water and Power], Yaounde. 10pp.
- Kling, G.W., Tuttle, M.L. and Evans, W.C. 1989. The evolution of thermal structure and water chemistry in Lake Nyos. J. Volcanol. Geotherm. Res. 39, 151-165.
- Kusakabe, M., Ohsumi, T. and Aramaki, S. 1989. The Lake Nyos disaster: chemical and isotopic evidence in waters and dissolved gases from three Cameroonian crater lakes, Nyos, Monoun and Wum. J. Volcanol. Geotherm. Res. 39, 167-185.
- Kusakabe, M. and Sano, Y. 1992. The origin of the gas in Lake Nyos, Cameroon. in: Natural Hazards in West and Central Africa (eds. S.J.Freeth, K.M.Onuoha & C.O.Ofoegbu) pp.83-95 Vieweg, Braunschweig.
- Nojiri, Y., Kusakabe, M., Hirabayashi, J., Sato, H., Sano, Y., Sinohara, H., Njine, T. and Tanyileke, G. 1990. Gas discharge at Lake Nyos. Nature 346, 322-323.
- Sano, Y., Wakita, H., Ohsumi, T. and Kusakabe, M. 1987. Helium isotope evidence for magmatic gases in Lake Nyos, Cameroon. Geophys. Res. Lett. 14, 1039-1041.
- Sigvaldason, G.E. 1989. International conference on Lake Nyos disaster, Yaounde, Cameroon 16-20 March 1987: conclusions and recommendations. J. Volcanol. Geotherm. Res. 39, 97-107.
- Tietze, K. 1987. Results of the German-Cameroon research expedition to Lake Nyos (Cameroon) October/November 1986. Bundesanstalt für Geowissenschaften und Rohstoffe, Report no. 100 470, 34pp.

- Tietze, K. 1992. Cyclic gas bursts. are they a 'usual' feature of Lake Nyos and other gas-bearing lakes? in: Natural Hazards in West and Central Africa (eds. S.J.Freeth, K.M.Onuoha & C.O.Ofoegbu) pp.97-108 Vieweg, Braunschweig.
- Tuttle, M.L., Clark, M.A., Compton, H.R., Devine, J.D., Evans, W.C., Humphrey, A.M., Kling, G.W., Koenigsberg, E.J., Lockwood, J.P. and Wagner, G.N. 1987. The 21 August 1986 Lake Nyos gas disaster, Cameroon. U. S. Geol. Surv. Open-File Report no.87-97, 58pp.
- Walker, A.B., Redmayne, D.W. and Browitt, C.W.A. 1992. Seismic monitoring of Lake Nyos, Cameroon. in: Natural Hazards in West and Central Africa (eds. S.J.Freeth, K.M.Onuoha & C.O.Ofoegbu) pp.109-136 Vieweg, Braunschweig.

## THE NEED OF REAL-TIME DEVICES FOR MEASURING VOLCANIC AND SEISMIC SIGNALS

M BALCAZAR, N SEGOVIA, M MONNIN,  
A CHAVEZ, J H FLORES  
Instituto Nacional de Investigaciones Nucleares,  
Mexico City, Mexico

### Abstract

Radon emanation measurements in Mexican volcanic and seismic regions have been carried out since 1980. Radon stations are mainly located near the active volcanoes and along the Ocean Pacific coast where tectonic plaques produce most of the earthquakes in Mexico.

Data has been collected by means of plastic passive detectors, automatic passive radon monitor, scintillation counters and recently with active solid state detectors. Developments and/or adaptations of passive and active monitors have been necessary due to the lack of commercial existence specially in the early days.

### 1 INTRODUCTION

Since 1980, The Nuclear Centre of Mexico has been working together with several Mexican institutions in order to detect Radon gas in air, soil and water. Detection purposes have been for monitoring volcanic and seismic activities [1], assessing anomalous radon concentrations in a research reactor [2], prospecting geothermal energy sources [3][4][5], determining uranium mineral distribution in a low radioactive waste storage [6] and measuring indoor radon concentrations [7][8][9].

The mayor radon data collected so far, for seismic and volcanic monitoring has been using passive solid state nuclear track detectors, for which it has been necessary to develop both automatic counting methods [10][11] and equipment for detector calibrations [12]. Passive plastic detectors have the disadvantage of being collected point by point after exposures of 20 to 40 days, so for a large country having important tectonic and volcanic areas to be covered in Mexico, this means a 4000 km travelling detector collection campaign each month. An additional disadvantage is the missing observation of the very short time radon variations, whose analysis provides important data for modelling.

Besides the Mexican experiences on data analysis presented by De la Cruz-Reyna S et al. [1] it is worth to mention two additional aspects: development of home made

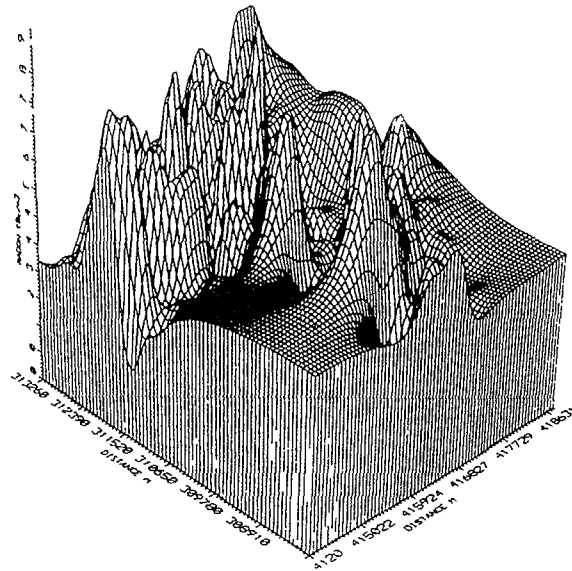


Figure 1 Radon anomalies from soil in a geothermal field having active faults are affected by seismic activity

radon monitoring equipment and radon anomalies observations in geothermal fields, situated rather close to seismic and volcanic regions

## 2 RADON MEASUREMENTS IN GEOTHERMAL FIELDS

Radon measurements in soils have been carried out in geothermal fields under prospection, as well as those fields already in production. Radon data started to be collected in Mexican geothermal fields for determining active faults to which there is a probability to find an associated heat source [3][5]

Passive radon monitors (PRM) were developed and calibrated [12] to place hundreds of them, at the same time in large geothermal areas. Figure 1 is a typical preliminary radon distribution obtained from 400 PRM, covering an area of 25 km<sup>2</sup>. Having these results, a geostatistical approach [13] is then used to optimize the size of the sampling net for obtaining additional radon concentration distributions. Usually geothermal faults are well correlated with a few exceptions, to high radon activity

Radon concentrations in soils from four geothermal fields situated in the so called Mexican volcanic belt are in the order of a few thousands of Bequerels/m<sup>3</sup> [14]. Their analysis have identified, in high radon emanation fields, several faults across of which it is worth to search for seismic signals [15][16]

Our radon investigations in geothermal fluids from producing geothermal wells led to unexpected results [4] on the big earthquake ( $M_s = 8.1$ ) occurred in Mexico on 19 September 1985. A long-term observation of radon content in fluids from producing geothermal wells, in Los Azufres Mexican geothermal energy field, was carried out in order to look for a correlation of radon concentration with specific volume of the geothermal fluids, the reason being that the specific volume is directly proportional to the enthalpy of the well, i.e. the energy production

Sampling fluids were taken in the field through a small "T" pipe connected to the main vapour output line and then radon was insulated and evaluated in the laboratory by means of a scintillation counter, everything according to a standard procedure [17]. Results of radon sampling from 1983 to 1988 are presented in Figure 2, the numbers in the graph at the left side of Figure 2 correspond to the monitored geothermal well,

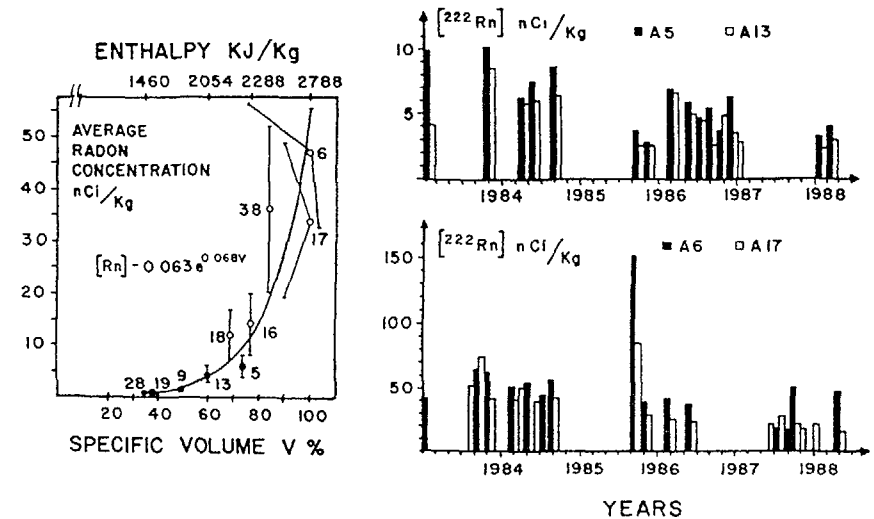


Figure 2 There is an exponential dependence of radon specific activity with enthalpy in fluids from producing geothermal wells (left graph). Big radon fluctuations in high enthalpy wells are influenced by seismic activity (histograms at the right)

additionally to the high dependence of specific activity with specific volume obtained, it is observed that big fluctuations of radon specific activity (see error bars) are present in high enthalpy wells; among other factors, we believe that these fluctuations are influenced by extra radon liberation induced by earthquakes. Histograms on the right side of Figure 2 shows radon specific activity for low enthalpy wells A5 and A13 and for high enthalpy wells A6 and A17; the general tendency in those histograms for the earthquake mentioned above is a decreasing of radon activity for wells of low enthalpy and an opposite behaviour for wells of high enthalpy. Unfortunately there is lack of information in some periods and the program run out of money in 1988.

### 3. PASSIVE AND ACTIVE AUTOMATIC RADON MONITORS

Because there are quite a few recent review papers on radon detection systems [18][19], this section deals only with the Mexican experience in setting and operating both passive and automatic radon monitors in seismic and volcanic regions.

Through the ININ-MontPellier collaboration, it was designed constructed and tested a passive automatic radon monitor. This monitor is a 1.5 m long PVC tube, 10 cm in diameter, in which it is possible to place up to 25 thin plastic detectors in such a way that, only one detector is exposed to environmental radon, remaining the other 24 detectors protected from radon gas. A mechanical device automatically controlled by an electronic clock, removes the uncovered detector from radon exposition and bares another one. Calibration of the passive automatic radon monitor in a controlled radon chamber led to results displayed in Figure 3: top histogram shows the radon activity registered by 19 detectors. A signal to noise ratio of 4.8 is obtained from the 5 unexposed detectors in the monitor; detectors marked with  $T_1$  y  $T_2$  were left outside the monitor exposed to environmental radon in the laboratory. If the open-end of the monitor is covered by a thin polycarbonate film, the signal to noise ratio increases up to 7.2 (middle histogram, Figure 3). Field results, at the bottom histogram of Figure 3, clearly show strong radon variations in short periods of time. This particular monitor is useful for placing it in those areas of either difficult access or where high radon concentration of a few thousands Bq/m<sup>3</sup> are commonly found. Exposition time is constant for all the 25 detectors however, it is possible to select exposition time from a minimum of 10 hours up to a maximum of 7 days. Adjustments in the clock allow to change this interval of exposition time, and a couple of rechargeable portable 12V batteries provide energy to the monitor during six months.

Two kinds of active radon detectors have been recently put into operation; the first one is a silicon surface barrier detector (SSBD) which has been adapted for assessing

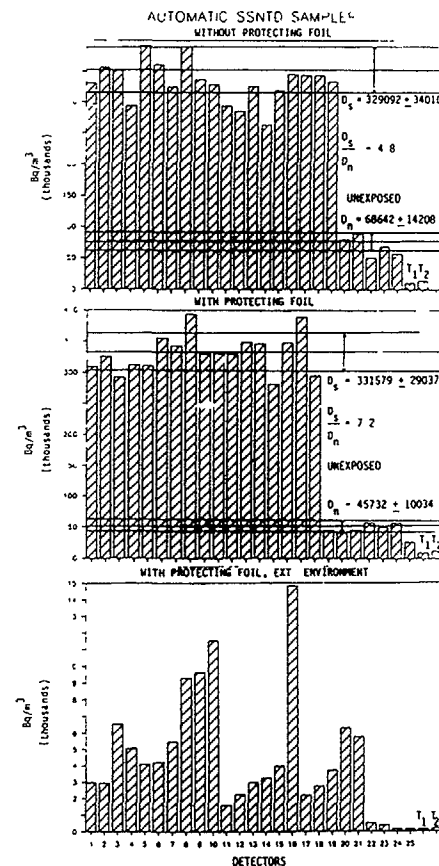


Figure 3. During calibration procedure, an increase of the radon signal to noise ratio from 4.8 (top histogram) to 7.2 (middle histogram) is achieved by covering the open-end of the home-made passive automatic radon monitor. Field performance (bottom histogram) shows short-time radon-variations.

real-time radon signals in soil. Monoenergetic  $\alpha$ -emitting sources permits to performe a fine calibration (Figure 4a), in order to avoid overestimation of radon signals; this is achieved by fixing an electronic window for separating radon decay products (Figure 4b)



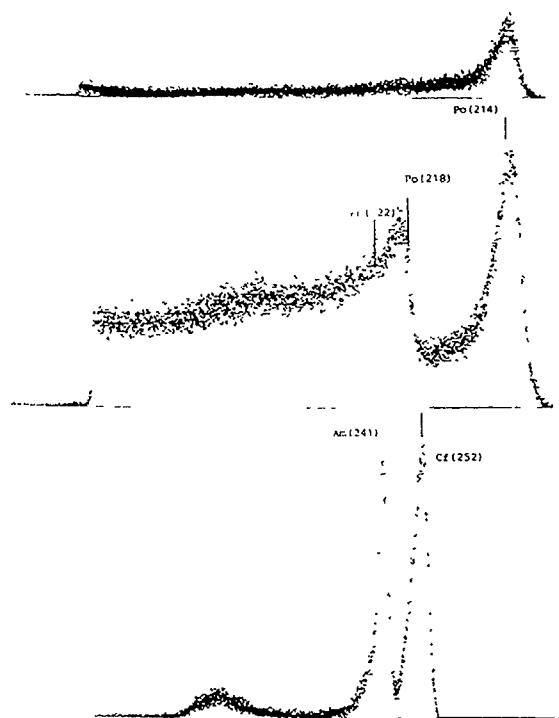


Figure 4. Calibrations of active solid state semiconductor detectors and a appropriated software permits to substract radon daughters from radon avoiding radon overestimation.

The SSBD is covered by a thin polyethylene to protect it from humidity and corrosive gases which are usually present in geothermal fields. The thin cover protects also the SSBD from the deposition of  $^{214}\text{Po}$  on its active surface; Figure 4c shows the  $\alpha$ -counting by other SSBD of the removed cover from the SSBD exposed in the field. This SSBD has the disadvantage of using bulk electronics and standard power supply limiting its use to those areas where there is a laboratory near by.

A second real-time device is a commercial  $\text{Si}(\text{Li})$  detector manufactured by Alpha Nuclear Co., Canada, a small portable detector which operates with batteries.

#### 4. CONCLUSIONS AND PROPOSAL

Amongs the possible precursors of earthquakes and volcano eruptions is Radon emanation. The encouraging fact is that scientists around the world have observed that about 70% of earthquakes are associated to radon anomalies; although at the same time 40% of radon anomalies occur without any earthquake.

A filtering of factors, others than earthquakes which influence radon emission are needed; the following recomendations may contribute to improve radon data analysis.

- Identification of areas where radon data has a bigger probability of being affected, mainly by earthquakes and volcano eruptions.
- Installation of real-time radon detection devices at specific sites, preferably with telemetry equipment to capture the signal at a central station.
- Installation of other geochemical precursors at the same sites.
- Starting a multidisciplinary approach to data processing in order to establishing a continuous data feed-back to improve the already existing models.

From the radon-data collection-campaign carried out for the last 13 years by the Instituto Nacional de Investigaciones Nucleares (ININ), it is possible to propose a few active faults and producing geothermal wells in two geothermal fields (Los Azufres and Cerro Prieto) and in some selective sites at the west coast of Mexico. As far as volcanoes in concerned Colima, the most active one and Popocatepetl seems suitable places; the former is already under study by several laboratories not just by mexicans but from abroad as well, the later is an active volcano 100 km far from Mexico City, easy to reach by car.

Most of the preliminary selected sites have associated laboratories to install protected stations. In some cases, it would be possible to use the already existing telemetry facilities, for example, the Faculty of Engineering of the University of Mexico has been continuously operating for the last 16 years, ten telemetry seismic stations[20], the fareset being 300 km from Mexico City. Seismometers of those stations identified in 1990, 52 earthquakes with  $M_s > 4$ , 4 with  $M_s > 5$  and zero with  $M_s < 5.97$ . A conection between this central laboratory in Mexico City and ININ is possible via commercial systems (TELECOM, TELENET, TELEPAK, TYMNET, etc.) or parabolic antennas both through standard modems.

The collaboration of good geochemistry groups at the University of Mexico (UNAM), Centre of Scientific Research and High Education (CICESE), Institute of Electric Research (IIE) and others would be possible, perhaps through a coordinate program supported by the IAEA. The economical support of this collaboration, is compulsory to achieve a multidisciplinary approach to the problem and so, to perform a better data modelling and to ensure long-term data collection.

#### REFERENCES

- [1] De la Cruz-Reyna S, et al. Some Isotopic and Geochemical Anomalies observed in Mexico prior to Large Scale Earthquakes and Volcanic Eruptions. This Technical IAEA Publication.
- [2] Balcázar M., Chávez A.. Anomalous Indoor Radon Concentration in a research reactor building. 29th Hanford Symposium on Health and the Environment. Richland, USA. October (1990).
- [3] López A., Gutiérrez R., Balcázar M. Radon Mapping for Locating Geothermal Energy Sources. Nuclear Instrument and Methods in Physics Research A-255 (1987) 426-429.
- [4] Balcázar M., Santoyo E., González E., González D.. Radon Measurements in Heat-Producing Geothermal Wells. Nucl. Tracks Radiat. Meas. 19 (1991). 283-287.
- [5] Balcázar M., González E., Ortega M., Flores J. H. Geothermal Energy Prospecting in El Salvador. To be published in Nucl. Tracks Radiat. Meas.
- [6] Balcázar M., Chávez A., Tavera L. Environmental Radon Monitoring in a Low-Radiative Waste Storage. To be published in Contamina. Int. J. on Environmental Sciences.
- [7] Balcázar M., Chávez A. Evidence of Radon Build up in utilities service conduits. Nuclear Tracks Radiat. Meas. 19 (1991) 289-290.
- [8] Segovia N., Gaso I., Chávez A., Tejera A., Gutiérrez A., Azorín J., Balcázar M. Environmental alpha and gamma survey. Radiat. Prot. Dos. J.
- [9] Segovia N., Peña P., Tamez E. Radon Survey in Mexico City. Nucl. Tracks Radiat. Meas. 19 (1991) 405-408.
- [10] Lira J., Balcázar M. Image processing technique for the evaluation of electrochemically etched spots. Nuclear Tracks 7 (1983) 101-103.
- [11] Balcázar M., Chávez A. A modified version of a spark counter for  $\alpha$  spectroscopy. Nuclear Tracks and Radiat. Meas. 8 (1984) 617.
- [12] Balcázar M., Pineda H. Versatile Irradiation Chamber to Perform Experiments with SSNTD. The Nucleus 20 (1983) 75.
- [13] Flores Ruiz J. H., Balcázar M. Optimum radon sampling distance in the Ceboruco geothermal field. ININ, Internal Report, IA 91-41, May 1991.
- [14] Balcázar M., López A., Cuapio L. Radon as a Signal to Locate Geothermal Energy Sources. International Workshop on Radon Monitoring in Radioprotection, Environmental Radioactivity and Earth Sciences. ICTP, Ed.: World Scientific, Singapore; (Tommasino L., Furlan G., Khan H. A., Monnin M. Ed.) Trieste, Italy (1990) 463-468.
- [15] Segovia N., De la Cruz-Reyna S., Mena M., Ramos E., Monnin M., Seidel J. L. Radon in Soil Anomaly observed at Los Azufres Geothermal Field, Michoacan. A Possible Precursor of the 1985 Mexico Earthquake ( $M_s = 8.1$ ). Natural Hazards 1 (1989) 319-329.
- [16] De la Cruz-Reyna S., Isabelle D. B., Mena M., Monnin M., Romero M., Segovia N., Seidel J. L., Pialox P., Armienta M. A. Radon Emanation Related to Geothermal Faults. Int. J. Radiat. Appl. Instrum. Part D. Nucl. Tracks 12 (1986) 875-878.
- [17] Santoyo F., Verma S. P. and Nieva C. Metodología y Principios Utilizados en el Monitoreo de  $^{222}\text{Rn}$  en Fluidos Geotérmicos. Los Azufres, Mich. V Seminario sobre Especialidades Tecnológicas IIE-IMP-ININ 14 (1990) 9-20.
- [18] Urban M., Schmitz. Radon and Radon Daughters Metrology: Basic Aspects. To be published in Proceedings of the Fifth International Symposium on the Natural Radiation Environment, Salzburg, Austria, September 1991.
- [19] Monnin M., Seidel J. L. Radon in Soil-Air and in Groundwater Related to major Geophysical Events. A Survey. To be published in Proceedings of the Fifth International Symposium on Radiation Physics. Dubrovnik, Croatia, June 1991.
- [20] Torres-Nogues M. Operation and Improvements of the SISMEC Network. Final Report. Faculty of Engineering, UNAM, Mexico. August 1991.

## GEOCHEMICAL SURVEILLANCE OF ACTIVE VOLCANIC AREAS IN ITALY: CAMPI FLEGREI CALDERA AND VULCANO ISLAND

D TEDESCO

Osservatorio Vesuviano,  
Naples, Italy

### Abstract

In the last ten years the prediction of volcanic eruptions with geochemical methods has largely increased his reputation in the volcanological community. Nevertheless since today, unfortunately no one eruption has been studied and followed systematically and predicted with geochemistry.

In this article we discussed about our experience on Italian volcanoes.

Two main areas have been studied in the last years: Campi Flegrei caldera and Vulcano island. In both volcanic areas the volcanism is at the moment quiescent with the last eruptions in the 1538 in Campi Flegrei and 1888 at Vulcano island.

At the moment the volcanic activity is in a different stage between these two sites. In fact at Campi Flegrei we experienced two bradyseismic crises, the second one is described from a geochemical point of view in this article. We should remind that the volcanological system in Campi Flegrei shows its maximum temperature of about 160°C at the Solfatara crater. Of course we are clearly in presence of an hydrothermal system, this is confirmed by the chemical and isotopic composition of the fluids. At the same time several very active fumarolic fields are also present in Pozzuoli harbor.

Fumaroles at Vulcano island show a systematic variations in content of the chemical and isotopic species. These oscillations together with an increase of the outlet temperature of the fumaroles at about 650°C, largely increase the interest of scientists for the Vulcano activity for a possible future eruption. However our data seem to indicate a different explanation. Two main systems are present on the island, the first one mostly controlled by the superficial water tables in the beach area with a maximum temperature of about 100°C. The second one at the Fossa crater mostly controlled by magmatic fluids with a temperature of about 650°C.

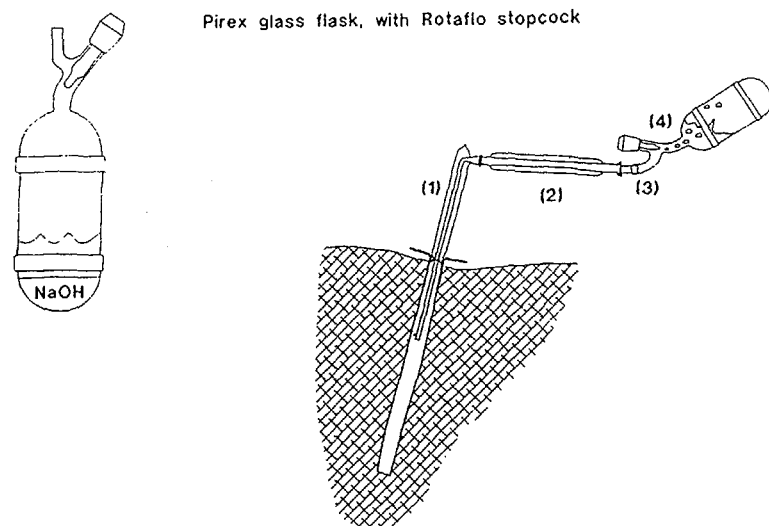
In this work our chemical and isotopic data will be discussed and for each volcanic area a simple volcanological model will be elaborated.

The surveillance of active volcanic areas and the prediction of volcanic eruptions is the tool of several international programs for the last decade of this century. In these programs the geochemistry of volcanic fluids play an important role to understand how volcanoes work. At the present moment the modelization of volcanoes with geochemical methods follows most of the time the philosophy of the researcher and often it is not based only on the real experience. In fact, unfortunately no one geochemist until today have had the possibility to study, to follow and to predict with geochemical techniques any volcanic crisis followed by an eruption. Nevertheless, in several countries studies on volcanic fumarolic fluids emanations, soil gases and thermal waters has been done for long time and today a solid basic knowledge exists. So, it is possible to extrapolate some main rules to follow the volcanic activity and to try to predict volcanic eruptions by geochemical parameters. Following our experience, it is necessary to start the study of active volcanic areas in a quiescent stage, because it might be easier to detect a baseline for all parameters that should be monitored.

### SAMPLING AND ANALYTICAL TECHNIQUES

Volcanic gases can be analysed by very different methods but in the last years most of the geochemists try to standardize the analytical techniques.

Volcanic fluids are conveyed from the fumarolic vents to the flask with a special device: quartz dewar tubes (until 500°C) or titanium tubes (> 500°C) to avoid chemical reaction and condensation of water vapor during the sampling. The gas is usually collected for chemical analysis in a pre-evacuated flask partly filled with a 4N sodium hydroxide alkaline absorbing solution (Giggenbach, 1975) which may concentrate by several hundred times the content of the so-called uncondensable gases (fig. 1). Typically more than one mole of fumarolic fluids (dry gas + water vapour) is introduced into the sampling volume of ca. 250 cm<sup>3</sup>. The enrichment occurs because water vapour (H<sub>2</sub>O) and acid species (CO<sub>2</sub>, SO<sub>2</sub>, H<sub>2</sub>S, HCl)



SAMPLING LINE: dewar quartz tubes (1-2); pirex and rubber connection (for temperatures less than 300°C at the pipe exit) (3); pirex flask (4).

Fig. 1 - Sampling device routinely used to collect volcanic gases from fumaroles.

and HF) labelled condensable species, that account for more than 99,5% of the total gases, are trapped and dissolved in the alkaline solution until the solution will be saturated. At the same time the uncondensable species (He, H<sub>2</sub>, O<sub>2</sub>, Ar, N<sub>2</sub>, CO and CH<sub>4</sub>) remain above the alkaline solution. To analyse the gas composition, a flame ionization detector (FID) is used downstream from a methanizing oven, in series with a 3 m. Porapak R column at room temperature. The other gas species were analysed with a thermal conductivity detector (TCD) downstream from 3 m. molecular sieve 5A column, either at 65°C with helium as carrier gas (for analysing He, H<sub>2</sub>). After determining the volume ratio between the liquid phase and the gas phase in the sampling bottle, the CO<sub>3</sub><sup>=</sup> and S<sup>=</sup> ions in the alkaline solution were analysed by conventional methods of neutralization by HCl and titration by Pb(ClO<sub>4</sub>)<sub>2</sub> using pH-electrode and sulphide ion-sulphide electrode (Tedesco, 1987). SO<sub>2</sub> is first

Table 1. Volumetric composition of sample VC FA 034

H <sub>2</sub> O (%)	CO <sub>2</sub> (%)	SO <sub>2</sub> (%)	H <sub>2</sub> S (%)	HCl (%)	HF (%)	H <sub>2</sub> (%)	N <sub>2</sub> (%)	CO (%)	He (%)	O <sub>2</sub> +Ar (%)	CH <sub>4</sub> (%)
Uncondensable	gases										
						63,32	34,79	1,65	0,04	0,20	0,03
Dry gases	81,05	8,52	4,61	3,87	0,54	0,90	0,49	0,027	0,0007	0,0032	0,0005
Overall 85,59	chemical 11,68	composition 1,23	0,66	0,56	0,077	0,13	0,071	0,0034	0,00	0,0004	0,000073
Accuracy (%) 2	2	4	3	4	4	5	10	2	10	15	2

oxidized by peroxide in an oven at 100°C, then analysed as sulfate (SO<sub>4</sub><sup>=</sup>) by liquid chromatography, and then determined as the difference between the total sulphur (SO<sub>4</sub><sup>=</sup>) and H<sub>2</sub>S. HF and HCl analysis were also determined by liquid chromatography in the same analytical sequence with SO<sub>4</sub><sup>=</sup>. The mass of water vapour could then determined as the difference between the total mass of fluid and the mass of the so-called dry gases (Table 1).

The helium isotope ratios were measured after the separation and purification of the gases, following procedure as described by Sano and Wakita, (1985, 1988). About 0.3 cm<sup>3</sup> STP of each gas sample were introduced into a high-vacuum metallic line in which helium and neon were separated from the other components, using hot Ti-Zr getters and two charcoal traps held at liquid nitrogen temperature. The <sup>4</sup>He/<sup>20</sup>Ne ratio was measured on-line with a quadrupole mass spectrometer (Balzers, MG 112). Interference of doubly charged ions of <sup>40</sup>Ar with <sup>20</sup>Ne is controlled to be negligible. Helium was then complete purified from Neon by trapping the latter on activated charcoal at 40°K. Isotopic analyses were made with a dual collector modified VG 5400 mass spectrometer (Sano and Wakita, 1988). Complete separation of <sup>3</sup>He from H<sub>3</sub> and HD is insured by a resolving power of 600 at the 5% peak height. The experimental blanks were negligibly small compared to actual sample sizes. Both <sup>3</sup>He/<sup>4</sup>He and <sup>4</sup>He/<sup>20</sup>Ne ratios were

determined by comparison with a calibrated air standard and their accuracy reaches 3 and 10%, respectively.

## INTRODUCTION

Several active volcanic areas in the last years have been intensely studied from a geochemical point of view. Campi Flegrei caldera, Vulcano island, Kilauea crater, White island, Kusatsu Shirane are some of those. Also other volcanoes are currently studied, as well in the past, from the geochemical point of view by several researchers. However, the number of samples collected for each area is, in our opinion, not sufficient to have a complete spectra of chemical and isotopic data. In the past, the way of working on volcanoes has been discontinuous, and often we had several geochemical data concentrated in a very short period, and after for years no one analysis was made on the same volcanic area. These results show in most of the cases only a moment of the life of the volcano, that is not enough to have a complete and successful model of a volcano. We believe that these data are useful, but it is also necessary to collect routinely hundreds of samples for each fumarolic area all long the year. This work is important to detect a stable baseline for each parameter and to quantify the influence on chemical and isotopic species of physical parameters, sometime external to volcanoes: marine and meteoric waters additions, earthquakes, tides, atmospheric pressure variations, and some others. This new kind of work is necessary, for example, to avoid "wrong warnings" in active volcanic areas densely populated, when some geochemical parameter starts to vary. It has been the case of Vulcano island.

After collecting volcanic fluids for years, and following all the available literature, we can say that from both low and high fumarolic gases is almost impossible to study a pure juvenile fluid. We have always to reason in terms of mixing between deep and surficial fluids or we can say, magmatic and hydrothermal fluids. Only in case of gases trapped in rocks as fluid inclusions as the MORB for example, it is possible to analyse the real content of

gases before the eruption. The quantification of this mixing and the variations/oscillations occurring with time, should give the exact proportion of each different member participating to the mixing. One more thing, is that at the contrary to what is believed, variations on fumarolic fluids usually occur in a very short time and only collecting a big number of samples it is possible to record them. One of this case has been the chemical variations occurred at the Solfatara of Pozzuoli during and after the bradyseismic crisis (Carapezza et al., 1984; Cioni et al., 1984; Tedesco and Sabroux, 1987). One more example is the variations occurred on Halemaumau fumaroles (Kilauea crater-Hawaii) (Stokes, unpubl. data), or on Vulcano crater fumaroles (see this chapter). We cannot state that all volcanoes, if sufficiently well monitored, shown the same type of variations, but it is also true that all fumaroles on volcanoes we intensely studied, have shown that chemical and isotopic parameters are continuously affected by variations, sometime independently from what it is strictly called "volcanic activity". In this chapter we will discuss about the Campi Flegrei and the Vulcano island activity from a geochemical point of view.

## THE CAMPI FLEGREI CALDERA: AN INTERPRETATION OF CHEMICAL AND ISOTOPE DATA

### A UNIQUE CASE: THE BRADYSEISMIC CRISIS OF 1982-1984;

The Campi Flegrei caldera (fig. 2) has been in the last 20 years affected by two different bradyseismic crisis (seismic activity and ground deformation). The first one occurred in the 1970-1972 and the second one in the 1982-1984. Since 1982, the Campi Flegrei volcanic district, on the west coast of Italy, has experienced a period of ground uplift (fig. 3) (with a maximum of 180 cm) and sustained seismicity including several hundred felt earthquakes (Barberi et al., 1984) with a maximum  $M=4.0$ . The vents are being monitored by a permanent surveillance network, which, in common with similar systems deployed elsewhere, e.g.

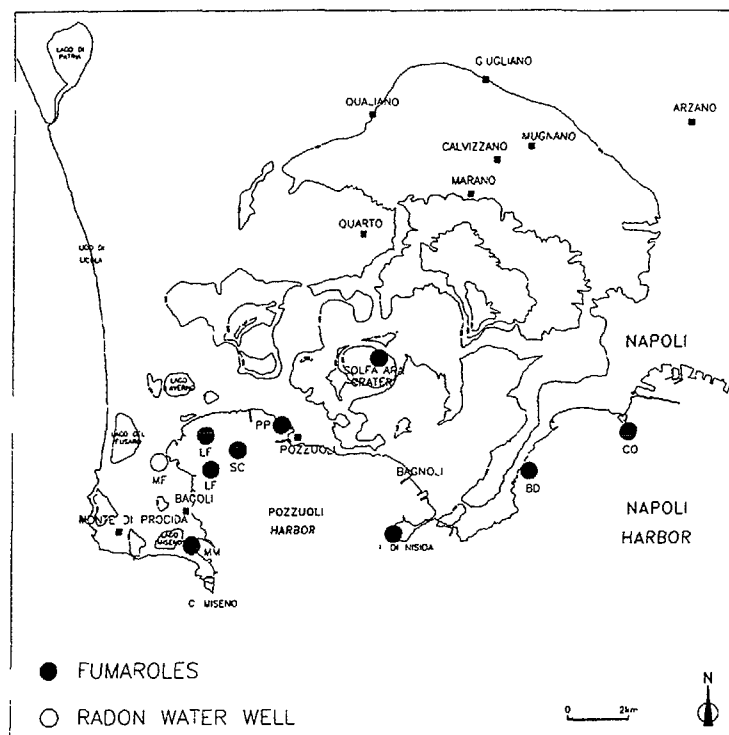


Fig. 2 - Campi Flegrei caldera map. Full circles indicate location of fumaroles. Open circle indicate Radon water well.

the Long Valley/Mono Basin volcanic complex (Hermance, 1983) or the Rabaul caldera (McKee et al., 1985), utilizes predominantly geophysical methods (such as seismometry, microgravimetry and high precision ground levelling). In the Campi Flegrei, however, the additional possibility exists of conducting geochemical monitoring of fumarolic gases, particularly those escaping from the crater of the Solfatara, the site of the most conspicuous superficial thermal anomaly in the area and from several submarine fumaroles seated in the gulf of Pozzuoli and in the gulf of Napoli. If sufficiently accurate, the analysis of such gases provide informations on the conditions of temperatures and pressures in the hydrothermal or

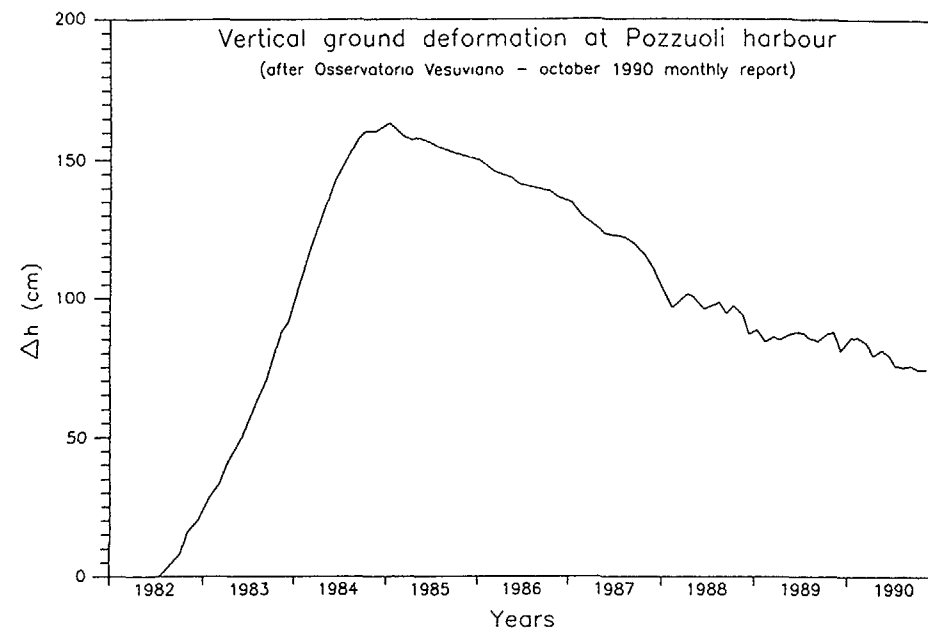


Fig. 3 - Vertical ground deformation at Pozzuoli harbor. Uplift started on 1982 (March) and stopped on December 1984. Since then a slow negative movement occurred with a total downlift of 80 cm.

magmatic reservoirs feeding the fumaroles, on the physico chemical evolution of that reservoir, and on any connections between it and an underlying body of hot magma. At the same time to better constrain the genesis of these fluids and the extension of these reservoirs (superficial and deep) several isotope analysis has been carried out in order to define the relationships between deeper and superficial systems. We have therefore collected and analysed a series of volcanic gas samples from the Solfatara crater and from several submarine fumaroles in Pozzuoli and Napoli harbors, obtained at intervals after October 1983. We also assessed the data to determine how closely these fluids meet the conditions necessary to be used as geothermometers and geobarometers. It has been pointed out that several variations affected the fumarolic fluids of the Solfatara crater during the

decline of seismic activity. Cioni et al., (1984) pointed out that some variations in the content of chemical species probably occurred also before the starting of the bradiseismic crisis.

#### Presentation and discussion of data

Water vapor ( $H_2O$ ) started to increase between 1981 and 1982, Hydrogen Sulfide ( $H_2S$ ) and the Carbon/Sulfur (C/S) ratio started to increase between the end of 1980 and the beginning of 1981. Data on methane ( $CH_4$ ) that seem less reliable for their reduced accuracy (Cioni et al., 1984) also seem to vary since 1981. All other species ( $H_2$ ,  $N_2$ , Ar, CO and He) except carbon dioxide ( $CO_2$ ) that decreased, exhibits practically constant values (Martini et al., 1986).

A first approach to understand the cause of these chemical variations seem to be a correlation between these changes and an increase in the flow of the heat flux from deeper reservoirs to near-surface hydrothermal systems, one of these feeding the Solfatara crater (Tedesco et al., 1988 a, b; Tedesco et al., 1990) rather than to a direct injection of magmatic fluids towards the surface. In fact, given the lack of variations and increase in content of the so-called magmatic species such as carbon monoxide, present only as a minor species (0,1 ppm of the total fluid) and the constancy of the helium isotope ratio, we consider that no new magmatic fluids were involved before and during the bradysismic crisis (Tedesco et al., 1988b). From the beginning of 1984 starts a new phase of variations of the chemical composition of these fluids (fig. 4). Firstly  $H_2S$ ,  $CH_4$ ,  $N_2$  and  $H_2$  strongly decrease followed at the beginning of 1985 by the  $H_2O$ . During this period the content of helium and carbon monoxide remained practically constant. We interpreted these variations as a decrease in the energy transfer (as thermal flux) from deeper reservoirs. This simple model, graphically showed in fig. 5 is also supported by thermodynamic calculations obtained using the water-gas-shift reaction.

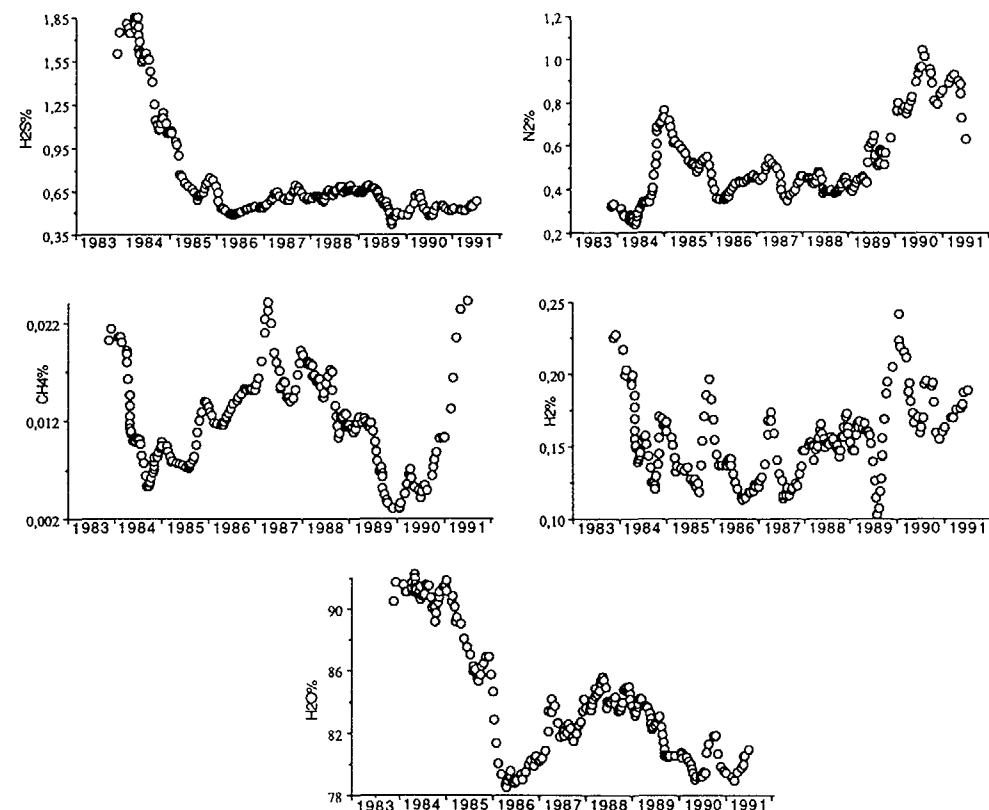
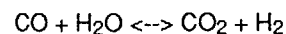


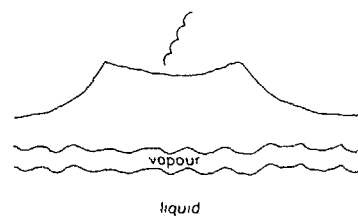
Fig. 4 - Several chemical species have shown dramatic changes in their content:  $H_2S$ ,  $N_2$ ,  $H_2$ ,  $CH_4$  and  $H_2O$  started to decrease at the beginning of 1984 (February-March), before the end of both ground deformations and seismicity.

A new increase phase started from 1985-1986 until 1988.

Seasonal variations sometimes overlapped the main trends.

This reaction allowed us to calculate an equilibrium temperature for the Solfatara crater system of about  $250^\circ C$  in 1983-1984 (fig. 6) (Barin and Knacke, 1973; Barin et al., 1977). From 1985, in two different stages, the equilibrium temperature dropped of about  $50^\circ C$ : (a) the first stage occurred from the end of the bradyseism (1985) until the beginning of 1986 followed by a new increase; (b) the second phase, of decreasing temperature, has taken place

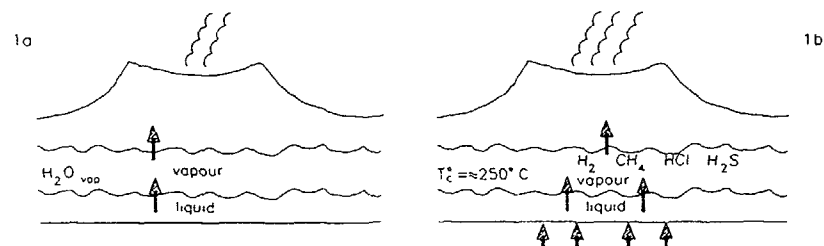
Situation after 1970–1972 bradyseismic crisis



Calculated Equilibrium Temperature  
is observed by  
 $\text{CO} + \text{H}_2\text{O} \rightleftharpoons \text{CO}_2 + \text{H}_2$

$T_c \approx 200^\circ \text{C}$

Situation before and during the crisis



After bradyseismic crisis

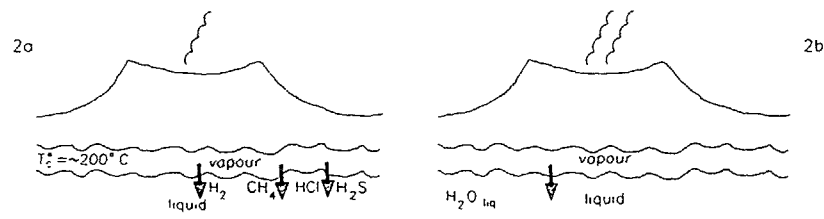


Fig. 5 - Physical variations probably occurring at the Solfatara hydrothermal system. Variations of the level of the Solfatara crater reservoir during the different phases of the bradyseismic crisis.

during the last two years since the beginning of 1989. These two events may also have been preceded, before the seismic activity started in 1982, by a similar increase of the temperature of the hydrothermal reservoir, probably of the same magnitude. In agreement with this hypothesis, Cioni et al., (1984) estimated a positive  $\Delta T$  of at least  $20^\circ \text{C}$  from the variations of the  $\text{CO}_2$ /vapor ratio before the crisis.

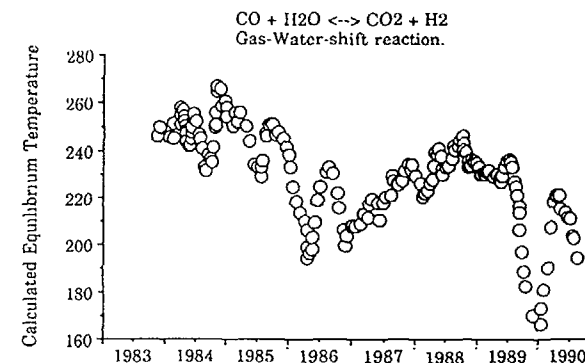


Fig. 6 - The calculated equilibrium temperature also show a wide variations. We can follow 3 different periods: (1) from 1983 to 1986, from  $\approx 250^\circ \text{C}$  to  $\approx 200^\circ \text{C}$ , (2) from 1987 to 1988, from  $\approx 200^\circ \text{C}$  to  $\approx 240^\circ \text{C}$  and finally (3) from 1989 until today, from  $\approx 240^\circ \text{C}$  to  $\approx 240^\circ \text{C}$  with a negative peak of  $\approx 160^\circ \text{C}$  (nearly the sampling temperature).

### Origin and variations of $\delta^{13}\text{C}$

Being  $\text{CO}$  and  $\text{CH}_4$  present in the whole gas phase in Solfatara fumaroles only in a few ppm species (Table 1), the only  $\text{CO}_2$  accounts for the  $\delta^{13}$  values. The data obtained at the Solfatara fumaroles since 1970 indicate values of  $\delta^{13}$  between  $-1.9$  and  $-0.8\%$  before the bradyseismic crisis of 1982-1984. Data obtained after the crisis seem more stable (Allard et al., 1991) and they range between  $-1.9$  and  $-1.6\%$ . Other values also very close to previous one were obtained by Carapezza (Carapezza et al., 1984) on 1983 range between  $-1.73$  and  $-1.49\%$ . These results show that despite the strong variation of the  $\text{CO}_2$  content in gas phase, the  $\delta^{13}$  remained quite stable over more than 20 years.

Allard et al. (1991) deeply discuss the origin of carbon in Solfatara and Campi Flegrei fluids. They argue that the constant  $\delta^{13}$  values over the period 1970-1988 is an evidence for a stable source of carbon. This source should be also both large and deep enough for conciling the lack of isotopic balance effects with, respectively, the  $\text{CO}_2$  output from the crater [170-350 tons/day; (Carapezza et al., 1984)] and the extensive mechanical and hydrological disturbances which affected the last few km of the



caldera's basement during the bradyseismic crisis of 1982-1984 (Barberi et al., 1984) As well as for helium isotopic data,  $\delta^{13}$  values obtained in Campi Flegrei caldera, are much higher than those normally obtained for mantle-magmatic carbon [ $-6 \pm 2\%$ , (Allard, 1983, 1986; Javoy et al., 1984)] and are more similar to typical marine carbonates that have a range between  $0 \pm 2\%$  (Degens 1969) Also other fumaroles seated in the east part of the caldera - Mare Morto, Secca Caruso, Le Fumose a and b, Porto Pozzuoli - (fig. 2) as well fluids from geothermal wells showed values between the range of marine carbonates

#### Temporal $^3\text{He}$ variations

In 1978, four years before the onset of the 1982-1984 bradyseismic crisis, Poliak and Tolstikin (1980) measured a  $R/R_a$  value of 2.7 for the Solfione fumarole, using a special container for helium isotopic analysis Our results for the same fumarole in October and December 1983, during the acme of the crisis, are very close ( $2.8 \pm 0.1$ ) and, therefore, show no evidence of increasing  $^3\text{He}/^4\text{He}$  due to the events During the same time, the Bocca Grande fumarole displayed somewhat lower  $R/R_a$  values (2.4-2.5) in spite of its proximity to Solfione (a few tens of meters) A value of 2.9, typical of Solfione, was however measured in this fumarole in June 1988, nearly four years after the end of the crisis, values from 2.9 to 3.2  $R/R_a$  were then measured from 1988 to 1991 (fig. 7)

It is noteworthy that in December 1984, as the bradyseism was vanishing, the Pozzuoli Porto (PP) submarine fumarole, the closest to Solfatara, displayed a similar  $^3\text{He}/^4\text{He}$  ratio as the Bocca Grande fumarole during the crisis This similarity thus lends support to the idea that the helium isotopic composition of Campi Flegrei fumaroles remains steady over the whole bradyseismic period In contrast the result obtained in 1986 show a tendency to increasing  $^3\text{He}/^4\text{He}$  in the PP, SC and LF-bg fumaroles (Tedesco et al., 1990) The variations well exceed the analytical uncertainty and are thus considered significant They represent a true  $^3\text{He}$  increase in these fluids after the crisis and correspond to a temporary

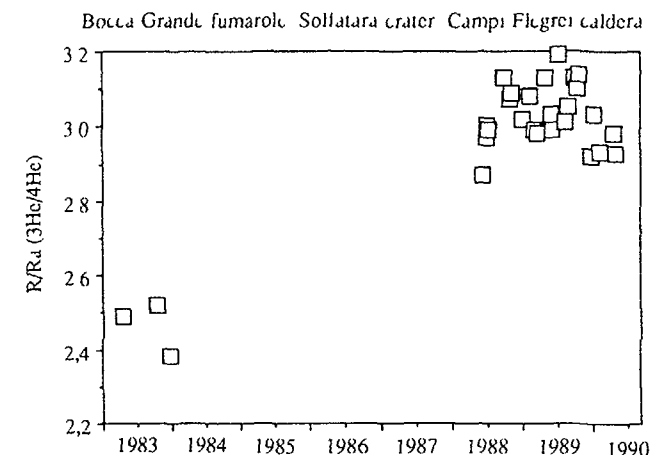


Fig. 7 - The helium isotope ratio show in 1983 - 1984 similar values to those obtained in 1978 by Poliak and Tolstikin (1982) Since 1988 the data are much higher than previous one, from 2.5  $R/R_a$  to  $\approx 3.0$   $R/R_a$  This variation is correlated to all others occurred in the caldera

variation that can be settled from the high number of data and the long interval of investigation These data are in good agreement with the chemical variations recorded at the Bocca Grande fumarole during the same period The results of radon monitoring in the caldera (e.g., Tedesco et al., 1988a) may provide some indications (Fig. 8) The variations of this radiogenic rare gas in monitored hot water wells follow a seasonal pattern, its activity increasing during the rainy winter season and then decreasing during the drier May-September period Such a pattern, which suggests a rapid input of meteoric water into the hydrogeological system, is attributed to enhanced/lower stripping of radon by circulating groundwaters from larger/smaller volumes of rocks, depending on the extent of water inflow If radiogenic  $^4\text{He}$  accumulated in the same rocks is extracted as well, then we might expect a lower supply of this isotope to hot waters and fumarolic gases during the dry season than in winter Observed seasonal variations of helium in the Bocca Grande fumarole (Tedesco, 1987; Tedesco et al., 1988b) are consistent with this hypothesis At the same time, a Radon increasing trend has been

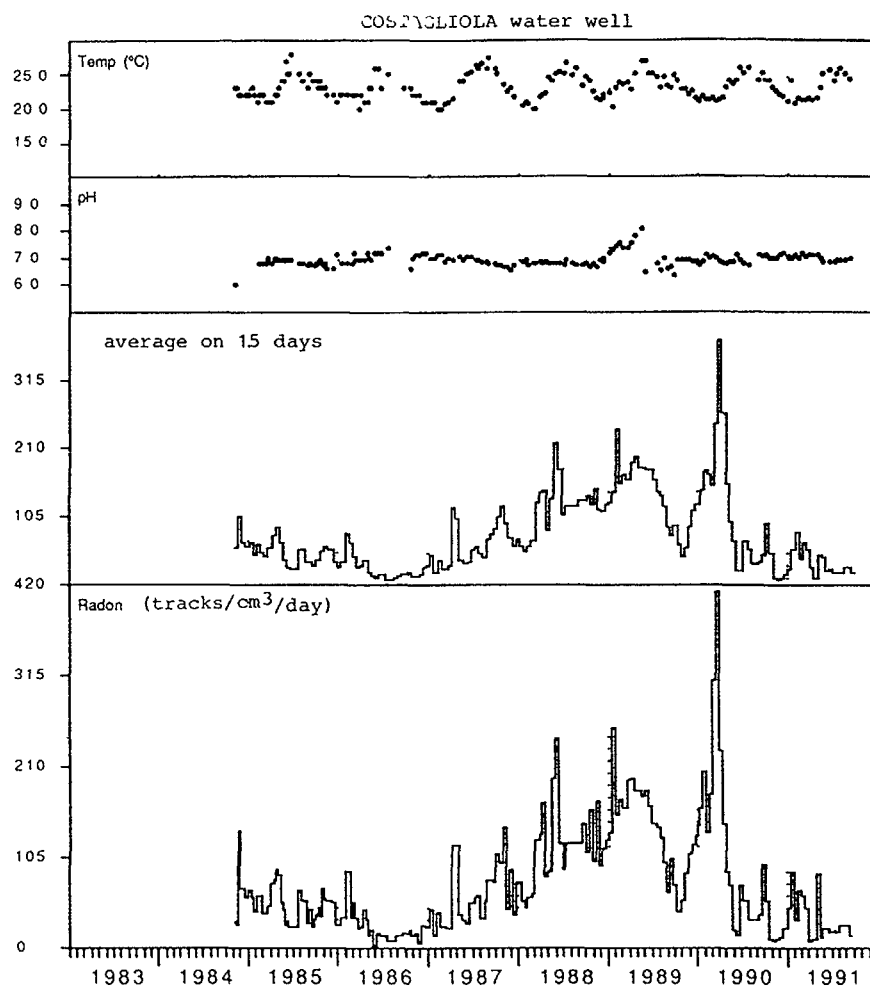


Fig. 8 - The Radon activity is closely related to the variations of the other chemical species collected at the Solfatara crater fumarole. Here is showed the continuous monitoring of Costagliola water well

monitored in different thermal wells of the Campi Flegrei region and it perfectly follow the chemical and isotopic variations registered at the Bocca Grande fumarole. Such a mechanism could thus explain the trend of increasing helium  $^3\text{He}/^4\text{He}$  ratio in some of the submarine gases collected in May-June 1986, but not the

higher  $^3\text{He}/^4\text{He}$  ratio of the Bocca Grande fumarole from June 1988 until today (fig. 7). It would also not account, however, for the high value measured at Solfione measured in December 1983, during the period of high seismicity and ground deformation. Nor can it preclude the possibility of a true  $^3\text{He}/^4\text{He}$  and Radon increase at Campi Flegrei after the 1982-1984 events.

Using these  $^3\text{He}/^4\text{He}$  data it has been possible to calculate that a maximum of 35% of the helium has a magmatic origin. During our studies we first hypothesized that the occurrence in the central part of the caldera of the hottest fluids (Solfatara of Pozzuoli,  $155^\circ\text{C}$ ) with also the highest helium isotope ratio, compared to the lower values obtained in the more peripheral fumarolic fluids (Secca Caruso, Le Fumose and Mare Morto fumaroles) indicated a greater leakage of magmatic species and higher heat flux from the central part of the caldera (Tedesco et al., 1990). Further results obtained on the same as well on new fumaroles do not agree with this model (fig. 9).

New helium data indicate that the  $^3\text{He}/^4\text{He}$  ratio is similar inside and outside the caldera, ranging from 2.5 to 2.9  $R/R_a$ , with values of 2.8 and 2.7 (close to the maximum, 2.9  $R/R_a$ ) up to 5 and 14 Km respectively from the central part of the caldera (fig. 10). These values do not support the notion that the magmatic leak and heat flow are mostly concentrated in the central part of the caldera. It appears, instead, that an homogeneous gas phase is present both in the Campi Flegrei caldera and its surroundings as has already been hypothesized by Tedesco (1987). The slight differences in the  $^3\text{He}/^4\text{He}$  ratio can be attributed to the different paths followed by fluids to reach the surface and to the different depth of local superficial hydrological systems present in and outside the inner caldera, through which the gases pass (Rosi and Sbrana, 1987). In this context, the origin of the gas is considered to be the same for all fumaroles collected in this area, even those belonging to neapolitan harbor. Slight isotopic changes occurring as it approach the surface and, passes through different layers and aquifers, where small amounts of crustal helium might be added. Accordingly, the gases from each fumarole appear to be characterised by their own chemical and isotopic history indeed.

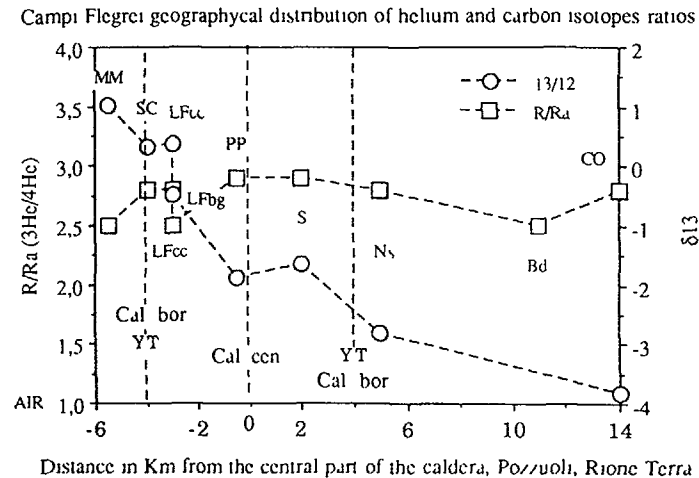
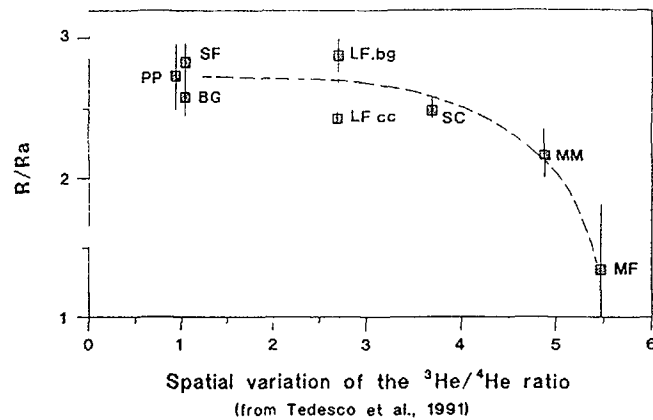


Fig. 9, 10 - The geographical distribution of the  $^3\text{He}/^4\text{He}$  and  $^{13}\text{C}/^{12}\text{C}$  ratios is different. Homogeneous all over the caldera ( $\approx$ almost 20 km) is the distribution of the helium isotope ratio. On the contrary the  $^{13}\text{C}/^{12}\text{C}$  ratio shows a different values from fumarole to fumarole with a trend from positive to negative going from Mare Morto (west) to Castel dell'Ovo (east) fumaroles.

even fluids collected at distance of only a few meters apart (10 meters) as is the case of the Le Fumose fumaroles (a and b), or in the Solfatara crater for the Soffione and Bocca Grande fumaroles (Tedesco, 1987) show different ( $^3\text{He}/^4\text{He}$ )  $R/R_a$ , 2.5 and 2.8,

which are almost the minimum and the maximum values recorded in the whole area (2.4 and 2.9  $R/R_a$ ). In conclusion even if the the  $^3\text{He}/^4\text{He}$  ratio in this volcanic area is not very high compared to other active volcanic areas (Tedesco et al., 1990; see Vulcano island) it seems to be uniform over a very wide area. Nevertheless, most of the conclusions reached in Tedesco et al. (1990) are still valid:

a) Measurements of He isotopes in the volcanic fumaroles of Campi Flegrei confirm that mantle-derived helium escapes from this caldera (Poliak and Tolstikin, 1980). The  $^3\text{He}/^4\text{He}$  ratios ranges between 2.5 and 2.9  $R/R_a$ , and there are no peculiar difference between subaerial and submarine fumaroles of the caldera, which indicates that both types of fluid are fed by a common helium source.

b) The  $^3\text{He}/^4\text{He}$  ratio of Campi Flegrei fumaroles is significantly lower than that of upper mantle volatiles and volcanic gases from other areas. Such a feature may reflect either a low mantle-magmatic He supply, a strong dilution of mantle gas by  $^4\text{He}$  from the crust, the radioactive aging of an isolated magma chamber, and/or a true characteristic of the local mantle. Further isotopic analysis of helium in both volcanic rocks and mantle-derived xenoliths from this area could help to distinguish between these alternatives. A shallow dilution by  $^4\text{He}$ -rich fluids, coupled with a decrease in the flux of the magmatic helium component, may be responsible for some of the lower  $^3\text{He}/^4\text{He}$  ratios. Otherwise, we point out that the low  $^3\text{He}/^4\text{He}$  of most volcanic gases and hydrothermal fluids in Western Italy coincides with a strong enrichment of the related volcanic rocks in radiogenic Sr, LIL-elements, and  $^{18}\text{O}$ , a feature primarily attributed to anomalous mantle composition.

c) Although limited in number, our data indicate that the proportion of  $^3\text{He}$  in the emitted helium did not increase during 1982-1984 bradyseismic crisis. This observation has important bearing as regards the origin of the crisis, particularly, it would exclude the

hypothesis of a shallow magma intrusion, associated with an increasing release of  $^3\text{He}$ -rich mantle magmatic gas. However, its significance could be strongly weakened if the magma chamber, for any of the reason mentioned above, does have a low  $^3\text{He}/^4\text{He}$  ratio, closer to that of the maximum helium isotope ratio of the caldera than of typical mantle helium.

#### GEOCHEMICAL MEASUREMENTS AT VULCANO ISLAND: A CHANGE IN THE VOLCANIC REGIME OR CONTINUOUS FLUCTUATIONS IN THE MIXING OF TWO DIFFERENT SYSTEMS?

##### Introduction

The Aeolian Archipelago (Southern Italy) consists of seven volcanic islands and numerous seamounts and is interpreted as a typical volcanic arc, generated by subduction processes beneath the Tyrrhenian sea (e.g. **Barberi et al., 1973 - 1974; Beccaluva et al., 1985**). Recent investigations about petrology and K/Ar ages of volcanics support this global scheme. Vulcano, the southernmost island is one of the active volcanoes of the archipelago. It lies a few tenth of kilometers north of the coast of Sicily (**fig. 11**). Its active cone (Fossa), 391 m high above sea level, last erupted in 1888-1890 (**Keller, 1980**). Since then intense fumarolic degassing has persisted in the Fossa crater with a peak in 1926 when fumaroles temperatures reached  $600^\circ\text{C}$  (**Sicardi, 1955**). More recently, after regional seismic event in April 15, 1978, reaching  $M=5.5$  and the following volcanic seismic swarm (e.g. Patti earthquake; **Del Pezzo and Martini, 1981; Falsaperla et al., 1989**), fumaroles underwent a temperature increase of more than  $100^\circ\text{C}$ , and variations in the chemical composition (**Martini et al., 1980; 1989; Carapezza et al., 1981**). Temperature decreased followed few years later. Again in 1987, the temperature of some crater rim fumaroles started to increase, and in particular we monitored at F5 fumarole an increasing temperature from about  $200^\circ\text{C}$  to  $330^\circ\text{C}$ . Since 1988, temperature rises were recorded at other fumaroles,  $470^\circ\text{C}$  being measured in mid-1988,  $550^\circ\text{C}$  in mid-1989 and about  $630\text{--}650^\circ\text{C}$  in 1991-1992,

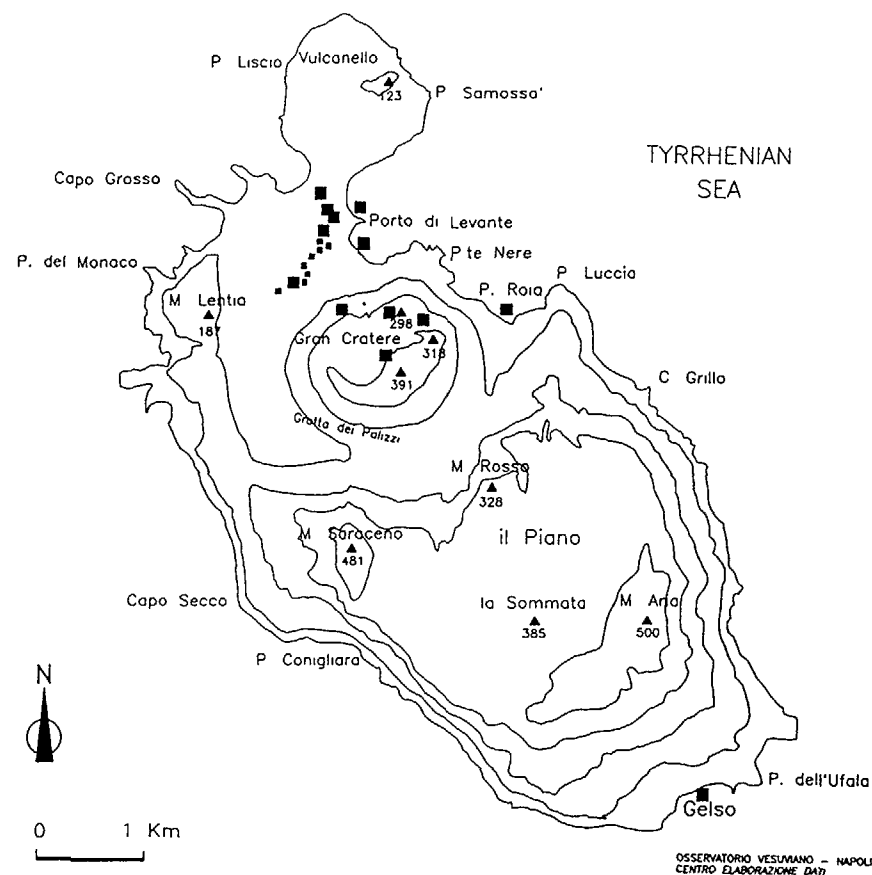


Fig. 11 - Vulcano island map. Large full dots indicate location of fumaroles and small full dots indicate water wells.

at the same site indicated by **Sicardi (1955)** as area A with  $600^\circ\text{C}$  in 1926. This recent thermal change was associated with an increasing gas flow, an aerial extension of the fumarolic field, and the opening of new fractures across the rim of the crater (**Martini, 1988; Tedesco et al., 1991**) and after, also inside the crater. Because of the highly explosive potential of Vulcano eruptions (**Sheridan and Malin, 1983; Frazzetta et al., 1984**) and for the presence of dense population on the island during

summer time (until 25,000 persons/day), these events brought some concern about increasing volcanic hazard. Accordingly, in order to determine their cause we performed an intensive monitoring of the F5 and FA crater fumaroles and several other beach fumaroles since mid-1987) (Tedesco et al., 1991). In particular, the F5 fumarole, located on the eastern rim of the Fossa crater, has been preferentially studied since many years by various authors (Tonani, 1971; Allard 1978; Martini et al., 1980, 1984; Carapezza et al., 1981; Cioni and Corazza, 1981; Le Guern and Faivre Pierret, 1982; Cioni and D'Amore, 1984; Mazor et al., 1988) owing to its steady temperature and access.

#### Total fluid

Figure 12 shows that the amount of water vapour in the fluid widely oscillate in content during the sampling period (Tedesco et al., 1990). It increased from 81% in July 1987 up to 95% in May 1988, and then decreased back to about 85% on December 1988. Since then a new variation occurred with a trend slightly different: an increase with the same slope of the previous one from January 1989, but once reached the maximum, 97%, the water content remained for a few months (3) stable and after started to decrease with a gentle slope (fig. 12). Actually we are still monitoring a decreasing trend, the value reached is between 88 - 90%. Hydrogen followed a similar pattern, its content varying by a factor 3 (fig. 12).  $\text{SO}_2$ ,  $\text{CO}_2$ ,  $\text{N}_2$ , He and HCl (fig. 13) exhibit an exact opposite pattern, which reflects their complementary response to the variations of water vapour, the dominant compound. Only  $\text{H}_2\text{S}$  shows comparatively limited oscillations (fig. 13).

In order to eliminate the influence of water changes, dry gas proportions and ratios were further considered. Hydrogen is the compound which fluctuates most remarkably, by about one order magnitude. A relative enrichment of sulphur with respect to carbon is observed and the S/C atomic ratio shows significant variation (-50%), matching that of  $\text{H}_2\text{O}$ , and peaks at the time of maximum of  $\text{H}_2\text{O}$  content. Simultaneously, total sulphur ( $\text{H}_2\text{S} + \text{SO}_2$ ) increased to

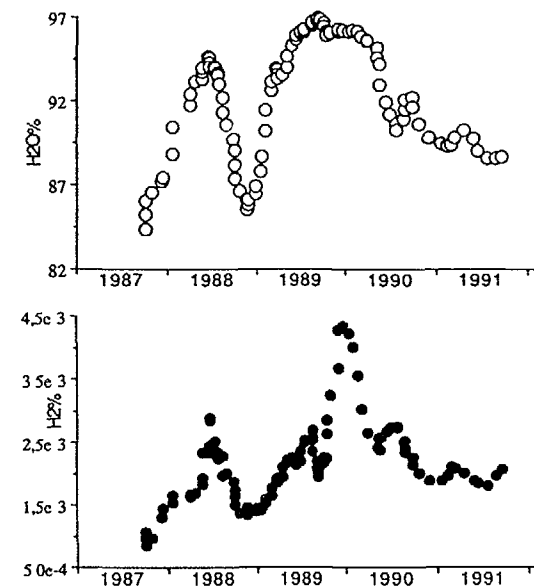


Fig. 12 -  $\text{H}_2\text{O}$  and  $\text{H}_2$  content at crater fumarole F5 show large oscillations in the chemical composition.

about 18% of the dry gases, and then returned close to the initial value, around 8%, again a new phase of variation started in 1989 with a similar pattern. Nitrogen and helium display comparable trends.

#### Discussion

Recent investigations on Vulcano island have shown that intensive gas emanations occur throughout the island. Particularly significant gas emissions are observed both in the crater of the volcano and in the beach area at the northern foot of the Fossa cone (Fig. 11). Differences have been found in the beach and crater fumaroles. Most gas emission is concentrated within two principal areas: (1) in and around the Fossa crater and (2) in the beach area immediately to the north. Emissions from the two areas are characterized by distinctive chemical and carbon isotopic

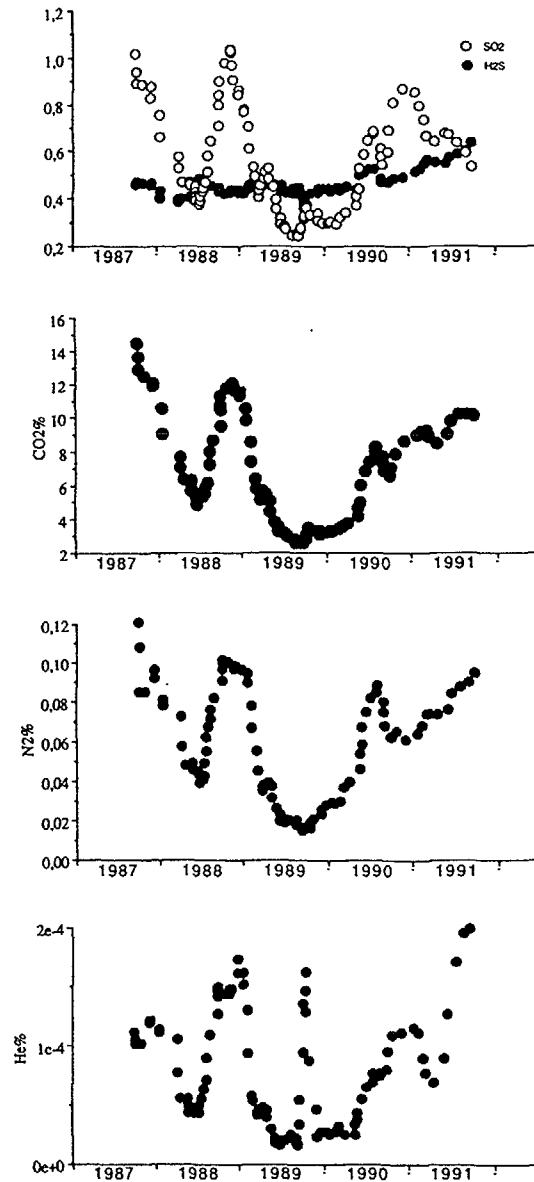


Fig. 13 -  $\text{H}_2\text{S}$ ,  $\text{SO}_2$ ,  $\text{CO}_2$ ,  $\text{N}_2$ , and He content also showed during our sampling period large oscillation, opposite to those of  $\text{H}_2\text{O}$  and  $\text{H}_2$ .

signatures (Baubron 1987-1990, Baubron et al., 1990; Tedesco et al., 1991; Le Guern et al., 1980; Martini et al., 1980; Carapezza et al., 1981; Cioni et al., 1984; Mazor et al., 1988). In particular, gases in the crater area contain large proportions of acidic compounds (e.g.  $\text{SO}_2$ ,  $\text{HCl}$ ,  $\text{HF}$  and are rich in helium (ca. 10 ppm of dry gases, while the beach emissions contain no acid components and are relatively poor in helium (ca. 2-3 ppm of dry gases). The difference in acid contents has been related to the distribution of near-surface aquifers. Such aquifers are common in the beach area and it has been suggested that they act as traps for the acidic components (Martini et al., 1984; Carapezza et al., 1981; Cioni et al., 1984). This interpretation, however, cannot explain the observed differences in helium content (Baubron et al., 1990; Tedesco et al., 1991): if the original gases feeding the two areas were the same, the beach gases would be expected to have higher proportions of helium (and other uncondensable phases) after removal of the acid species. The different helium contents may thus reflect that, in addition to different near-surface conditions, the two areas are underlain at intermediate depth by distinct and independent systems. However, geochemical studies conducted in the past 15 years on the fumaroles of both crater and beach systems suggest that deep magmatic fluids ascend through a shallower aquifer system, a biphasic reservoir (Tonani, 1971; Allard 1978; Le Guern, 1980; Carapezza et al., 1981; Mazor et al., 1988) or through a mono-phase reservoir (Cioni and D'Amore, 1984) below the Fossa cone and then feed the crater fumaroles. All these authors did not find evidence from their work of the existence of other different system below the superficial one. The clearest evidence of a magmatic contribution is provided by the isotopic ratio of helium, which ranges from 5-6  $R/R_a$  at the crater fumaroles and around 5  $R/R_a$  at the beach fumaroles (Poliak and Tolstikin, 1980; Hooker et al., 1985; Marty, pers. commun.; Shinohara and Matsuo, 1984; Tedesco, 1987; Sano et al., 1989) contrary to what stated by Mazor et al., (1988). These values, which are typical for arc volcanism (e.g. Poreda and Craig, 1989), indicate at least 65-80% of upper mantle helium in the fumaroles. The probable presence of a shallow

aquifer (meteoric or marine water) adjacent to the Fossa cone and strictly related to it, is also supported by our results, showing continuous rapid variations of the water vapour content of the fumaroles which seems to follow a seasonal trend (fig. 12), even if some other parameters seems to affect its trend.

The aim of this part of the chapter is to check the possible mechanism(s) in the fluid reservoir which could explain the observed chemical and isotopic variations of the F5, FA and other fumaroles since 1987.

Four mechanisms can be considered to explain these chemical oscillations:

- 1 - Seasonal dilution of deep gas reservoir with meteoric water.
- 2 - Variable injection(s) of hot gas from a magmatic reservoir. The existence of a magma intrusion at 2-4 Km depth below the Fossa is suggested by gravimetric data (Barberi et al., 1973), and seismic data (Ferrucci et al., 1991; Vilardo et al., 1991)
- 3 - Pressure variations in the fluid reservoir feeding the fumaroles as a result of either tectonic or hydrodynamic events.
- 4 - Mixing between different magmatic and hydrothermal systems.

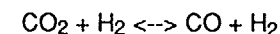
#### Mixing with superficial water

The hydrothermal fluid may be variably diluted by superficial water through two processes: (a) addition of meteoric water (according to the  $\delta D$  of fumarolic condensates, e.g., Cheminée et al., 1969; Allard, 1983) seasonally feeding the system and (b) infiltration of meteoric and/or marine water as a result of stress field variations due to earth tides. A dilution effect indeed could explain the annual variations of  $H_2O$  and the consequent decrease of the other species but  $H_2$ . The more soluble species, such as  $SO_2$  and  $HCl$ , can be specifically removed by enhanced dissolution; a higher increase of  $H_2/HCl$  and  $H_2/SO_2$  than of  $H_2/CO_2$ ,  $H_2/N_2$  or  $H_2/CO_2$

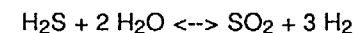
ratios is actually noticeable at the time of the two maximum water content peaks in our series of data.

#### Injection of new magmatic fluids

New injections of magmatic gas into a shallower reservoir (hydrothermal, or an old magmatic dyke) should be followed by an increase of the reservoir temperature, a higher a constant steam/liquid water ratio in the ascending fluid, and then, by a rise in the equilibrium temperature. The superficial temperature are from 335°C to 275°C, 415°C to 476°C and between 535°C and 661°C at F5, F5<sub>HT</sub> and FA respectively. In particular since the beginning of 1991, following the temperature drop from 335°C to 275°C and the drastic reduction of its flux, the fumarole F5 was no more sampled, and substituted by the so-called F5<sub>HT</sub>. We have calculated the so-called apparent equilibrium temperature of the fumarolic gases (Sabroux, 1979; Sabroux 1983). Based on our results on the F5, F5<sub>HT</sub> and on the FA fumaroles, equilibrium temperatures were computed from thermodynamic data for both the pressure independent water-gas-shift reaction:



and the pressure-dependent  $H_2S/SO_2$  equilibrium:



Temperatures calculated for F5 and F5<sub>HT</sub> from reaction (1) range between 315°C and 420°C for F5 (Fig. 14) and until 440°C for F5<sub>HT</sub> fumarole and thus are close to the higher outlet temperature, and do not provide evidence of higher conditions at depth. Those calculated from reaction (2) are slightly higher, ranging from 360°C and 440°C with some isolated higher values for both fumaroles. The differences between the outlet and the equilibrium temperatures given by the pressure-independent reaction (1), indicate that cooling of the fluid during its transit from the reservoir to the surface is limited to 80-100°C at most.

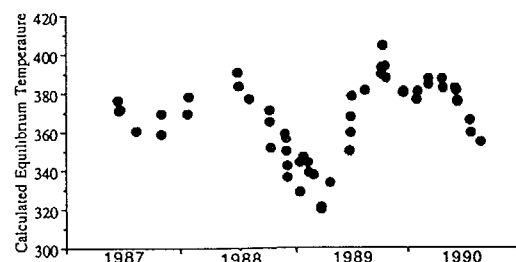


Fig. 14 - The calculated equilibrium temperature also show a wide variations, fairly correlated with the chemical oscillations.

Carapezza et al., (1981) calculated a slightly different  $\Delta T$  of 20-40°C for cooling of the Vulcano crater fluids in a previous period.

Such values therefore suggest that the fumarolic fluid equilibrates (for F5 and F5<sub>HT</sub> fumaroles) at a maximum temperature of around 410-440°C in a reservoir which must be shallow enough for limiting gas re-equilibration during ascent. On the other hand FA fluids reached an outlet temperature during our sampling period between 535°C and 661°C. It seems that the temperature variation is strictly dependent from the sampling point; in fact we realized that the highest temperature fumarolic point slowly migrate from one place to another inside the fumarolic field and thus it is difficult to find always the same point. Calculated equilibrium temperatures from reactions 1 and 2 indicate different results. Reaction (1) showed always temperature lower or at most similar to the emission point, indicating that chemical composition, as already showed for the F5 fumarole, re-equilibrate very fast at superficial conditions. On the contrary reaction (2) shows results indicating chemical equilibrium of higher temperatures. The calculated equilibrium temperature range between 670°C and 900°C suggesting an increasing trend with time. These results suggest an evolution of the superficial system, compared to reaction 2, of deeper equilibrium, probably closer to a magmatic reservoir.

The possibility of an increasing input of magmatic gas since 1982 is not supported by two features:

(a) Particularly at F5 fumarole, carbon monoxide, which forms at high temperature and under low oxygen fugacity conditions, occurs only in trace amounts in the gas and did not increase in the recent period compared to previous years. If an increasing magmatic gas input had been the cause of the recent thermal increase at the crater fumaroles, then a significant increase of both CO and CO/CO<sub>2</sub> ratio would have been expected in all crater fumaroles, included F5 and F5<sub>HT</sub> vents. This was not observed during the 5 years period of investigation, the CO content remaining 0,5 and 1,5 ppm of the anhydrous phase (Tedesco et al., 1991). On the other hand, the FA fumarole at a temperature of 600-650°C shows a higher CO content compatible with the outlet temperature. Nevertheless, as already shown by thermodynamical calculations (1) it seems that also in this case, fluids reach chemical equilibriums always close to the outlet temperature. The increase of the CO content in fumaroles at higher temperature show a slow variations with time. Unfortunately from our work and from the literature, we cannot affirm that the FA fumarole (inside crater) with the highest crater temperature just appeared during the last 5 years. It is also possible that this fumarole already existed with a temperature higher than rim crater fumarole and was not yet identified from researchers working on the island.

(b) The <sup>3</sup>He/<sup>4</sup>He ratio of the fumarole has continuously oscillated at the crater fumaroles over the same period, with high values from 5,0 to more than 6,0 R<sub>a</sub> (Sano et al., 1989; Tedesco et al., 1992), similar to those already obtained by other authors. On the contrary, at the beach fumarolic field, the helium ratio remain constant, with a value of 5,0 R<sub>a</sub>. The higher values at the crater fumaroles can be explained by a direct connection between the deep magmatic reservoir, about 4 km deep or less (Vilardo et al., 1991), and a shallower reservoir, -the magmatic intrusion of the 1888-1890 eruption- with only very slight interactions with the superficial system(s). At the same time, mixing with superficial



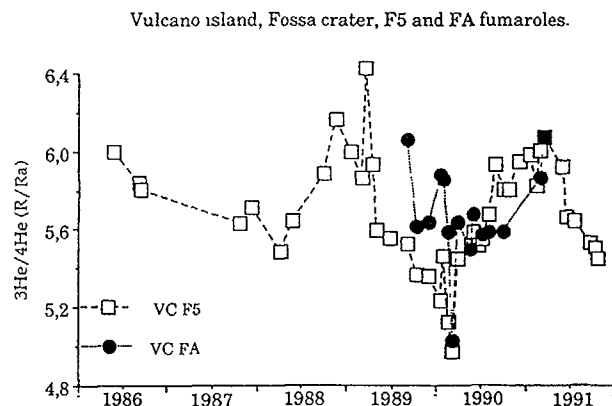
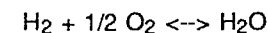


Fig. 15 - The helium isotopic composition at F5 and FA crater fumaroles. This is probably the first time on fumarolic fluids that the helium isotope ratios is changing at the same time that other chemical components.

reservoirs, and marine or meteoric waters (Tedesco et al., 1991), all of which are poor in 3-He, could produce the lower values recorded for  $^3\text{He}/^4\text{He}$ . The variations of the  $^3\text{He}/^4\text{He}$  ratios recorded at the F5 and FA crater fumaroles (Fig. 15) are explained by this model as a consequence of a continuous mixing between deep magmatic fluids (3-He rich) and superficial or deep marine waters (4-He rich). The highest  $^3\text{He}/^4\text{He}$  value at the crater fumaroles may be representative of uncontaminated juvenile fluid coming directly from the deepest magmatic reservoir. On the other hand, the lowest values of the  $^3\text{He}/^4\text{He}$  ratio (always recorded on the same fumaroles) show the time of the increasing mixing between the two reservoirs, when the addition of the superficial 4-He is at maximum. It is worth noting that the minimum  $^3\text{He}/^4\text{He}$  value at the crater fumaroles is the same as the ratio constantly obtained at the beach fumaroles, further suggesting that the two systems are influenced by the same phenomena, however, more evident on beach fluids for the uniformity of the helium isotopic ratio. The presence of very high  $^4\text{He}/^{20}\text{Ne}$  (Tedesco et al., 1992) ratios from almost all sampling sites, implies that the superficial helium source, mixed to the deeper one, is crustal and not

atmospheric. These results are in good agreement with the interpretation that an older superficial eruptive fracture could exist located close to the beach fumarolic system. This reservoir should be slightly depleted in 3-He compared to what actually feeds the crater reservoir and comparatively richer in 4-He, without addition of atmospheric helium trapped and carried in the superficial meteoric waters but probably buffered by deep marine waters. In Fig. (16) the  $\text{C}/^3\text{He}$  ratio has been plotted versus the  $\delta^{13}\text{C}$  values. In the diagram is possible to follow a continuous evolution of the composition of the fluid along a mixing line. The two end members can be recognized as follow: (a) S like superficial or sedimentary (crustal) with a lower 3-He content and a heavier carbon, close to typical limestone value (around 0‰), and (b) M as magmatic, close to the MORB values found by Marty and Jambon (1990), with a higher 3-He content and a lighter carbon closer to MORB values (between -4 and -8‰). From this graphic the variations that we monitored occurred all along this straight line and only between these two poles. It seems in this case that only two sources participate to the final fluid.

c) An injection of deep  $\text{CO}_2$  and  $\text{H}_2$ -rich magmatic fluid could also be hypothesized. Oskarsson (1984) has shown that a non equilibrated degassing magma can produce hydrogen pulses through diffusion processes,  $\text{H}_2$  being the most mobile compound due to its low molecular weight. Although  $\text{H}_2$ , actually increased in the first period of our sampling, its variation appear mostly related to that of water and the  $\text{H}_2/\text{H}_2\text{O}$  ratio suggests rather steady redox conditions in the fluid equilibration zone. An increase in  $P(\text{H}_2)$  could result from a simple increase of  $P(\text{H}_2\text{O})$ , if  $P(\text{O}_2)$  remains constant (Gerlach, 1980):



Finally, increasing vaporization of the underground reservoir would be associated with higher release of the less soluble ( $\text{H}_2\text{S}$ ,  $\text{CO}_2$ ) gas species compared to others ( $\text{HCl}$ ,  $\text{HF}$ ,  $\text{SO}_2$ ) and with higher  $\text{H}_2\text{S}/\text{SO}_2$  or  $\text{CO}_2/\text{H}_2$  ratios.

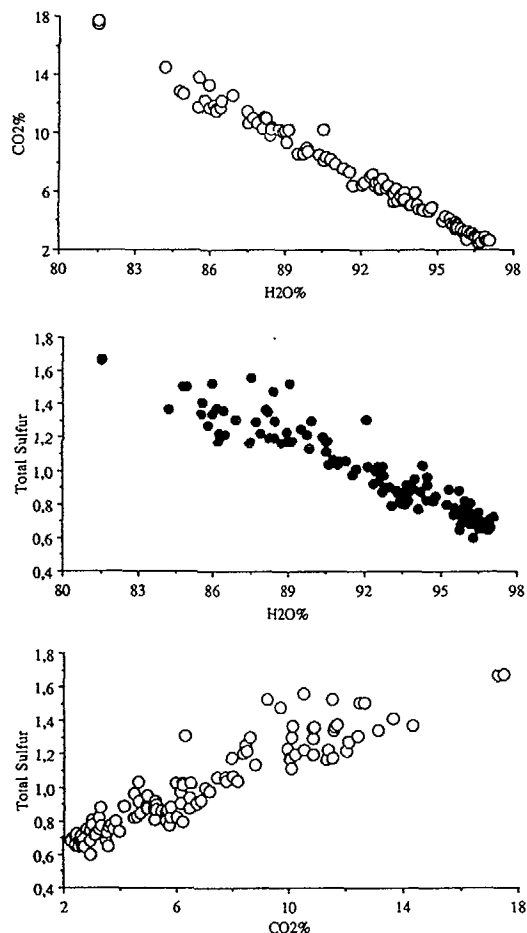


Fig 16 - The 3 diagrams in this figure try to explain the possible existence under the Vulcano crater of at least two different sources. In fact the inverse correlation between carbon dioxide and water vapor and total sulfur ( $\text{H}_2\text{S} + \text{SO}_2$ ) and water vapor indicate that both should come from two distinct source. On the other hand carbon dioxide and sulfur seems both to come from a unique source, probably deeper than that of water vapor.

d) One more evidence of the continuous mixing between different sources has given by Fig. 17. It is possible to separate different contribution from the different reservoirs: superficial and deep. It is also possible from these graphics to characterize the chemical

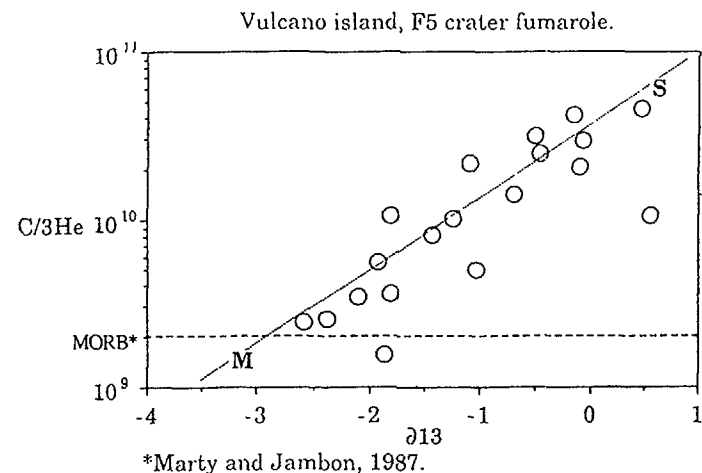


Fig. 17 - The existence of a mixing between two different sources is also suggested by the straight correlation between  $\text{C}/^3\text{He}$  and  $\delta^{13}\text{C}$ . Two possible source are found: 1) a superficial or crustal one related to heavier carbon and to a lower contribution of  $^3\text{He}$ . A magmatic one with light carbon, closer to typical M.O.R.B. values and richer in juvenile  $^3\text{He}$ .

composition of the sampled fluids in two different moments: (a) when the maximum mixing, between the superficial and deep reservoirs occur, and (b) when the gas reaches the surface directly from its departure reservoir with a small or no addition of superficial fluids. Evidently all intermediate points should represent all different moments of the mixing between the two end members. The inverse correlation between  $\text{CO}_2$ , total sulfur ( $\text{SO}_2 + \text{H}_2\text{S}$ ) and  $\text{N}_2$  versus  $\text{H}_2\text{O}$  (Fig.18), suggests that if water vapor has surely a superficial origin (Chemineé et al., 1969; Allard, 1983), the other species should come all together from another reservoir deeper than  $\text{H}_2\text{O}$ 's reservoir, without addition of any amount of the same compounds en route to the surface. Unfortunately this is not completely true, as it possible to realize from the Fig. 18, in which we plotted the  $\text{CO}_2$  content versus the  $\delta^{13}\text{C}$  values. In fact, if we hypothesize that carbon dioxide is generated from only one source, the isotopic value should not change at the changing of the  $\text{CO}_2$  content. The trend in Fig. 18

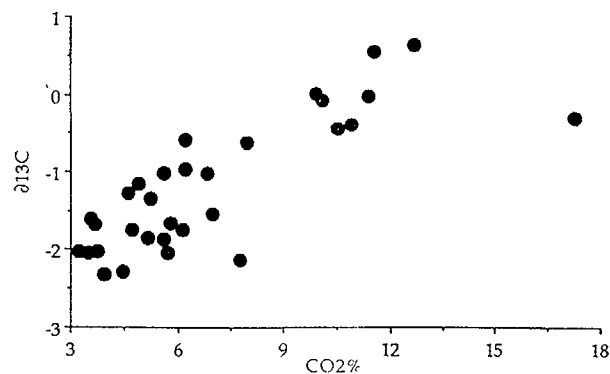


Fig. 18 - One more correlation is that of  $\delta^{13}\text{C}$  and carbon dioxide. Once again the data suggest two possible sources for the  $\text{CO}_2$ . One superficial or crustal with heavy carbon and the second with a light carbon closer to magmatic values.

suggests that also for the carbon dioxide exist at least two different sources, both deep with two different isotopic signatures: one crustal (metamorphic?) and one magmatic. The inverse correlation, between the  $\delta^{13}\text{C}$  and the  $^3\text{He}/^4\text{He}$  ratio suggests that the carbon values in the Vulcano island magmatic reservoir might be completely different from what expected from typical carbon values in magmatic reservoirs.

#### Seismic events

No significant earthquakes nor abnormal ground deformation occurred in the area over the 5 years of survey. No significant tectonic earthquake occurred in this area in the previous years (Ferrucci et al., 1991). So, it seems difficult to attribute the chemical variations to a disturbance of the hydrothermal system as a consequence of an increasing regional or local geophysical activity.

#### Mixing between crater and beach fluids

The sea level fumaroles of Vulcano are generally interpreted as resulting from percolation of a crater-type fluid through superficial

water tables, leading to a preferential loss of soluble species such as  $\text{SO}_2$ ,  $\text{HCl}$ ,  $\text{HF}$  (Martini et al., 1980, 1984; Cioni and D'Amore, 1984; Mazar et al., 1988). However, compared to crater fumarole, these fumaroles have not only chemical particularities (high  $\text{H}_2$ ,  $\text{CH}_4$ , low  $\text{He}$  and the  $\text{He}/\text{CO}_2$  ratio) but also different carbon isotope ratio (Allard, 1978; Cannata et al., 1988) and helium isotope ratio (Tedesco et al., 1992) which according to Baubron et al. (1990) and Tedesco et al. (1991), may reflect their feeding by a separate hydrothermal system, distinct from the superficial reservoir feeding the crater. This hydrothermal system could be fed by late degassing of a cooling magma body probably related to the Vulcanello complex, erupting from the 183 BC through the 16<sup>th</sup> century (Keller, 1980).

Interactions between the two systems could occur, considering the proximity of the respective fumarolic field (less than one kilometer). Some of the chemical variations in the F5 fumarole are compatible with such a mixing process. For example in Tedesco et al. (1991) is showed that the inverse relation between  $\text{He}$  and  $\text{H}_2\text{O}$ ; in fact we can see that  $\text{He}$  decreases when  $\text{H}_2\text{O}$  increases, which can interpreted as due to simple water dilution effect or to a mixing between a  $\text{He}$ -rich and  $\text{H}_2\text{O}$ -poor crater fluid and a  $\text{He}$ -poor and  $\text{H}_2\text{O}$ -rich beach fluids. On the other hand always the inverse correlation between the calculated equilibrium temperature and the  $\text{H}_2\text{S}/\text{SO}_2$  ratio (Tedesco et al., 1991) is also an evidence between a hot (high- $\text{SO}_2$ ) crater fluid and a colder (high- $\text{H}_2\text{S}$ ) beach fluid. One more indication that a mixing between two different reservoirs occurs is the trend of the  $\text{R}/\text{Ra}$  values at F5 and F5<sub>HT</sub> fumaroles showed in fig. 16. Is worth noting that the minimum value obtained at the crater fluid 5  $\text{R}/\text{Ra}$  is the same that the normal value obtained at the beach fluids. In this case we can always imagine a mixing between a  $^3\text{He}$  poor reservoir (beach) with a  $^3\text{He}$  rich reservoir (crater) (Tedesco et al., 1992).

From all chemical and isotopical data the hypothesis of a new injection of deep magmatic fluids as the source of the observed variations and the recent increase in activity is not supported by the constant and low  $\text{CO}$  content (fumaroles F5 and F5<sub>HT</sub>), the

continuous oscillation of the  $^3\text{He}/^4\text{He}$  ratio without any increasing trend and the rather low calculated equilibrium temperatures close to the emission temperatures and comparable to those inferred in previous periods. Nevertheless the increasing trend vent temperature at the FA fumarole of 660°C max, and the high CO content should be explained differently then with only the simple hypothesis of a new magmatic fluids injection. First of all the  $^3\text{He}/^4\text{He}$  ratio at the FA fumarole follows the same general trend showed by the F5 fumarole, on the other hand the increasing temperature and the chemical composition closer to a typical magmatic fluid, can be related to a major efficiency of the transfert of the deep fluid to the surface and not to an uprising magma body. With this hypothesis is possible to explain both the increase of the outlet temperature and the chemical equilibrium (reaction 2) and composition of higher temperatures. At the same time, if the reaction 1 always showed a superficial equilibrium, with a very low temperature, we should think that a partial re-equilibration of the CO content compared to the  $\text{H}_2$  content (or viceversa) surely occurs before the fluids reach the surface.

A more complete study, chemical and isotopical, on wider area of the island, including both systems is need to verify our interpretations and to better constrain the actual volcanological model here discussed. This model is only the first steep towards a better understanding of the dynamic evolution of the Vulcano island volcanic system.

#### REFERENCES

- Allard P., 1978. Composition isotopique et origine des constituants majeurs des gaz volcaniques ( $\text{H}_2\text{O}$ , C, S). Thèse d'Université, Paris VII, 340p.
- Allard P., 1983. Stable isotope composition of fumarolic gases from Vulcano island, Eolian island arc. IUGG Assembly, Hambourg, Proc. IAVCEI Symposium on Volcanic Gases, p. 4.
- Allard P. (1986). Géochimie isotopique et origine de l'eau, du carbone et du soufre dans le gaz volcaniques: zone du rift, marges continentales et arcs insulaires. Ph. D. thesis, Paris, France.
- Allard P., Baubron J.C., Luongo G., Pece R. and Tedesco D., 1988. Geochemical survey of soil gas emanations and eruption forecasting: the Vesuvius case, Italy. Proceedings of Int. Conf. on Volcanoes, Kagoshima, Japan, 212.
- Allard P., Maiorani A., Tedesco D., Cortecchi Turi B. Isotopic constraints on the origin of sulfur and carbon in Solfatara fumaroles, Campi Flegrei (Italy). J. Volcanol. Geoth. Res., 1991.
- Barberi F., Gasparini P., Innocenti F. and Villari L., 1973. Volcanism of the Southern Tyrrhenian Sea and its geodynamic implications. J. Geophys. Res., 78: 5221-5232.
- Barberi F., Innocenti F., Ferrara G., Keller J. and Villari L., 1974. Evolution of Eolian arc volcanism (Southern Tyrrhenian sea). Earth Planet. Sci. Lett. 21, 269-276.
- Barberi F., Corrado G., Innocenti F. Luongo G. Phlegraena Fields 1982-1984: Brief chronicle of a volcano emergency in a densely populated area. Bull. Volcanol. 47-2: 175-185, 1984.
- Barin I., Knacke O., 1973. Thermochemical properties of inorganic substances. Springer Berlin Heidelberg, New York, 921 p.
- Barin I., Knacke O. and Kobascewsky L., 1977. Thermochemical properties of inorganic substances (Supplement). 861 Springer Verlag, Berlin.
- Baubron J.C., Geochemical surveillance of some Italian volcanoes (Vulcano, Vesuvio, Solfatara). B.R.G.M. reports ANA DT 86-87-88-89-90 (1986-1987-1988-1989-1990).
- Baubron, J.C., Allard P. & Toutain J.P., 1990. Diffuse volcanic emissions of carbon dioxide from Vulcano island, Italy. Nature 344, 51-53.
- Beccaluva L., Gabbianelli G., Lucchini R., Rossi P.L., & Savelli C., 1985. Petrology and K/Ar ages of volcanics dredged from the Eolian seamounts: implications for geodynamic evolution of the southern Tyrrhenian basin. Earth Planet. Sci. Lett. 74, 187-208.
- Cannata S., Hauser S., Parello F. and Valenza M. 1988. Caratterizzazione isotopica della  $\text{CO}_2$  presente nelle manifestazioni gassose dell'isola di Vulcano. Rend. Soc. It. Min. Petr. vol. 43-1, 153-161.
- Carapezza M., Nuccio M. & Valenza M., 1981. Genesis and evolution of the fumaroles of Vulcano (Aeolian islands, Italy): a geochemical model. Bull. Volcanol. 44, 547-563.
- Carapezza M., Nuccio M. & Valenza M. (1984). Geochemical surveillance of the Solfatara of Pozzuoli (Campi Flegrei) during 1983. Bull. Volcanol. 47, 303-311.
- Cioni R. and Corazza E., 1981. Medium-temperature fumarolic gas sampling. Bull. Volcanol., 41: 23-29.
- Cioni R. & D'Amore F., 1984. A genetic model for the crater fumaroles of Vulcano island (Sicily, Italy). Geothermics 13, 375-384.

- Cioni R., Corazza E., Marini L. The gas/steam ratio as indicator of heat transfer at the Solfatara fumaroles, Phlegraean Fields (Italy). *Bull. Volcanol.*, 47-2: 295-302, 1984.
- Cioni R., Corazza E., Fratta M., Magro G. Sorveglianza geochimica dei Campi Flegrei. *Boll. Gruppo Nazionale Vulcanol.*, CNR, 167-173, 1986.
- Cheminée J. L., Letolle R., Olive P. H. 1969. Premières données isotopiques sur des fumerolles de volcans italiens. *Bull. Volcanol.*, vol. 45-3: 173-178.
- Degens E.T. 1969. Biogeochemistry of stable carbon isotopes. In *Organic geochemistry: methods and results*. Eglinton and Murphy. 304-329.
- Del Pezzo E. & Martini M. (1981). Seismic events under Vulcano, Aeolian island, Italy. *Bull. Volcanol.*, 44-3, 521-525.
- De Natale G., Pingue F., Allard P., Zollo A. Geophysical and geochemical modelling of the 1982-1984 bradyseismic phenomena at Campi Flegrei caldera (southern Italy). *J. Volcanol. Geoth. Res.*, 1991.
- Falsaperla S., Frazzetta G., Neri G., Nunnari G., Velardita R. & Villari L. (1989). Vulcano monitoring in the aeolian islands (Southern Tyrrhenian sea): the Lipari-Vulcano eruptive complex. In: *Volcanic Hazards, Assessment and Monitoring*. J. H. Latter (ed): 339-356. Springer-Verlag, Berlin, Heidelberg.
- Ferrara G., Magro G. Rare gas systematics (He, Ne, Ar) as a tool in the study of volcanic eruption precursors. *Per. Mineral.*, special volume, 55; 5-13, 1986.
- Ferrucci F., Gaudiosi G., Hirn A., Luongo G., Mirabile L. and Pino N.A. 1991. Seismological exploration of Vulcano (Aeolian Islands, Southern Tyrrhenian sea): case history. *Acta Vulcanologica* n. 1, 143-152.
- Frazzetta G., La Volpe L. and Sheridan M. 1984. Hazards at Fossa of Vulcano: data from the last 6,000 years. *Bull. Volcanol.*, 47: 106-124.
- Gerlach T. M., 1980. Evaluation of volcanic gas analyses from Kilauea Volcano. *J. Volcanol. Geother. Res.*, 7: 295-317.
- Giggenbach W. F., 1975. A simple method for collection and analysis of volcanic gases. *Bull. Volcanol.* 39: 132-145.
- Giggenbach W.F. Geothermal gas equilibria. *Geoch. Cosmoch. Acta*, 43: 2021-2032, 1983.
- Hermance J.F. (1983). The Long Valley/Mono Basin volcanic complex in eastern California: Status of present knowledge and future research need. *Rev. Geophys. Space Phys.* 21, 1545-1565.
- Hooker P.J., Bertrami R., Lombardi S., O'Nions R.K. & Oxburg E.R., 1985. Helium-3 anomalies and crustal-mantle interactions in Italy. *Geoch. Cosmoch. Acta* 49, 2505-2513.
- Jaggar T.A. (1940). Magmatic gases. *Am. J. Sci.*, 238: 313-353.
- Javoy M., Pineau F. & Demaiffe D. (1984). Nitrogen and carbon isotopic composition in the diamonds of Mbuji Maji (Zaire). *Earth Plan. Sci. Letters*, n° 68, 399-412.
- Keller J., 1980. The island of Vulcano. In L. Villari (editor), *The Eolian Islands, an active volcanic arc in the Mediterranean sea*. C.N.R. Catania.
- Le Guern F. and Faivre Pierret R., 1980. Différentiation de l'émanation magmatique: réaction  $H_2S + SO_2$  dans le gaz volcaniques. Vulcano (Italie), 1923-1979. *Bull. Volcanol.* 45 (3), 179-190.
- Le Guern F., 1983. Magmatic gas monitoring. In Tazieff H. and Sabroux J.C. (editors). *Forecasting Volcanic Events*, Elsevier, pp. 293-310.
- Le Guern F., 1987. Ecoulements gazeux réactif à hautes températures, mesures et modélisation. Thèse, université Paris 7, 314 pp.
- Matsuo S., 1961. On the chemical nature of fumarolic gases of volcano Showashinzan, Hokkaido, Japan. *J. Earth Sc., Nagoya Univ.* 80-100.
- Martini M., Piccardi G. & Cellini Legittimo P., 1980. Geochemical surveillance of active volcanoes: data on the fumaroles of Vulcano (Aeolian islands, Italy) *Bull. Volcanol.* 43: 255-263.
- Martini M., Cellini Legittimo P., Piccardi G., Giannini L., 1984. Composition of hydrothermal fluids during the bradyseismic crisis which commenced at Phlegraean Fields in 1982. *Bull. Volcanol.*, 47-2: 267-273.
- Martini M., 1986. Thermal activity and ground deformations at Phlegraean Fields, Italy: precursors of eruptions or fluctuations of quiescent volcanism? A contribution of geochemical study. *J. Geophys. Res.* 91-12: 255.
- Martini M., 1988. S.E.A.N. *Bull.* 6.
- Marty B. & Janbon A., 1987  $C/^{3}He$  in volatile fluxes from the solid earth: implications for carbon geodynamics. *Earth Planet. Sci. Lett.*, 83: 16-26.
- Marty B., Janbon A., Sano Y., 1989. Helium isotopes and  $CO_2$  in volcanic gases of Japan. *Chem. Geol.* 76, 25-40.
- Mazor E., Cioni R., Corazza E., Fratta M., Magro G., Matsuo S., Hirabayashi J., Shinohara H., Martini M., Piccardi G. & Cellini Legittimo P., 1988. Evolution of fumarolic gases boundary conditions set by measured parameters: case study at Vulcano, Italy. *Bull. Volcanol.* 50, 71-85.
- McKee C.O., Johnson R.W., Lowenstein P.L., Riley S.J., Blong R.J., De Saint Ours P., Talai B., 1984. Rabaul caldera, Papua New Guinea: volcanic hazards, surveillance and eruption contingency planning. *Bull. Volcanol.* 47-2: 195-327.
- Oskarsson N., 1984. Monitoring of fumarole discharge during the 1975-1982 rifting in Krafla volcanic center, North Iceland. *J. Volcanol. Geoth. Res.*, 22: 97-121.
- Poliak B.G. & Tolstikin I.N., 1980. Geotectonics, heat flux and helium isotopes: tripple relationship. In: *Proc. Int. Symp. KAPG 1-4, 1979*.

- Poreda R. and Craig H., 1989. Helium isotope ratios in circumpacific volcanism arcs. *Nature*, 338: 473-478.
- Rosi M., Sbrana A. (eds), Phlegraean Fields. CNR, Quaderni della Ricerca Scientifica, n° 114, vol. 9, pp. 1-5, 1987.
- Sabroux J. C., 1979. Equilibre thermodynamique en phase gazeuse volcanique. In *Haute temperatures et sciences de la terre*. C.N.R.S., Toulouse, 37-46.
- Sabroux J.C. Volcano energetics: volcanic gases and vapours as geothermometers and geobarometers. In: *Forecasting Volcanic Events*. Tazieff H., Sabroux J.C. (eds), Amsterdam, Elsevier pp. 17-25.
- Saint Claire Deville C., Leblanc F. & Fouquet F. (1863). Sur les emanations à gas combustible qui se sont échappé des fissures de la lave de 1794 à Torre del Graco lors de la dernière eruption du Vesuve. *C.R. Acad. Sc. Paris*, tome LVI.
- Sano Y and Wakita H., 1985. Geographical distribution of  $^3\text{He}/^4\text{He}$  ratios in Japan: implications for arc tectonics and incipient magmatism. *J. Geophys. Res.* 90, 8729-8741.
- Sano Y. and Wakita H., 1988. Precise measurement of helium isotopes in terrestrial gases. *Bull. Chem. Soc. Japan* 61, 1153-1157.
- Sano Y., Wakita H., Italiano F. & Nuccio M., 1989. Helium isotopes and tectonics interactions in Italy. *J. Res. Lett.* 16 (6), 511-514.
- Shepherd E.S. (1921). Kilauea gases, 1919. *Hawaiian Volcano Observatory Bulletin*, v. 9, n°5, 83-88.
- Sheridan M. F. and Malin M. C., 1983. Application of computer-assisted mapping to volcanic hazard evaluation of surge eruptions: Vulcano, Lipari and Vesuvius. *J. Volcanol. Geoth. Res.*, 17: 182-202.
- Shinohara H. & Matsuo S. Results and analysis on fumarolic gases from F-1 and F-5 fumaroles of Vulcano, Italy. *Geothermics* 15, 211-215, 1984.
- Sicardi L., 1955. Captazione ed analisi chimica dei gas della esalazione solfidrico-solforosa dei vulcani in fase solfatarica. *Bull. Volcanol.* 17, 107-112.
- Tedesco D., 1987. Significato ed elaborazione termodinamica dei fluidi di ambienti geotermici (Campi Flegrei, Long Valley) e vulcanici (Hawaii, Usu). Ph. D. Thesis, University of Napoli, pp. 239.
- Tedesco D. and Sabroux J.C. The determination of deep temperatures by means of the  $\text{CO-CO}_2\text{-H}_2\text{-H}_2\text{O}$  geothermometer: an example using fumaroles in Campi Flegrei, Italy. *Bull. Volcanology*, 49: 381-387, 1987.
- Tedesco D., Bottiglieri L., Pece R. 10<sup>th</sup> of April 1987 seismic swarm: correlation with geochemical parameters in Campi Flegrei caldera (southern Italy). *Geoph. Res. Lett.*, 15-7, 661-664, 1988 a.
- Tedesco D., Pece R., Sabroux J.C. No evidences of a new magmatic gas contribution to the Solfatara volcanic gas, during the bradyseismic crisis at Campi Flegrei caldera (Italy). *Geoph. Res. Lett.* 15-12: 1441-1444, 1988 b.
- Tedesco D., Allard P., Sano Y., Pece R., Wakita H. Helium-3 in subaerial and submarine fumaroles at Campi Flegrei caldera, Italy. *Geoch. Cosmoch. Acta*, 54, 1105-1116, 1990.
- Tedesco D., Toutain J.P., Allard P. & Losno R. Chemical variations in fumarolic gases at Vulcano island: seasonal and volcanic effects. *J. Volcan. Geotherm. Res.* 45, 325-334, 1991.
- Tedesco D. Helium and Carbon isotope data at Vulcano island. Poster at G.N.V. March, 1992.
- Tonani F. Concepts and techniques for the geochemical of volcanic eruptions. In: *The surveillance and prediction of volcanic activity*. UNESCO, Paris, pp. 145-166, 1971.
- Vilardo G., Castellano M., Gaudiosi G. and Ferrucci F. Seismic surveillance at Vulcano by use a portable digital array: features o the seismicity and relocation of the evnts in a 3-D heterogeneous structure. *Acta Vulcanol.*, vol. 1, 171-177, 1991.

# LIST OF PARTICIPANTS

Armenta-Hernandez, M A National Autonomous University of Mexico  
Institute of Geophysics  
Ciudad Universitaria, 04510 Mexico DF, Mexico

Balcazar, M National Institute of Nuclear Research  
Apartado Postal 18-1027  
Col Escandon, 11801 Mexico DF, Mexico

Balderer, W Ingenieur-Geology, ETH-Honggerberg  
CH-8093 Zurich, Switzerland

Belyaev, A Geochemistry Institute, Academy of Sciences  
Kossygina ul 19, 117975 GSP-1, Moscow, Russian Federation

Dall'Aglia, M Dipartimento di Scienze della Terra  
Citta Universita La Sapienza  
Piazzale Aldo Moro 5, 00185 Rome, Italy

de la Cruz-Reyna, S National Autonomous University of Mexico  
Institute of Geophysics  
Ciudad Universitaria, 04510 Mexico DF, Mexico

Dubinchuk, V T All-Russian Research Institute for Hydrology and Engineering  
Geology, Center for Geoenvironment  
142452 Zeleny Village, Noginsk District  
Moscow Region, Russian Federation

Freeth, S J Geological Hazards Research Unit  
University College of Swansea  
Natural Sciences Building  
Singleton Park, Swansea SA2 8PP, United Kingdom

Friedmann, H University of Vienna  
Institute of Radio Research and Nuclear Physics  
Boltzmanngasse 3, A-1090 Vienna, Austria

Gupta, H K Ministry of Science and Technology  
Department of Science and Technology  
New Mehrauli Road, New Delhi 110016, India

Heimcke, J Bergakademie Freiberg, Institute of Physics  
Bernhard-von-Cotta-Strasse 4, 9200 Freiberg, Germany

Keilis-Borok, V I International Institute for Earthquake Prediction, Theory  
and Mathematical Geophysics  
ul Warshavskaja 79, pr korp 2, Moscow 1113556  
Russian Federation

King, Chi-Yu US Department of the Interior  
Geological Survey  
345 Middlefield Road, Menlo Park, CA 94025  
United States of America

Kusakabe, M Institute for Study of the Earth's Interior  
Okayama University  
Misasa, Tottori-ken 682 01, Japan

Martinelli, G Regione Emilia Romagna, Servizio Informativo e Statistica  
Viale Silvani 4/3, I-40122 Bologna, Italy

Monnin, M Centre National de la Recherche Scientifique  
Place Eugene Bataillon, F-34060 Montpellier, France

Moosbauer, L University of Vienna  
Institute of Geology  
Universitätsstrasse 7/III, A-1010 Vienna, Austria

Nuccio, P M Institute of Mineralogy, Petrography and Geochemistry  
University of Palermo  
Via Archirafi 36, I-90123 Palermo, Italy

Sato, M US Department of the Interior  
Geological Survey, Office of Earthquakes, Volcanoes and  
Engineering  
959 National Centre, Reston, VA 22092, USA

Tedesco, D Osservatorio Vesuviano  
Via A Manzoni 249, 80123 Naples, Italy

Vartanyan, G S VSEGINGEO, All-Union Research Institute for Hydrogeology  
and Engineering Geology  
1424542 Zeleny Village, Noginsk District  
Moscow Oblast, Russian Federation

Valenza, M Institute of Geochemistry of Fluids (CNR)  
Via Torino 27d, I-90100 Palermo, Italy

Wang, Chengmin Centre of Earthquake Predictions and Analysis  
National Bureau of Earthquakes, Office of IAEA Affairs  
P O Box 2101, Beijing, China